Entwicklung und präklinische Evaluation immunologischer und nuklearmedizinischer diagnostischer Tests für Schimmelpilz-assoziierte Hypersensitivität und invasive Mykosen

Development and preclinical evaluation of immunological and nuclear medical diagnostic assays for mould-associated hypersensitivity and invasive mycoses

Dissertation zur Erlangung des naturwissenschaftlichen Doktorgrades
der Graduate School of Life Sciences,
Julius-Maximilians-Universität Würzburg,
Sektion: Infektion und Immunität

Vorgelegt von

Lukas Page

aus

Nürnberg

Würzburg 2020

This document is licensed under the Creative Commons Attribution-ShareAlike 4.0 International License (CC BY-SA 4.0):
http://creativecommons.org/licenses/by-sa/4.0 This CC license does not apply to third party material (attributed to another source) in this publication.

Eingereicht am: ……

Bürostempel

Mitglieder des Promotionskomitees:

Vorsitzender: Prof. Dr. Christian J. Janzen

1. Betreuer: Prof. Dr. Andrew J. Ullmann

2. Betreuer: Prof. Dr. Jürgen Löffler

3. Betreuer: Prof. Dr. Samuel Samnick

4. Betreuer: Prof. Dr. Ulrike Holzgrabe

Tag des Promotionskolloquiums: ……

Doktorurkunden ausgehändigt am: ……

Inhaltsverzeichnis

1. EINLEITUNG

1.1 Übersicht der Immunabwehr gegen Schimmelpilze

Täglich atmen Menschen hunderte Sporen unterschiedlicher Schimmelpilze ein. Diese ubiquitär vorkommenden saprophytisch lebenden Organismen nehmen eine dominante Rolle als Destruenten in der Umwelt ein (Ribes et al., 2000). Die Inhalation von Pilzsporen hat für gewöhnlich kaum negative Effekte auf die Gesundheit immunkompetenter Personen, da die Pilzsporen über mehrere Abwehrsysteme des menschlichen Körpers eliminiert werden können.

Die erste Verteidigungslinie stellt die Epithelbarriere des Atmungstrakts dar, deren Mukus-Schicht und sezernierte antimikrobielle Peptide (AMP) inhalierte Pathogene eliminieren (Park & Mehrad, 2009). Leukozyten des innaten Immunsystems, namentlich Makrophagen, neutrophile, eosinophile und basophile Granulozyten, sowie Mastzellen und dendritische Zellen (DC) stellen die zweite Verteidigungslinie gegen inkorporierte Mikroben dar. Sie identifizieren mithilfe von *Pattern Recognition*-Rezeptoren (PRR) auf ihrer Zelloberfläche *Pathogen Associated Molecular Patterns* (PAMP) verschiedener Mikroorganismen (Romani, 2011). Im Fall von Schimmelpilzen handelt es sich dabei u. a. um Mannan und β-Glucan, die von Makrophagen beispielsweise über die Rezeptoren Mannose-bindendes Lectin bzw. Dectin-1 erkannt werden (Brown et al., 2002, Worthley et al., 2005). Polymorphkernige Neutrophile sind die zahlenmäßig im Blut häufigsten Leukozyten und verfügen über eine Vielzahl antiinfektiver Funktionen. Dazu zählen Exozytose toxischer Granula, Generation reaktiver Sauerstoff-Spezies, Phagozytose und intrazelluläre Degradation von Mikroorganismen, sowie der programmierte Zelltod unter Freisetzung ihrer DNA zur Erzeugung von *Neutrophil Extracellular Traps* (Gazendam et al., 2016, Zawrotniak et al., 2013). Mit einer Lebensdauer von weniger als einem Tag muss ihre Population konstant regeneriert werden, um die Immunantwort effizient aufrecht zu erhalten (Lahoz-Beneytez et al., 2016). Ihre Bedeutung wird dadurch unterstrichen, dass Neutropenie und Neutrophilendysfunktion die Haupt-Risikofaktoren für die Entwicklung invasiver Mykosen darstellen (Baehner, 1980, Chamilos et al., 2006, Chen et al., 2017).

In den Alveolen der Lunge sind alveoläre Makrophagen (AM) stationiert, die in diesen Bereich vorgedrungene Sporen phagozytieren und mithilfe von in Lysosomen enthaltenen Proteasen und Peroxiden eliminieren (Ibrahim-Granet et al., 2003, Park & Mehrad, 2009). Die degradierten Peptide des Pathogens werden über Moleküle des Haupthistokompatibilitätskomplexes (MHC) Klasse II an die Oberfläche der Makrophagen gebracht und so den T-Zellen präsentiert. Parallel werden u. a. proinflammatorische Mediatoren wie Tumornekrosefaktor (TNF) α und die Interleukine (IL) 1α, 1β, 2 und 6 sezerniert (Steele et al., 2005). IL-2 ist dabei essenziell für eine funktionale spezifische T-Zell-Antwort und deren Regulation (Abbas et al., 2018b). Chemokine (CXCL2, CCL3) rekrutieren weitere Leukozyten über chemotaktische Signale zum Infektionsherd und induzieren parallel chemokin- und populationsspezifische Differenzierungen von unterschiedlichen T-Zell-Fraktionen (Rossi & Zlotnik, 2000, Steele et al., 2005). Granulozyten-Kolonie-stimulierende Faktoren (G-CSF) bzw. Granulozyten-Monozyten-CSF (GM-CSF) dienen der Proliferationsstimulation der entsprechenden Zielpopulationen (Steele et al., 2005).

DC phagozytieren Schimmelpilzsporen und präsentieren die Produkte des lysosomalen Verdaus über MHC II an ihrer Oberfläche (Guermonprez et al., 2002). Diese durchqueren daraufhin den Blutkreislauf in Richtung lymphatischer Organe, während sie reifen und eine Vielzahl Chemo- und Zytokine sezernieren, welche weitere Populationen rekrutieren (Gafa et al., 2007). In lymphatischen Organen präsentieren sie die Antigene einer konzentrierten Population an T-Zellen, sodass diese effizient in großer Zahl aktiviert werden können. Die spezifisch gegen die präsentierten Antigene gerichtete T-Zell-Variante wird in den Lymphknoten klonal expandiert und in den Blutkreislauf entlassen (Merad et al., 2013). DC stellen somit eine Brücke zwischen innater und adaptiver Immunität dar.

T-Zellen erkennen auf MHC-Molekülen präsentierte Peptide über variierende T-Zell-Rezeptoren (TCR), benötigen für ihre Aktivierung aber zusätzliche kostimulatorische Signale. Der wichtigste Rezeptor hierfür ist CD28. Auf diesen können antigenpräsentierende Zellen (APC) über die Liganden CD80 und CD86 kostimulatorisch einwirken (Esensten et al., 2016). Zusätzliche kostimulatorische Signale können über das auf der Zelloberfläche von T-Zellen befindliche Integrin *Very Late Antigen* (VLA) 4, einem CD29/CD49d-Komplex, vermittelt werden (Thakur

et al., 2013). VLA 4 bindet an Fibronectin und das *Vascular Cell Adhesion Molecule* (VCAM) 1, womit neben der Aktivierung der Zelle auch die zielgerichtete Migration der Zellen zu Entzündungsherden und Extravasation in Gewebe unterstützt wird (Udagawa et al., 1996).

CD4-positive T-Zellen (T-Helfer-Zellen, Th) exprimieren nach ihrer Aktivierung CD154 (alternativ CD40L) auf ihrer Oberfläche. Mit diesem können sie an CD40 auf der Oberfläche von Makrophagen binden, die ein korrespondierendes Antigen über MHC II präsentieren, diese hierdurch aktivieren und so eine effizientere Degradation phagozytierten Materials initiieren (Elgueta et al., 2009). Es existieren unterschiedliche Subpopulationen von T-Helfer-Zellen, welche je nach ihren Effektorfunktionen und Zytokinprofilen maßgeblich an der Balance zwischen Toleranz und Abwehr von Schimmelpilzen beteiligt sind (Dewi et al., 2017).

Die über Schimmelpilz-spezifische Th-Zellen vermittelte Immunreaktion ist schematisch zusammengefasst in Abb. 1.1 dargestellt (Dewi et al., 2017). Fehlfunktionen einzelner Bestandteile dieses Systems können in der Folge bereits eine Vielzahl von Schimmelpilz-assoziierten Erkrankungen hevorrufen.

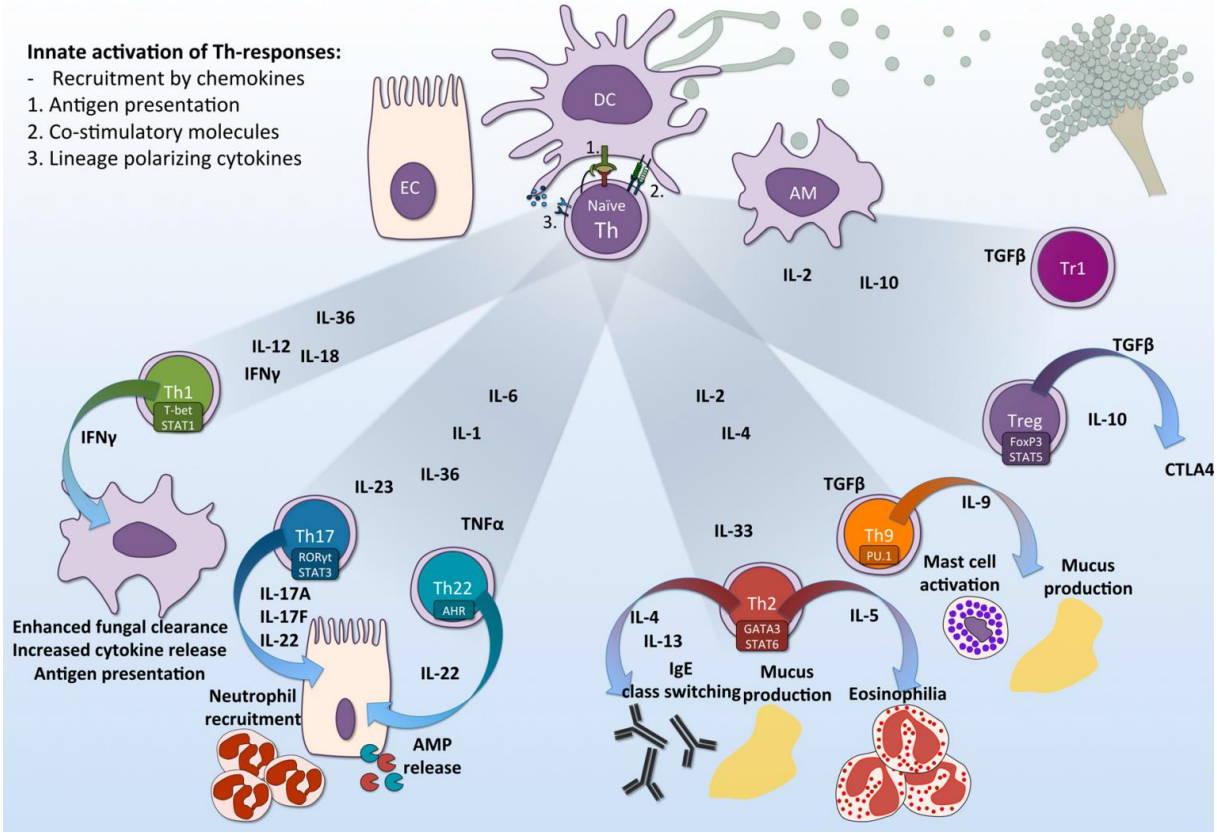

Abb. 1.1 Schematische Darstellung der Rolle verschiedener Th-Populationen bei der Immunantwort gegen Schimmelpilze (Dewi et al., 2017).

Aktivierte Makrophagen sezernieren proinflammatorische Faktoren und Zytokine, z. B. IL-12, welche primär T-Helfer 1 Zellen (Th1) stimulieren. Diese führen eine systemische proinflammatorische Reaktion über die Zytokine Interferon (IFN) γ, TNF-α und IL-2 herbei, die zusätzlich durch die Rekrutierung weiterer Leukozyten die Elimination fungaler Erreger begünstigt (Romagnani, 1991, Romani, 2011). Eine funktionale Th1-Antwort wird mit einer positiven Prognose im Falle einer invasiven Aspergillose in Verbindung gebracht, u. a. da diese die antifungalen Effektor-mechanismen der innaten Immunabwehr, welche letztendlich zur Eradikation der fungalen Erreger führt, effizient stimuliert (Cenci et al., 1998, Dewi et al., 2017, Jolink et al., 2014).

Th2 Zellen verfügen über ein differentes Zytokinprofil (IL-4, IL-5, IL-13), welche der durch Th1-Zellen induzierten Immunantwort entgegensteht und so potentiellen Gewebeschädigungen vorbeugt (Romani, 2011). Aktivierte Th2 induzieren dabei insbesondere Eosinophilie und in antikörperproduzierenden B-Zellen des Körpers einen Klassenwechsel zu IgE (Dewi et al., 2017). Antikörper der IgE-Klasse verfügen über eine hohe Affinität zu den F_c-Rezeptoren von Mastzellen, welche mittels toxischer Granula in der Lage sind, Pathogene effizient zu eliminieren, jedoch auch mit verantwortlich für die bei allergischen Reaktionen auftretenden gewebeschädigenden Symptome sind (Rick et al., 2016, Toniato et al., 2017). Eine Th2-dominierte Immunantwort gegenüber Schimmelpilzen wird mit Hypersensitivität und allergischen Symptomen assoziiert (Lordan et al., 2002, Muller et al., 2007, Park & Mehrad, 2009, Romani, 2011) und geht mit einer schlechteren Prognose im Fall einer invasiven Aspergillose einher, da die von Th2 induzierten Immunreaktionen nicht in der Lage sind, die Erreger effizient zu eliminieren (Cenci et al., 1998 und 1999, Dewi et al., 2017).

Die von Th17 Zellen hauptsächlich sezernierten Zytokine IL17A und IL17F führen zu einer effizienten Rekrutierung und gesteigerten Stimulation von Neutrophilen, womit eine rasche Elimination der invadierenden Erreger begünstigt wird (Werner et al., 2009). Parallel freigesetztes IL-22 führt zu einer gleichzeitigen Aktivierung von Epithelzellen, worauf mitunter eine gesteigerte Sekretion antimikrobieller Peptide folgen kann (Dudakov et al., 2015). Eine prolongierte exazerbierende Th17-polarisierte Immunantwort kann jedoch auch zu unproduktiven inflammatorischen Reaktionen mit fungaler Persistenz führen (Zelante et al., 2007).

Regulatorische T-Zellen (T_{Reg}) wirken der proinflammatorischen Antwort anderer Immunzellen entgegen und sezernieren antiinflammatorische Zytokine wie IL-10 und *Transforming Growth Factor* (TGF) β, um eine überschießende Immunantwort und kollaterale Schäden an gesundem Gewebe zu minimieren. Zusätzlich verfügen T_{Reg} über das zytotoxische T-Lymphozyten-Antigen (CTLA) 4, welches andere T-Zellen über direkten Kontakt inhibiert (Dewi et al., 2017, Montagnoli et al., 2006, Vignali et al., 2008).

CD8 positive T-Zellen, auch zytotoxische T-Zellen genannt, erkennen Antigene, welche über MHC Klasse I Moleküle präsentiert werden. Jede Zelle im Besitz eines Zellkerns exprimiert diese Art von MHC Molekülen und präsentiert auf ihnen Peptide, welche im Zytosol proteasomal abgebaut wurden. Gesunde Zellen sollten hierbei nur körpereigene Peptide aufweisen, gegen die im Regelfall keine spezifischen CD8 T-Zellen im Blutkreislauf vorhanden sind, da autoreaktive T-Zellen während des Reifungsprozesses im Thymus negativ selektiert werden (Abbas et al. 2018a). Mutierte oder mit intrazellullären Erregern infizierte Zellen präsentieren jedoch entsprechend fremdartige Peptide auf den MHC I Molekülen an der Zelloberfläche, die von den CD8 T-Zellen erkannt werden und eine zytotoxische Antwort provozieren, welche die entartete Zelle eliminiert (Miller-Kittrell & Sparer, 2009). Hierdurch werden beispielsweise Infektionen mit Influenza- und Cytomegalieviren (CMV) abgewehrt, Risikofaktoren für schwere Pilzinfektionen (Vanderbeke et al., 2018, Yong et al., 2018). Es existieren nur wenige Nachweise eines prominenten funktionellen Beitrages zytotoxischer T-Zellen zur Abwehr von Schimmelpilzen (Cui et al., 2017), durch Vakzinierungsstrategien (Nanjappa et al., 2012 Wuthrich et al., 2003) oder die immuntherapeutische Anwendung von mit chimären Antigenrezeptoren versehenen CD8 T-Zellen (Kumaresan et al., 2017) könnte eine solche jedoch artifiziell hervorgerufen werden.

1.2 Klinik und Immunpathologie Schimmelpilz-assoziierter Erkrankungen

Eine fein regulierte Immunantwort ist insbesondere bei der Abwehr von Schimmelpilzen essenziell, da das Immunsystem konstant durch Antigene der aerogen dispergierenden Sporen stimuliert wird (Ribes et al., 2000). Dies führt bei immungesunden Menschen aufgrund effizienter Eradikation der Sporen durch die in Kap. 1.1 genannten Mechanismen nur selten zu assoziierten Komplikationen, überschießende Reaktionen können jedoch zu Allergien und Hypersensitivitäts-erkrankungen führen. Als opportunistische Krankheitserreger stellen Schimmelpilze insbesondere eine Gefahr für immunkompromittierte Patienten dar, deren insuffiziente Immunreaktionen ein Auskeimen der Sporen im Lungengewebe ermöglichen, was beispielsweise zu Aspergillomen und invasiven Mykosen führen kann (Park & Mehrad, 2009).

Die wichtigsten Risikofaktoren für invasive Mykosen stellen wie in Kap. 1.1 beschrieben Neutropenie und Neutrophilendysfunktionen dar (Chamilos et al., 2006, Chen et al., 2017, Marr et al., 2002a und 2002b). Diese treten vor allem bei Patienten mit leukämischen Erkrankungen oder nach Transplantation hämatopoietischer Stammzellen (HSZT) auf, mitunter verbunden mit einer global verzögerten Rekonstitution des Immunsystems (Baron & Nagler, 2017). Dies erhöht das Risiko der Patienten eine Vielzahl opportunistischer Infektionserkrankungen zu erleiden, insbesondere jedoch Schimmelpilzinfektionen wie invasive Aspergillosen und Mucormykosen (Marr et al., 2002a und b). Zusätzlich erhalten Patienten nach Transplantationen von Stammzellen oder soliden Organen häufig immunsuppressive Medikation, welche das Risiko einer Abstoßungsreaktion des Transplantats und *Graft-versus-Host-Disease* (GvHD) minimieren (Fukuda et al., 2003, Ratanatharathorn et al., 2001). Häufig werden Inhibitoren der Calcineurin- und JNK-Signalwege verwendet (beispielsweise Ciclosporin A). Diese interferieren mit der Aktivierung des Transkriptionsfaktors *Nuclear Factor Activating T cell* (NF-AT), sodass insbesondere die T-Zell-Antworten der Patienten geschwächt werden (Matsuda & Koyasu, 2000). Weitere häufig verwendete Immunsuppressiva sind u. a. Kortikosteroide wie Prednisolon, welche nach Bindung an Glucocorticoid-Rezeptoren in den Zellkern translozieren und dort direkt die Expression antiinflammatorischer

Proteine induzieren (Vandevyver et al., 2013). Des Weiteren inhibieren Kortikosteroide zentrale proinflammatorische Signalwege, wie z. B. den NF-κB-Signalweg, sowie eine Vielzahl pyrogener Zyto- und Chemokine (IL-2, IL-4, IL-5, GM-CSF, CXCL8) und die Adhäsionsmoleküle ICAM-1 und VCAM-1 (Barnes, 2017). Immunsuppressiva interferieren dadurch aber auch mit der Abwehr von Infektionen, sodass diese Patienten insbesondere in der frühen Phase nach der Transplantation eine strikte Expositionsprophylaxe einhalten müssen, um das Risiko einer Infektion mit opportunistischen Erregern zu reduzieren. Nichtsdestotrotz erleiden bis zu 10 % der HSZT-Patienten eine invasive Aspergillose (Maschmeyer et al., 2007), wobei *Aspergillus fumigatus* den häufigsten ursächlichen Erreger darstellt (Hohl, 2017). Bei Patienten, die über einen Zeitraum von 30 Tagen unter Neutropenie leiden, erhöht sich die Inzidenz der invasiven Aspergillose auf bis zu 70 % (Darling & Milder, 2018). In den meisten Fällen handelt es sich um pulmonale oder tracheale Manifestationen, deren Letalität bei 50-70 % liegt (Maertens et al., 2018, Taccone et al., 2015). Neben *A. fumigatus* als häufigsten Erreger invasiver Schimmelpilzinfektionen werden inzwischen auch vermehrt Infektionen mit Pilzen der Ordnung Mucorales diagnostiziert (Goncalves et al., 2016, Roden et al., 2005). Eine frühzeitige Diagnose und antimykotische Therapie sind in jedem Fall essenziell für das Überleben der an invasiven Mykosen erkrankten Patienten (Chamilos et al., 2008a, Karthaus & Buchheidt, 2013, Maertens et al., 2018). Um einer Infektion vorzubeugen wird in vielen Fällen für transplantierte Patienten neben der genannten GvHD-Prophylaxe auch eine antimykotische Prophylaxe verordnet (Mellinghoff et al., 2017, Ullmann et al., 2018).

Auch vordergründig immunkompetente Personen ohne klassische Risikofaktoren wie Neutropenie können jedoch an schweren Schimmelpilzinfektionen erkranken. So werden diese auch vermehrt bei Patienten mit chronisch-obstruktiver Lungenerkrankung (COPD, Guinea et al., 2010), Diabetes mellitus (Petrikkos et al., 2012), sowie nach Influenzavirus-Infektionen (Vanderbeke et al., 2018, Wauters et al., 2012) diagnostiziert. In der Folge geophysikalischer und meteorologischer Naturkatastrophen wie Vulkanausbrüchen und Überschwemmungen werden ebenfalls vermehrt invasive Pilzinfektionen beobachtet (Benedict & Park, 2014), v. a. durch die traumatische Inkorporation der Erreger, zumeist Mucorales, in tieferliegende Hautschichten oder die Inhalation kontaminierten Wassers (Garzoni et al., 2005, Kawakami et al., 2012, Neblett Fanfair et al., 2012, Patino et al., 1991).

Die allergische broncho-pulmonale Aspergillose (ABPA) stellt eine hypersensitive Erkrankung dar, welche insbesondere mit IgE-basierten Sensibilisierungen gegenüber *Aspergillus* assoziiert ist (Agarwal et al., 2016). Wie in Kap. 1.1 dargestellt, führen die zugrunde liegenden Mechanismen über eine Th2-polarisierte Immunantwort zu exazerbierenden Inflammationen unter Beteiligung von Mastzellen und insbesondere eosinophilen Granulozyten, wobei eine Sensibilisierung gegenüber *Aspergillus*-Antigenen einer manifesten ABPA zumeist vorhergeht (Agarwal et al., 2013, Dewi et al., 2017). Prädisponierende Erkrankungen für eine ABPA sind Asthma und CF (Patel & Greenberger, 2019). Zudem konnte die Exposition gegenüber hohen Konzentrationen von Schimmelpilzsporen mit der Entwicklung von ABPA in Verbindung gebracht werden (Agarwal et al., 2013).

COPD, CF, sowie Infektionen mit *Mycobacterium tuberculosis* erzeugen durch chronische Inflammationen und Fibrosen Kavitäten im Lungengewebe (Page et al., 2019). Sie stellen damit neben ABPA prädisponierende Erkrankungen der chronisch-pulmonalen Aspergillose (CPA) dar, da sich in diesen Kavitäten *A. fumigatus*-Sporen festsetzen können (Agarwal et al., 2013, Denning et al., 2016). Dort können sie auskeimen und chronische Infektionen verursachen, wobei die Inflammationsprozesse progressiv exazerbieren. Die Folgen sind u. a. chronisch-kavernöse pulmonale Aspergillosen, chronisch-fibrotische Aspergillosen oder subakute invasive Infektionen (Denning et al., 2016).

Eine weitere Form hypersensitiver Reaktionen auf Schimmelpilze stellt die Hypersensitivitätspneumonitis dar. Hypersensitivitätsreaktionen treten gehäuft im beruflichen Umfeld von stark schimmelpilzexponierten Berufsgruppen auf, so etwa im landwirtschaftlichen Bereich (Kotimaa et al., 1984, Liu et al., 2015), holz-verarbeitender Industrie (Halpin et al., 1994, Faerden et al., 2014) oder bei Klimatisierungstechnikern (Quirce et al., 2016). Zystische Fibrose (CF) stellt einen weiteren Risikofaktor für eine Sensibilisierung und bronchopulmonale Komplikationen durch Schimmelpilze dar (Schwarz et al., 2018). Die auch als allergische Alveolitis bezeichnete Lungenerkrankung basiert auf einer granulomatösen lymphozytischen Alveolitis, der neben einer Th1- v. a. eine verstärkte Th17-polarisierte Immunantwort zugrunde liegt (Joshi et al., 2009, Selman et al., 2012, Simonian et al., 2009). Neben Schimmelpilzen unterschiedlicher Spezies (z. B. *Aspergillus*, *Alternaria* oder *Rhizopus*) kann diese auch gegenüber einer Vielzahl weiterer Antigene auftreten,

darunter (myko-) bakterielle, aviane oder chemische Auslöser (Selman et al., 2012, Spagnolo et al., 2015). Da diese Erkrankung in den meisten Fällen das Resultat einer chronischen Antigen-Exposition am Arbeitsplatz darstellt, entstanden u. a. entsprechende Bezeichnungen wie *Farmer's Lung*, *Pigeon Breeder's Lung* und *Chemical Worker's Lung* (Spagnolo et al., 2015). Die stetige Progression der subakuten und chronischen Formen dieser Erkrankung kann zu letalen Lungenfibrosen und pulmonaler Hypertension führen (Selman et al., 2012, Spagnolo et al., 2015).

Zur Erforschung der Pathophysiologie dieser Erkrankungen, sowie neuer Biomarker und Therapeutika sind Studien im Tiermodell oder an Menschen oftmals ein wichtiger Schritt der Validierung. Insbesondere während der frühen experimentellen Phasen sind *in vivo* Studien jedoch nicht immer indiziert bzw. praktikabel. *In vitro* Experimente bezüglich der Infektions- und Immunbiologie pulmonaler Schimmelpilzinfektionen tragen verglichen mit diesen jedoch stets einen artifiziellen Charakter mit sich. Um dem zu begegnen wurde ein *Transwell*®-Modell entworfen, welches mittels eines epithelialen und endothelialen Kompartiments die physiologischen Gegebenheiten des humanen Alveolus akkurater approximieren soll als planktonische Zellkulturen. Dieses Modell wurde von Hope et al. (2007) auf Basis humaner pulmonalarterieller Endothelzellen (HPAEC) und A549 Typ 2 Pneumozyten entwickelt. Diese wurden durch eine semipermeable Polyestermembran mit einer Porengröße von 3 µm separiert. Nach Infektion des alveolären Kompartiments wurde die Invasivität von *A. fumigatus* in das endotheliale Kompartiment über einen Anstieg der Galactomannan-Konzentration verifiziert und mit Werten aus *Aspergillus*-infizierten Kaninchen verglichen. Eine Suppression des Pilzwachstums nach Zugabe von Makrophagen oder Amphotericin B (AMB) konnte ebenfalls dargestellt werden (Hope et al., 2007). Weitere immun- und infektionsbiologische Studien konnten anhand dieses bzw. adaptierter *Monolayer*-Varianten des Modells mit *A. fumigatus* durchgeführt werden (Morton et al., 2014 und 2018). Weiterhin soll nun evaluiert werden, ob sich das *Bilayer*-Modell ebenfalls zur Simulation pulmonal-invasiver Infektionen mit den hiermit bisher nicht untersuchten Mucorales eignet. Neben immunpathologischen Gesichtspunkten sollen dabei auch klinische Phänomene von Mucormykosen dargestellt werden. Wenn dies gewährleistet ist könnten auch Mucorales anhand des *Transwell*®-Modells in zukünftigen Studien experimenteller Biomarker oder Antimykotika effizienter untersucht werden.

1.3 Experimentelle Biomarker zur Diagnostik Schimmelpilz-assoziierter Hypersensitivität und invasiver Mykosen

1.3.1 Etablierte Diagnostik von Schimmelpilzinfektionen

Mithilfe der Kriterien der *European Organization for Research and Treatment of Cancer* wird die Diagnose einer invasiven Mykose in verschiedene Wahrscheinlichkeitsgrade unterteilt (De Pauw et al., 2008). So stellen positive Kulturen, Mikroskopie oder Zytopathologie aus sterilem Patientenmaterial bzw. Biopsaten Voraussetzungen für den Nachweis einer Schimmelpilzinfektion dar. Zusätzlich müssen radiologische Hinweise auf eine invasive Pilzinfektion oder Gewebeschädigungen vorliegen (De Pauw et al., 2008). Der direkte Erregernachweis über Kulturen setzt jedoch voraus, dass sich der Organismus mittels minimaler Inokula rapide im Labor anzüchten lässt. Mikroskopische Charakterisierungen führen zudem nur selten zu einer eindeutigen Speziesbestimmung (Cornely et al., 2014, Ostrosky-Zeichner, 2012). Bei vielen Risikopatienten ist außerdem aufgrund deren hämatologischer (Neutropenie, Thrombozytopenie) oder klinischer Konstitution die Entnahme von Biopsaten kontraindiziert (Ostrosky-Zeichner, 2012). Radiologische Surrogatmarker pulmonaler Mykosen, z. B. Halo-Zeichen, können anhand von Computertomographie (CT) detektiert werden, was sich als sensitiver als die Röntgendiagnostik erwiesen hat und somit gegebenenfalls auch frühe Stadien pulmonal-invasiver Infektionen erkannt werden können (Greene et al., 2007, Sherif et al., 2010). Diese Anzeichen treten bei individuellen Patienten jedoch nicht immer bzw. in unterschiedlichen Ausprägungen auf und erlauben keinerlei Rückschlüsse auf die Erregerspezies (Ostrosky-Zeichner, 2012).

Für *Aspergillus*-Infektionen existieren mikrobiologische Surrogatmarker in Form der fungalen Zellwandbestandteile Galactomannan und β-D-Glucan. Diese können aus Serum- oder BAL-Proben (Bronchoalveoläre Lavage) mithilfe eines *Enzyme Linked Immunosorbent Assay* (ELISA) detektiert werden (Marty et al., 2009, Meerssemann et al., 2008). Es wird empfohlen, diese Surrogatmarker zur Erhöhung der Sensitivität parallel einzusetzen, insbesondere im Fall nicht-neutropenischer Patienten, da besonders bei diesen die Verlässlichkeit negativer Galactomannan-Werte als Ausschlusskriterium abnimmt (Ullmann et al., 2018). Zudem führen diese *Assays* bei Mucorales-Infektionen meist zu negativen Ergebnissen (Cornely et al., 2014,

Karageorgopoulos et al., 2011, Paiva et al., 2018, Sinko et al., 2008). Als weiterer mikrobiologischer diagnostischer Nachweis dient über Polymerase-Kettenreaktion (PCR) detektierte *Aspergillus*-DNA aus Blut, BAL oder Biopsiematerial (Mengoli et al., 2009, Springer & Löffler, 2017, Ullmann et al., 2018). Analog hierzu lassen sich Mucorales- und *Fusarium*-Infektionen ebenfalls über deren DNA nachweisen (Springer et al., 2016a und b und 2019).

Zur Diagnostik von Hypersensitivitätserkrankungen bedient man sich primär der mit diesen assoziierten IgE-Antikörpern. IgE-basierte Sensibilisierung wird in vielen Fällen Schimmelpilz-assoziierter Lungenerkrankungen diagnostiziert, wie z. B. allergischer Rhinosinusitis, Asthma und ABPA (Rick et al., 2016). Aufgrund der durch die mitunter chronischen Inflammationen und darauffolgenden pulmonalen Fibrosen bei ABPA und CPA können radiologisch sichtbare Infiltrate ebenfalls als Marker schwerer Manifestationen dienen (Denning et al., 2016, Patel & Greenberger, 2019). Die Diagnostik der Hypersensitivitätspneumonitis gestaltet sich als komplex, da diese keine spezifischen Merkmale im Vergleich zu anderen Lungenerkrankungen mit ähnlicher Symptomatik aufweist. Gängige diagnostische Methoden wie Radiologie, Histologie und Serologie führen ebenfalls zu vergleichsweise unspezifischen Ergebnissen, welche zusätzlich mit der originären Antigenexposition in Verbindung gebracht werden müssen (Selman et al., 2012). Zumeist behilft man sich zur Sicherung der Diagnose einer Inhalation des mutmaßlichen stimulierenden Antigens und der darauffolgenden symptomatischen Episode des Patienten (Selman et al., 2012).

Existierende Biomarker sind demnach kaum in der Lage, frühzeitig verlässliche Diagnosen Schimmelpilz-assoziierter Erkrankungen zu liefern. Gegenwärtig wird jedoch intensiv an der Etablierung und Evaluation neuer supportiver experimenteller Biomarker gearbeitet.

1.3.2 Schimmelpilz-reaktive T-Zellen als supportiver Biomarker

Pathogen-spezifische T-Zellen können als supportive Biomarker für Infektionskrankheiten herangezogen werden, oftmals auch in Verbindung mit deren sezernierten Zytokinen (Kim et al., 2015, Potenza et al., 2016). Im Falle von Tuberkulose und CMV-Infektionen werden Antigen-reaktive T-Zell-Antworten anhand deren Zytokinsekretion über *Enzyme Linked Immuno Spot Assays* (ELISPOT)

quantitativ analysiert und als Diagnostikum angewandt (Kim et al., 2015, Silveira et al., 2018). Eine T-Zell-basierte Immundiagnostik ist nach initialen Studien an Risikopatienten eventuell auch für Pilzinfektionen möglich (Bacher et al., 2015b, Koehler et al., 2018, Potenza et al., 2011 und 2016). Für diese Untersuchungen werden in der Regel isolierte mononukleäre Zellen des peripheren Blutes (PBMC) verwendet und mit Antigenen oder Lysaten der Erreger stimuliert. Nach geeigneten Stimulationszeiten können die von den PBMC sezernierten Zytokine analysiert (Potenza et al., 2011 und 2016) oder durchflusszytometrisch die Frequenz reaktiver CD4-positiver Th-Zellen über den Aktivierungs-Marker CD154 bestimmt werden (Bacher et al., 2013 und 2015b, Bacher & Scheffold, 2015). Im Gegensatz zur Analyse der Expression einzelner Zytokine wie IFN-γ, welche sich über individuelle Th-Populationen wie in Kap. 1.2 beschrieben deutlich unterscheiden, stellt CD154 einen globalen Aktivierungsmarker von Th-Zellen dar. Dieser zeichnet sich durch eine minimale Hintergrundexpression bei jedoch raschem Anstieg nach Stimulation aus (Bacher & Scheffold, 2013 und 2015a, Meier et al., 2008). CD154 dient als Ligand für CD40, welches sich auf APC befindet (Elgueta et al., 2009) und lokalisiert mittels Exozytose nach der Proteinbiosynthese an der Zelloberfläche. Da CD154 nach Reinternalisierung degradiert wird und keiner Quantifizierung mehr zur Verfügung stehen würde, muss zur durchflusszytometrischen Analyse $CD4^+CD154^+$-Zellen dieser Vorgang unterbunden werden. Hierfür wird der Exozytoseinhibitor Brefeldin A der Kultur beigegeben, da ohne vorhergehende Exozytose das Protein nicht reinternalisiert werden kann, und somit auch dessen Abbauprozess nicht induziert wird (Miller et al., 1992).

Bacher et al. (2015b) konnte zeigen, dass sich *Aspergillus*- und Mucorales-spezifische T-Zellen als supportiver Marker zur Diagnostik und Verlaufskontrolle invasiver Mykosen eignen könnten, da die reaktiven T-Zell-Frequenzen bei einer Infektion anstiegen, im Verlauf antimykotischer Therapien jedoch wieder sanken. Ein hoher Anteil *Aspergillus*-reaktiver T-Zellen muss jedoch nicht zwangsläufig mit einer Infektion koinzidieren, sondern kann auch das Resultat erhöhter Schimmel-Exposition im beruflichen oder residentiellen Umfeld sein (Wurster et al., 2017b). Bisher wurde jedoch noch nicht untersucht, ob dies auch für ebenfalls ubiquitär vorkommende Mucorales zutrifft. Die Kombination durchflusszytometrischer Marker mit zusätzlichen Tests wie Messungen von T-Zell-Zytokinprofilen könnte die Differenzierungsleistung hinsichtlich physiologischer und pathologischer Immun-

antworten gegenüber Schimmelpilzen möglicherweise weiter optimieren. Besonders in arbeitsmedizinischen Risikogruppen von ABPA, CPA oder Hypersensitivitäts-pneumonitis könnten hiermit potenziell übermäßig expandierende und reagierende T-Zell-Populationen frühzeitig detektiert werden.

Ex vivo isolierte PBMC erwiesen sich jedoch als anfällig gegenüber prä-analytischen Störungen wie etwa prolongierte Bearbeitungszeit. So führten bereits präanalytische Lagerungszeiten der Blutproben von mehr als 30 min vor Beginn der *Ficoll*-basierten Aufreinigung zu einer signifikant reduzierten Detektionsleistung *Aspergillus*-spezifischer T-Zellen (Wurster et al., 2017c). Im Verlauf von bis zu 6 h werden Granulozyten unspezifisch aktiviert, die dabei ablaufenden Prozesse können spezifische T-Zell-Reaktionen inhibieren (McKenna et al., 2009). Dem kann durch kontinuierliche Agitation, Verdünnung mit RPMI 1640-Medium oder Erwärmen auf 37 °C in begrenztem Maße entgegengewirkt werden (Wurster et al., 2016, Kongress für Infektionskrankheiten und Tropenmedizin, Würzburg, Deutschland), da insbesondere die Verdünnung der Blutproben mit RPMI bzw. PBS die Vitalität der Granulozyten verbessern kann, wodurch die Beeinträchtigung der T-Zellen verringert wird (McKenna et al., 2009).

Im Rahmen multizentrischer klinischer Studien und der klinischen Praxis werden längere Lagerungs- und Transportzeiten jedoch mitunter unvermeidbar, u. a. da bei lokalen Kliniken nicht immer Sterilwerkbänke und die zur Durchflusszytometrie benötigte Ausrüstung verfügbar sind. Von Weis et al. (2019) wurde daher ein Vollblut-basiertes Protokoll entwickelt, welches bettseitig mit Patientenblut beimpft und anschließend an spezialisierte Zentren versandt werden kann, da die Anfälligkeit gegenüber präanalytischen Transportzeiten verglichen mit dem konventionellen PBMC-basierten Protokoll geringer ausfiel (Page et al., 2017, *8th Trends in Medical Mycology*, Belgrad, Serbien). Im Unterschied zum PBMC-basierten Protokoll muss dem Vollblut-Testsystem jedoch für ein zuverlässiges Ergebnis neben dem ko-stimulatorischen Faktor α-CD28 zusätzlich α-CD49d hinzugefügt werden (Weis et al., 2019).

Ein Abfall detektierter reaktiver T-Zellen kann zudem auch auf immunsuppressive Medikation zurückzuführen sein (Kamperschroer et al., 2014, Sester et al., 2009), welche Risikopatienten invasiver Mykosen mitunter erhalten (siehe Kap. 1.2). Während immunsuppressive Medikation zu Beeinträchtigungen der Funktionalität *ex*

vivo kultivierter T-Zellen führte (Fellman et al., 2011, Guzera et al., 2016, Tsiavou et al., 2002), wurden zumindest für T-Zell-Zytokin-basierte *Assays* noch keine Einbußen durch Antimykotika dokumentiert, tendenziell sogar Steigerungen der Reaktivität auf zugegebene Stimuli (Fidan et al., 2014, Tramsen et al., 2013).

Es wurde bisher jedoch für keines der beiden genannten durchflusszytometrischen Protokolle die direkte Anfälligkeit der Detektionsleistung Schimmelpilz-spezifischer T-Zellen gegenüber antimykotischer und immunsuppressiver Medikation evaluiert. Da diese in Risikogruppen hypersensitiver Erkrankungen und invasiver Mykosen, wie in Kap. 1.2 dargestellt, häufig angewandt werden, soll im Rahmen dieser Arbeit deren Einfluss auf die durchflusszytometrische Bestimmung $CD154^+CD4^+$ T-Zellen untersucht werden.

1.3.3 Nuklearmedizinische Bildgebung

Ein wesentlicher Ansatz weiterer potenzieller Diagnostika ist die Entwicklung nuklearmedizinischer Detektionsverfahren wie Positronenemissionstomographie (PET) und Einzelphotonenemissionscomputertomografie (SPECT). Neben dem direkten Nachweis einer Schimmelpilzinfektion könnte durch die hohe Spezifität nuklearmedizinischer *Tracer* zusätzlich Lokalisation und Ausdehnung des befallenen Gewebes präzise bestimmt und von Inflammationen anderen Ursprungs differenziert werden.

In der Vergangenheit wurden nuklearmedizinische *Tracer* zur Bildgebung von Infektionserkrankungen bereits vielfach untersucht, insbesondere für bakterielle Infektionen (Zhang et al., 2011, Gowrishankar et al., 2014, Nielsen et al., 2015, Sellmyer et al., 2017). ^{18}F-Fluorodesoxyglucose (FDG) stellt einen etablierten Marker zur Bildgebung metabolisch hyperaktiver Gewebe dar. Um (ggf. okkulte) Infektionserkrankungen anhand nuklearmedizinischer Bildgebung zu detektieren wurde FDG im PET/CT klinisch getestet, wies allerdings kaum Spezifität gegenüber bakteriellen Erregern und Tumorgewebe auf (Douglas et al., 2017, Sharma et al., 2014, Rolle et al., 2016). Unterstrichen wird dies dadurch, dass anhand eines porzinen Modells ^{18}F-FDG als potenzieller PET-*Tracer* zur Diagnostik *S. aureus*-induzierter Osteomyelitis vorgeschlagen wurde (Nielsen et al., 2015). Erste Erfolge im klinischen Kontext wurden für bakterielle Erreger mit radioaktiv markiertem Ciprofloxacin erreicht, wobei die Sensitivität und Spezifität > 80 % betrugen (Britton

et al, 2002). Zudem wurden bereits bekannte antimikrobielle Moleküle untersucht, diese sind aufgrund ihrer Aktivität gegen unterschiedliche Erreger jedoch ebenfalls ungeeignet zur Differenzierung von Pilzen und Bakterien (Lupetti et al., 2011). Zur Detektion von Schimmelpilzen wurden mit ^{68}Ga-markierte Siderophore Triacetylfusarinin C und Ferrioxamin E (TAFC bzw. FOXE) im Rattenmodell etabliert. Während TAFC eine hohe Spezifität für *A. fumigatus* Infektionen aufwies, fiel FOXE durch hohe Sensitivität mit gleichzeitig jedoch deutlich verringerter Unterscheidbarkeit zu bakteriellen Infektionen auf (Petrik et al., 2014). TAFC konnte zudem *Aspergillus terreus* und *Aspergillus flavus* nicht detektieren, während FOXE auch *R. arrhizus*, *Fusarium solani* erkannte. Beide *Tracer* wiesen jedoch auch Anreichungen im Bereich steriler Inflammationen auf (Petrik et al., 2014). Um nun die Spezifität gezielt für Pilzinfektionen zu erhöhen stehen potenziell mehrere Möglichkeiten zur Verfügung. Wang et al. (2014) untersuchte ^{99m}Tc-markierte MORF Oligomere: Nukleinsäure-Analoga, die komplementär zur ribosomalen RNA von *Aspergillus spp.* bzw. *A. fumigatus* synthetisiert wurden. Diese konnten im Mausmodell spezifisch *A. fumigatus* nachweisen, stehen aber nicht für alle relevanten Pilze zur Verfügung und müssten für jede zu diagnostizierende Spezies einzeln generiert und evaluiert werden. Antikörper können ebenfalls synthetisch hergestellt und auf Spezifität optimiert werden, sodass Rolle et al. 2016 eine Kombination aus ImmunoPET und Magnetresonanztomographie zur Diagnostik im Mausmodell etablieren konnten. Diese Technologie stellt jedoch hohe Anforderungen an Ressourcen und Ausrüstung, sodass sie primär an spezialisierten Zentren zum Einsatz kommen würde.

Antimykotika stellen im Vergleich dazu kostengünstige Alternativen dar, welche sich analog zu antibakteriellen Substanzen ebenfalls radioaktiv markieren lassen und an definierte Zielstrukturen fungaler Zellen binden: Polyene wie Amphotericin B binden an Ergosterole in der fungalen Zellmembranen und führen dort zur Formation von Poren (Hammond, 1977). Azole wie Fluconazol, Voriconazol, Posaconazol und Isavuconazol hemmen das zur Ergosterolsynthese benötigte Enzym Lanosterol-14α-Demethylase, was in der Folge ebenfalls die Zellmembranen von Pilzen beeinträchtigt (Dogan et al., 2017). Echinocandine inhibieren die 1,3-β-Glucansynthase, einem essenziellen Enzym zum Aufbau einer intakten Zellwand (Patil & Majumdar, 2017).

Einige dieser Substanzen wurden bereits auf ihre Eignung als potenzielle *Tracer* hin evaluiert. So wurden Versuche mit ^{99m}Tc-markiertem Fluconazol im *A. fumigatus* und *C. albicans* infizierten Mausmodell vorgenommen, hier konnte jedoch nur *C. albicans* verlässlich detektiert werden (Lupetti et al., 2002 und 2005). ^{99m}Tc-Tricarbonyl-Caspofungin konnte über Szintigrafie *C. albicans* und *Aspergillus niger* verursachte Mykosen im murinen Modell diagnostizieren (Reyes et al., 2014).

Das Polyen-Makrolakton Amphotericin B (AMB) stellt ein Antimykotikum mit Aktivitäten gegenüber *Aspergillus* und *Candida spp*., sowie Erreger der Ordnung Mucorales dar. Der Wirkmechanismus basiert auf der Bindung von Ergosterol, einem essentiellen Zellwandbestandteil von Pilzen, der sich von dem auf Säugerzellen befindlichen Cholesterol unterscheidet (Hamill, 2013, Hammond, 1977). Aufgrund des amphiphilen Charakters des Wirkstoffs führt eine Akkumulation von ca. acht AMB-Molekülen zur Porenbildung in der Zellmembran und somit zu unkontrolliertem Ionenfluss, welcher schließlich zur Lyse der betroffenen Zelle führt (Hamill, 2013, Hammond, 1977). Aufgrund seines breiten Wirkspektrums könnte AMB nach Markierung mit geeigneten radioaktiven Isotopen potenziell in der Lage sein, ebenjenes Spektrum an Erregern über nuklearmedizinische Methoden nachweisen zu können. Aufgrund multipler Hydroxygruppen in geeigneten sterischen Konformationen ließe es sich potenziell über die Komplexierung mit dreiwertigen Kationen radioaktiver Metalle markieren (Abb. 1.2).

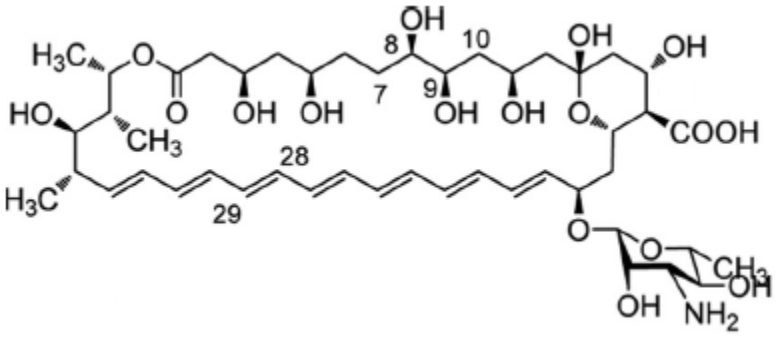

Abb. 1.2 Strukturformel von Amphotericin B (modifiziert nach Tevyashova et al., 2013). Die Positionen 7 – 10 und 28 – 29 bezeichnen für die antimykotische Wirksamkeit essenzielle funktionellen Gruppen.

Die antimykotische Aktivität von AMB ließ sich hauptsächlich auf die funktionellen Gruppen der Positionen 7 – 10 und 28 – 29 zurückführen (Tevyashova et al., 2013), wobei die hydrophoben Areale des Moleküls, welche an Plasmamembranen binden, vom Markierungsprozess vermutlich nicht betroffen werden. Zum Zwecke der

Bildgebung ist bei gewährleisteter Bindung eine fungizide Wirkung ohnehin nur sekundär von Bedeutung.

Eines der in der konventionellen Nuklearmedizin am meisten eingesetzten Radioisotope stellt ^{99m}Tc dar. Als Gamma-Emitter mit einer Halbwertszeit von 6 h wird es häufig zur diagnostischen Bildgebung und Verlaufskontrolle über SPECT unterschiedlicher Erkrankungen angewandt, darunter neuronale, kardiovaskuläre und Tumor-erkrankungen (Papagiannopoulou, 2017). ^{68}Ga kann als Positronstrahler zur Bildgebung mittels PET genutzt werden, welche mit bis zu 2 mm eine höhere räumliche Auflösung als SPECT (gegenwärtig bis zu 6,7 mm) ermöglicht, allerdings zu einem deutlich höheren Kostenpunkt (Martiniova et al., 2016, Slomka et al., 2015).

Fernandez et al. (2017) konnten bereits einen ^{99m}Tc-markierten AMB-*Tracer* zur Detektion von Schimmelpilzen entwickeln, welcher im Mausmodell Infektionen erfolgreich darstellen konnte. Verglichen mit der dort beschriebenen Methodik zur Markierung von AMB über eine Tricarbonyl-^{99m}Tc-Verbindung könnte alternativ jedoch unter Ausnutzung der zahlreichen Hydroxygruppen des AMB-Moleküls eine zeit- und ressourceneffizientere Komplex-Synthese entworfen werden. Zusätzlich sollen Möglichkeiten weiterer geeigneter Radioisotope, wie das für die PET-Bildgebung zunehmend eingesetzte Radionuklid ^{68}Ga, hinzugezogen werden. Sollte dies zu ausreichend reinen und stabilen Produkten führen, soll anschließend die Spezifität und Detektionsleistung des *Tracers* anhand von Schimmelpilzinfektionen in einem *Transwell*®-Modell des humanen Alveolus (basierend auf Hope et al., 2007 und Morton et al., 2014, siehe Kap. 1.1) verifiziert werden.

1.4 Zielsetzung

Im Rahmen der vorliegenden Arbeit sollten supportive experimentelle Biomarker zur Diagnostik Schimmelpilz-assoziierter Erkrankungen in unterschiedlichen Entwicklungsstadien optimiert und evaluiert werden.

1.) Die durchflusszytometrische Bestimmung Schimmelpilz-spezifischer T-Zellen über CD154 wurde als supportiver Biomarker invasiver Mykosen und Schimmelpilz-Exposition im beruflichen und privaten Umfeld vorgeschlagen. Hier soll nun evaluiert werden, ob die Kombination dieses Markers mit *Aspergillus*- und Mucorales-reaktiven Zytokinprofilen und Phänotypen der T-Zell-Populationen die Klassifizierungsleistung von Expositionsprofilen gegenüber Schimmelpilzen optimieren kann.

2.) Neben dem PBMC-basierten Protokoll zur Quantifizierung spezifischer T-Zellen wurde ein Vollblut-basiertes Protokoll entwickelt. Es sollte weiterhin evaluiert werden, inwiefern Antimykotika und Immunsuppressiva in Abhängigkeit der Testmatrix und verwendeter Kostimulation diese *Assays* beeinflussen, da für beide Pharmakaklassen immunmodulatorische Aspekte dokumentiert sind. So soll zudem die Robustheit der Tests gegenüber geläufigen Störfaktoren in Risikopatienten zu evaluiert werden.

3.) Ein *in vitro Transwell*®-Alveolarmodell invasiver Aspergillosen wurde zur präliminären Evaluation neuer Biomarker und antimykotischer Wirkstoffe publiziert und soll hier für Erreger der Ordnung Mucorales etabliert werden. Dafür sollen neben der Validierung anhand technischer Qualitätsmerkmale Charakteristika der unterschiedlichen Erreger wie Invasivität und Immunpathologie rekonstruiert und verglichen werden.

4.) Als potenzieller weiterer neuer Biomarker sollte eine Methode entwickelt werden, Amphotericin B mit den Radionukliden ^{68}Ga und ^{99m}Tc zu markieren, und deren Eignung als potenzielle nuklearmedizinischer *Tracer* zu untersuchen. Nach Evaluation von Ausbeute, Reinheit und Stabilität der *Tracer* sollte unter Verwendung eines *Transwell*®-Modells zur Simulation pulmonaler invasiver Mykosen *in vitro* die Fähigkeit der *Tracer* untersucht werden, Schimmelpilze unterschiedlicher Spezies von bakteriellen Infektionen differenzieren zu können.

2. MATERIALIEN UND METHODEN

2.1 Materialien

2.1.1 Technische Ausrüstung

2.1.1.1 Kühl- und Gefrierschränke

Comfort	Liebherr
MedLINE	Liebherr
Premium	Liebherr

2.1.1.2 Vortexer

Harmony Mixer Uzusio VTX-3000L	LMS Laboratory and Medical Supplies
Vortex-Genie 2	Scientific Industries

2.1.1.3 Heizblock

neoBLOCK 1	neoLab

2.1.1.4 Zentrifugen

Fresco 17 Centrifuge	Thermo Scientific
Megafuge 16 Centrifuge	Thermo Scientific
Multifuge 3s	Thermo Scientific
Sunlab Mini-Zentrifuge	neoLab

2.1.1.5 Sterilwerkbank

HERAsafe HS 12	Thermo Electron Corporation

2.1.1.6 Inkubatoren

HERACELL 150i CO_2 Incubator	Thermo Scientific
HERATHERM Incubator	Thermo Scientific
Minitron	INFORS HT

2.1.1.7 Mikroplatten-*Reader*

Luminex 200	Luminex Corporation
NanoQuant infinite M200 PRO	Tecan
Reader GENios	Tecan

2.1.1.8 Waagen

KERN 440-33N	Kern & Sohn GmbH
KERN AEJ 120-4M	Kern & Sohn GmbH

2.1.1.9 Geräte und Materialien zur Dosierung von Flüssigkeiten

Accu-Jet Pro	Brand
BD Discardit II Spritzen	Becton Dickinson SA
BD Eclipse Needle 20G	Becton Dickinson SA
BD Plastipak 1 ml	Becton Dickinson SA
Biosphere Filter Tips	Sarstedt
Pipettierhilfe Macro	Brand
Mikroliterpipetten Research Plus	Eppendorf
Multipette M4	Eppendorf
Pasteur Pipette 3 ml	Biosigma
Serologische Pipetten Cellstar	Greiner bio-one

2.1.1.10 Reaktionsgefäße

Reaktionsgefäße 5 ml, PP	Nerbe plus
Cellstar Tubes 15 ml / 50 ml	Greiner bio-one
SafeSeal Gefäße 1,5 ml / 2 ml	Sarstedt

2.1.1.11 Material zur Blutabnahme und Wundversorgung

Cutasept F Haut-Desinfiziens	BODE Chemie
Gazin Mullkompresse	Lohmann und Rauscher
Leukomed Wundverband	BSN medical
Multi-Adapter	Sarstedt
S-Monovette® 2,7 ml	Sarstedt
S-Monovette® 2,7 ml K3E	Sarstedt
S-Monovette® 7,5 ml Z	Sarstedt
S-Monovette® 9 ml AH	Sarstedt
S-Monovette® 9 ml K3E	Sarstedt
Venenstaubinde	Megro
Venofix Safety 19G	B. Braun Melsungen AG

2.1.1.12 Material für mikrobiologische Arbeiten und die Zellkultur

Cell Scraper, 16 cm	Sarstedt
Cell Strainer 40 µm Nylon	Falcon
Cellstar Cell culture flasks, 250 ml	Greiner
Costar Transwell® Permeable Supports 6.5 mm Insert, 24 Well Plate, 3.0 µm Polyester Membrane, Tissue Culture Treated, Polystyrene	Corning

Dialysekanüle Plume-S A17L15SG	Plume
Falcon 6-/24-/96-well Clear Flat Bottom TC-treated Multiwell Cell Culture Plates	Falcon
Filtropur S 0,2	Sarstedt
Filtropur S 0,45	Sarstedt
Hypodermic Needle-Pro Needle 23G	B. Braun Melsungen AG
LS Columns	Miltenyi Biotec
MACS Multistand	Miltenyi Biotec
Sterican Mix Halbstumpf, G 18	B. Braun Melsungen AG
Wattestäbchen steril	Applimed SA
Zählkammer Neubauer Improved	Assistent
Zählkammer Neubauer Improved	Marienfeld

2.1.1.13 Geräte und Materialien für die Durchflusszytometrie

5 ml Polystyrene Round-Bottom Tubes	Falcon
BD FACSCalibur	Becton Dickinson
CytoFLEX	Beckmann Coulter

2.1.1.14 Geräte zum Arbeiten mit Nukleinsäuren

Mastercycler epgradient	Eppendorf
Nanodrop ND-1000 Spectrophotometer	Peqlab Biotechnologie GmbH
Step One Plus Real-Time PCR System	Applied Biosystems

2.1.1.15 Geräte und Materialien zur Herstellung nuklearmedizinischer *Tracer*

^{68}Ge/^{68}Ga-Generator	Eckert & Ziegler
^{99}Mo/^{99m}Tc-Generator	Curium
HPLC	Scintomics
ITLC-SG Streifen	Varian
mini-GITA®	Raytest
Nucleosil 100-5 C18 Säule	Macherey-Nagel
TLC-SG Streifen SGI0001	Agilent

2.1.1.16 Geräte und Materialien zur Detektion radioaktiver Strahlung

2480 WIZARD2 Automatic Gamma Counter	PerkinElmer
CR-35 BIO Reader	Dürr Medical
Phosphor Imaging Plate	Dürr Medical
Szintillationsfläschchen	Hartenstein

2.1.2 Reagenzien

2.1.2.1 Reagenzien für mikrobiologische Arbeiten

Bierwürz-Agarplatten	IHM Würzburg
Penicillin-Streptomycin (10.000 U/ml Penicillin und 10 mg/ml Streptomycin in 0.9% NaCl)	Sigma-Aldrich

2.1.2.2 Reagenzien und Kits für Arbeiten mit Proteinen

Aqua ad iniectabilia	B. Braun Melsungen AG
Aspergillus fumigatus Lysate	Miltenyi Biotec
Bead Tube Holder	Macherey-Nagel
Bovines Serumalbumin (BSA)	Sigma-Aldrich
DC Protein Assay Kit	Bio-Rad
HCYTOMAG Milliplex Kit	EMD Millipore
NucleoSpin Bead Tubes Type A	Macherey-Nagel
Pierce LAL Chromogenic Endotoxin Quantitation Kit	Thermo Scientific
Wasser für Injektionszwecke	Berlin-Chemie Menarini

2.1.2.3 Reagenzien für die PBMC-Isolation und -Kultur

Liposomales Amphotericin B (AmBisome® 50 mg Pulver)	Gilead
Anti-CD28 pure – functional grade, human	Miltenyi Biotec
Anti-CD40 pure – functional grade, human	Miltenyi Biotec
Anti-CD49d pure, human	Miltenyi Biotec
Biocoll Separating Solution (1,077 g/ml)	Biochrom
CD14 MicroBeads, human	Miltenyi Biotec
Ciclosporin A (Sandimmun® 50 mg/ml Konzentrat)	Novartis
CPI Positive Control Solution	CTL Europe
EDTA salt solution	Sigma-Aldrich

Fötales Kälberserum (FCS)	Sigma-Aldrich
Hanks‘ buffered salt solution (HBSS)	Sigma-Aldrich
Human GM-CSF, premium grade	Miltenyi Biotec
Human IL-1β (ELISA MAX™ Deluxe Kit Standard)	BioLegend
Human IL-4, premium grade	Miltenyi Biotec
PepTivator CMV IE-1 – premium grade, human	Miltenyi Biotec
PepTivator CMV pp65 – premium grade, human	Miltenyi Biotec
PHA	Lophius Biosciences
Posaconazol (Noxafil® 300 mg Konzentrat)	MSD
Prednisolon-21-hydrogensuccinat (Prednisolut 250 mg Pulver)	mibe
Purified anti-human HLA-DR, DP, DQ Antibody	BioLegend
Refobacin 80 mg Injektionslösung Gentamicin	MerckSerono
RPMI-Medium 1640 + GlutaMAX™	Gibco
TNF-α (ELISA MAX™ Deluxe Kit Standard)	BioLegend
Trypanblau	Fluka
Voriconazol (Vfend® 200 mg Pulver)	Pfizer

2.1.2.4 Reagenzien und Kits für Immunfluoreszenzfärbungen

7-AAD Staining Solution	Miltenyi Biotec
Anti-CD4-FITC, human	Miltenyi Biotec
Anti-CD4-VioGreen(TM), human	Miltenyi Biotec
Anti-CD4-VIT4-FITC, human	Miltenyi Biotec
Anti-CD8-PerCP, human	Miltenyi Biotec
Anti-CD8-PerCP-Vio® 700, human	Miltenyi Biotec
Anti-CD45RA-APC-Vio® 770, human	Miltenyi Biotec
Anti-CD45RO-PerCP, human	Miltenyi Biotec
Anti-CD69-VioBlue®, human	Miltenyi Biotec
Anti-CD154-APC, human	Miltenyi Biotec
Anti-CD154-PE-Vio® 770, human	Miltenyi Biotec
Anti-CD197 (CCR7)-FITC, human	Miltenyi Biotec
Anti-CD197 (CCR7)-PE, human	Miltenyi Biotec
Anti-IFN-g-APC, human	Miltenyi Biotec
Anti-IFN-g-PE, human	Miltenyi Biotec
Anti-IL-2-PE, human	Miltenyi Biotec
Anti-TNF-a-PE, human	Miltenyi Biotec
Brefeldin A	Sigma-Aldrich
Erythrocyte lysis buffer	Qiagen
Inside Stain Kit	Miltenyi Biotec

2.1.2.5 Reagenzien für die Durchflusszytometrie

Contrad 70	Beckmann Coulter
CytoFLEX Sheath Fluid	Beckmann Coulter
FACS Clean	Becton Dickinson
FACS Flow	Becton Dickinson
FACS Rinse	Becton Dickinson
FlowClean Cleaning Agent	Beckmann Coulter

2.1.2.6 Reagenzien für Endothel- und Epithelzellkulturen und das *Transwell*®-Modell

3-Hydroxybutyric acid	Sigma-Aldrich
Dextranblau 5 kDa	Sigma
Dextranblau 20 kDa	Sigma
Dextranblau 70 kDa	Sigma
D-(+)-Glucose	Sigma
Dimethylsulfoxid (DMSO) – Lösung Ph.Eur.	Apotheke des Universitätsklinikums Würzburg
EBM-2 Endothelial Cell Growth Basal Medium 2	Lonza
EGM-2 Endothelial SingleQuots Kit	Lonza
Gefitinib	ChemCruz
Isotone Natriumchloridlösung 0,9 % Braun Injektionslösung	B. Braun Melsungen AG

2.1.2.7 Reagenzien und Kits für Arbeiten mit Nukleinsäuren

Ethanol	Sigma-Aldrich
High Capacity cDNA Reverse Transcription Kit	Applied Biosystems
iTaq Universal SYBR Green Supermix	Bio-Rad
Nukleasefreies Wasser	Qiagen
RNAprotect Cell Reagent	Qiagen
RNeasy Mini Kit	Qiagen

2.1.2.8 Oligonukleotide für die quantitative Echtzeit-PCR

Gen	Bezeichnung	Sequenz (5‘ – 3‘)
Alas1 (Referenz-Gen)	Alas1fw1	GGCAGCACAGATGAATCAGA
	Alas1rv1	CCTCCATCGGTTTTCACACT
Cas3	Cas3fw1	CTCTGGTTTTCGGTGGGTGT
	Cas3rv1	TCCAGAGTCCATTGATTCGCT
Cas9	Cas9fw1	CAGGCCCCATATGATCGAGG
	Cas9rv1	TCGACAACTTTGCTGCTTGC
CCL2	CCL2fw1	CCCCAGTCACCTGCTGTTAT
	CCL2rv1	AGATCTCCTTGGCCACAATG
CCL5	CCL5fw1	TCATTGCTACTGCCCTCTGC
	CCL5rv1	TACTCCTTGATGTGGGCACG
ICAM-1	ICAM1fw1	ACCCCGTTGCCTAAAAAGGA
	ICAM1rv1	AGGGTAAGGTTCTTGCCCAC
IL-6	IL6fw1	AAAGAGGCACTGGCAGAGAAAAC
	IL6rv1	AAAGCTGCGCAGAATGAGATG

IL-8	IL8fw1	AAGAAACCACCGGAAGGAAC
	IL8rv1	ACTCCTTGGCAAAACTGCAC

Bezugsquelle: Sigma-Aldrich

2.1.2.9 Reagenzien für die Herstellung nuklearmedizinischer *Tracer*

Acetonitril	Sigma-Aldrich
Ammoniumacetat	Sigma-Aldrich
Amphotericin B European Pharmacopoeia (EP) Reference Standard	Sigma-Aldrich
Essigsäure 0,1 M	Merck
Methanol	Carl Roth
Natriumchlorid (0.9 %)	B. Braun Melsungen AG
Natriumacetat	Merck
Phosphate Buffered Saline	B. Braun Melsungen AG
Salzsäure 0,1 N	Merck
Trifluoressigsäure	Sigma-Aldrich
Wasser ad injectabilia	B. Braun Melsungen AG
Zinn(II)chloride dihydrate	Sigma-Aldrich

2.1.3 Pathogene

Spezies	CBS-Nummer	ATCC-Nummer	IHM-Nummer
Aspergillus fumigatus	-	46645	-
Aspergillus niger	553.65	-	B016
Aspergillus terreus	594.65	-	B022
Cunninghamella bertholletiae	187.84	-	B046
Fusarium solani	181.29	-	B70
Mucor circinelloides	192.68	-	B091B
Rhizomucor pusillus	245.58	-	B148
Rhizopus arrhizus	110.17	-	B149
Staphylococcus aureus	-	-	Klinisches Isolat

2.1.4 Software

AIDA Image Data Analyzing Software	Raytest
BD CellQuest Pro Version 0.3.9f7B	Becton Dickinson
CytExpert 1.2	Beckmann Coulter
FLOWJO Single Cell Analysis Software V10.6.1	FlowJo, LLC
FLOWJO Single Cell Analysis Software V10 vX.0.7	FlowJo, LLC
i-Control 1.12	Tecan
Microsoft Office 2010	Microsoft
ND-1000 V3.1.0	Peqlab Biotechnologie GmbH
P Value from Pearson (R) Calculator	Social Science Statistics
Statistical software package R (Version	R Project

3.2.2)	
Step One Software v 2.2.2	Applied Biosystems
Wilcoxon-Mann-Whitney Test Calculator	Saarland University
WIZARD2	PerkinElmer
xPONENT 3	Luminex Corporation

2.2 Methoden

2.2.1 Kultur von Schimmelpilzen

Aus Sporensuspensionen oder Glycerolstocks wurden mithilfe steriler Watteträger Sporen entnommen und auf Bierwürz-Agarplatten ausgestrichen. Die Ernte der Pilze wurde vorgenommen, sobald die Agarplatten konfluent bewachsen waren. Die hierfür benötigten Inkubationszeiten sind in Tab. 2.1 zusammengefasst.

Spezies	Temperatur	Inkubationszeit [Tage]
Aspergillus fumigatus	35 °C	2,5 – 4
Aspergillus niger	35 °C	4 – 6
Aspergillus terreus	35 °C	4 – 6
Cunninghamella bertholletiae	35 °C	4 – 6
Fusarium solani	21 °C	6 – 8
Mucor circinelloides	21 °C	6 – 8
Rhizomucor pusillus	35 °C	4 – 6
Rhizopus arrhizus	35 °C	6 – 8

Tab. 2.1 Kulturbedingungen der verwendeten Schimmelpilz-Spezies

Die Ernte der Sporen von den Agarplatten wurde mittels eines feuchten, sterilen Watteträgers durchgeführt. Konfluent bewachsene Platten wurden während der Aufnahme der Sporen mit Wasser überschichtet. Die abgenommenen Sporen wurden in 50 ml sterilem Wasser suspendiert, Hyphenmaterial wurde anschließend

mithilfe eines 40 µm Zellfilters abgetrennt. 10 µl einer 1:50 Verdünnung der jeweiligen Suspension wurde zur Bestimmung der Zellzahlen in eine Neubauer-Zählkammer verbracht.

Zur Anzucht von Hyphen wurden 1 x 10^8 Sporen in 20 ml RPMI 1640 Medium (+ GlutaMAX™, Gibco) gegeben und bei 37 °C unter Schütteln (200 rpm) und Luftzufuhr inkubiert. Im Falle von *R. pusillus* wurde dem Medium 10 % FCS zugesetzt. Das Wachstum der Hyphen wurde visuell und mikroskopisch überprüft.

Die Bestimmung minimaler Hemmkonzentrationen (MIC) gegenüber AMB der genannten Pilze wurde gemäß den Richtlinien des *European Committee on Antimicrobial Susceptibility Testing* (EUCAST) durchgeführt. Hierfür wurde eine Verdünnungsreihe in RPMI + 2 % Glucose angesetzt, wobei das Spektrum der Konzentrationen von 0.0625 mg/l bis 32 mg/l AMB reichte (Verdünnungsfaktor 2). In einer 96-*Well*-Platte wurden zu je 100 µl der AMB-Verdünnungen 5 x 10^4 Pilzsporen gegeben und bei 35 °C inkubiert. Proben ohne Zugabe von AMB dienten als Wachstumskontrollen, während Proben ohne Sporen als Sterilitätskontrollen fungierten. Das Wachstum der Pilze wurde nach 24 h und 48 h überprüft.

2.2.2 Herstellung von Schimmelpilz-Lysaten und Lysatprozessierung

Wie in 2.2.1 beschrieben kultivierte Hyphensuspensionen wurden bei 5000 g für 10 min zentrifugiert. Der Überstand wurde abgenommen und die Hyphen aus mehreren Gefäßen in *Hank's buffered salt solution* (HBSS) suspendiert und mehrfach durch eine 17 G Kanüle (Plume) passiert. Die Suspension wurde erneut bei 5000 g für 10 min zentrifugiert, der Überstand entfernt und die trockenen Hyphen gewogen. Durch Zugabe von HBSS wurde die Suspension auf 228 mg/ml eingestellt.

Je 350 µl dieser Suspension (80 mg) wurden auf (im Fall von Hyphenlysaten mindestens drei) *NucleoSpin Bead Tubes Type A* (Macherey-Nagel) gegeben und unter Zuhilfenahme eines *Bead Tube Holder*-Adapter (Macherey-Nagel) auf einem *Vortex-Genie 2* (Scientific Industries) für die in Tab. 2.2 angegebenen Zeiträume bei maximaler Geschwindigkeit lysiert. Sporenlysate wurden 1:5 mit HBSS verdünnt und durch einen Spritzenvorsatzfilter mit Porengröße 0,2 µm passiert. *A. fumigatus* Konidienlysate wurden nur 1:2 verdünnt. Die Lysate mehrerer *Bead Tubes* wurden im Fall von Hyphenlysaten in einer Spritze gesammelt und unverdünnt filtriert. Da für *A.*

fumigatus ein kommerziell erhältliches Hyphenlysat verfügbar war (Miltenyi Biotec), wurde von einer Herstellung nach diesem Protokoll abgesehen.

	A. fumigatus	*R. arrhizus*	*R. pusillus*	*C. bertholletiae*
Sporen	5 min	2 min	5 min	5 min
Hyphen	-	2 min	2 min	1 min

Tab. 2.2 Zeiträume des *Bead Beatings* für optimale Proteinkonzentrationen des erhaltenen Lysats unter Verwendung von *Bead Tubes Type A*.

Die Proteinkonzentration der Lysate wurden mithilfe des *DC Protein Assay Kits* (Bio-Rad) nach Angaben des Herstellers ermittelt. Die Absorption der Proben wurde in Duplikaten bei einer Wellenlänge von 750 nm gemessen. Zur Erstellung der Standardreihe wurden Konzentrationen von 0,125 mg bis 8 mg bovinen Serumalbumins (BSA) verwendet. Mithilfe des *Pierce LAL Chromogenic Endotoxin Quantitation Kit* (Thermo Scientific) wurde nach Angaben des Herstellers verifiziert, dass der Endotoxin-Gehalt des so erhaltenen Lysats unter 0,1 EU/ml lag.

2.2.3 Rekrutierung und Erstellung von Expositionsprofilen freiwilliger gesunder Blutspender

Die in diese Studie eingeschlossenen freiwilligen Spender waren zwischen 18 und 75 Jahren alt und unterzeichneten eine schriftliche Einverständniserklärung. Die Kennzeichen der positiven Ethikvoten der Ethikkomission der Julius-Maximilians-Universität Würzburg waren 105/15 und 42/17.

Die Erfüllung eines der folgenden Kriterien führte bei gesunden Probanden zum Ausschluss aus der Studie:

- Schwangerschaft oder stillende Mütter
- Einnahme von Immunsuppressiva oder Immunmodulatoren in den letzten 12 Wochen
- Vakzinierung oder Einnahme von Antiinfektiva in den letzten 4 Wochen
- Akute oder chronische Infektionserkrankung
- Insulinpflichtiger Diabetes mellitus
- Bereits an derselben Versuchsserie dieser Studie teilgenommen

- Vulnerable Personengruppe

Zur Erstellung individueller Expositionsprofile wurden anhand eines Fragebogens mit Schimmelpilzexposition assoziierte Faktoren im beruflichen und Wohnumfeld der Probanden ermittelt. Die Expositionsfaktor-Kategorien sind in Tab. 2.3 dargestellt (nach Wurster et al., 2017b).

Expositionsfaktor-Kategorie	Expositionsfaktoren (eine Kategorie wurde als positiv angesehen, wenn ein Proband mindestens einen Faktor aufweist)
Langzeitexposition	• Leben in ruralem Wohnort mit weniger als 2000 Einwohnern oder in einer Kleinstadt mit weniger als 20000 Einwohnern bei gleichzeitig landwirtschaftlichen Betrieben / Nutzflächen (inkl. Weinbau) bzw. holzverarbeitender Industrie im Umkreis von 1 km für mindestens 5 Jahre • Exposition im beruflichen Umfeld für mindestens 5 Jahre
Exposition im beruflichen Umfeld	• Intensiver Kontakt mit organischen Abfällen • Intensiver Kontakt mit landwirtschaftlichen Rohstoffen • Verarbeitung von Holz oder Holzprodukten • Sanierungs- bzw. Renovierungsarbeiten in Altbauten • Längerer Aufenthalt in Schimmel-belasteten Räumen inkl. Büroräumen • Intensiver Umgang mit Pflanzen, inkl. Topfpflanzen und Hydrokultur • Umgang mit Klimaanlagen, Abluftanlagen oder Kühltechnik • Sonstige Arbeiten, bei denen intensiver Umgang mit Schimmelpilzen bestanden haben könnte (nach Angabe des Probanden)
Exposition im Wohnungsumfeld	• ruraler Wohnort mit weniger als 2000 Einwohnern • landwirtschaftliche Betriebe / Nutzflächen (inkl. Weinbau) bzw. holzverarbeitende Industrie im Umkreis von 1 km
Exposition innerhalb des Wohnumfelds	• Eigener Nutzgarten • Teichanlage, Wasserlauf oder ähnliche Anlagen im Gartenbereich • Zimmerspringbrunnen oder Aquarium • Topfpflanzen inkl. Hydrokultur im Wohn- oder Schlafbereich • Haltung von Haustieren (jeglicher Art) • Intensive Nutzung von Kellerräumen z. B. als Lagerräume • Bekannte Schimmelpilzbelastung in der Wohnung oder dem Wohngebäude

Tab. 2.3 Kriterien, die mit Schimmelpilzexposition assoziiert sind (nach Wurster et al., 2017b)

Ein Spender wurde als hoch exponierter Proband eingestuft, wenn er entweder mindestens einen Langzeit- und einen aktuellen Expositionsfaktor-Kategorie aufwies oder positiv für mindestens 3 der Expositionsfaktorkategorien war. Bei geringerer Exposition wurde die Einstufung „gering exponiert“ vorgenommen (Wurster et al., 2017b).

2.2.4 Blutentnahme

Die Einstichstelle wurde vor der Blutentnahme aus einer Kubitalvene zweimal unter Beachtung einer Einwirkzeit von 30 Sekunden desinfiziert. Über *Venofix Safety* 19G Kanülen wurden je nach Versuchsaufbau S-Monovetten® (Sarstedt) befüllt, die mit einem der Gerinnungshemmer EDTA bzw. NH_4-Heparin oder einem Gerinnungsaktivator zur Serumgewinnung befüllt waren.

2.2.5 Gewinnung von autologem Serum aus Spenderblut

Die mit Vollblut befüllten Serum-Monovetten® (Sarstedt) mit Gerinnungsaktivator wurden bei 3000 g für 7 min zentrifugiert. Das Serum wurde abgenommen und mithilfe eines 0,2 µm Spritzenvorsatzfilters sterilisiert. Aliquots zu 1 ml wurden in 1,5 ml Reaktionsgefäße überführt und 30 min bei 56 °C inkubiert, um das Komplementsystem zu inaktivieren.

2.2.6 PBMC-Isolation und Stimulation

Zur Isolation von PBMC wurde EDTA-Vollblut verwendet. 5 ml Ficoll-Lösung wurden in 15 ml Zentrifugenröhrchen vorgelegt, welche mit jeweils 7,5 ml Vollblut überschichtet wurden. Die Röhrchen wurden für 25 min bei 2000 rpm mit verringerter Beschleunigung und Bremse zentrifugiert (5 Acc / 5 Dec der Heraeus Megafuge 16 von Thermo Scientific, gültig für alle Zentrifugationsschritte der PBMC Isolationen). Die resultierenden Interphasen wurden mit einer Pasteurpipette abgenommen und in einem 50 ml Zentrifugenröhrchen gesammelt. Nach Auffüllen der Zentrifugenröhrchen auf 50 ml mit HBSS-Puffer wurde die Suspension für 15 min bei 900 rpm zentrifugiert. Dieser Waschschritt wurde anschließend einmal wiederholt.

Die Zellen wurden schließlich in 1 ml RPMI 1640 + 5 % autologem Serum aufgenommen. 10 µl der Suspension wurden mit 40 µl RPMI 1640 und 50 µl Trypanblau versetzt und die Zellzahl und Zellviabilität mittels einer Neubauer-Zählkammer mikroskopisch bestimmt. Sollte der Einfluss immunsuppressiver oder antimykotischer Medikation auf den Test überprüft werden, wurde dem experimentellen Ablauf an dieser Stelle die Inkubation mit klinisch relevanten Konzentrationen der entsprechenden Pharmaka hinzugefügt (siehe Kap. 2.2.8).

Die Suspension wurde auf eine Zielkonzentration von 1 x 10^7 Zellen/ml mit RPMI 1640 + 5 % autologem Serum verdünnt. 1 x 10^6 Zellen wurden je Vertiefung einer 96-*Well*-Platte ausplattiert (Reaktionsvolumen 100 µl) und bei 37 °C / 5 % CO_2 inkubiert.

Die Stimulation wurde 1 h nach Beginn der Inkubation vorgenommen. Während dieser 1-stündigen Ruheperiode wurde ggf. 10 µg/ml eines MHC II-blockierenden Antikörpers zugegeben (α-HLA-DR, -DP, -DQ, BioLegend). Während der Stimulation wurde zunächst 1 µg/ml α-CD28 als kostimulierender Faktor zu allen Konditionen gegeben, ggf. zusätzlich 1 µg/ml α-CD49d. Anschließend wurden die jeweiligen Stimuli hinzugefügt, wobei es sich um Pilzlysate (50 µg/ml) bzw. die CMV-Antigen-Peptid-Mischungen pp65 (Phosphoprotein 65, Miltenyi Biotec, 1 µg/Peptid/ml) und IE-1 (*Immediate Early*-Protein 1, Miltenyi Biotec, 1 µg/Peptid/ml) handelte. Als Positivkontrollen dienten Phytohämagglutinin (PHA, 4 µg/ml) oder eine Antigenmischung von Cytomegalovirus, Parainfluenzavirus und Influenzavirus (CPI, 50 µg/ml).

Hieran schloss sich eine Inkubationsperiode von insgesamt 18 bis 20 h bei 37 °C / 5 % CO_2 an. Während dieser Inkubationsperiode wurde 2 h nach Stimulation der PBMC 10 µg/ml Brefeldin A zu den Proben gegeben, welche später einer durchflusszytometrischen Analyse zugeführt werden sollten (Kap. 2.2.7). Proben, die einer Analyse über Multiplex-Zytokin-*Assays* zugeführt werden sollten (Kap. 2.2.11), wurden 120 h ohne Brefeldin A stimuliert. Der experimentelle Ablauf ist schematisch in Abb. 2.1 dargestellt.

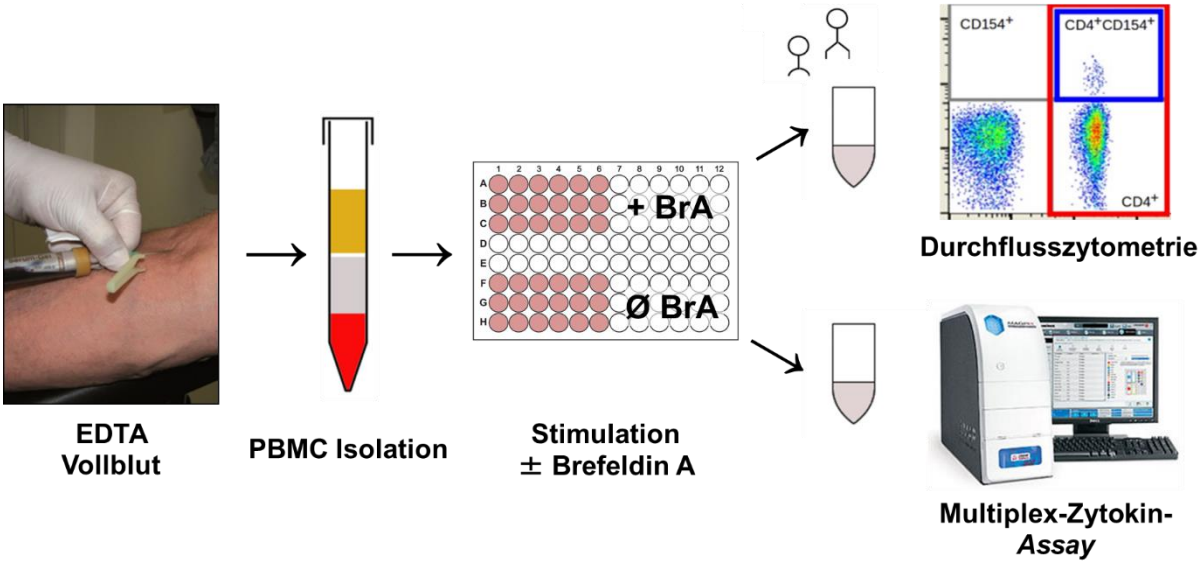

Abb. 2.1 Schematischer Ablauf der Isolation und anschließenden Stimulation von PBMC-Proben gesunder Probanden. Die Isolation erfolgte mittels Ficoll-Gradientenzentrifugation. Die Zellen wurden in RPMI 1640 + 5 % autologem Serum aufgenommen und auf eine Konzentration von 1 x 10^7 /ml eingestellt. Nach Inkubation für 1 h bei 37 °C wurden die Proben wie in Kap. 2.2.6 beschrieben stimuliert. Sollten die Proben durchflusszytometrisch analysiert werden, wurde 2 h nach Beginn der Stimulation 10 µg/ml Brefeldin A zugegeben und nach weiteren 18 h Inkubation die Zellen geerntet und wie in Kap. 2.2.7 beschrieben gefärbt. Sollten Zytokinkonzentrationen aus den Überständen bestimmt werden, wurden die stimulierten Proben 120 h ohne Brefeldin A inkubiert und nach Kap. 2.2.11 weiterverarbeitet. Entnommen und übersetzt aus der Posterpräsentation von Wurster et al., 2017, *European Congress of Clinical Microbiology and Infectious Diseases*, Wien, Österreich.

2.2.7 Immunfluoreszenzfärbung von PBMC

Die Überstände der Zellkulturen wurden in 2 ml Reaktionsgefäße überführt. Die Zellen wurden vorsichtig mit einer 1000 µl Pipettenspitze aus den Vertiefungen gelöst, in 200 µl Waschpuffer (HBSS + 0,5 % autologes Serum) aufgenommen und mit den zugehörigen Überständen vereint. Die Zentrifugation wurde für 5 min bei 400 g und 4 °C vollzogen, analog zu allen folgenden Zentrifugationsschritten des Färbeprozesses. Die Antikörper-Lösungen wurden nach vorhergehendem Titrationsprozess in der Hälfte der in den Herstellerangaben definierten Konzentrationen angesetzt. Je Probe wurden 100 µl Waschpuffer mit α-CD4-FITC und ggf. zusätzlich mit α-CD8-PerCP oder α-CCR7-PE und α-CD45RO-PerCP angesetzt. Für einzelne Experimente wurde stattdessen α-CD4-VioGreen(TM), α-CD197 (CCR7)-FITC, α-CD45RA-APC-Vio® 770 und α-CD69-VioBlue® für die Oberflächenfärbung verwendet, sowie nach Herstellerangaben 7-AAD *Staining Solution* (Vitalitätsfärbung mit 7-Amino-Actinomycin D, Miltenyi Biotec). Die Proben

wurden in 95 µl der Antikörperlösung resuspendiert und 20 min bei Raumtemperatur inkubiert. Alle Inkubationsschritte wurden im Dunkeln durchgeführt. Nach Zugabe von 1 ml Waschpuffer wurden die Proben zentrifugiert und die Überstände verworfen. Die Zellen wurden in 400 µl Fixierlösung resuspendiert (1:1 HBSS-Puffer und *Inside Fix*) und 20 min bei Raumtemperatur inkubiert. Nach erneuter Zentrifugation und Verwerfen des Überstands wurden die Proben in je 95 µl Zweit-Antikörper-Lösung resuspendiert, für die je Probe 100 µl *Inside-Perm* mit α-CD154-APC und ggf. zusätzlich α-IFN-γ-PE oder α-TNF-α-PE angesetzt wurden. Für einzelne Experimente wurden für die intrazelluläre Färbung stattdessen α-IL-2-PE, α-IFN-γ-APC und α-CD154-PE-Vio® 770 verwendet. Die Inkubation erfolgte für 10 min bei Raumtemperatur. Anschließend wurden 750 µl *Inside-Perm* zu den Proben gegeben, diese zentrifugiert und die Überstände verworfen. Abschließend wurden die Proben in 200 µl HBSS-Puffer aufgenommen und in 5 ml Polystyrol-Röhrchen überführt.

2.2.8 Behandlung von PBMC mit Antimykotika und Immunsuppressiva

Die PBMC wurden nach der Isolation mit RPMI 1640 + 5 % autologem Serum auf eine Konzentration von 5 x 10^6 /ml verdünnt und in 6-*Well*-Platten für 3 h bei 37 °C, 5 % CO_2 mit Pharmaka in den folgenden Konzentrationen inkubiert: 50 µg/ml liposomales Amphotericin B (LAMB), 5 µg/ml Voriconazol (VRC), 4 µg/ml Posaconazol (PCZ), 200 ng/ml Ciclosporin A (CsA) oder 200 ng/ml Prednisolon (Pred). Die Zellen wurden anschließend mit einer 1000 µl Pipettenspitze von der Platte gelöst, bei 400 g für 10 min zentrifugiert, in 1 ml RPMI 1640 + 5 % autologem Serum aufgenommen und einer erneuten Zellzählung unterzogen, bevor sie wie in Kap. 2.2.6 und 2.2.7 beschrieben weiterverarbeitet wurden. Die unbehandelten Referenzproben wurden mit Ausnahme der Zugabe der Pharmaka identisch behandelt, um einem möglichen Einfluss der zusätzlichen Arbeitsschritte und der prolongierten Bearbeitungsdauer auf die Zellfunktionalität Rechnung zu tragen.

Bei einzelnen Experimenten wurde EDTA-Vollblut vor der PBMC-Isolation mit den oben genannten Konzentrationen von CsA oder Prednisolon versetzt und für 2 h bei 37 °C inkubiert. Die darauffolgende PBMC-Isolation und Stimulation erfolgte wie in Kap. 2.2.6-7 beschrieben.

2.2.9 Stimulation und Immunfluoreszenzfärbung von Vollblut-Proben

Für jede zu testende Kondition wurden nach dem von Weis et al. (2019) beschriebenen Protokoll Stimulantien in neutrale 2,7 ml Monovetten® (Sarstedt, ohne Antikoagulans) vorgelegt und diese bei -20 °C für einen Zeitraum von maximal 4 Wochen kryopräserviert. Alle nachfolgenden Konzentrationsangaben beziehen sich auf ein finales Reaktionsvolumen von 500 µl. Mit Ausnahme der Positivkontrolle PHA (4 µg/ml) wurden als kostimulatorische Faktoren je 1 µg/ml α-CD28 Antikörper und α-CD49d Antikörper zu jeder Probe vorgelegt. Monovetten® zur Quantifizierung Antigen-spezifischer T-Zellen wurden mit 50 µg/ml des jeweiligen Pilzlysats oder pp65 und IE-1 (Miltenyi Biotec, je 1 µg/Peptid/ml befüllt. Um das Probenvolumen zu normieren, wurden die Ansätze mit RPMI 1640 auf insgesamt 50 µl aufgefüllt.

Mithilfe einer Insulinspritze wurden je 500 µl heparinisiertes Vollblut in die wie beschrieben präparierten 2,7 ml Monovetten® (Sarstedt) injiziert, welche vorher auf Raumtemperatur gebracht wurden. Ggf. wurde dem entnommenen Vollblut vor der Injektion in die 2,7 ml Monovetten® LAMB, VRC, PCZ, CsA oder Prednisolon in den unter 2.2.6 genannten Konzentrationen zugesetzt. Bei einzelnen Experimenten wurde das Blut nach Zugabe von CsA oder Prednisolon zunächst 2 h bei 37 °C inkubiert und anschließend in die Monovetten® injiziert. 4 h nach Stimulation und Inkubation bei 37 °C wurde 10 µg/ml Brefeldin A zu den Zellen gegeben, wonach die Proben für weitere 16 bis 18 h bei 37 °C inkubiert wurden.

Nach Ende der Inkubationszeit wurden 0,5 ml einer 0,5 M EDTA-Lösung zu den Proben gegeben und für 15 min bei Raumtemperatur inkubiert. Die Proben wurden in 15 ml Zentrifugenröhrchen überführt, wobei die Monovette® mit 1 ml Erythrolyse-Puffer gespült wurde, um etwaige Probenrückstände nicht zu verlieren. Nach Zentrifugation bei 600 g für 7 min wurde der Überstand dekantiert und die Proben in 3 ml Erythrolyse-Puffer resuspendiert. Die Inkubation erfolgte, bis die Blutproben optisch klar erschienen, höchstens jedoch für 6 min, um einer Schädigung der Leukozyten und Granulozyten-Aktivierung durch den Puffer vorzubeugen. Die Proben wurden erneut bei 600 g für 7 min zentrifugiert und nach Abnahme des Überstandes in je 1 ml HBSS resuspendiert und in 2 ml Reaktionsgefäße überführt. Die Antikörper-Färbung wurde analog Kap. 2.2.7 durchgeführt, mit dem Unterschied, dass die Antikörper nach Herstellerangaben und im Falle der Oberflächenfärbungen

in 100 µl HBSS angesetzt wurden. Der experimentelle Ablauf der Stimulation und Färbung von Vollblutproben ist schematisch in Abb. 2.2 dargestellt.

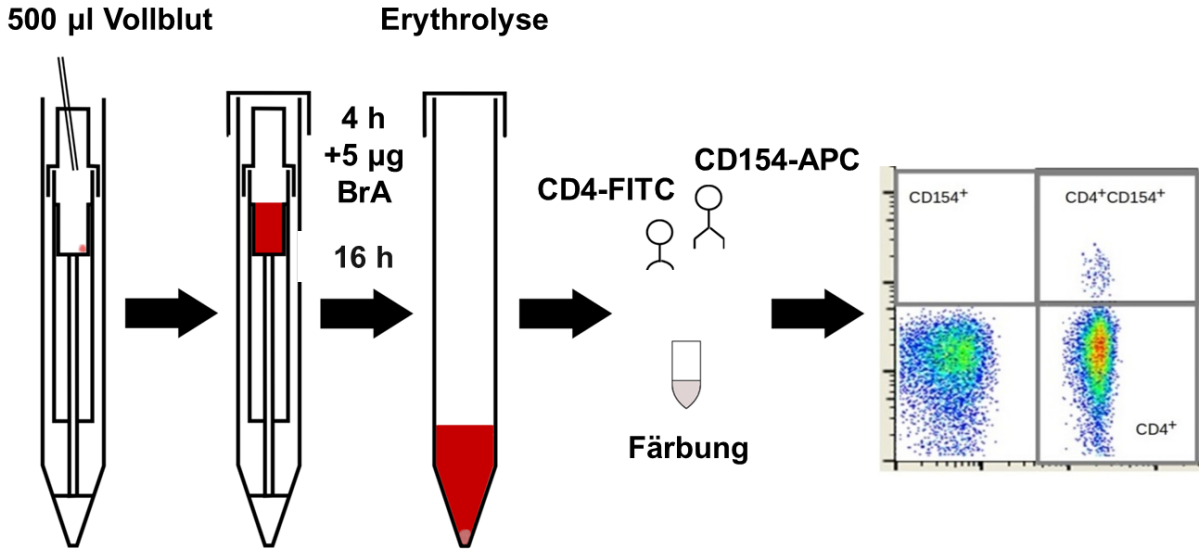

Abb. 2.2 Schematische Darstellung des Vollblut-basierten Protokolls zur Quantifizierung CD154+ Antigen-reaktiver T-Helfer-Zell-Frequenzen gemäß der in Kap. 2.2.9 bzw. 2.2.7 beschriebenen Methodik. Adaptiert aus Weis et al., 2019.

2.2.10 Durchflusszytometrie

Durchflusszytometrische Untersuchungen erfolgten mithilfe eines FACSCalibur Zytometers (Becton Dickinson) unter Verwendung der *BD Cell Quest Pro* Software. Die Lymphozyten-Fraktion wurde anhand von Größe (*FSC Height*) und Granularität (*SSC Height*) identifiziert und mit einem *Gate* markiert. Innerhalb des gesetzten *Gates* wurden je Probe 100000 Zellen akquiriert. Zur Analyse wurde die Software FlowJo V10 vX.0.7 verwendet. Die *Gating*-Strategie ist in Abb. 2.3 repräsentativ für PBMC-Proben an einem Beispiel aus Page et al., 2018 dargestellt.

Einzelne Experimente wurden an einem CytoFLEX Zytometer (Beckmann Coulter) mit der zugehörigen CytExpert Software durchgeführt. Diese wurden mit der Software FlowJo V10.6.1 analysiert.

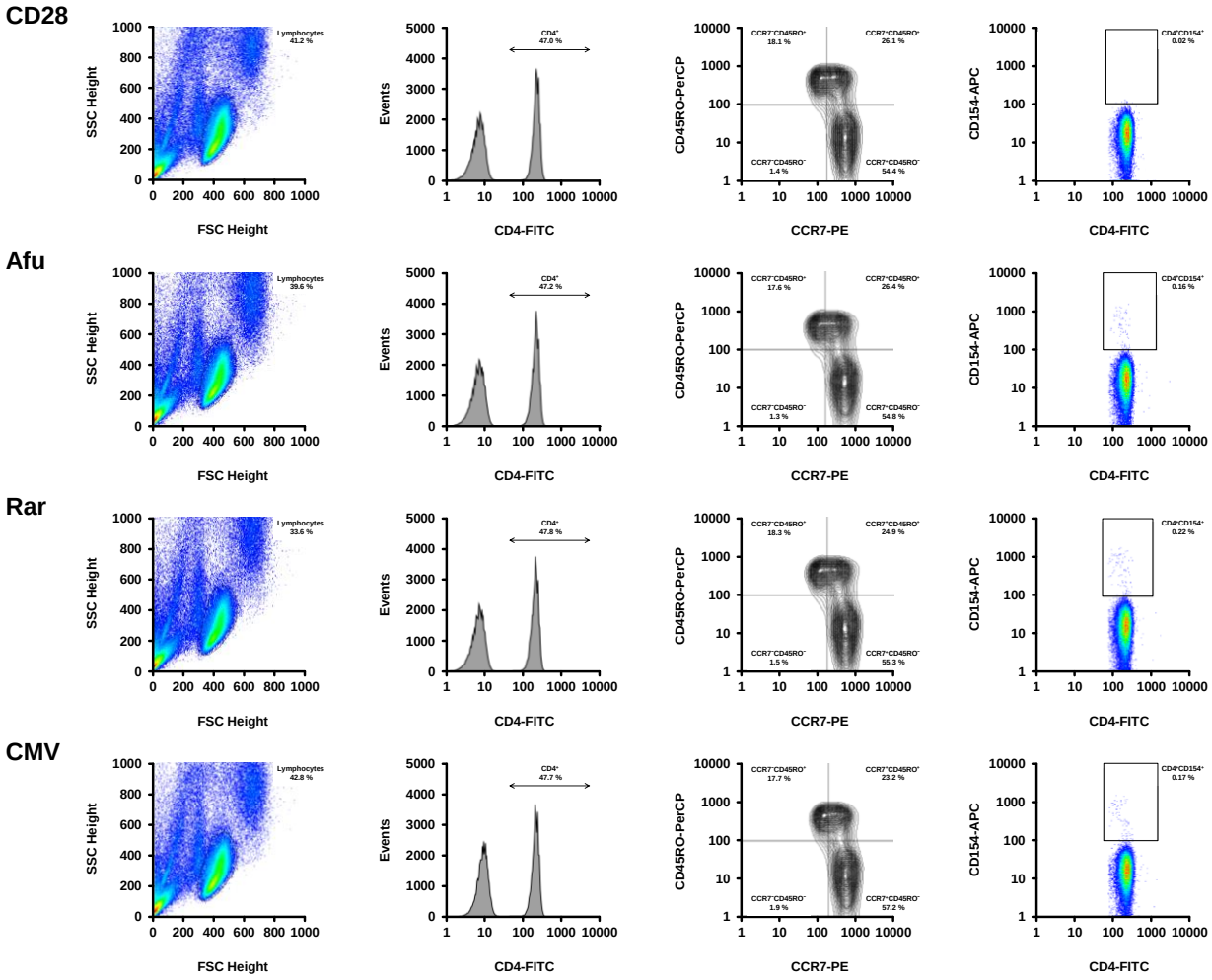

Abb. 2.3 *Gating*-Strategie zur Quantifizierung der CD154⁺ T-Helfer-Zellen und zur Bestimmung deren CCR7/CD45RO Phänotyp. Die Oberflächenfärbung wurde mit α-CD4-FITC, α-CCR7-PE und α-CD45RO-PerCP durchgeführt, mit α-CD154-APC wurden die Zellen intrazellulär gefärbt. 100000 Lymphozyten wurden je Messung anhand eines approximativ gesetzten FSC/SSC-*Gates* analysiert. Mittels FlowJo-Software wurde das *Gate* in der finalen Auswertung präzisiert (1. Spalte). CD4⁺ Zellen wurden innerhalb der Lymphozyten-Fraktionen anhand eines Histogramms detektiert (2. Spalte). Das CCR7/CD45RO-Quadranten-*Gate* wurde anhand eines 2 % Konturplots über den CD4⁺ Zellen gesetzt (3. Spalte). CD154⁺ wurden anhand eines CD4/CD154-Pseudocolor-Plots definiert (4. Spalte). Das zuvor in der CD4⁺ Zellfraktion gesetzte CCR7/CD45RO-*Gate* wurde abschließend auf die CD4⁺CD154⁺ Zellen angewandt. CD28 = unspezifische Kontrolle, enthielt zur Stimulation nur α-CD28, Afu = *A. fumigatus*, Rar = *R. arrhizus*, CMV = pp65 + IE-1. Entnommen und übersetzt aus Page et al., 2018.

2.2.11 Multiplex Zytokinanalysen

Von den wie oben beschrieben stimulierten PBMC-Proben wurde nach 120 h Inkubation (ohne Brefeldin A) der Überstand abgenommen und in 2 ml Reaktionsgefäße überführt. Nach einem Zentrifugationsschritt bei 7000 g, 5 min, 4 °C zur Abtrennung von kontaminierenden Zellen und Zellfragmenten wurden die Überstande bei -20 °C gelagert, bevor sie mittels eines 14-plex HCYTOMAG Milliplex Kits (EMD Millipore) nach Angaben des Herstellers analysiert wurden.

2.2.12 Generation dendritischer Zellen aus Monozyten

Zur Gewinnung der Monozyten wurden zunächst PBMC aus Leukozytenreduktionssystemen (LZRS) isoliert. Hierzu wurde die aus den LZRS erhaltene Zellsuspension mit HBSS + 1 % Fötales Kälberserum (FCS, Sigma-Aldrich) + 0,4 % EDTA ($HBSS^{++}$) auf 50 ml aufgefüllt und jeweils 25 ml der Suspension auf Ficoll überschichtet. Die Zentrifugation erfolgte bei 600 g in der Heraeus Megafuge für 25 min mit Acc/Dec 5. Nach Isolation der Interphase wurde diese mit $HBSS^{++}$ auf 50 ml aufgefüllt und für 15 min bei 120 g, Acc/Dec 5 zentrifugiert. Dieser Schritt wurde nach Dekantieren des Überstands einmal wiederholt, bevor die Zellen in 1 ml $HBSS^{++}$ aufgenommen wurden. Vor Bestimmung der Zellzahl und Vitalität über Trypanblau-Exklusion mithilfe einer Neubauer-Zählkammer analog zu 2.2.6 wurde eine Vorverdünnung der Zellsuspension von 1:25 in $HBSS^{++}$ vorgenommen. Anschließend wurde mit $HBSS^{++}$ eine Zielkonzentration von 3×10^8 /ml eingestellt.

1×10^8 PBMC wurden mit jeweils 60 µl CD14-*MicroBeads* (Miltenyi Biotec) versetzt und für 15 min bei 4 °C inkubiert. Nach Auffüllen auf 50 ml mit $HBSS^{++}$ wurde der Ansatz 10 min bei 400 g zentrifugiert, der Überstand entfernt, und die Zellen in 2 ml $HBSS^{++}$ aufgenommen.

Zur magnetischen Separation der $CD14^+$ Zellfraktion wurde eine LS-Säule in die zugehörige Magnetvorrichtung (MACS Multistand, Miltenyi Biotec) eingesetzt und mit 3 ml $HBSS^{++}$ äquilibriert, bevor die Zellsuspension auf die Säule pipettiert wurde. Die Säule wurde 3 x mit je 3 ml $HBSS^{++}$ gespült und die Durchläufe verworfen. Die so beladene LS-Säule wurde aus dem Magneten entfernt und auf ein 15 ml Zentrifugenröhrchen gestellt. 5 ml $HBSS^{++}$ wurden auf die Säule gegeben und die

$CD14^+$ Zellen schnell mit dem zugehörigen Stempel von der Säule eluiert. Die Zellzahl im Eluat wurde wie in 2.2.6 beschrieben bestimmt.

Nach Zentrifugation (400 g, 10 min) wurden die Zellen in moDC-Differenzierungsmedium (RPMI 1640 + 10 % FCS + 100 ng/ml GM-CSF + 20 ng/ml IL-4 + 100 µg/ml Gentamicin) auf 0,83 x 10^6 Zellen/ml eingestellt und je 3 ml der Suspension in je eine Vertiefung einer 6-*Well*-Platte gegeben. Die Zellen wurden zur moDC-Differenzierung für 6 Tage bei 37 °C kultiviert, wobei an jedem 2. Tag das Medium erneuert wurde. Hierfür wurde je Vertiefung 1 ml entnommen, 10 min bei 400 g zentrifugiert und die Zellen nach Resuspension in 1 ml frischem Medium wieder der Kultur zugeführt. Das verwendete frische Medium enthielt 300 ng/ml GM-CSF und 60 ng/ml IL-4. Zum Zeitpunkt der Ernte wurden die Zellen aller *Wells* desselben Spenders vereint, bei 400 g für 10 min zentrifugiert und in 1 ml EBM-2 + *EGM-2 SingleQuots* Medium (Lonza) + 10 % FCS resuspendiert (siehe 2.2.12.1). Die Zielkonzentration betrug 1 x 10^7 /ml.

2.2.13 Markierung von Amphotericin B mit ^{99m}Tc und ^{68}Ga

Radioaktive *Tracer* wurden in der Radiopharmazie der Klinik und Poliklinik für Nuklearmedizin des Universitätsklinikums Würzburg unter GMP-Bedingungen hergestellt. Die aus dem Strahlenschutzbereich überführten *Tracer*-Mengen wiesen stets Aktivitäten unterhalb der Freigrenze auf (^{99m}Tc < 10 MBq, ^{68}Ga < 1 MBq).

2.2.13.1 Herstellung und Qualitätskontrolle von ^{99m}Tc-Amphotericin B

Aus einer 0,5 mg/ml AMB-Lösung (in HBSS) wurden 100 µl (50 µg Amphotericin B, 54 nMol) in einem 2 ml-Reaktionsgefäß vorgelegt. Nach Zugabe von ^{99m}Tc-Pertechnetat (mit einer Aktivität von 1000 ± 100 MBq) in 200 ± 50 µl 0,9 % NaCl-Lösung, welches aus einem ^{99}Mo/^{99m}Tc-Generator eluiert wurde, wurden 20 µl Sn(II)-Lösung (10 mg $SnCl_2$-Dihydrat / ml 0,1 N HCl) hinzugefügt. Die Reduktion lief unter gelegentlichem Invertieren über einen Zeitraum von 20 min bei Raumtemperatur ab. Nach vollendeter Reaktion wurden 3 ml PBS (pH = 7,0) hinzugegeben. Die klare Lösung wurde anschließend in einer 5 ml-Spritze aufgezogen und mittels 0,2 µl Spritzenvorsatzfilter sterilfiltriert.

Die Reinheit des Produkts wurde mit Hilfe von zwei unterschiedlichen Dünnschichtchromatografie-Ansätzen (TLC) und einem Mini-GITA®-TLC-Scanner (Raytest) bestimmt (Tab. 2.4). Die radiochemische Ausbeute lag bei allen Experimenten über 98 %. Die radiochemische Reinheit basierend auf TLC betrug > 99 %. Die Gesamtaktivität der ^{99m}Tc-Amphotericin B-Lösung (^{99m}Tc-AMB) lag bei 800 MBq.

Laufmittel	Retentionsfaktor von ^{99m}Tc-Amphotericin B	Retentionsfaktor von freiem ^{99m}Tc-Pertechnetat
ITLC-SG/Methylethylketon	0,0	> 0,9
ITLC-SG/0,9 % NaCl	0,0	0,8

Tab. 2.4 Qualitätskontrolle basierend auf TLC von ^{99m}Tc-Amphotericin B

Für die Zellkulturexperimente wurden die benötigten 10 MBq entnommen und mit sterilem PBS (pH = 7,0) auf 1 ml verdünnt, was unter Berücksichtigung der Ausbeute und Reinheit einer Konzentration von 1 µg/ml entspricht.

Die Reaktionsbedingungen zur Herstellung von ^{99m}Tc-AMB wurden zuvor hinsichtlich der optimalen Stoffmengen von AMB (schrittweise von 12,5 – 75 µg), Sn(II) (0,1 – 0,5 mg), Temperatur (Raumtemperatur, 35 °C und 45 °C) und Inkubationszeit (10, 15, 20 und 30 min) evaluiert.

2.2.13.2 Herstellung und Qualitätskontrolle von ^{68}Ga-Amphotericin B

100 µl einer 0,5 mg/ml AMB-Lösung (in HBSS) wurden in einem 2 ml-Reaktionsgefäß vorgelegt (50 µg, 54 nMol). Es wurden nacheinander 350 µl einer 0,1 N Na-Acetat-Lösung (pH = 3,4) und 1000 µl einer mit 0,1 N HCl frisch eluierten Lösung $^{68}GaCl_3$ mit einer Aktivität von 450 – 500 MBq zugegeben. Das Reaktionsgefäß wurde anschließend für 10 min bei 90 °C inkubiert. Nach Abkühlen auf Raumtemperatur wurde die Mischung mit 1,5 ml PBS verdünnt und neutralisiert.

Die Qualitätskontrolle erfolgte ebenfalls mittels Dünnschichtchromatografie und nachfolgender Messung der Aktivität der detektierten Produkte (Tab. 2.5). Die radiochemische Ausbeute lag bei > 97 % und die radiochemische Reinheit des Produkts bei > 99 %.

Laufmittel	Retentionsfaktor von ^{68}Ga-Amphotericin B	Retentionsfaktor von freiem ^{68}Ga
ITLC-SG/Methylethylketon	0,0	> 0,85

Tab. 2.5 Qualitätskontrolle basierend auf TLC von ^{68}Ga-Amphotericin B

Für die Zellkulturexperimente wurde 1 MBq entnommen und mit sterilem PBS (pH 7,0) auf 1 ml verdünnt (0,1 µg/ml).

2.2.13.3 *In vitro* Stabilitätsbestimmungen der *Tracer*

Die Stabilität von ^{99m}Tc-AMB und ^{68}Ga-AMB wurde sowohl in PBS, als auch humanem Serum mittels Hochleistungsflüssigchromatographie (HPLC) bestimmt.

5 MBq ^{99m}Tc-AMB oder 10 MBq ^{68}Ga-AMB wurden in 950 µl humanem Serum für 1, 2 und 4 h bei 37 °C / 5 % CO_2 inkubiert. Anschließend wurden 10 µl der Mischungen analog der Ausführungen in 2.2.13.1 und 2.2.13.2 über TLC analysiert und mit ^{99m}Tc-Natriumpertechnetat bzw. $^{68}GaCl_3$, sowie ^{99m}Tc-AMB bzw. ^{68}Ga-AMB, welche in PBS bei Raumtemperatur inkubiert wurden, verglichen. 500 µl wurden 1 ml Ethanol versetzt und für 15 min bei 14000 rpm zentrifugiert. Die resultierenden Überstände wurden per HPLC über einer Nucleosil 100-5 C_{18} Säule (125 x 4,7 mm) analysiert. Die Aktivität der Proben wurde mit einem *WIZARD2 Gamma Counter* gemessen.

2.2.14 Aufbau des *in vitro Transwell*®-Alveolarmodells

2.2.14.1 Zellkultur

Für den Aufbau des Alveolarmodells wurden humane pulmonale arterielle Endothelzellen (HPAEC, Lonza) und humane alveolare Adenokarzinom-Basalepithelzellen (A549, DSMZ) verwendet. In der Zellkultur wurde *Endothelial Cell Basal Medium-2* (EBM-2, Lonza) verwendet, wobei dieses für die Kultur der HPAEC nach Angaben des Herstellers mit den Zusätzen der *EGM-2 SingleQuots* (Lonza, ohne FCS und GA-1000) versetzt wurde. 10 % FCS und die benötigten Antiinfektiva wurden dem Medium stets unmittelbar vor der Verwendung zugesetzt. Die genaue Zusammensetzung der verwendeten Medien ist Tab. 2.6 zu entnehmen. Die Medien

wurden grundsätzlich vor Gebrauch mittels Spritzenvorsatzfiltern mit einer Porengröße von 0,2 µm sterilfiltriert und für mindestens 30 min bei 37 °C temperiert.

	EBM-2	**EBM-2 *+ EGM-2 Single-Quots***	**Genta-micin**	**liposom. Ampho-tericin B**	**GA-1000**	**FCS**
Hersteller	Lonza	Lonza	Merck-Serono	Gilead	Lonza	Sigma-Aldrich
Ausgans-konzentration	---	---	40 mg/ml	4 mg/ml	30 mg/ml Gentamicin 15 mg/ml AMB	---
Medien zur Vorbereitung der Zelllinien						
Auftaumedium	100 %	---	Ø	Ø	Ø	Ø
HPAEC-Medium nach dem Auftauen	---	88,45 %	0,3 % = 120 µg/ml	1,25 % = 50 µg/ml	Ø	10 %
Medium zur Kultur von HPAEC	---	89,9 %	Ø	Ø	0,1 %	10 %
A549-Medium nach dem Auftauen	88,45 %	---	0,3 % = 120 µg/ml	1,25 % = 50 µg/ml	Ø	10 %
Medium zur Kultur von A549	89,9 %	---	Ø	Ø	0,1 %	10 %
Medien für das Alveolarmodell						
Unteres Komparti-ment (1. Wechsel)	---	89,9 %	Ø	Ø	0,1 %	10 %
Unteres Komparti-ment (ab 2. Wechsel)	---	90 %	Ø	Ø	Ø	10 %
Oberes Kompartiment	---	90 %	Ø	Ø	Ø	10 %

Tab. 2.6 Zusammensetzungen der Kulturmedien des Alveolarmodells

Zum Auftauen wurden die kryokonservierten Zellen (HPAEC maximal in Passage 3, A549 maximal in Passage 5) in 15 ml EBM-2 ohne Zusätze aufgenommen und bei

400 g für 10 min zentrifugiert. Nach Entfernen des Überstandes wurden die Zellen in 15 ml des jeweiligen Kulturmediums (Tab. 2.6) aufgenommen und in einer 75 cm² Zellkulturflasche bei 37 °C und 5 % CO_2 inkubiert. Nach einem Tag wurde das Medium durch 15 ml frisches, GA-1000-haltiges Kulturmedium substituiert. Weitere Wechsel des Mediums erfolgten in 48-stündigen Abständen, wobei entsprechend der zunehmenden Konfluenz das Mediumvolumen um jeweils 5 ml erhöht wurde.

Bei einer Konfluenz der Zellen von 90 – 100 % wurde die Ernte der Zellen vorgenommen. Hierzu wurde das Kulturmedium entfernt und die Zellenschicht vorsichtig mit 15 ml sterilfiltriertem HBSS gewaschen. Nach Zugabe von 3 ml einer Trypsin / EDTA-Lösung (Lonza) wurden die Zellen für 2 min (HPAEC) bzw. 3 min (A549) bei 37 °C inkubiert, wonach die Trypsin-Reaktion mit 12 ml HBSS + 10 % FCS abgestoppt wurde. Die Zellen wurden mithilfe eines Zellschabers vom Boden der Kulturflasche abgelöst und anschließend in 15 ml Zentrifugenröhrchen überführt. Nach Zentrifugation bei 400 g für 10 min wurden die Zellen in 1 ml des jeweiligen Zellkulturmedium (Tab. 2.6) resuspendiert, mithilfe einer Neubauer-Zählkammer quantifiziert und mit dem entsprechenden Medium auf eine Zielkonzentration von 1 x 10^6 (HPAEC) bzw. 5 x 10^5 (A549) Zellen / ml verdünnt.

100 µl der HPAEC-Suspension (1 x 10^5 Zellen) wurden auf die Unterseite von 6,5 mm *Transwell*®-Einsätzen mit einer Porengröße von 3,0 µm (Sigma Aldrich) gegeben, welche in 6-*Well*-Platten in invertierter Position aufgestellt wurden, und für 2 h bei 37 °C inkubiert. Daraufhin wurden die Einsätze in 24-*Well*-Platten überführt, die mit 600 µl Kulturmedium pro *Well* befüllt waren. Das weitere Vorgehen erfolgte entsprechend der gewünschten Komplexität des Modells gemäß den Ausführungen in Kap. 2.2.14.2-3.

2.2.14.2 Endotheliales *Monolayer*-Modell

Alle 48 h wurde ein Mediumwechsel der Einsätze durchgeführt, wobei diese in 24-*Well*-Platten mit frischem Medium umgesetzt wurden. Nach dem ersten Mediumwechsel wurde auf die weitere Zugabe von GA-1000 verzichtet. 15 h vor der geplanten *Tracer*-Markierung wurden die Unterseiten der *Transwell*®-Einsätze mit 12,5 µl einer Pathogen-haltigen Lösung oder (als Kontrolle) 12,5 µl Pathogen-freiem EGM-2-Medium infiziert. Hierzu wurden 2 x 10^2 bis 2 x 10^7 Pilz- oder Bakterienzellen pro ml in EGM-2 aufgenommen (2,5 x 10^1 – 2,5 x 10^6 Zellen in 12,5 µl). Die

verwendeten Stämme sind in Kap. 2.1.3 gelistet. Nach 2-stündiger Inkubation der invertierten Einsätze in 6-*Well*-Platten wurden diese in 24-*Well*-Platten, welche mit 600 µl frischem Kulturmedium versehen waren, verbracht. Eine schematische Darstellung des experimentellen Ablaufs der Infektion ist in Abb. 2.4 dargestellt.

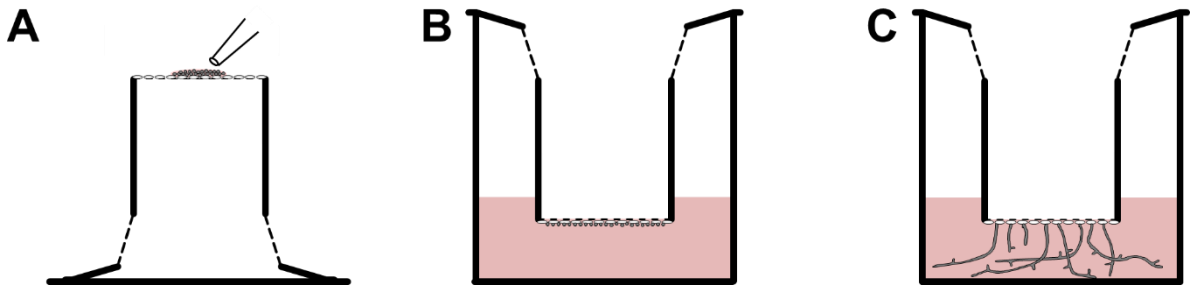

Abb. 2.4 Schematische Darstellung der Infektion des endothelialen *Monolayer*-Modells. 2,5 x 10^1 – 2,5 x 10^6 Pilz- oder Bakterienzellen wurden in 12,5 µl EGM-2 auf die Unterseite der Membran eines *Transwell*®-Einsatzes gegeben (A). Nach 2 h Inkubation bei 37 °C wurden sie in 24-Well-Platten überführt, die mit 600 µl EGM-2 befüllt waren (B). Während der anschließenden 15-stündigen Inkubation keimten die Pilzsporen im unteren Kompartiment zu Hyphen aus (C). Adaptiert übernommen aus der Posterpräsentation von Page et al., 2019, *9th Trends in Medical Mycology*, Nizza, Frankreich.

2.2.14.3 *Bilayer*-Modell

24 h nach dem Ausplattieren der HPAEC wurden die Einsätze in neue 24-*Well*-Platten, welche mit 600 µl frischem Kulturmedium versehen waren, umgesetzt. Anschließend wurden in das obere Kompartiment 100 µl der wie oben beschriebenen A549-Suspension (5 x 10^4 Zellen) zugegeben. 72 h und 120 h nach dem Ausplattieren der HPAEC wurden die Einsätze erneut in 24-*Well*-Platten mit 600 µl frischem Kulturmedium umgesetzt, wobei ab dem 72 h-Zeitpunkt kein GA-1000 mehr zugegeben wurde.

Nach dem 120 h-Mediumwechsel wurden 100 µl einer Pilz- oder Bakterien-haltigen Lösung (2,5 x 10^6 / ml, entsprechend 2,5 x 10^5 Zellen in 100 µl) oder 100 µl EGM-2 (Negativkontrolle) in das obere Kompartiment pipettiert. Die verwendeten Pathogene entsprachen dabei den unter Kap. 2.1.3 genannten Organismen. Die Einsätze wurden nach der Infektion je nach Endpunkt des Experiments für 30 min bis 30 h bei 37 °C und 5 % CO_2 inkubiert. Der experimentelle Aufbau ist in Abb. 2.5 schematisch dargestellt.

Um den Einfluss unterschiedlicher Kulturbedingungen und Pharmaka auf das Wachstum von Mucorales zu untersuchen wurden bei einigen Experimenten dem Medium im unteren Kompartiment während der Infektion 8 mg/ml Glucose, 1 mg/ml 3-Hydroxybutansäure oder 50 µg/ml Gefitinib zugesetzt.

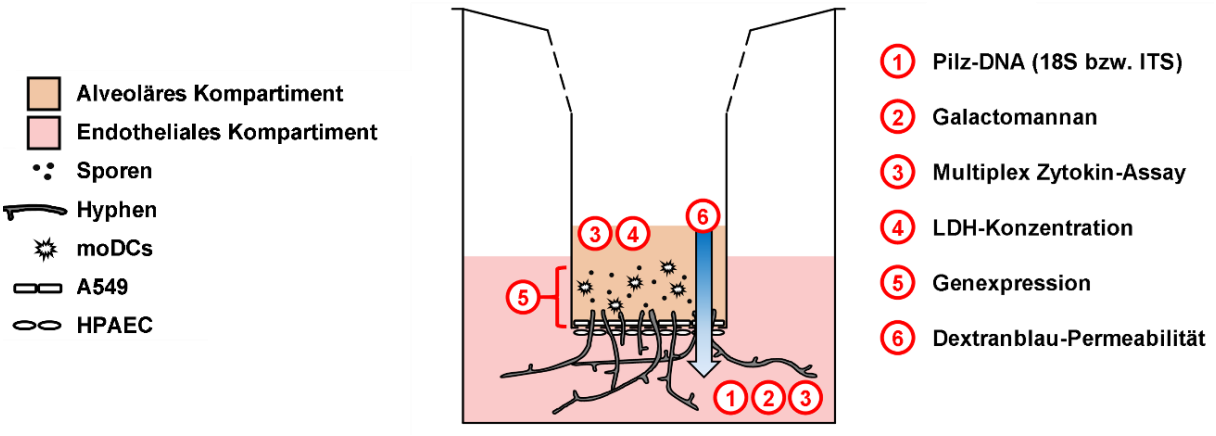

Abb. 2.5 Schematischer experimenteller Aufbau der unterschiedlichen Studien im *Bilayer-Transwell*®-Modell (entnommen aus der Posterpräsentation von Wurster et al., 2018, PEG Frühjahrstagung Sektion antimykotische Therapie, Bonn, Deutschland, bzw. übersetzt aus Belic et al., 2019).

2.2.15 Genexpressionsanalysen des epithelialen Kompartiments im *Bilayer*-Modell

2.2.15.1 Ernte von RNA aus dem epithelialen Kompartiment

Von den Zellkulturproben, die Genexpressionsanalysen zugeführt werden sollten, wurden Endothelzellen und Myzel nach der wie in Kap. 2.2.14.3 beschrieben erfolgten Infektion und Inkubation mithilfe eines Zellschabers entfernt. Die *Transwell*®-Einsätze und darin verbliebenen A549-Zellen und moDC im oberen Kompartiment wurden 5-mal in 12-*Well*-Platten mit je 4 ml HBSS gewaschen. Die Einsätze wurden anschließend in 24-*Well*-Platten mit 800 µl *RNAprotect* überführt. Nach Zugabe von weiteren 200 µl *RNAprotect* in das obere wurde die Membran mit einer Pipette mechanisch perforiert und durch multiples Pipettieren des *RNAprotect* gespült. Der *Transwell*®-Einsatz wurde daraufhin verworfen und die suspendierten Proben bis zur RNA-Isolation bei -20 °C eingefroren.

2.2.15.2 RNA-Isolation mithilfe des *RNeasy Mini Kit*

Die in *RNAprotect* (Qiagen) gelösten Zellen wurden aufgetaut und bei 5000 g für 5 min zentrifugiert. Der Überstand wurde abgenommen und verworfen, die Zellen in 350 µl RLT-Puffer (ohne β-Mercaptoethanol) resuspendiert. Die Gesamt-RNA der Zellen wurde mithilfe des *RNeasy Mini Kits* (Qiagen) gemäß Herstellerangaben aufgereinigt und in 30 µl nukleasefreiem Wasser eluiert. Die Konzentration der so isolierten RNA wurde mittels Nanodrop gemessen, wobei das verwendete nukleasefreie Wasser als Referenzwert diente.

2.2.15.3 cDNA Synthese aus isolierter RNA mittels *High capacity cDNA reverse transcriptase Kit*

300 ng isolierter RNA wurden mit nukleasefreiem Wasser bis zu einem Volumen von 12 µl aufgefüllt und dann nach Angaben des Herstellers (Applied Biosystems) mit den Bestandteilen des Kits versetzt:

Reverse Transcriptase	1 µl
dNTPs	0,8 µl
Random Primer	2 µl
10x Reaktionspuffer	2 µl
Nukleasefreies Wasser	2,2 µl

Zur Synthese wurde der *Thermocycler* folgendermaßen programmiert:

25 °C	10 min	Vortemperierung
37 °C	2 h	Synthese
85 °C	5 min	Enzyminaktivierung
4 °C	Pause	Lagerung

2.2.15.4 Quantitative Echtzeit-Polymerase-Kettenreaktion

Je Probe wurde 1 µl eines *Primer Mix* hinzugegeben, welcher sowohl *reverse* als auch *forward Primer* des jeweiligen Gens enthielt (die Konzentration betrug für beide Primer jeweils 10 µM). Die Sequenzen der verwendeten Oligonukleotide zur Amplifikation der mRNA von Alas1, Cas3, Cas9, CCL2, CCL5, ICAM-1, IL-6 und IL-8 sind in Kap. 2.1.2.8 dargestellt. Zusätzlich wurden je 10 µl 2x *iTaq Universal SYBR Green Supermix* (Bio-Rad) zugegeben, sowie je 5 µl nukleasefreies Wasser. Die wie

in 2.2.15.3 beschrieben hergestellte cDNA wurde mit 180 µl nukleasefreiem Wasser 1:10 verdünnt. Je Probe wurden dann 4 µl der verdünnten cDNA für die qPCR verwendet.

Zur Amplifikation und Erstellung von Schmelzkurven wurde das folgende Programm am *Step-One plus PCR Cycler* (Applied Biosciences) verwendet:

95 °C	30 sec	Initiale Denaturierung
95 °C	3 sec	Denaturierung
60 °C	30 sec	*Annealing* und Elongation
(40 Amplifikationszyklen)		
95 °C	15 sec	Denaturierung
60 °C	60 sec	*Annealing* und finale Elongation
+ 0,5 °C	nach je 15 sec	Schmelzkurve
95 °C	15 sec	Endpunkt der Schmelzkurve
4 °C	Pause	Lagerung

Die relativen Expressionslevel der detektierten mRNA der amplifizierten Gene wurden mithilfe der ΔΔCt-Methodik ermittelt. Als Referenzgen diente Alas1.

2.2.16 Muc18S-*Assay* im *Bilayer*-Modell

Der Echtzeit-PCR-*Assay* „Muc18S“ wurde zur semi-quantitativen Bestimmung der Mucorales-DNA in den Kulturüberständen des unteren Kompartiments durchgeführt. Der Test wurde im Labor der molekularen Hämatologie des Universitätsklinikums Würzburg (AG Löffler) entsprechend des von Springer und Kollegen publizierten Protokolls durchgeführt (Springer et al., 2016a und b).

2.2.17 Dextranblau-Diffusions-*Assay* im *Bilayer*-Modell

Zum Zeitpunkt der Infektion des wie in 2.2.12.3 aufgebautem *Transwell®-Bilayer*-Modells wurden in das obere Kompartiment 250 µg Dextranblau der Molekülmassen 5 kDa, 20 kDa oder 70 kDa sowie ggf. 2.5 x 10^5 moDCs oder 1 ng/ml IL-1β und TNF-α in einem Volumen von insgesamt 50 µl Medium zugegeben. Die Infektion wurde

wie in 2.2.12.3 beschrieben mit 2,5 x 10^5 Sporen bzw. Bakterien durchgeführt, welche hierfür allerdings in nur je 50 µl Medium aufgenommen wurden.

Zur Bestimmung des prozentualen Anteils des vom oberen in das untere Kompartiment diffundierten Dextranblaus wurden die *Transwell*®-Einsätze zu definierten Zeitpunkten nach der Infektion in 24-*Well*-Platten mit frischem Kulturmedium umgesetzt, um die Rückdiffusion von Dextranblau in das obere Kompartiment zu vermeiden (30 min, 90 min, 5 h, 10 h, 20 h und 30 h). 100 µl des Mediums der vorherigen Platte wurden in eine 96-*Well*-Platte überführt und die Absorption bei 622 nm gemessen. Als Referenz wurde eine Verdünnungsreihe erstellt, wobei 250 µg Dextranblau / 600 µl Medium als 100 %-Probe angesetzt wurde.

2.2.18 Inkubation von Kulturüberständen von Schimmelpilzen im *Bilayer*-Modell

Zur Gewinnung von Kulturüberständen der Schimmelpilze wurden je 1 x 10^7 Sporen in 2 ml EBM-2 für 30 h bei 37 °C inkubiert. Die Überstände wurden abgenommen und mittels 0,2 µm-Filtern sterilfiltriert. Vor Zugabe von 100 µl der einzelnen Überstände in das obere Kompartiment des *Bilayer*-Modells zum Zeitpunkt der Infektion wurden sie 1:1 mit EBM-2 verdünnt. Die Inkubation des Alveolarmodells mit den Überständen erfolgte für 30 h bei 37 °C.

2.2.19 Bestimmung von Zytokin- und Lactatdehydrogenase-Konzentrationen des epithelialen Kompartiments des *Bilayer*-Modells

Aus dem oberen Kompartiment des *Bilayer*-Modells wurden 10, 20 oder 30 h nach der Infektion 100 µl Flüssigkeit entnommen und diese bei 5000 g und 4 °C für 5 min zentrifugiert. 30 µl des daraus resultierenden Überstands wurden mit 120 µl 0,9 % NaCl versetzt und umgehend einer Lactatdehydrogenase-Bestimmung im Zentrallabor des Universitätsklinikums Würzburg zugeführt. Dort wurde der LDHI2-*Assay* mittels eines *Cobas Integra Analyzer* durchgeführt. Sollte die Proben stattdessen zur Messung von Zytokinkonzentrationen wie in Kap. 2.2.11 beschrieben Multiplex-Zytokinassay zugeführt werden, wurden die Überstände nach der Zentrifugation nicht mit 0,9 % NaCl verdünnt.

2.2.20 *Tracer*-basierte Detektion von Schimmelpilzen im endothelialen *Monolayer*-Modell

Die *Tracer* wurden wie in Kap. 2.2.13 beschrieben hergestellt, mit temperiertem (37 °C) HPAEC-Kulturmedium (ohne GA-1000) auf eine Konzentration von 50 ng/ml (^{99m}Tc) bzw. 5 ng/ml (^{68}Ga) verdünnt und jeweils 600 µl pro Vertiefung in 24-*Well*-Platten vorgelegt.

Die infizierten *Transwell*®-Einsätze wurden in die mit dem *Tracer* vorbereiteten 24-*Well*-Platten umgesetzt und für 5 bis 240 min (entsprechend der Anforderungen des jeweiligen Experiments) bei 37 °C und 5 % CO_2 inkubiert. Anschließend wurden die Einsätze durch fünfmaliges Umsetzen und 1-minütige Inkubation in jeweils frischem, gekühltem HBSS (4 °C) gewaschen. Hierdurch wurde die *Tracer*-Aufnahme gestoppt und ungebundener *Tracer* von den Zellen entfernt. Der experimentelle Ablauf ist schematisch in Abb. 2.6 dargestellt.

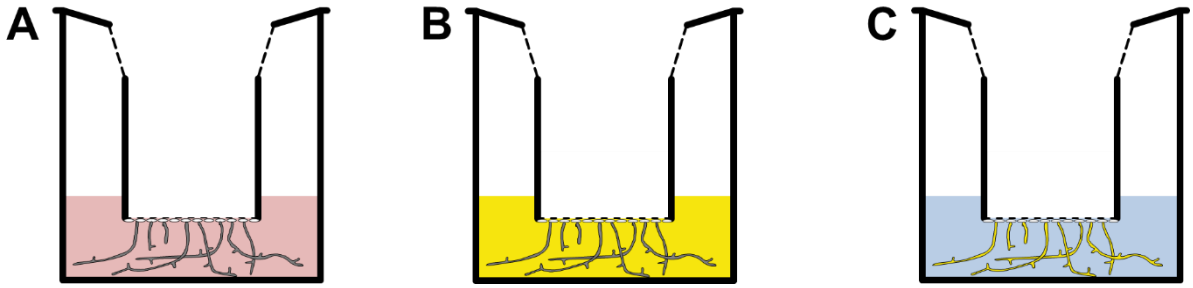

Abb. 2.6 Schematische Darstellung der Detektion von Schimmelpilzen im *Monolayer*-Modell. 15 h nach der wie in Kap. 2.2.14.2 beschriebenen Infektion (A) wurden die *Transwell*®-Einsätze für 5 – 240 min mit 50 ng/ml ^{99m}Tc-AMB bzw. 5 ng/ml ^{68}Ga-AMB bei 37 °C inkubiert (B). Anschließend wurden die Einsätze je 5-mal in 1 ml gekühltem HBSS gewaschen (C), bevor die Proben mittels *Gamma Counting* oder Autoradiographie analysiert wurden. Entnommen aus der Posterpräsentation von Page et al., 2019, *9th Trends in Medical Mycology*, Nizza, Frankreich.

Zur anschließenden Analyse der Proben mittels eines *Gamma Counters* wurden drei Aliquots der *Tracer* zu je 600 µl, sowie drei Aliquots einer 1:10 Verdünnung dieser Lösung als 100 %- bzw. 10 %-Standardmesswerte in 1,5 ml Reaktionsgefäße verbracht. Die *Transwell*®-Einsätze und Reaktionsgefäße mit Standard-Verdünnungen wurden in Polyethylen-Szintillationsfläschchen (Hartenstein) überführt und die Aktivität der Proben mithilfe eines *WIZARD2 Gamma Counters* quantifiziert.

Alternativ wurden die Proben mittels Autoradiographie analysiert. Hierzu wurden die Einsätze nach dem Waschvorgang in eine trockene 24-*Well*-Platte überführt. Mit dieser wurde eine *Phosphor Imaging Plate* (Dürr Medical) für 120 min (^{99m}Tc) bzw. 5 min (^{68}Ga) belichtet, welche anschließend mit einem *CR-35 Readers* gescannt und mittels der zugehörigen *AIDA Image Data Analyzing Software* (Raytest) ausgewertet wurde.

2.2.21 Statistik

2.2.21.1 Signifikanzprüfungen

Signifikanzprüfungen der Unterschiede verschiedener Werteverteilungen erfolgten meist mithilfe des ungepaarten, zweiseitigen Mann-Whitney-U-Tests, t-Tests oder einfaktorieller ANOVA. Ausgenommen sind hiervon die Signifikanzprüfungen des Manuskripts *„In vitro evaluation of radiolabeled Amphotericin B for molecular imaging of mold infections“*, welche aufgrund der Vielzahl experimenteller Konditionen und Variablen mit zweifaktorieller ANOVA durchgeführt wurden. Korrelationen wurden anhand des Pearson-Korrelationskoeffizienten (r) bewertet und dessen Signifikanz in Abhängigkeit von der Anzahl der untersuchten Probanden evaluiert. Für die Wertebereiche des p-Werts wurde in den dieser Dissertation zugrundeliegenden Manuskripten folgende Symbolik definiert: ns $p > 0{,}05$ (nicht signifikant); * $p < 0{,}05$; ** $p < 0{,}01$; *** $p < 0{,}001$. In einigen Fällen wurde, v. a. bei geringer Stichprobengröße, zusätzlich ein p-Wert zwischen 0.05 und 0.1 ausgewiesen (■).

2.2.21.2 Berechnung von Konfidenzintervallen durchflusszytometrisch bestimmter Zellfrequenzen

Zur Abschätzung der 95 % Konfidenzintervalle für die durchflusszytometrische Bestimmung seltener Zellpopulationen wurde zunächst nach Allan & Keeney (2010) die Standardabweichung (SA) der unstimulierten Probe berechnet, mit f als Frequenz und n als Anzahl gemessener antigen-reaktiver Zellen:

$$SA_{uns} = \frac{f\,[CD154^{+}/CD4^{+}]}{\sqrt{n\,[CD154^{+}/CD4^{+}]}}$$

Da für die Bestimmung *A. fumigatus*-reaktiver T-Zellen Duplikate erstellt wurden, wurde in diesen Fällen folgende Formel für die Berechnung der SA reaktiver T-Zell-Frequenzen verwendet:

$$SA_{Afu} = \frac{0{,}5\ x\ (f\ [CD154^+/CD4^+]_{Well\ 1} + f\ [CD154^+/CD4^+]_{Well\ 2})}{\sqrt{n\ [CD154^+/CD4^+]_{Well\ 1} + n\ [CD154^+/CD4^+]_{Well\ 2}}}$$

Gemäß der Gauss'schen Fehlerfortpflanzung wurden die gesamte SA der unstimulierten und stimulierten Proben kombiniert:

$$SA_{gesamt} = \sqrt{SA_{uns}^2 + SA_{Afu}^2}$$

Die 95 %-Konfidenzintervalle wurden schließlich mit dem 1,96-fachen der jeweiligen Gesamt-SA der Proben approximiert.

2.2.21.3 Logistische Regression

Die Analysen mittels logistischer Regression wurden am Lehrstuhl für Bioinformatik am Biozentrum der Julius-Maximilians-Universität Würzburg unter Leitung von Prof. Dr. Thomas Dandekar durchgeführt. Basierend auf den mittels Multiplex-Zytokin-*Assay* ermittelten Zytokinkonzentration und den $CD154^+$ reaktiven T-Helfer-Zell-Frequenzen sollten hoch und niedrig exponierte Gesunde über uni- und multivariate logistische Regressionsanalysen differenziert werden. Die Zytokinkonzentrationen wurden dabei logarithmisch transformiert, wobei zu jeder Messung ein *Pseudocount* addiert wurde. Die Signifikanzniveaus der Regressionskoeffizienten wurde mittels Plausibilitätsquotiententests berechnet. Jedes Zytokin wurde hierbei gegen das verschachtelte Modell getestet, wobei entweder die Ordinate oder der CD154-Koeffizient überprüft wurden. Um die prädiktive *Power* der einzelnen Modelle zu ermitteln wurde eine 10-fache Kreuzvalidierung genutzt, wobei sowohl die interne Präzision, als auch die Präzision der Kreuzvalidierung berechnet wurden. Die Berechnungen wurden mithilfe des *Statistical Software Package R* (Version 3.2.2) durchgeführt (Übersetzt aus Page et al., 2018).

3. ERGEBNISSE

Die hier dargestellten Manuskripte wurden modifiziert, um dem Format dieser Dissertation zu entsprechen. Die Versionen entsprechen jeweils der bei der jeweiligen Zeitschrift eingereichten Fassung nach Bearbeitung der Revisionen. Diese Dissertation wurde auf Basis folgender Publikationen angefertigt:

Page L, Weis P, Müller T, Dittrich M, Lazariotou M, Dragan M, Waaga-Gasser AM, Helm J, Dandekar T, Einsele H, Löffler J, Ullmann AJ, Wurster S (2018). "Evaluation of Aspergillus and Mucorales specific T-cells and peripheral blood mononuclear cell cytokine signatures as biomarkers of environmental mold exposure." Int J Med Microbiol. **308**(8):1018-1026.

Page L, Lauruschkat CD, Helm J, Weis P, Lazariotou M, Einsele H, Ullmann AJ, Loeffler J, Wurster S (2020). "Impact of immunosuppressive and antifungal drugs on PBMC- and whole blood-based flow cytometric CD154+ Aspergillus fumigatus specific T-cell quantification" Med Microbiol Immunol. https://doi.org/10.1007/s00430-020-00665-3.

Belic S, Page L, Lazariotou M, Waaga-Gasser AM, Dragan M, Springer J, Loeffler J, Morton CO, Einsele H, Ullmann AJ, Wurster S (2019). "Comparative Analysis of Inflammatory Cytokine Release and Alveolar Epithelial Barrier Invasion in a Transwell® Bilayer Model of Mucormycosis." Front Microbiol. **9**:3204.

Page L, Ullmann AJ, Schadt F, Einsele H, Wurster S, Samnick S (2020). "In vitro evaluation of radiolabeled Amphotericin B for molecular imaging of mold infections." Antimicrob Agents Chemother. doi:10.1128/AAC.02377-19

3.1 Evaluation of *Aspergillus* and Mucorales specific T-cells and peripheral blood mononuclear cell cytokine signatures as biomarkers of environmental mold exposure

Lukas Page[1], Philipp Weis[1], Tobias Müller[2], Marcus Dittrich[2], Maria Lazariotou[1], Mariola Dragan[3], Ana Maria Waaga-Gasser[3], Johanna Helm[1], Thomas Dandekar[2], Hermann Einsele[1], Jürgen Löffler[1], Andrew J. Ullmann[1], Sebastian Wurster[1,4,‡]

1) University Hospital of Wuerzburg, Department of Internal Medicine II, Division of Infectious Diseases, Josef-Schneider-Str. 2, 97080 Wuerzburg, Germany

2) University of Wuerzburg, Biocenter, Department of Bioinformatics, Am Hubland, 97074 Wuerzburg, Germany

3) University Hospital of Wuerzburg, Department of Surgery I, Oberduerrbacher Str. 6, 97080 Wuerzburg, Germany

4) The University of Texas MD Anderson Cancer Center, Department of Infectious Diseases, 1515 Holcombe Boulevard, Houston, Texas, 77030, United States of America

‡ Corresponding author:

University Hospital of Wuerzburg Laboratory (Billing Address for Publication Charges):

University Hospital of Wuerzburg, Department of Internal Medicine II

Josef-Schneider-Str. 2, C11, Room 0.205, 97080 Wuerzburg, Germany

Email address: Wurster_S@ukw.de

Phone: +49931-201-36402

Present Contact Address:

The University of Texas MD Anderson Cancer Center, Department of Infectious Diseases

1515 Holcombe Boulevard, Y5.5725, Houston, TX 77030, United States of America

Email address: stwurster@mdanderson.org

Phone: 1-713-745-1371

Abstract

Mold specific T-cells have been described as a supportive biomarker to monitor invasive mycoses and mold exposure. This study comparatively evaluated frequencies and cytokine profiles of *Aspergillus fumigatus* and Mucorales reactive T-cells depending on environmental mold exposure. Peripheral blood mononuclear cells (PBMCs) obtained from 35 healthy donors were stimulated with mycelial lysates of *A. fumigatus* and three human pathogenic Mucorales species. $CD154^+$ specific T-cells were quantified by flow cytometry. In a second cohort of 20 additional donors, flow cytometry was complemented by 13-plex cytokine assays. Mold exposure of the subjects was determined using a previously established questionnaire. Highly exposed subjects exhibited significantly greater $CD154^+$ *A. fumigatus* and Mucorales specific naïve and memory T-helper cell frequencies. Significant correlation (r = 0.48 – 0.79) was found between *A. fumigatus* and Mucorales specific T-cell numbers. Logistic regression analyses revealed that combined analysis of mold specific T-cell frequencies and selected cytokine markers (*A. fumigatus*: IL-5 and TNF-α, *R. arrhizus*: IL-17 and IL-13) significantly improved classification performance, resulting in 75 – 90 % predictive power using 10-fold cross-validation. In conclusion, mold specific T-cell frequencies and their cytokine signatures offer promising potential in the assessment of environmental mold exposure. The cytokines identified in this pilot study should be validated in the clinical setting, e. g. in patients with hypersensitivity pneumonitis.

Keywords: Mold exposure, Biomarker, T-cells, Flow cytometry, CD154, Cytokines

Highlights

- Subjects with intensive mold exposure harbor greater Mucorales specific T-cell frequencies
- Naïve and memory T-cells equally contribute to elevated specific T-cell numbers
- Aspergillus and Mucorales specific T-cell frequencies significantly correlate in healthy subjects
- Cytokine markers improve the classification performance of mold specific T-cell monitoring

Introduction

Airborne spores of opportunistic mold pathogens are ubiquitously present in the environment (Park & Mehrad, 2009; Richardson, 2009). In case of aberrant immune status, mold exposure is associated with a broad spectrum of illnesses ranging from invasive mycoses (IM) to mold associated hypersensitivity syndromes (Park & Mehrad, 2009; Ribes et al., 2000). While *Aspergillus* species are the most frequent cause of invasive mold infections and belong to the most common causes of mold related allergy (Park & Mehrad, 2009; Twaroch et al., 2015), other emerging fungal pathogens attract growing clinical and scientific attention (Madney et al., 2017; Walsh et al., 2004). The largest burden of non-*Aspergillus* IM is attributable to the order Mucorales that also causes allergy and hypersensitivity pneumonitis. Mucorales are thermotolerant molds ubiquitously found on organic substrate. Their mycelium is characterized by rapid and abundant growth (Ribes et al., 2000). Mucorales spores, released from sporangiums containing 10^2 to 10^5 spores, are efficiently dispersed and easily aerosolized (Richardson, 2009). Inhalative exposure to Mucorales spores has been linked to mucormycosis outbreaks (England et al., 1981; Lueg et al., 1986; Richardson, 2009) and occupational hypersensitivity pneumonitis (Bellanger et al., 2010; Cote et al., 1991; Eduard et al., 1992; Prabhu & Patel, 2004; Weber et al., 2015).

While antibody measurements have demonstrable merit in the diagnosis of allergic diseases or allergic bronchopulmonary mycosis (Woolnough et al., 2015), their value in the assessment of environmental mold exposure is limited, as they cannot provide an estimation of time, location or dose of exposure (Bush et al., 2006). Similarly, air sampling is only helpful to determine current exposure at the sampling location, but does not facilitate evaluation of long-term exposure and thresholds for tolerable aerosolized spore concentrations are yet to be defined (Bush et al., 2006). Therefore, new biomarkers for the assessment of environmental mold exposure including immune monitoring strategies are subject of current research (Daschner, 2017).

The T-cell system with its various subsets, distinguishable by specific cytokine profiles and lineage markers, is pivotal to orchestrate a balanced immune response mediating tolerance to commensals while eliminating invasive pathogens (Romani, 2011). Different groups studied *Aspergillus* and Mucorales specific T-helper cell

responses in healthy subjects or immunocompromised patients (Bacher et al., 2015a; Jolink et al., 2013; Potenza et al., 2011, 2013, and 2016; Wurster et al., 2017a). Applying flow cytometry (Bacher et al., 2015a) or immunospot assays (Potenza et al., 2011, 2013, and 2016), elevated specific T-cell frequencies were found in hematological patients suffering from invasive pulmonary aspergillosis or mucormycosis. Interestingly, significant mold specific T-cell counts were also detected in healthy subjects (Bacher et al., 2015a; Jolink et al., 2013; Wurster et al., 2017a). We have previously demonstrated that *Aspergillus fumigatus* reactive T-helper and T-memory cell frequencies in healthy subjects correlate with mold exposure in the residential and working environment (Wurster et al., 2017a). Building upon this observation, the present study comparatively assessed the performance of *A. fumigatus* and Mucorales specific T-cell frequencies and PBMC (peripheral blood mononuclear cells) cytokine profiles in the assessment of environmental mold exposure.

Material and Methods

Generation of Mucorales lysates

Spores of *Rhizopus arrhizus* (CBS 110.17), *Rhizomucor pusillus* (CBS 245.58), and *Cunninghamella bertholletiae* (CBS 187.84) were harvested from mature fungal cultures grown on beer wort agar. To generate hyphae, 1 x 10^8 conidia were incubated in 20 ml RPMI 1640 overnight at 37 °C under constant agitation at 200 rpm. After a washing step (HBSS), hyphae were resuspended in HBSS (80 mg in 350 µl) and bead beating was performed for 2 min (*R. arrhizus* and *R. pusillus*) or 1 min (*C. bertholletiae*) using a Vortex Genie 2 apparatus (Scientific Industries) with an attached bead tube adaptor (Macherey-Nagel). The contents of three bead tubes were combined and passed through a 0.2 µl sterile filter. Protein concentrations were determined using the DC Protein Assay Kit (Bio-Rad). Endotoxin testing was performed using the Pierce LAL Chromogenic Endotoxin Quantitation Kit (Thermo Scientific) according to the manufacturer's instructions. Endotoxin concentrations were consistently below 1 EU/ml.

Donor selection and blood collection

After obtaining informed consent approved by the ethics committee of the University of Wuerzburg, 27 ml EDTA whole blood and 7 ml serum were collected from healthy volunteers. Donors were screened for absence of acute or chronic infection, diabetes mellitus, immunosuppressive or antimicrobial therapy, and pregnancy. Risk factors for mold exposure were recorded using a previously published questionnaire (Wurster et al., 2017a). Demographic details of the study cohort are summarized in **Table 1**.

	Cohort 1 n = 35	Cohort 2 n = 20
Mean Age ± SD	24.9 ± 2.8	25.3 ± 1.8
Gender Distribution	17 male 18 female	13 male 7 female
Long Term Exposure in Rural Environment	21 (60 %)	13 (65 %)
Mold Exposure in Professional Environment	8 (23 %)	3 (15 %)
Place of Residence in 1 km Surrounding of Farmlands	26 (74 %)	13 (65 %)
Mold Exposure in Residential Environment	24 (69 %)	14 (70 %)
No Risk Factor	2 (6 %)	2 (10 %)
High Exposure Category (3 positive items or Long Term Exposure + ≥ 1 additional item)	22 (63 %)	13 (65 %)
Low Exposure Category	13 (37 %)	7 (35 %)

Table 1

Characteristics of study cohort

PBMC isolation and stimulation

Peripheral blood mononuclear cell (PBMC) isolation was performed by ficoll gradient centrifugation. PBMCs were diluted in RPMI 1640 containing 5 % autologous serum at a final concentration of 1 x 10^7 cells per ml. 100 µl of the cell suspension were seeded per well of a 96 well flat bottom plate. Fungal lysates (final concentration: 50 µg/ml, *A. fumigatus*: Miltenyi Biotec, Mucorales: generated as described above) or

CMV PepTivators IE-1 and pp65 (final concentration: 60 pmol per peptide), as well as 0.1 µg CD28 costimulatory antibody were added for cell stimulation. To determine unspecific background, control samples were treated with the costimulatory antibody only. Cell incubation was performed for 2 h at 37 °C, 5 % CO_2. Thereafter, brefeldin A was added at a final concentration of 10 µg/ml followed by an 18 h incubation period at 37 °C, 5 % CO_2.

Determination of specific T-cell frequencies

Antibody staining was performed using the Inside Stain Kit (Miltenyi Biotec) according to the manufacturer's instructions. α-CD4-VIT4-FITC, α-CD3-PerCP, α-CCR7-PE, and α-CD45RO-PerCP were used for extracellular staining, and α-CD154-APC, α-IFN-γ-PE as well as α-TNF-α-PE for intracellular staining (all antibodies: Miltenyi Biotec). Gating strategy and calculation of specific T-cell frequencies in consideration of unspecific background are described in **Supplementary Figures 1 and 2**. MIATA compliant reporting (Britten et al., 2012) of detailed workflow, data analysis, and quality control parameters is provided in **Supplementary Table 1**.

Assessment of cytokine secretion

PBMC were isolated and stimulated as described above, but not treated with brefeldin A. Cells were incubated for 120 hours at 37 °C, 5 % CO_2. Cytokine secretion into the culture supernatant was analyzed using a 13-plex HCYTOMAG Milliplex Kit (EMD Millipore) according to the manufacturer's instructions. Quality control samples provided by the manufacturer were used to validate proper assay performance.

Statistical analysis

A first cohort of 35 healthy volunteers was assessed to compare Mucorales specific T-cell frequencies and their correlation with mold exposure as well as the correlation of *Aspergillus* and Mucorales specific T-cell frequencies. T-cell phenotypes and cytokine secretion were characterized in a second cohort of 20 healthy adults. Significance testing was performed using the unpaired Mann-Whitney-U test.

Uni- and multivariate logistic regression models were used to classify samples into high and low exposure groups based on cytokine and CD154 measurements. Cytokine concentrations were log-transformed (adding a pseudo count of one to each

measurement) prior to model fitting. Significance of regression coefficients have been tested using likelihood ratio tests. Each cytokine was tested against the nested model including only the intercept (to test the marginal effect) or the CD154 coefficient (to test the cytokine effect adjusted for CD154), respectively. To assess the predictive power of each model, a 10-fold cross-validation was performed and the internal and cross-validation accuracy were calculated. Calculations were performed with the statistical software package R (version 3.2.2).

Results

Assessment of A. fumigatus and Mucorales specific T-cell frequencies depending on environmental mold exposure profiles

Mean frequencies of T-helper cells upregulating CD154 in response to mycelial lysates of *A. fumigatus* (0.113 % ± 0.071 %), *R. arrhizus* (0.124 % ± 0.068 %), *R. pusillus* (0.188 % ± 0.102 %), and *C. bertholletiae* (0.143 % ± 0.100 %) were determined in PBMC samples from 35 donors (donor characteristics: **Table 1**). Subjects whose questionnaires revealed a high mold exposure profile (as defined in Wurster et al., 2017a) harbored significantly greater mean frequencies of *A. fumigatus* (3.1 fold) and Mucorales (1.9 – 2.5 fold) specific T-helper cells compared to subjects with low exposure (**Figure 1**). The number of positive categories of surrogate markers for mold exposure strongly correlated with specific T-cell frequencies (**Figure 2**). For *A. fumigatus* and *R. arrhizus* specific T-cells a significant incline was already observed in case of two positive categories (**Figure 2A-B**), whereas only subjects with three or four positive categories showed significantly elevated *R. pusillus* and *C. bertholletiae* specific T-helper cell counts (**Figure 2C-D**).

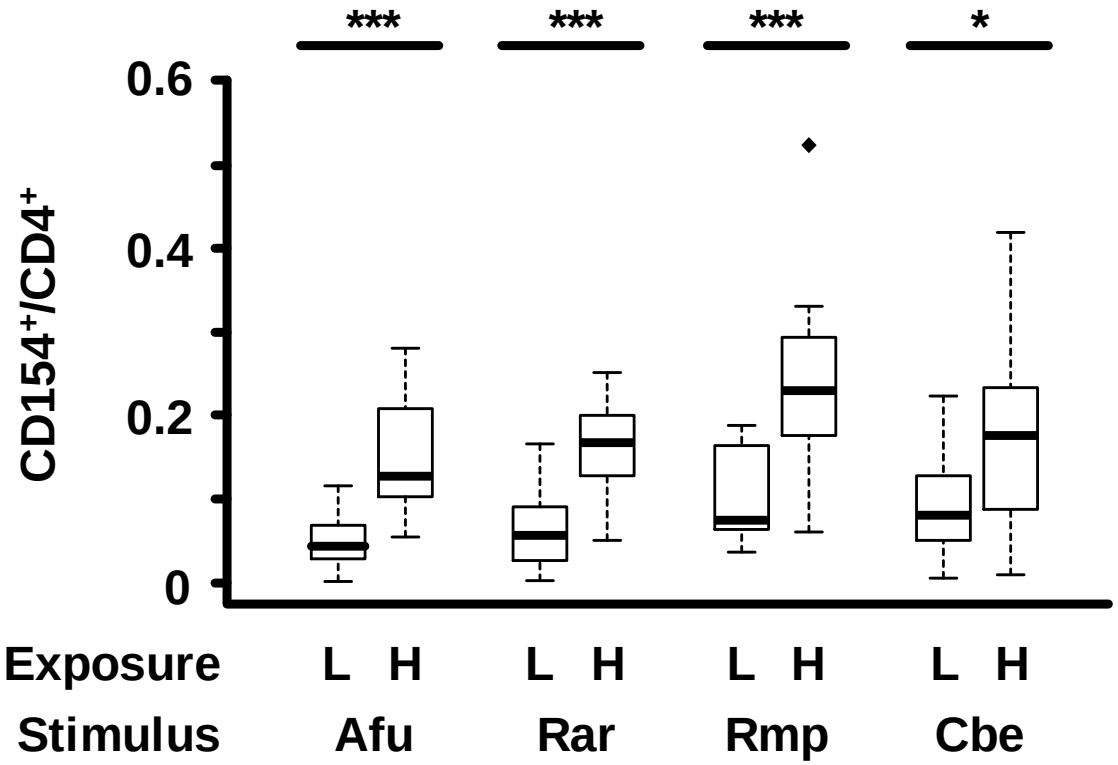

Figure 1: Frequencies of mold specific CD154$^+$/CD4$^+$ T-cells depending on the subjects' mold exposure profile

Frequencies of mold specific CD154$^+$/CD4$^+$ cells were determined in a cohort of 35 healthy donors (**Table 1**, cohort 1). Subjects with ≥ 3 positive categories of risk factors for environmental mold exposure or a combination of long-term exposure and at least one current risk factor were assigned to the "high exposure" group (as described in Wurster et al., 2017a). All other subjects were assigned to the "low exposure" cohort. Box-whisker plots represent minimum, first quartile, median, third quartile, and maximum values observed in both cohorts. Outliers exceeding the 1.5-fold inter-quartile-range are shown individually. The two-sided Mann-Whitney-U test was used for significance testing. * $p < 0.05$, ** $p < 0.01$, *** $p < 0.001$.

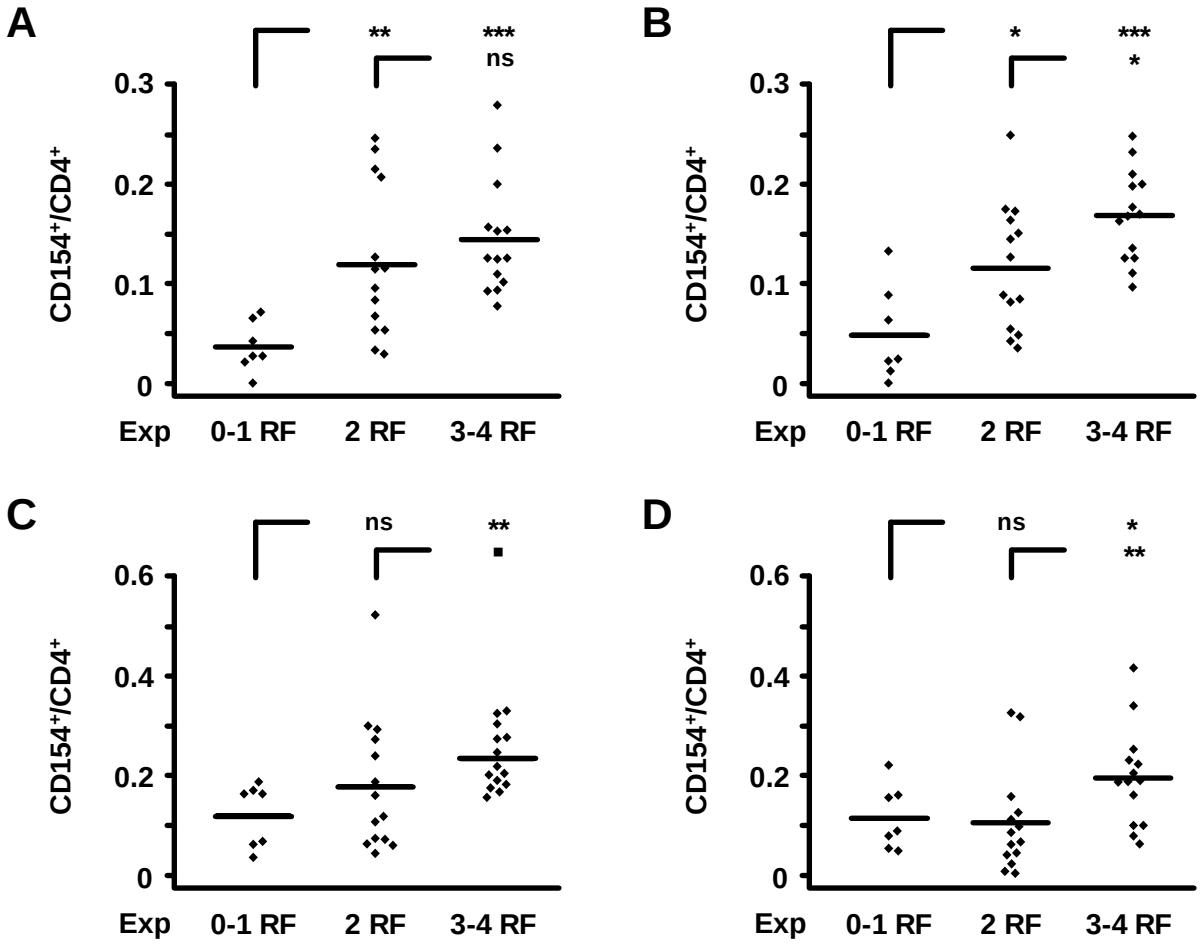

Figure 2: Frequencies of mold specific CD154⁺/CD4⁺ T-cells depending on the amount of risk factors for occupational or residential mold exposure

The diagrams show individual (n = 35, cohort 1) *A. fumigatus* (**A**), *R. arrhizus* (**B**), *R. pusillus* (**C**), and *C. bertholletiae* (**D**) specific T-cell frequencies in dependency of the number of positive risk factor (RF) categories for mold exposure (as described in Wurster et al., 2017a). Black bars represent arithmetic means. The two-sided Mann-Whitney-U test was used for significance testing. ■ $p < 0.1$, * $p < 0.05$, ** $p < 0.01$, *** $p < 0.001$.

Correlation of Aspergillus and Mucorales specific T-cell frequencies in healthy subjects

Comparing *A. fumigatus* and Mucorales specific T-cell frequencies, significant positive correlation was found (**Figure 3**). Coefficients of correlation between *A. fumigatus* and Mucorales specific CD154⁺/CD4⁺ cell numbers ranged from 0.48 (*C. bertholletiae*, $p = 0.004$) to 0.79 (*R. arrhizus*, $p < 0.001$). Between the studied Mucorales species, coefficients of correlation ranged from 0.59 ($p = 0.002$) to 0.65 ($p < 0.001$).

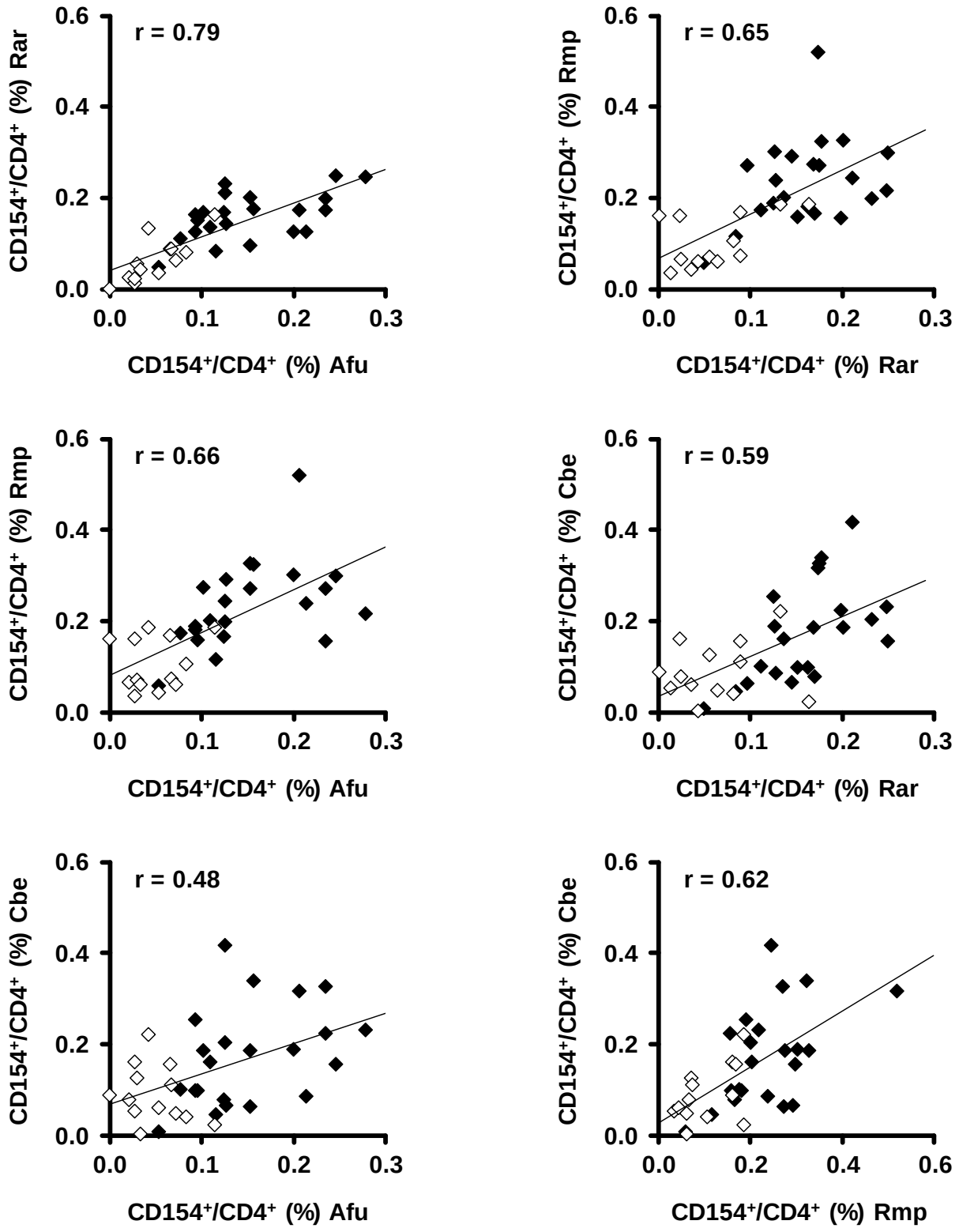

Figure 3: Correlation of *A. fumigatus* and Mucorales specific T-cell frequencies

Coefficients of correlation (r) were determined for individual frequencies of *A. fumigatus* (Afu), *R. arrhizus* (Rar), *R. pusillus* (Rmp), and *C. bertholletiae* (Cbe) specific T-helper cells. Black and white diamonds represent the high (n = 22) and low (n = 13) exposure cohort, respectively. Coefficients of correlation (r) are given in the charts.

To confirm these observations and to characterize phenotypes of T-helper cells upregulating CD154 in response to *A. fumigatus* or *R. arrhizus* lysates, 20 additional subjects were enrolled (**Table 1**, cohort 2). Similar to the first cohort, highly exposed subjects showed markedly greater *A. fumigatus* and *R. arrhizus* specific T-cell frequencies, with a coefficient of correlation of 0.61 (**Figure 4A**). Importantly, $CD154^+$ CMV-specific (pp65 + IE1) T-cell frequencies neither correlated with the subjects' mold exposure profiles nor with mold reactive T-cell frequencies (**Figure 4B**).

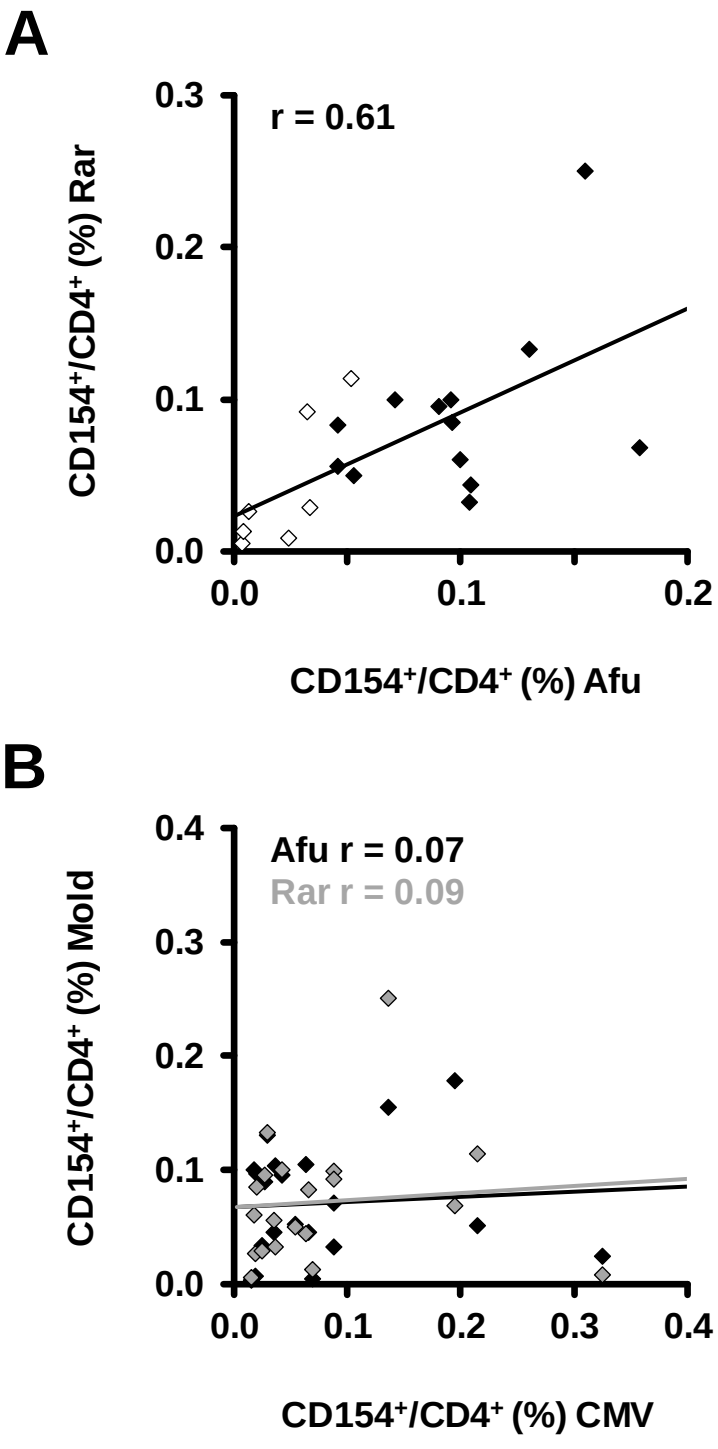

Figure 4: Comparison of mold and CMV specific T-cells in a second cohort of 20 donors

A. fumigatus, *R. arrhizus*, and CMV pp65 + IE-1 specific T-cell frequencies were determined in a second cohort of 20 additional donors. Correlation of *A. fumigatus* and *R. arrhizus* specific T-cells (**A**) as well as mold and CMV specific T-cells (**B**) was analyzed. Black and white diamonds represent the high (n = 13) and low (n = 7) exposure cohort, respectively. Coefficients of correlation (r) are given in the charts.

CCR7/CD45RO Phenotype of A. fumigatus and Mucorales specific T-helper cells

CCR7 and CD45RO phenotypes of $CD4^+CD154^+$ mold specific T-helper cells were assessed in the second cohort (n = 20). Significantly higher mean numbers of *A. fumigatus* reactive $CCR7^-CD45RO^+$ effector memory T-cells (0.031 % vs. 0.006 %, $p < 0.001$), $CCR7^+CD45RO^+$ central memory T-cells (0.034 % vs. 0.010 %, $p = 0.002$), and $CCR7^+CD45RO^-$ naïve T-cells (0.039 % vs. 0.019 %, $p = 0.018$) were found in highly exposed donors (**Figure 5A**). These data indicate that memory and naïve T-cells similarly contribute to elevated *A. fumigatus* specific T-cell frequencies in highly exposed subjects. For *R. arrhizus* specific T-cells, elevations of central (0.029 % vs. 0.013 %, $p = 0.082$) and effector memory cells (0.023 % vs. 0.011 %, $p = 0.052$) were found in donors with high mold exposure, whereas specific naïve T-cell frequencies were only slightly increased (**Figure 5B**). *A. fumigatus* and *R. arrhizus* specific $CCR7^-CD45RO^-$ effector T-cell frequencies did not significantly depend on the subjects' mold exposure profiles.

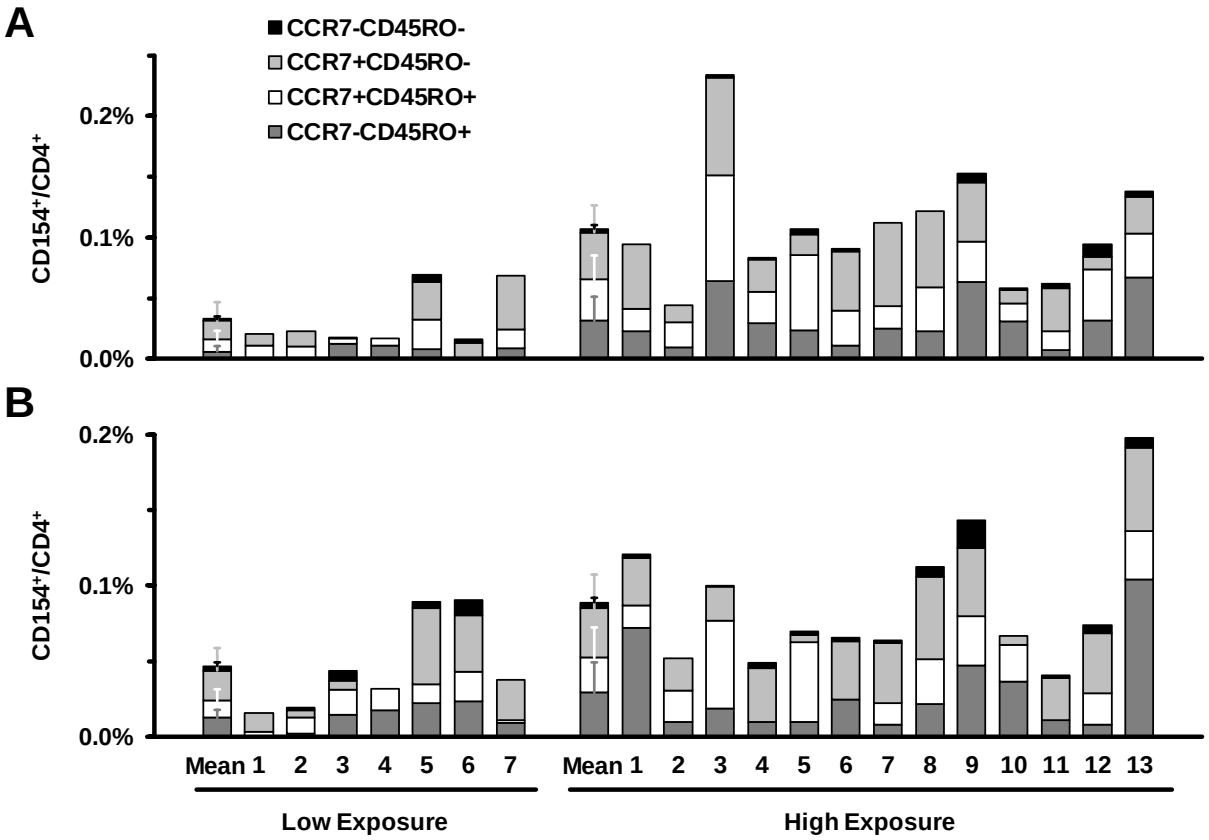

Figure 5: Characterization of CCR7/CD45RO profiles of mold specific T-helper cells in dependency of the subjects' exposure profiles

CCR7 and CD45RO phenotypes of $CD154^+/CD4^+$ *A. fumigatus* (A) and *R. arrhizus* (B) specific T-cells were comparatively assessed in subjects with low (n = 7) or high (n = 13) mold exposure profiles. Mean values and standard deviations are shown in the left column of each group.

Cytokine profiles of lysate stimulated PBMCs and their classification performance

Cytokine concentrations in the culture medium were assessed upon PBMC stimulation with *A. fumigatus* and *R. arrhizus* lysates. Comparing cytokine response patterns and the subjects' mold exposure profiles, significantly greater elevations of IL-5 and IL-17A and a tendency towards higher IL-13 levels were found in *A. fumigatus* lysate stimulated PBMC samples from highly exposed donors (**Figure 6A, Supplementary Table 4**). For *R. arrhizus* stimulation, more than 2-fold greater mean levels of IFN-γ, TNF-α, IL-5, IL-1β, and IL-17A were observed in PBMC supernatants from highly exposed subjects, though statistical significance was not reached (**Figure 6B, Supplementary Table 4**).

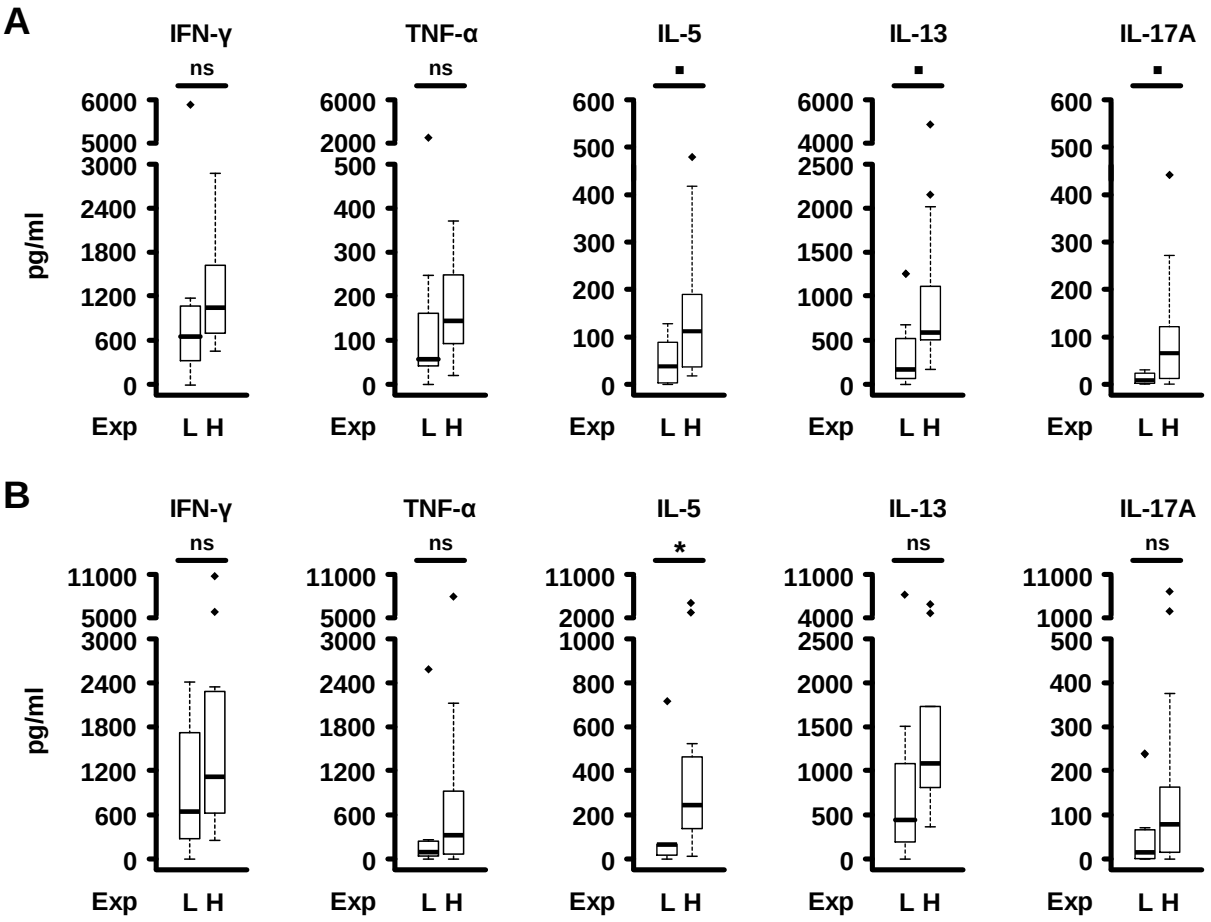

Figure 6: Cytokine secretion of PBMCs stimulated with *A. fumigatus* or *R. arrhizus* lysates in dependency of the subjects' mold exposure profiles

PBMCs isolated from 20 healthy adults (cohort 2, 7 low exposure and 13 high exposure subjects) were stimulated with α-CD28 and *A. fumigatus* (**A**) or *R. arrhizus* (**B**) mycelial lysates. Concentrations of cytokines in the culture medium were determined using a 13-plex T-cell cytokine panel. Cytokine concentrations of unspecific background controls (α-CD28 only) were deduced from lysate stimulated measurements. Box-whisker plots represent minimum, first quartile, median, third quartile, and maximum values of both cohorts. Outliers exceeding the 1.5-fold inter-quartile-range are shown individually. The two-sided Mann-Whitney-U test was used for significance testing. ■ $p < 0.1$, * $p < 0.05$, ** $p < 0.01$, *** $p < 0.001$. Raw data of cytokines not included in the figure are provided in **Supplementary Table 4**.

Logistic regression analyses were performed to determine the classification performance of cytokine concentrations alone or in combination with $CD154^+/CD4^+$ specific T-cell frequencies (**Figure 7**). Using the *A. fumigatus* lysate, $CD154^+/CD4^+$ frequencies alone showed a 95 % internal accuracy and 85 % cross-validation accuracy ($p < 0.001$, **Figure 7A**), followed by IL-13 (80 % / 75 %) and IL-5 (75 % / 70 %). Combination of $CD154^+/CD4^+$ frequencies and IL-5 concentrations led to a 5 %

increase of prediction performance of exposure profiles in the cross-validation procedure (90 %, $p < 0.05$, **Figure 7B**). Whereas TNF-α alone showed poor classification accuracy, its combination with specific T-cell frequencies also resulted in a 90 % prediction performance ($p < 0.05$). Inclusion of other cytokines did not lead to an improved predictive power compared with CD154 alone. Stimulating samples with the *R. arrhizus* lysate, internal and cross-validation performance of $CD154^+/CD4^+$ frequencies were 85 % and 75%, respectively (**Figure 7C**, $p < 0.05$). Addition of IL-17A increased predictive power in 10-fold cross-validation to 80 % ($p < 0.01$, **Figure 7D**).

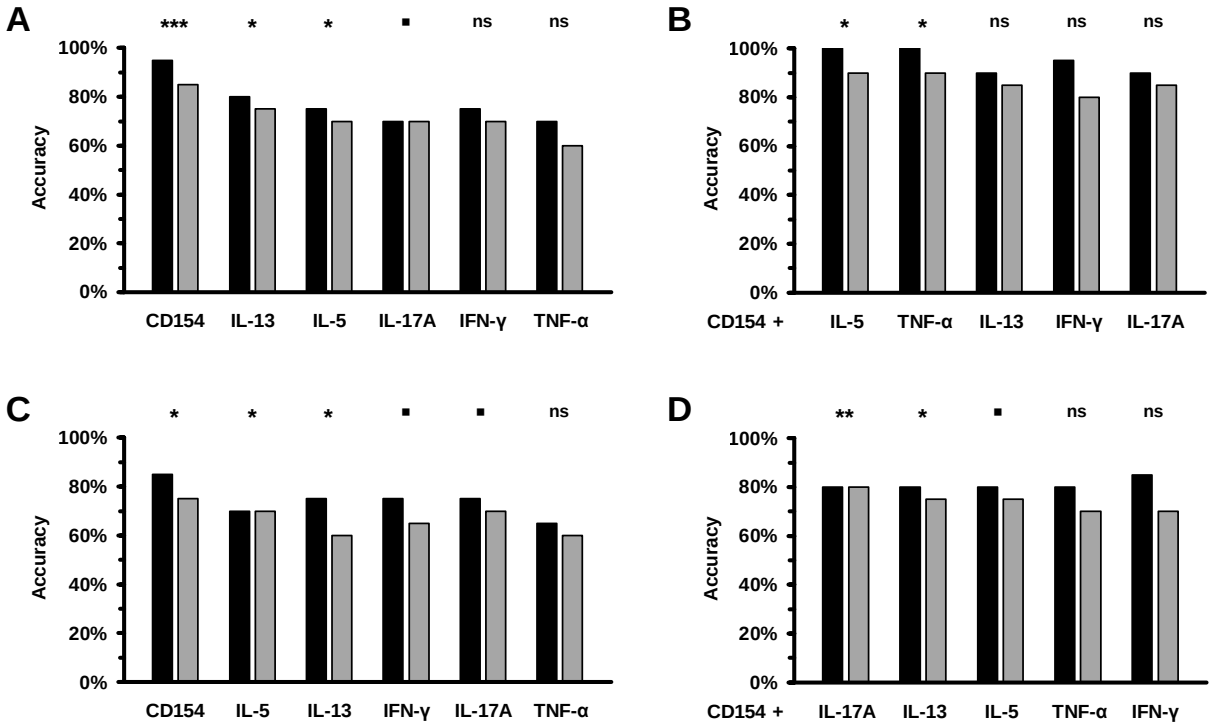

Figure 7: Univariate und bivariate prediction accuracy of exposure profiles

Logistic regression analyses were performed to determine internal (black columns) and 10-fold cross-validation accuracy (grey columns) for each cytokine marker or $CD154^+/CD4^+$ frequencies ("CD154") alone (**A**: *A. fumigatus*, **C**: *R. arrhizus*) and cytokines combined with $CD154^+/CD4^+$ frequencies (**B**: *A. fumigatus*, **D**: *R. arrhizus*). Asterisks indicate significance of regression coefficients based on likelihood ratio tests for each marker alone and cytokine effects adjusted for the CD154 measurements. ■ $p < 0.1$, * $p < 0.05$, ** $p < 0.01$, *** $p < 0.001$.

Discussion

Humans constantly inhale airborne mold spores from environmental sources. Sensitization to molds is a major risk factor for developing asthma, hypersensitivity pneumonitis, and allergic fungal rhinosinusitis (Hulin et al., 2013; Jacob et al., 2002; Mendell et al., 2011; Verhoeff & Burge, 1997). A significant portion of asthma and hypersensitivity pneumonitis incidence in adults is attributable to occupational mold exposure (Denning et al., 2014; Quirce et al., 2016), particularly common in farmers (Kotimaa et al., 1984; Liu et al., 2015) and wood workers (Faerden et al., 2014; Halpin et al., 1994). On the other hand, inhalative mold exposure of immunocompromised patients can result in life-threatening infections including invasive aspergillosis and mucormycosis.

The mammalian T-cell system, co-evolved with fungal commensals, is crucial to maintain a balanced immune status preventing both invasive infections and hypersensitivity (Romani, 2011). Several studies focused on the quantification and characterization of mold specific T-cell responses in healthy subjects (Wurster et al., 2017a; Stuehler et al., 2015) or patients with a wide spectrum of medical conditions ranging from invasive mold infections (Bacher et al., 2015a; Potenza et al., 2011, 2013, and 2016) to mold related hypersensitivity syndromes (Jolink et al., 2015; Pant & Macardle, 2014). Though allergic syndromes are hard-wired to environmental mold exposure and humoral immunity was extensively characterized (Cano-Jimenez et al., 2017; Edmondson et al., 2009; Rognon et al., 2015), the crosslink between mold encounter and specific T-helper cell frequencies and phenotypes is poorly studied.

We have previously reported that subjects with intensive mold exposure in their occupational or residential surrounding exhibit elevated numbers of *A. fumigatus* specific T-helper cells (Wurster et al., 2017a). Corroborating these data in two additional cohorts, the present study also provides evidence of elevated Mucorales specific T-cell frequencies in dependency of environmental mold exposure. This observation was surprising, given that Mucorales spore concentrations in indoor and outdoor air sampling studies tend to be low and subject to seasonal variation (Klaric & Pepeljnjak, 2005; Richardson, 2009; Shelton et al., 2007). There is, however, ample evidence that Mucorales exposure and transmission are associated with specific environmental niches and occupational settings including construction work,

ventilation systems, potted plant soil, poultry facilities, and decaying organic matter (Ribes et al., 2002; Richardson, 2009). Low baseline spore concentrations in ambient air in combination with specific residential and occupational exposure scenarios appear to provide a favorable constellation for bio-effect monitoring using immune markers. In contrast to the other tested species, *C. bertholletiae* specific T-cell frequencies showed considerable overlap of interquartile ranges of high and low exposure cohorts, which may be attributable to the large spore diameter (7-14 µm, Nimmo et al., 1988) limiting penetration into the terminal bronchioles and alveoli.

In both cohorts assessed in this study, considerable correlation of *A. fumigatus* and Mucorales specific T-cell frequencies was observed. A number of earlier studies provided insights in T-cell cross-reactivity among clinically important molds and yeasts. Schmidt and colleagues (Schmidt et al., 2012) showed that *R. arrhizus* specific $CD4^+$ lymphocytes elicit significant IFN-γ response when restimulated with *R. pusillus*, *Rhizopus microsporus*, or *Candida albicans*. Enriched *A. fumigatus* specific T-helper cells cross-react to clinical isolates of several molds and yeasts (Jolink et al., 2015; Bacher et al., 2015b). In addition, highly exposed subjects often encounter various molds including *Aspergillus* and Mucorales, which possess similar environmental niches (Garcia-Cela et al., 2015; Yamamoto et al., 2011; Zielinska-Jankiewicz et al., 2008), possibly resulting in enhanced T-helper cell response against multiple fungi. This hypothesis is supported by studies of humoral immunity documenting enhanced humoral response to various molds in exposed subjects (Gamboa et al., 2005; Sterclova et al., 2011).

While CD154-based flow cytometry provides a global assessment of the total antigen reactive T-helper cell repertoire, the present study also compared cytokine release from PBMCs stimulated with lysates of *A. fumigatus* and *R. arrhizus*, representing the most common human pathogenic Ascomycetes and Mucorales species. Previous reports documented significant antigen-dependent heterogeneity of cytokine release from T-cells (Bacher et al., 2013; Zielinski et al., 2012) or PBMCs (Simms et al., 2013). Moreover, markedly distinct influence of mold exposure on cytokine response patterns to different molds has been documented. For example, significantly greater IL-8 and IL-1β secretion in PBMC samples stimulated with *A. versicolor* was found in subjects with visible mold contamination of their domicile (Punsmann et al., 2013), whereas others described reduced pro-inflammatory cytokine response to *Penicillium*

chrysogenum and *Cladosporium herbarum* spores in exposed subjects (Rosenblum Lichtenstein et al., 2015).

Despite of previously documented morphotype-dependent differences in cytokine response of mononuclear cells to *Aspergillus* and Mucorales (Wurster et al., 2017b), the present study, using mycelial lysates, found largely similar cytokine signatures of stimulated PBMCs. Induction of T_H1 cytokines IFN-γ and TNF-α was paralleled by even higher fold changes of IL-5, IL-13, and IL-17 in highly exposed subjects. For *A. fumigatus*, these findings are in line with previous reports documenting induction of IL-5, IL-13, and IL-17 in fungal hypersensitivity pneumonitis, bronchopulmonary aspergillosis, and in response to mold exposure. For example, a T_H17-dominant phenotype was reported in lung derived *A. fumigatus* specific T-cells (Jolink et al., 2017) and repeated intranasal challenge of mice with *A. fumigatus* conidia resulted in sustained IL-17 induction driving a T_H2 polarized inflammatory response (Murdock et al., 2012). Others reported significantly increased IL-5 levels after inhalative challenge of patients with fungus-related hypersensitivity pneumonitis (Villar et al., 2014). Stimulation of PBMCs with *A. fumigatus* was found to induce strong IL-5 and IL-13 response to *A. fumigatus* conidia, whereas *C. albicans*, bacterial pathogens, fungal cell wall components, and synthetic PRR agonists did not alter the expression of these cytokines (Becker et al., 2015). The authors also described increased *A. fumigatus*-induced IL-5 and IL-13 levels, as well as elevated T_H2/T_H1 ratios in patients with ABPA or *Aspergillus*-associated asthma (Becker et al., 2015), corroborated by another study demonstrating a T_H2-polarized response to *A. fumigatus* antigens in ABPA patients (Jolink et al., 2015).

As of yet few studies are available on cytokine profiles of Mucorales specific T-cells. Potenza et al. (2011 and 2016) reported increased levels of IL-4 and IL-10 producing T-cells in patients with invasive mucormycosis or possible IM, indicating a T_H2-polarized phenotype. In healthy donors or non-IM patients, strong proinflammatory cytokine release of human PBMCs and T_H1-polarized T-cell response were observed, enhancing phagocytic activity and dendritic cell maturation marker expression (Potenza et al., 2016; Schmidt et al., 2012; Wurster et al., 2017b). Accordingly, greater absolute levels of TNF-α and IL-1β were found in the present study in response to *R. arrhizus* stimulation, whereas T_H2 and T_H17 cytokines were superior in the discrimination of high and low exposure subjects.

Though statistical significance was reached for few cytokine parameters individually, combined CD154-based antigen specific T-helper cell quantification and measurement of cytokine concentrations led to significantly improved classification performance of exposure profiles compared with $CD154^+/CD4^+$ T-cell frequencies alone. Combination of CD154 flow cytometry and the single best cytokine readout identified by bivariate logistic regression analysis resulted in a predictive performance (10-fold cross-validation) of 90 % for *A. fumigatus* (CD154 + IL-5) and 80 % for *R. arrhizus* (CD154 + IL-17A) stimulation, suggesting promising potential in the assessment of environmental mold exposure. The better performance of the *A. fumigatus* lysate is likely to be attributable to its commercial availability, guaranteeing lower inter-batch variability and higher quality control standards compared with the self-produced Mucorales lysates.

Naturally, the application of specific T-cell frequencies and PBMC cytokines in the evaluation of environmental mold exposure requires further validation in relevant patient cohorts and direct comparison with immunoglobulin markers. Our findings may contribute to a more streamlined study design facilitating less-expensive readout methods such as ELISPOT, intracellular cytokine staining, or standard ELISA assays. Moreover, this study highlights that environmental exposure needs to be considered as a potential confounder in approaches evaluating specific T-cell responses as a supportive biomarker in invasive mycoses (Bacher et al., 2015; Potenza et al., 2011, 2013, 2016).

Undoubtedly, functional T-cell analyses pose logistic challenges including long stimulation periods for reliable IL-5, IL-13, and IL-17 detection (Jeurink et al., 2008; Jolink et al., 2015) and impaired performance of specific T-cell detection after pre-analytic storage or cryopreservation (Lauruschkat et al., 2018; Wurster et al., 2017c). However, the availability of more sensitive and robust whole blood based techniques for mold specific T-cell quantification (Page et al., 2017) and evaluation of cytokine profiles (Brunet et al., 2016) as well as the development of multiplex ELISPOT and FLUOROSPOT assays (Janetzki et al., 2014) greatly contribute to the feasibility and standardization of T-cell based immune monitoring.

References

Bacher P, Schink C, Teutschbein J, Kniemeyer O, Assenmacher M, Brakhage AA, Scheffold A. 2013. Antigen-reactive T cell enrichment for direct, high-resolution analysis of the human naive and memory Th cell repertoire. J Immunol 190:3967-3976.

Bacher P, Steinbach A, Kniemeyer O, Hamprecht A, Assenmacher M, Vehreschild MJ, Vehreschild JJ, Brakhage AA, Cornely OA, Scheffold A. 2015a. Fungus-specific CD4(+) T cells for rapid identification of invasive pulmonary mold infection. Am J Respir Crit Care Med 191:348-352.

Bacher P, Jochheim-Richter A, Mockel-Tenbrink N, Kniemeyer O, Wingenfeld E, Alex R, Ortigao A, Karpova D, Lehrnbecher T, Ullmann AJ, Hamprecht A, Cornely O, Brakhage AA, Assenmacher M, Bonig H, Scheffold A. 2015b. Clinical-scale isolation of the total Aspergillus fumigatus-reactive T-helper cell repertoire for adoptive transfer. Cytotherapy 17:1396-1405.

Becker KL, Gresnigt MS, Smeekens SP, Jacobs CW, Magis-Escurra C, Jaeger M, Wang X, Lubbers R, Oosting M, Joosten LA, Netea MG, Reijers MH, van de Veerdonk FL. 2015. Pattern recognition pathways leading to a Th2 cytokine bias in allergic bronchopulmonary aspergillosis patients. Clin Exp Allergy 45:423-437.

Bellanger AP, Reboux G, Murat JB, Bex V, Millon L. 2010. Detection of Aspergillus fumigatus by quantitative polymerase chain reaction in air samples impacted on low-melt agar. Am J Infect Control 38:195-198.

Britten CM, Janetzki S, Butterfield LH, Ferrari G, Gouttefangeas C, Huber C, Kalos M, Levitsky HI, Maecker HT, Melief CJ, O'Donnell-Tormey J, Odunsi K, Old LJ, Ottenhoff TH, Ottensmeier C, Pawelec G, Roederer M, Roep BO, Romero P, van der Burg SH, Walter S, Hoos A, Davis MM. 2012. T cell assays and MIATA: the essential minimum for maximum impact. Immunity 37:1-2.

Brunet M, Millan Lopez O, Lopez-Hoyos M. 2016. T-Cell Cytokines as Predictive Markers of the Risk of Allograft Rejection. Ther Drug Monit 38 Suppl 1:S21-28.

Bush RK, Portnoy JM, Saxon A, Terr AI, Wood RA. 2006. The medical effects of mold exposure. J Allergy Clin Immunol 117:326-333.

Cano-Jimenez E, Rubal D, Perez de Llano LA, Mengual N, Castro-Anon O, Mendez L, Golpe R, Sanjuan P, Martin I, Veres A. 2017. Farmer's lung disease: Analysis of 75 cases. Med Clin (Barc) 149:429-435.

Cote J, Chan H, Brochu G, Chan-Yeung M. 1991. Occupational asthma caused by exposure to neurospora in a plywood factory worker. Br J Ind Med 48:279-282.

Daschner A. 2017. An Evolutionary-Based Framework for Analyzing Mold and Dampness-Associated Symptoms in DMHS. Front Immunol 7:672.

Denning DW, Pashley C, Hartl D, Wardlaw A, Godet C, Del Giacco S, Delhaes L, Sergejeva S. 2014. Fungal allergy in asthma-state of the art and research needs. Clin Transl Allergy 4:14.

Edmondson DA, Barrios CS, Brasel TL, Straus DC, Kurup VP, Fink JN. 2009. Immune response among patients exposed to molds. Int J Mol Sci 10:5471-5484.

Eduard W, Sandven P, Levy F. 1992. Relationships between exposure to spores from Rhizopus microsporus and Paecilomyces variotii and serum IgG antibodies in wood trimmers. Int Arch Allergy Immunol 97:274-282.

England AC, 3rd, Weinstein M, Ellner JJ, Ajello L. 1981. Two cases of rhinocerebral zygomycosis (mucormycosis) with common epidemiologic and environmental features. Am Rev Respir Dis 124:497-498.

Faerden K, Lund MB, Mogens Aalokken T, Eduard W, Sostrand P, Langard S, Kongerud J. 2014. Hypersensitivity pneumonitis in a cluster of sawmill workers: a 10-year follow-up of exposure, symptoms, and lung function. Int J Occup Environ Health 20:167-173.

Gamboa PM, Urbaneja F, Olaizola I, Boyra JA, Gonzalez G, Antepara I, Urrutia I, Jauregui I, Sanz ML. 2005. Specific IgG to Thermoactynomices vulgaris, Micropolyspora faeni and Aspergillus fumigatus in building workers exposed to esparto grass (plasterers) and in patients with esparto-induced hypersensitivity pneumonitis. J Investig Allergol Clin Immunol 15:17-21.

Garcia-Cela E, Crespo-Sempere A, Gil-Serna J, Porqueres A, Marin S. 2015. Fungal diversity, incidence and mycotoxin contamination in grapes from two agro-climatic Spanish regions with emphasis on Aspergillus species. J Sci Food Agric 95:1716-1729.

Halpin DM, Graneek BJ, Turner-Warwick M, Newman Taylor AJ. 1994. Extrinsic allergic alveolitis and asthma in a sawmill worker: case report and review of the literature. Occup Environ Med 51:160-164.

Hulin M, Moularat S, Kirchner S, Robine E, Mandin C, Annesi-Maesano I. 2013. Positive associations between respiratory outcomes and fungal index in rural inhabitants of a representative sample of French dwellings. Int J Hyg Environ Health 216:155-162.

Jacob B, Ritz B, Gehring U, Koch A, Bischof W, Wichmann HE, Heinrich J. 2002. Indoor exposure to molds and allergic sensitization. Environ Health Perspect 110:647-653.

Janetzki S, Rueger M, Dillenbeck T. 2014. Stepping up ELISpot: Multi-Level Analysis in FluoroSpot Assays. Cells 3:1102-1115.

Jeurink PV, Noguera CL, Savelkoul HF, Wichers HJ. 2008. Immunomodulatory capacity of fungal proteins on the cytokine production of human peripheral blood mononuclear cells. Int Immunopharmacol 8:1124-1133.

Jolink H, Meijssen IC, Hagedoorn RS, Arentshorst M, Drijfhout JW, Mulder A, Claas FH, van Dissel JT, Falkenburg JH, Heemskerk MH. 2013. Characterization of the T-cell-mediated immune response

against the Aspergillus fumigatus proteins Crf1 and catalase 1 in healthy individuals. J Infect Dis 208:847-856.

Jolink H, de Boer R, Willems LN, van Dissel JT, Falkenburg JH, Heemskerk MH. 2015. T helper 2 response in allergic bronchopulmonary aspergillosis is not driven by specific Aspergillus antigens. Allergy 70:1336-1339.

Jolink H, de Boer R, Hombrink P, Jonkers RE, van Dissel JT, Falkenburg JH, Heemskerk MH. 2017. Pulmonary immune responses against Aspergillus fumigatus are characterized by high frequencies of IL-17 producing T-cells. J Infect 74:81-88.

Klaric MS, Pepeljnjak S. 2005. [Beauvericin: chemical and biological aspects and occurrence]. Arh Hig Rada Toksikol 56:343-350.

Kotimaa MH, Husman KH, Terho EO, Mustonen MH. 1984. Airborne molds and actinomycetes in the work environment of farmer's lung patients in Finland. Scand J Work Environ Health 10:115-119.

Lauruschkat CD, Wurster S, Page L, Lazariotou M, Dragan M, Weis P, Ullmann AJ, Einsele H, Löffler J. 2018. Susceptibility of A. fumigatus specific T-cell assays to pre-analytic blood storage and PBMC cryopreservation greatly depends on readout platform and analytes. Mycoses. doi: 10.1111/myc.12780. [Epub ahead of print]

Liu S, Chen D, Fu S, Ren Y, Wang L, Zhang Y, Zhao M, He X, Wang X. 2015. Prevalence and risk factors for farmer's lung in greenhouse farmers: an epidemiological study of 5,880 farmers from Northeast China. Cell Biochem Biophys 71(2):1051-1057.

Lueg EA, Ballagh RH, Forte V. 1996. Analysis of the recent cluster of invasive fungal sinusitis at the Toronto Hospital for Sick Children. J Otolaryngol 25:366-370.

Madney Y, Khedr R, Al-Mahellawy H, Adel N, Taha H, Zaki I, Youssef A, Taha G, Hassanain O, Hafez H. 2017. "Mucormycosis" the Emerging Global Threat; Overview and Treatment Outcome Among Pediatric Cancer Patients in Egypt. Blood, 130(Suppl 1), 4830.

Mendell MJ, Mirer AG, Cheung K, Tong M, Douwes J. 2011. Respiratory and allergic health effects of dampness, mold, and dampness-related agents: a review of the epidemiologic evidence. Environ Health Perspect 119:748-756.

Murdock BJ, Falkowski NR, Shreiner AB, Sadighi Akha AA, McDonald RA, White ES, Toews GB, Huffnagle GB. 2012. Interleukin-17 drives pulmonary eosinophilia following repeated exposure to Aspergillus fumigatus conidia. Infect Immun 80:1424-1436.

Nimmo GR, Whiting RF, Strong RW. 1988. Disseminated mucormycosis due to Cunninghamella bertholletiae in a liver transplant recipient. Postgrad Med J 64:82-84.

Page L, Wurster S, Weis P, Helm J, Lazariotou M, Einsele H, Ullmann AJ. 2017. Evaluation of a whole blood based approach for the determination of mould reactive T-cell quantification and its susceptibility to pre-analytic delays. Mycoses 60(Suppl. 2):115.

Pant H, Macardle P. 2014. CD8(+) T cells implicated in the pathogenesis of allergic fungal rhinosinusitis. Allergy Rhinol (Providence) 5:146-156.

Park SJ, Mehrad B. 2009. Innate immunity to Aspergillus species. Clin Microbiol Rev 22:535-551.

Potenza L, Vallerini D, Barozzi P, Riva G, Forghieri F, Beauvais A, Beau R, Candoni A, Maertens J, Rossi G, Morselli M, Zanetti E, Quadrelli C, Codeluppi M, Guaraldi G, Pagano L, Caira M, Del Giovane C, Maccaferri M, Stefani A, Morandi U, Tazzioli G, Girardis M, Delia M, Specchia G, Longo G, Marasca R, Narni F, Merli F, Imovilli A, Apolone G, Carvalho A, Comoli P, Romani L, Latge JP, Luppi M. 2013. Characterization of specific immune responses to different Aspergillus antigens during the course of invasive Aspergillosis in hematologic patients. PLoS One 8:e74326.

Potenza L, Vallerini D, Barozzi P, Riva G, Forghieri F, Zanetti E, Quadrelli C, Candoni A, Maertens J, Rossi G, Morselli M, Codeluppi M, Paolini A, Maccaferri M, Del Giovane C, D'Amico R, Rumpianesi F, Pecorari M, Cavalleri F, Marasca R, Narni F, Luppi M. 2011. Mucorales-specific T cells emerge in the course of invasive mucormycosis and may be used as a surrogate diagnostic marker in high-risk patients. Blood 118:5416-5419.

Potenza L, Vallerini D, Barozzi P, Riva G, Gilioli A, Forghieri F, Candoni A, Cesaro S, Quadrelli C, Maertens J, Rossi G, Morselli M, Codeluppi M, Mussini C, Colaci E, Messerotti A, Paolini A, Maccaferri M, Fantuzzi V, Del Giovane C, Stefani A, Morandi U, Maffei R, Marasca R, Narni F, Fanin R, Comoli P, Romani L, Beauvais A, Viale PL, Latge JP, Lewis RE, Luppi M. 2016. Mucorales-Specific T Cells in Patients with Hematologic Malignancies. PLoS One 11:e0149108.

Prabhu RM, Patel R. 2004. Mucormycosis and entomophthoramycosis: a review of the clinical manifestations, diagnosis and treatment. Clin Microbiol Infect 10 Suppl 1:31-47.

Punsmann S, Liebers V, Stubel H, Bruning T, Raulf-Heimsoth M. 2013. Determination of inflammatory responses to Aspergillus versicolor and endotoxin with human cryo-preserved blood as a suitable tool. Int J Hyg Environ Health 216:402-407.

Quirce S, Vandenplas O, Campo P, Cruz MJ, de Blay F, Koschel D, Moscato G, Pala G, Raulf M, Sastre J, Siracusa A, Tarlo SM, Walusiak-Skorupa J, Cormier Y. 2016. Occupational hypersensitivity pneumonitis: an EAACI position paper. Allergy 71:765-779.

Ribes JA, Vanover-Sams CL, Baker DJ. 2000. Zygomycetes in human disease. Clin Microbiol Rev 13:236-301.

Richardson M. 2009. The ecology of the Zygomycetes and its impact on environmental exposure. Clin Microbiol Infect 15 Suppl 5:2-9.

Rognon B, Reboux G, Roussel S, Barrera C, Dalphin JC, Fellrath JM, Monod M, Millon L. 2015. Western blotting as a tool for the serodiagnosis of farmer's lung disease: validation with Lichtheimia corymbifera protein extracts. J Med Microbiol 64:359-368.

Romani L. 2011. Immunity to fungal infections. Nat Rev Immunol 11:275-288.

Rosenblum Lichtenstein JH, Hsu YH, Gavin IM, Donaghey TC, Molina RM, Thompson KJ, Chi CL, Gillis BS, Brain JD. 2015. Environmental mold and mycotoxin exposures elicit specific cytokine and chemokine responses. PLoS One 10:e0126926.

Schmidt S, Tramsen L, Perkhofer S, Lass-Florl C, Roger F, Schubert R, Lehrnbecher T. 2012. Characterization of the cellular immune responses to Rhizopus oryzae with potential impact on immunotherapeutic strategies in hematopoietic stem cell transplantation. J Infect Dis 206:135-139.

Shelton BG, Kirkland KH, Flanders WD, Morris GK. 2002. Profiles of airborne fungi in buildings and outdoor environments in the United States. Appl Environ Microbiol 68:1743-1753.

Simms E, Kjarsgaard M, Denis S, Hargreave FE, Nair P, Larche M. 2013. Cytokine responses of peripheral blood mononuclear cells to allergen do not identify asthma or asthma phenotypes. Clin Exp Allergy 43:1226-1235.

Sterclova M, Vasakova M, Metlicka M. 2011. Significance of specific IgG against sensitizing antigens in extrinsic allergic alveolitis: serological methods in EAA. Rev Port Pneumol 17:253-259.

Stuehler C, Nowakowska J, Bernardini C, Topp MS, Battegay M, Passweg J, Khanna N. 2015. Multispecific Aspergillus T cells selected by CD137 or CD154 induce protective immune responses against the most relevant mold infections. J Infect Dis 211:1251-1261.

Twaroch TE, Curin M, Valenta R, Swoboda I. 2015. Mold allergens in respiratory allergy: from structure to therapy. Allergy Asthma Immunol Res 7:205-220.

Verhoeff AP, Burge HA. 1997. Health risk assessment of fungi in home environments. Ann Allergy Asthma Immunol 78:544-554; quiz 555-546.

Villar A, Munoz X, Sanchez-Vidaurre S, Gomez-Olles S, Morell F, Cruz MJ. 2014. Bronchial inflammation in hypersensitivity pneumonitis after antigen-specific inhalation challenge. Respirology 19:891-899.

Walsh TJ, Groll A, Hiemenz J, Fleming R, Roilides E, Anaissie E. 2004. Infections due to emerging and uncommon medically important fungal pathogens. Clin Microbiol Infect 10 Suppl 1:48-66.

Weber J, Illi S, Nowak D, Schierl R, Holst O, von Mutius E, Ege MJ. 2015. Asthma and the hygiene hypothesis. Does cleanliness matter? Am J Respir Crit Care Med 191:522-529.

Woolnough K, Fairs A, Pashley CH, Wardlaw AJ. 2015. Allergic fungal airway disease: pathophysiologic and diagnostic considerations. Curr Opin Pulm Med 21:39-47.

Wurster S, Weis P, Page L, Helm J, Lazariotou M, Einsele H, Ullmann AJ. 2017a. Intra- and inter-individual variability of Aspergillus fumigatus reactive T-cell frequencies in healthy volunteers in dependency of mould exposure in residential and working environment. Mycoses 60:668-675.

Wurster S, Thielen V, Weis P, Walther P, Elias J, Waaga-Gasser AM, Dragan M, Dandekar T, Einsele H, Loffler J, Ullmann AJ. 2017b. Mucorales spores induce a proinflammatory cytokine response in human mononuclear phagocytes and harbor no rodlet hydrophobins. Virulence 8:1708-1718.

Wurster S, Weis P, Page L, Lazariotou M, Einsele H, Ullmann AJ. 2017c. Quantification of A. fumigatus-specific CD154+ T-cells-preanalytic considerations. Med Mycol 55:223-227.

Yamamoto N, Shendell DG, Peccia J. 2011. Assessing allergenic fungi in house dust by floor wipe sampling and quantitative PCR. Indoor Air 21:521-530.

Zielinska-Jankiewicz K, Kozajda A, Piotrowska M, Szadkowska-Stanczyk I. 2008. Microbiological contamination with moulds in work environment in libraries and archive storage facilities. Ann Agric Environ Med 15:71-78.

Zielinski CE, Mele F, Aschenbrenner D, Jarrossay D, Ronchi F, Gattorno M, Monticelli S, Lanzavecchia A, Sallusto F. 2012. Pathogen-induced human TH17 cells produce IFN-gamma or IL-10 and are regulated by IL-1beta. Nature 484:514-518.

Footnote Page

Acknowledgement

We want to thank the Institute for Hygiene and Microbiology Wuerzburg for provision of fungal strains.

Funding

This work was supported by the Interdisciplinary Centre for Clinical Research (IZKF) Wuerzburg (grant number Z-3/56 to SW) and the DFG Transregio 124 “Funginet” (project A2, to JL and HE, and project B2 to TD and MDi). Funding sources did not influence study design, data collection, and data analysis.

Disclosure of potential conflicts of interests

The authors have no conflicts of interest related to this study.

Meetings where the information has previously been presented

Preliminary data of this study have been presented at the European Congress of Clinical Microbiology and Infectious Diseases (ECCMID) 2017, Vienna, Austria.

Supplementary Materials

Module 1: Sample		
1.1	Essential donor info	55 healthy volunteers were enrolled (cohort 1: 35, cohort 2: 20). Demographic data are summarized in **Table 1**. Exclusion criteria: Signs and symptoms of acute or chronic infection, antimicrobial treatment within past 4 weeks, immunosuppressive treatment within past 12 weeks, diabetes mellitus, pregnancy.
1.2	Source of cell material	Venous whole blood
1.3	Collection methodology	Monovette® blood collection system + 19 G butterfly needle
1.4	Anti-coagulant	EDTA
1.5	Transportation / storage conditions for unprocessed samples	Venipuncture was performed in the laboratory and samples were processed within 30 min (no storage).
1.6	Cell processing methodology	PBMC isolation by ficoll gradient centrifugation
1.7	Median time and ranges from sample collection until end of cell processing	Time from blood collection until plating isolated PBMCs ranged from 75 to 100 min (Median: 80 min).
1.8	Cut-offs	PBMC isolation, cell counting, and plating had to be completed within 2 h after blood draw.
1.9	Fresh or cryopreserved	Fresh
1.10 - 1.14	Cryopreservation	n/a
1.15 - 1.18	Median cell yield and viability	Median yield of PBMC isolation: 2.46 x 10^6 PBMCs / ml whole blood. Median viability: > 99 % (determined by trypan blue exclusion).
1.19	Cut-offs	Viability after PBMC isolation > 95 %.
1.20	Cell counting methodology	Microscopic counting using a modified Neubauer chamber.
1.21	Additional assessments	n/a
Module 2: Assay		
2.1	Medium and serum details	RPMI 1640 (Gibco) + 5 % autologous heat-inactivated, sterile-filtered serum was used for PBMC culture and stimulation.
2.2	Pre-testing information	As sterile-filtered autologous serum was used, pre-testing was not necessary.
2.3	Treatment procedures of cells prior to assay	Described in Methods section
2.4	Sufficient assay details	
2.5	Internal assay controls	1 µg/ml α-CD28 were used as unspecific background control and reactive T-cell frequencies were deduced from all antigen stimulated measurements. Positive controls stimulated with PMA & ionomycin were used for adjusting instrument settings and confirmation of proper

		cell stimulation.
2.6	Acceptance criteria	Unspecific background of $CD154^+/CD4^+$ cells samples stimulated with α-CD28 only must not exceed 0.07 %.
2.7	External reference samples	n/a
2.8	Assay acceptance criteria	n/a
Module 3: Data acquisition		
3.1	Equipment and software	FACS Calibur & Cell Quest Pro Software (BD)
3.2	Basic equipment settings	Acquisition will stop when 100000 in G1=R1 (lymphocyte gate according to FSC/SSC properties), resolution: 1024. Compensation was performed individually for each donor.
3.3	Detailed gating strategy	**Sup. Fig. 1 and 2**
3.4	Representative data set	
3.5	Mean, median, ranges of event counts for relevant populations	Relevant populations and statistical details are summarized in **Sup. Table 2 and 3**.
3.6	Unusual strategies explained	n/a
3.7	Review of raw data	Raw data were reviewed by at least two authors.
Module 4: Results		
4.1	Background and ag-specific reactivity levels	Unspecific background and antigen-specific responses are summarized in **Sup. Table 2 and 3**.
4.2	Cut-off specifications	Unspecific background of $CD154^+/CD4^+$ cells samples stimulated with α-CD28 only must not exceed 0.07 %.
4.3	Accessibility of raw data	Donor record forms, flow cytometric files, and data printouts are stored onsite and were carefully reviewed by at least two authors. Relevant raw data are summarized in **Sup. Table 2 and 3**.
4.4	Definition of positive reactivity (above background) including tests applied	As mold reactive T-cells are detectable in most healthy donors, no cut-off specifications for reactivity were applied. In this study, reactive T-cells are defined as T-cells upregulating activation markers (e. g. CD154) upon stimulation with mycelial lysates + costimulatory factors, whereas specific T-cell frequencies are calculated by deducing unspecific background (costimulatory factors only) from *A. fumigatus* reactive T-cells numbers.
4.5	Parameters, software and version used for response determination	Analysis was performed using FlowJo vX.0.7.
4.6	Response definition predefined or post-hoc	n/a
4.7	Definition of response induced by treatment	n/a
4.8	Any data excluded and why	Two donors were excluded, one due to acute infection, and one for technical reasons (high unspecific background).
4.9	Why test was used	We have previously demonstrated that $CD154^+$ *A. fumigatus* specific T-cell frequencies are elevated in subjects with frequent mold exposure (Wurster et al., 2017a). This study sought to compare *Aspergillus* and

3.1 Evaluation of Aspergillus and Mucorales specific T-cells and peripheral blood mononuclear cell cytokine signatures as biomarkers of environmental mold exposure

		Mucorales specific T-cell frequencies, phenotypes, and PBMC cytokine responses.
Module 5: Laboratory		
5.1	Guidance of lab operations	Experiments were conducted under GLP principles. SOPs were prepared by SW and reviewed by all authors. Lab members were trained thoroughly. Process related parameters were documented in standardized case report forms.
5.2	Laboratory accreditations and certifications	n/a
5.3	Details on audits	n/a
5.4	Status of protocols	Monocentric study with SOPs followed by all authors.
5.5	Status of assays	The study was performed using qualified assays.
5.6	Specific performance criteria	n/a

Supplementary Table 1: MIATA sub-modules according to http://miataproject.org

			CD28	*A. fumigatus*	*R. arrhizus*	*R. pusillus*	*C. bertholl.*
Lymphocytes abs.	Low Exp.	Min	34358	48201	48875	48876	38654
		Median	49615	49753	49671	49653	49543
		Mean	48389	49622	49666	49661	48818
		Max	50426	50287	50367	50317	50516
	High Exp.	Min	40345	41745	48530	48665	48485
		Median	49214	49095	49397	49412	49305
		Mean	48607	48778	49416	49426	49318
		Max	50089	50482	50714	50487	50459
	All Donors	Min	34358	41745	48530	48665	38654
		Median	49308	49273	49492	49521	49389
		Mean	48526	49092	49509	49513	49132
		Max	50426	50482	50714	50487	50516
$CD4^+$ abs.	Low Exp.	Min	20830	20907	20411	20585	20654
		Median	25602	26922	26552	25714	25754
		Mean	26151	26991	26629	26581	26254
		Max	33448	33559	32885	32895	33091
	High Exp.	Min	16481	16719	16620	16356	16338
		Median	23249	23057	23243	22935	23510
		Mean	23702	23870	23777	23659	23728
		Max	30970	31436	31068	30872	31218
	All Donors	Min	16481	16719	16620	16356	16338
		Median	24067	24639	24697	24161	24001
		Mean	24612	25029	24836	24744	24666
		Max	33448	33559	32885	32895	33091
$CD4^+CD154^+$ abs.	Low Exp.	Min	0	6	5	12	3
		Median	3	15	14	28	30
		Mean	5	18	21	33	28
		Max	15	41	55	62	51
	High Exp.	Min	0	18	19	24	9
		Median	2	32	38	55	44
		Mean	2	38	40	56	43
		Max	13	88	77	89	96
	All Donors	Min	0	6	5	12	3
		Median	2	28	32	45	32
		Mean	3	31	33	48	37
		Max	15	88	77	89	96
$CD154^+/CD4^+$ (%)	Low Exp.	Min	0.000	0.022	0.016	0.039	0.012
		Median	0.014	0.061	0.057	0.114	0.102
		Mean	0.020	0.068	0.082	0.126	0.110
		Max	0.053	0.124	0.172	0.201	0.235
	High Exp.	Min	0.000	0.075	0.072	0.082	0.031
		Median	0.006	0.135	0.168	0.232	0.183
		Mean	0.009	0.159	0.169	0.245	0.184
		Max	0.059	0.293	0.269	0.531	0.428
	All Donors	Min	0.000	0.022	0.016	0.039	0.012
		Median	0.008	0.115	0.137	0.197	0.126
		Mean	0.013	0.126	0.137	0.201	0.156
		Max	0.059	0.293	0.269	0.531	0.428

Supplementary Table 2: Ranges of acquired event counts for lymphocytes, $CD4^+$ cells, $CD4^+CD154^+$ cells, and frequencies of $CD154^+/CD4^+$ cells in first cohort of 35 donors

			CD28	*A. fumigatus*	*R. arrhizus*	CMV pp65+IE-1
Lymphocytes abs.	Low Exp.	Min	80214	78855	82475	84687
		Median	99611	94143	100167	100426
		Mean	96947	92793	97112	97919
		Max	101243	101205	101144	101440
	High Exp.	Min	62777	73891	73533	89541
		Median	100016	100457	100559	100298
		Mean	95531	96932	97554	98785
		Max	101883	101455	101724	101945
	All Donors	Min	62777	73891	73533	84687
		Median	99813	100175	100505	100362
		Mean	96026	95484	97399	98482
		Max	101883	101455	101724	101945
$CD3^+CD4^+$ abs.	Low Exp.	Min	29773	28679	28844	30735
		Median	46147	48215	48130	47641
		Mean	45894	45292	45614	45942
		Max	58577	50860	58234	57513
	High Exp.	Min	27644	32095	31131	35983
		Median	46070	47263	45265	46050
		Mean	45280	46961	45329	47179
		Max	64482	64701	64536	64769
	All Donors	Min	27644	28679	28844	30735
		Median	46108	47265	46321	46353
		Mean	45495	46377	45429	46746
		Max	64482	64701	64536	64769
$CD3^+CD4^+CD154^+$ abs.	Low Exp.	Min	4	5	5	12
		Median	7	17	18	36
		Mean	7	16	23	56
		Max	9	35	65	162
	High Exp.	Min	2	23	24	15
		Median	6	49	44	26
		Mean	7	54	47	36
		Max	14	97	126	100
	All Donors	Min	2	5	5	12
		Median	7	37	39	28
		Mean	7	41	39	43
		Max	14	97	126	162
$CD154^+/CD4^+$ (%)	Low Exp.	Min	0.007	0.009	0.009	0.021
		Median	0.015	0.037	0.043	0.080
		Mean	0.015	0.037	0.056	0.123
		Max	0.027	0.069	0.131	0.339
	High Exp.	Min	0.003	0.062	0.055	0.026
		Median	0.017	0.108	0.098	0.064
		Mean	0.016	0.114	0.105	0.078
		Max	0.027	0.199	0.268	0.214
	All Donors	Min	0.003	0.009	0.009	0.021
		Median	0.017	0.082	0.085	0.065
		Mean	0.016	0.087	0.088	0.094
		Max	0.027	0.199	0.268	0.339

Supplementary Table 3: Ranges of acquired event counts for lymphocytes, $CD3^+CD4^+$ cells, $CD3^+CD4^+CD154^+$ cells, and frequencies of $CD154^+/CD3^+CD4^+$ cells in second cohort of 20 donors

3.1 Evaluation of Aspergillus and Mucorales specific T-cells and peripheral blood mononuclear cell cytokine signatures as biomarkers of environmental mold exposure

Lysate		*A. fumigatus*			*R. arrhizus*		
Exposure		Low (n = 7)	High (n = 13)	All (n = 20)	Low (n = 7)	High (n = 13)	All (n = 20)
IFN-γ	Min	0	1	0	0	1	0
	Median	655	1046	924	643	1114	934
	Mean	1329	1286	1301	1002	2258	1818
	Max	5852	2861	5852	2396	10644	10644
TNF-α	Min	0	1	0	0	0	0
	Median	57	143	120	94	323	218
	Mean	424	168	258	461	1140	903
	Max	2509	369	2509	2567	7922	7922
IL-1β	Min	0	0	0	0	0	0
	Median	1	16	11	2	4	4
	Mean	132	345	271	160	363	292
	Max	872	1738	1738	1104	4337	4337
IL-2	Min	0	0	0	0	0	0
	Median	107	110	108	254	13	51
	Mean	299	384	354	402	95	202
	Max	1080	2612	2612	1092	526	1092
IL-4	Min	0	0	0	0	0	0
	Median	4	24	23	0	0	0
	Mean	27	35	32	16	3	8
	Max	121	183	183	74	38	74
IL-5	Min	0	1	0	0	1	0
	Median	38	112	79	66	244	150
	Mean	50	150	115	135	794	563
	Max	128	479	479	708	4933	4933
IL-6	Min	0	1	0	0	1	0
	Median	71	212	159	70	401	289
	Mean	1686	2020	1903	2311	3122	2838
	Max	11227	9717	11227	11227	11307	11307
IL-10	Min	0	1	0	0	1	0
	Median	203	286	221	350	398	388
	Mean	389	368	375	646	619	629
	Max	1571	1377	1571	1719	1857	1857
IL-13	Min	0	1	0	0	1	0
	Median	169	586	565	442	1079	883
	Mean	370	1108	850	1485	1975	1803
	Max	1250	4817	4817	7412	5828	7412
IL-17A	Min	0	0	0	0	0	0
	Median	8	65	23	15	78	48
	Mean	13	104	72	55	221	163
	Max	30	441	441	236	1150	1150
IL-23	Min	0	0	0	0	0	0
	Median	0	0	0	0	2	2
	Mean	9	2	5	13	12	12
	Max	63	19	63	63	38	63
GM-CSF	Min	0	1	0	1	1	1
	Median	106	251	244	108	218	201
	Mean	187	272	242	309	444	397
	Max	513	665	665	1334	2123	2123

Supplementary Table 4: Concentrations of cytokines (pg/ml) in PBMC supernatants depending on exposure profiles (IL-12p70 values were < 5 pg/ml in all samples)

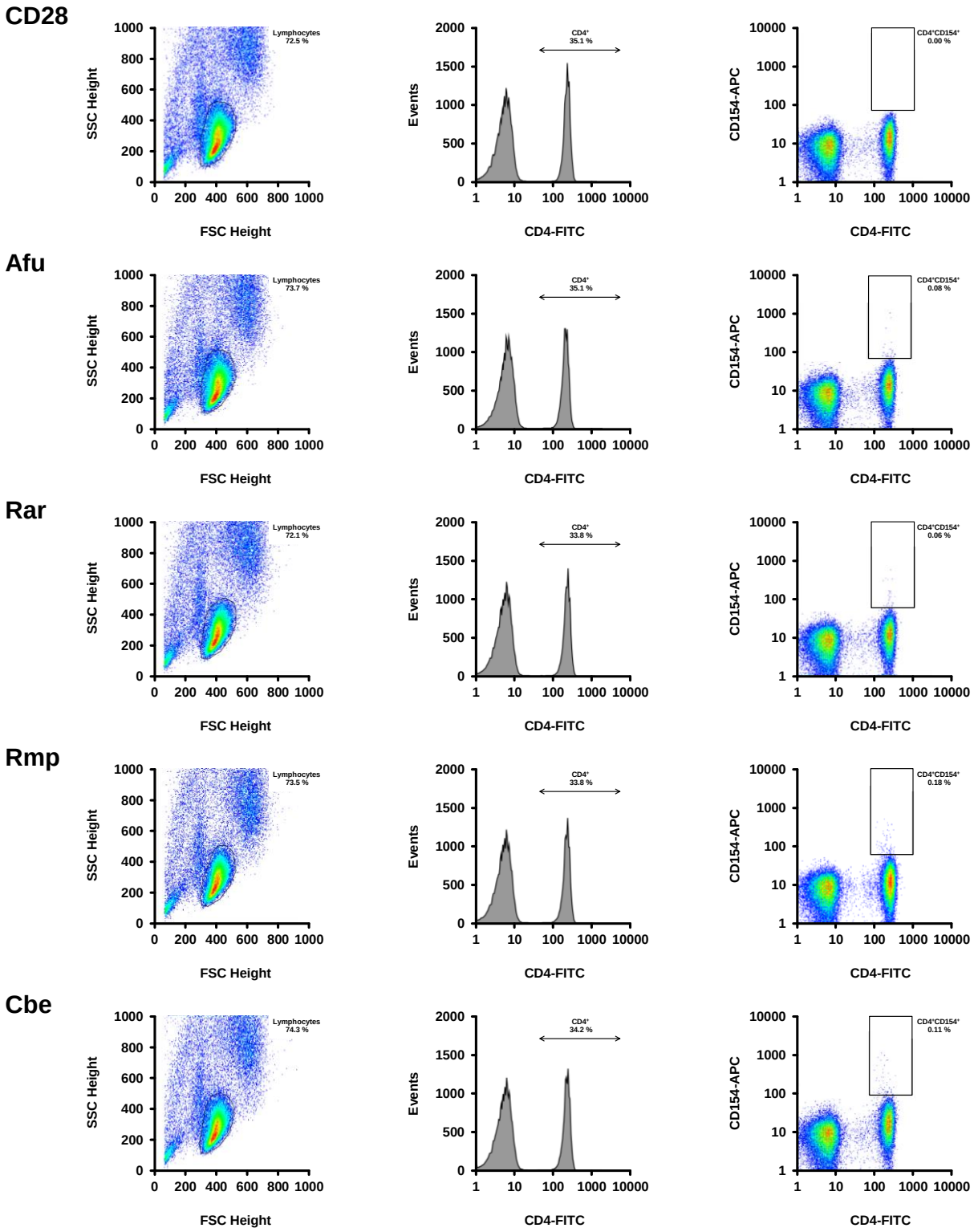

Supplementary Figure 1 → Gating strategy for enumeration of antigen specific T-cell frequencies (cohort 1)

Following surface staining with α-CD4-FITC and inside staining with α-CD154-APC, cells were resuspended in 200 µl HBSS. Measurement was performed on a FACS Calibur flow cytometer at low

acquisition speed (15 µl/min). 1 x 10^5 lymphocytes were acquired according to FSC/SSC properties. Using FlowJo software, the lymphocyte gate was adjusted precisely. $CD4^+$ cells were gated in a histogram plot. The $CD4^+CD154^+$ subset was determined using a CD4/CD154 pseudocolor plot. $CD4^+CD154^+$ events were divided by $CD4^+$ events to determine mold reactive T-cell frequencies and unspecific background. Mold specific T-cells frequencies were calculated by subtraction of unspecific background from mold reactive T-cell frequencies. CD28 = unspecific background control stimulated with α-CD28 only, Afu = *A. fumigatus*, Rar = *R. arrhizus*, Rmp = *R. pusillus*, Cbe = *C. bertholletiae*.

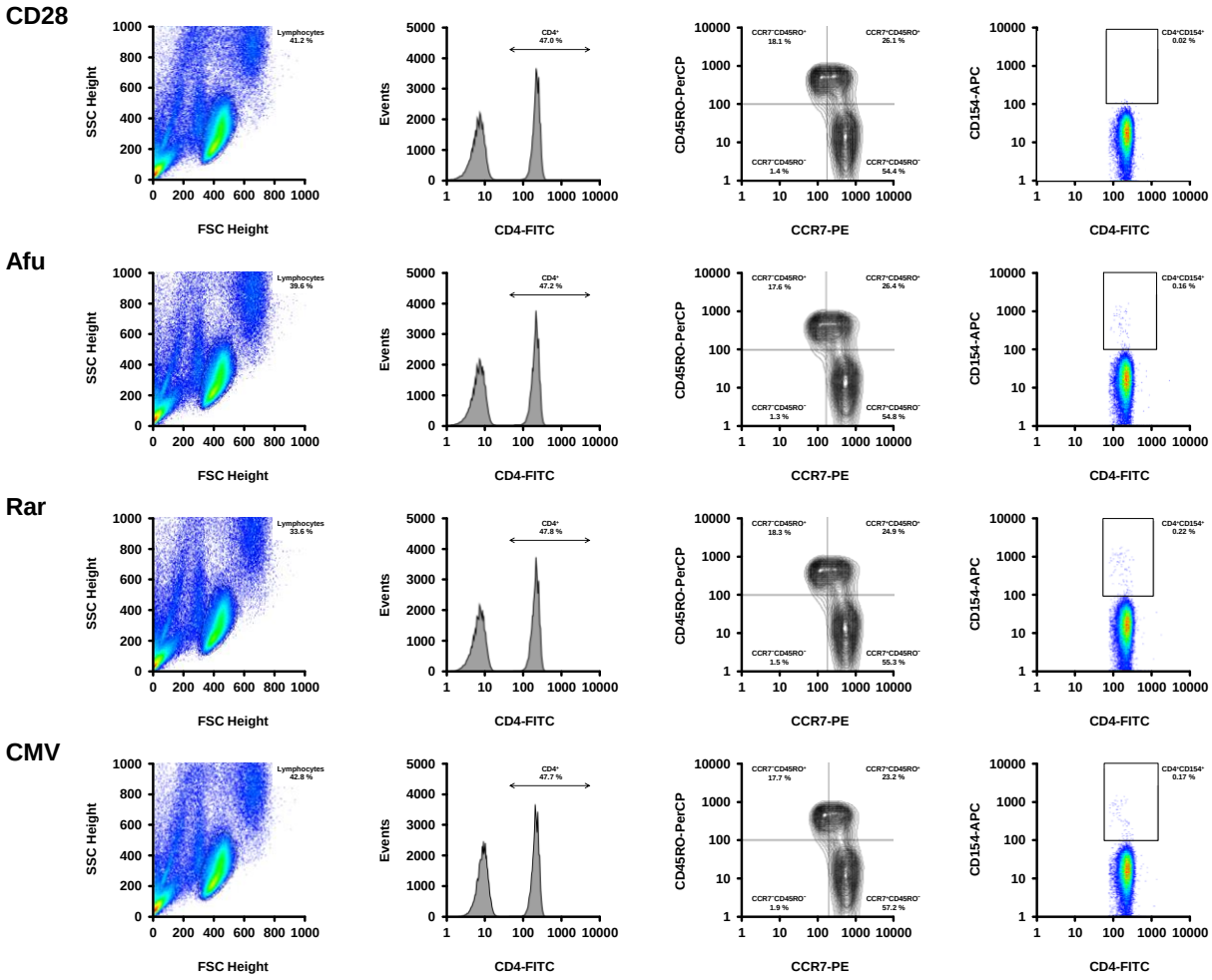

Supplementary Figure 2 → Gating strategy for determination of antigen specific T-cell frequencies and their CCR7/CD45RO phenotypes (cohort 2)

Following surface staining with α-CD4-FITC, α-CCR7-PE, and α-CD45RO-PerCP as well as inside staining with α-CD154-APC, cells were resuspended in 200 µl HBSS. Measurement was performed on a FACS Calibur flow cytometer at low acquisition speed (15 µl/min). 1 x 10^5 lymphocytes were acquired according to FSC/SSC properties. Using FlowJo software, the lymphocyte gate was adjusted precisely. $CD4^+$ cells were gated on a histogram plot. A CCR7/CD45RO quadrant gate was adjusted on a 2 % contour plot showing all $CD4^+$ events. $CD154^+$ cells were gated on a CD4/CD154 pseudocolor plot and the CCR7/CD45RO quadrant gate was applied to the $CD4^+CD154^+$ subset. CD28 = unspecific background control stimulated with α-CD28 only, Afu = *A. fumigatus*, Rar = *R. arrhizus*, CMV = pp65 + IE1 peptides.

3.2 Impact of immunosuppressive and antifungal drugs on PBMC- and whole blood-based flow cytometric CD154^{+} *Aspergillus fumigatus* specific T-cell quantification

Lukas Page[1], Chris D. Lauruschkat[1], Johanna Helm[1], Philipp Weis[1], Maria Lazariotou[1], Hermann Einsele[1], Andrew J. Ullmann[1], Juergen Loeffler[1], Sebastian Wurster[1,3,#]

[1] University Hospital of Wuerzburg, Department of Internal Medicine II, Division of Infectious Diseases, Wuerzburg, Germany

[2] The University of Texas MD Anderson Cancer Center, Department of Infectious Diseases, Houston, Texas, United States of America

Corresponding author: Sebastian Wurster, MD

The University of Texas MD Anderson Cancer Center

Department of Infectious Diseases, Infection Control and Employee Health

6565 MD Anderson Boulevard, Sheikh Zayed Building, Z8.3002

Houston, TX 77030, United States of America

Email address: stwurster@mdanderson.org

Phone: +1-713-563-1753

Abstract: 233 words

Main text (Original article): 3670 words

4 Figures, 4 Tables, 3 Supplementary Materials

Abstract

Flow cytometric quantification of $CD154^+$ mould specific T-cells in antigen-stimulated peripheral blood mononuclear cells (PBMCs) or whole blood has been described as a supportive biomarker to diagnose invasive mould infections and to monitor therapeutic outcomes. As patients at risk frequently receive immunosuppressive and antifungal medication, this study compared the matrix-dependent impact of representative drugs on $CD154^+$ T-cell detection rates. PBMCs and whole blood samples from healthy adults were pre-treated with therapeutic concentrations of liposomal amphotericin B, voriconazole, posaconazole, cyclosporine A (CsA) or prednisolone. Samples were then stimulated with an *Aspergillus fumigatus* lysate or a viral antigen cocktail (CPI) and assessed for $CD154^+$ T-helper cell frequencies. Specific T-cell detection rates and technical assay properties remained largely unaffected by exposure of both matrices to the studied antifungals. By contrast, CsA and prednisolone pre-treatment of isolated PBMCs and whole blood adversely impacted specific T-cell detection rates and caused elevated inter-replicate variation. Unexpectedly, the whole blood-based protocol that uses additional α-CD49d co-stimulation was less susceptible to CsA and prednisolone despite prolonged drug exposure in the test tube. Accordingly, addition of α-CD49d during PBMC stimulation partially attenuated the impact of immunosuppressive drugs on test performance. Translating these results into the clinical setting, false-negative results of $CD154^+$ antigen-specific T-cell quantification need to be considered in patients receiving T-cell-active immunosuppressive medication. Optimized co-stimulation regimes with α-CD49d could contribute to an improved feasibility of functional T-cell assays in immunocompromised patient populations.

Keywords

Antifungals, GvHD prophylaxis, *Aspergillus*, Biomarker, Flow cytometry, CD49d

Original article

Introduction

Humans are continuously confronted with airborne mould spores ubiquitously present in the environment (1). *Aspergillus fumigatus* remains the most frequent cause of life-threatening invasive mould infections in leukaemia patients or those requiring immunosuppressive therapy after hematopoietic stem cell or solid organ transplantation (2). The difficult and often delayed diagnosis is a major obstacle to reduce the significant mortality of invasive mould infections (3). Therefore, novel reliable diagnostic biomarkers remain a critical need in medical mycology (4-5).

Different laboratories established flow cytometric protocols or enzyme-linked immunospot assays to quantify T-lymphocyte responses to fungal antigens as a supportive approach to monitor invasive mycoses (6-10). $CD154^+$ mould-reactive T-cell detection showed promising potential in the diagnosis and therapeutic monitoring of invasive pulmonary mould infections (6, 10). However, conventional protocols based on isolated peripheral blood mononuclear cells (PBMCs) are highly susceptible to pre-analytical delays (11-14), complicating assay standardization and multi-centre studies, and exhibit considerable technical failure rates in haematological patient cohorts (10). To overcome these limitations, we have recently proposed a whole blood-based protocol with enhanced co-stimulation (15). A pilot study in healthy subjects revealed high technical reliability and superior detection rates of mould specific T-helper cells from whole blood, but the comparative applicability boundaries of both matrices remain to be defined (15).

Antigen-reactive lymphocyte assays crucially rely on cell viability and functional cellular interactions (13) that can be significantly modulated by the patient's concomitant medication. Both immunosuppressive (16-18) and antifungal (19-26) compounds diversely impact the *in vitro* response characteristics of a broad spectrum of leukocyte populations. However, their effect on the susceptibility of flow cytometric mould-reactive T-cell quantification depending on test matrix and co-stimulation is so far hardly investigated. Therefore, we compared the performance of flow cytometric $CD154^+$ *A. fumigatus*-specific T-cell quantification after exposure of PBMCs and whole blood samples to common immunosuppressive compounds and antifungal agents.

Material and Methods

Blood collection

54 ml EDTA blood (for PBMC isolation, + 15 ml autologous serum) or 36 ml Heparin-NH_4 blood (for whole blood assays) were collected from healthy volunteers with frequent mould exposure in their occupational or residential environment. Donors were screened for absence of acute or chronic infections, diabetes mellitus, immunosuppressive therapy, anti-infective agents, or pregnancy.

Isolation, drug exposure, and stimulation of PBMCs

PBMC isolation was performed by ficoll (Biochrom) gradient centrifugation. PBMCs were diluted in RPMI 1640 (+ GlutaMAX^{TM}, Gibco) containing 5 % autologous serum at a final concentration of 5 x 10^6 cells / ml. 2 ml aliquots of the cell suspension were seeded per well of a 6-well plate and exposed to antifungals or immunosuppressive drugs at the following, clinically relevant final concentrations: 50 µg/ml liposomal amphotericin B (AMB, Gilead), 5 µg/ml voriconazole (VRC, Pfizer), 4 µg/ml posaconazole (PCZ, Merck & Co.), 200 ng/ml cyclosporine A (CsA, Novartis), and 200 ng/ml prednisolone (mibe). Cells were incubated with the drugs for 3 h at 37 °C, 5 % CO_2. Thereafter, PBMCs were harvested, washed, and suspended in fresh medium at a concentration of 1 x 10^7 cells / ml. Importantly, non-drug exposed PBMCs for the reference measurement underwent the same re-collection and washing procedure to account for any procedure-related impact on specific T-cell detection rates. 100 µl aliquots of the cell suspensions were seeded per well of a 96-well plate. 5 µg *A. fumigatus* mycelial lysates (Miltenyi Biotec) and 0.1 µg α-CD28 ± 0.1 µg α-CD49d co-stimulatory antibody (Miltenyi Biotec) were added for cell stimulation. To determine unspecific background stimulation, control samples were treated with α-CD28 ± α-CD49d only. For selected experiments, cells were stimulated with 50 µg/ml cytomegalo-, parainfluenza-, and influenza virion antigen pool (CPI, C.T.L. Europe) in addition to co-stimulatory antibodies. After 2 h of incubation at 37 °C, 5 % CO_2, brefeldin A (Sigma) was added at a final concentration of 10 µg/ml, followed by another 18 h incubation period.

As an additional setting for direct comparison with the whole blood-based method (Fig. 4), EDTA blood was pre-treated with 200 ng/ml CsA or prednisolone for 2 h prior

to PBMC isolation. In this case, isolated PBMCs underwent no additional drug exposure, re-collection, and washing steps.

Drug treatment and stimulation of whole blood samples

For stimulation of whole blood samples, 2.7 ml blood collection tubes without anticoagulant (Sarstedt) were prepared with 0.5 µg α-CD28 and 0.5 µg α-CD49d costimulatory factors ± 25 µg mycelial lysate or 25 µg CPI pool (50 µg/ml) as previously described (15). The total reagent volume was adjusted to 50 µl by addition of RPMI 1640. 0.5 ml heparinized whole blood, supplemented with antifungals or immunosuppressive agents at the concentrations outlined above, was injected in each of the tubes using a graded 1 ml syringe. For selected experiments (Fig. 4), whole blood was pre-treated for 2 h with immunosuppressive agents prior to injection into the stimulation tubes instead of drug addition during antigen stimulation. Stimulation tubes were inverted ten times and incubated at 37 °C for 4 h. After addition of 10 µg/ml brefeldin A, tubes were incubated at 37 °C for another 18 h period.

Staining and flow cytometric analysis

Antibody staining was performed using the Inside Stain Kit, α-CD4-FITC, and α-CD154-APC (Miltenyi Biotec) according to the manufacturer's instructions. For selected experiments (Fig. 4), an extended panel was used consisting of 7-AAD Staining Solution (viability dye, Miltenyi Biotec), α-CD4-VioGreen, α-CD197 (CCR7)-FITC, α-CD45RA-APC-Vio 770, and α-CD69-VioBlue for surface staining, and α-IL-2-PE, α-IFN-γ-APC, as well as α-CD154-PE-Vio 770 for intracellular staining (all antibodies from Miltenyi Biotec). Prior to staining of whole blood, 0.5 ml of 0.5 M EDTA (Sigma) was added and erythrocytes were lysed using Buffer EL (Qiagen) as previously described (15). This study has been conducted in accordance with MIATA reporting requirements (27). The detailed workflow and quality control parameters are summarized in Appendix 1. Representative plots documenting the gating strategies are provided in Fig. 1B, Fig. 2B, and Appendix 2.

Statistics

To calculate the frequency of antigen specific (e.g. *A. fumigatus* specific) T-cells, the unspecific background percentage of $CD154^+/CD4^+$ events, determined in samples

containing co-stimulatory antibodies but no antigen, was subtracted from the antigen reactive $CD154^+/CD4^+$ frequency. This step was performed independently for each donor and condition (protocol and drug treatment). 95 % confidence intervals (CI) of reference measurements using untreated (non-drug-exposed) samples were estimated as described in Appendix 3. Results of drug-treated samples were considered significantly deviating if they did not fall within this interval. The Wilcoxon signed-rank test was used for pairwise comparison of different treatments or co-stimulation schemes.

Results

At first, we studied the influence of antifungals on *A. fumigatus* specific T-cell quantification. Applying the PBMC-based assay without antifungal pre-treatment, the mean *A. fumigatus* specific T-helper cell frequency in our donor cohort was 0.148 %. Upon exposure to AMB, VRC, and PCZ, reactive T-cell frequencies remained largely unaltered (Figure 1A, representative example in Figure 1B). Comparing drug-exposed and untreated samples, coefficients of correlation ranged from 0.97 to 0.99 and median fold changes were between 0.93 and 0.97 (Table 1). Analysing untreated whole blood samples from eight additional donors, 0.190 % *A. fumigatus* specific T-cells were found on average. Addition of antifungal drugs neither caused significant changes of median mould reactive T-cell frequencies (median fold change: 0.84-1.04) nor significant deviations of individual measurements (Figure 1C, Table 2).

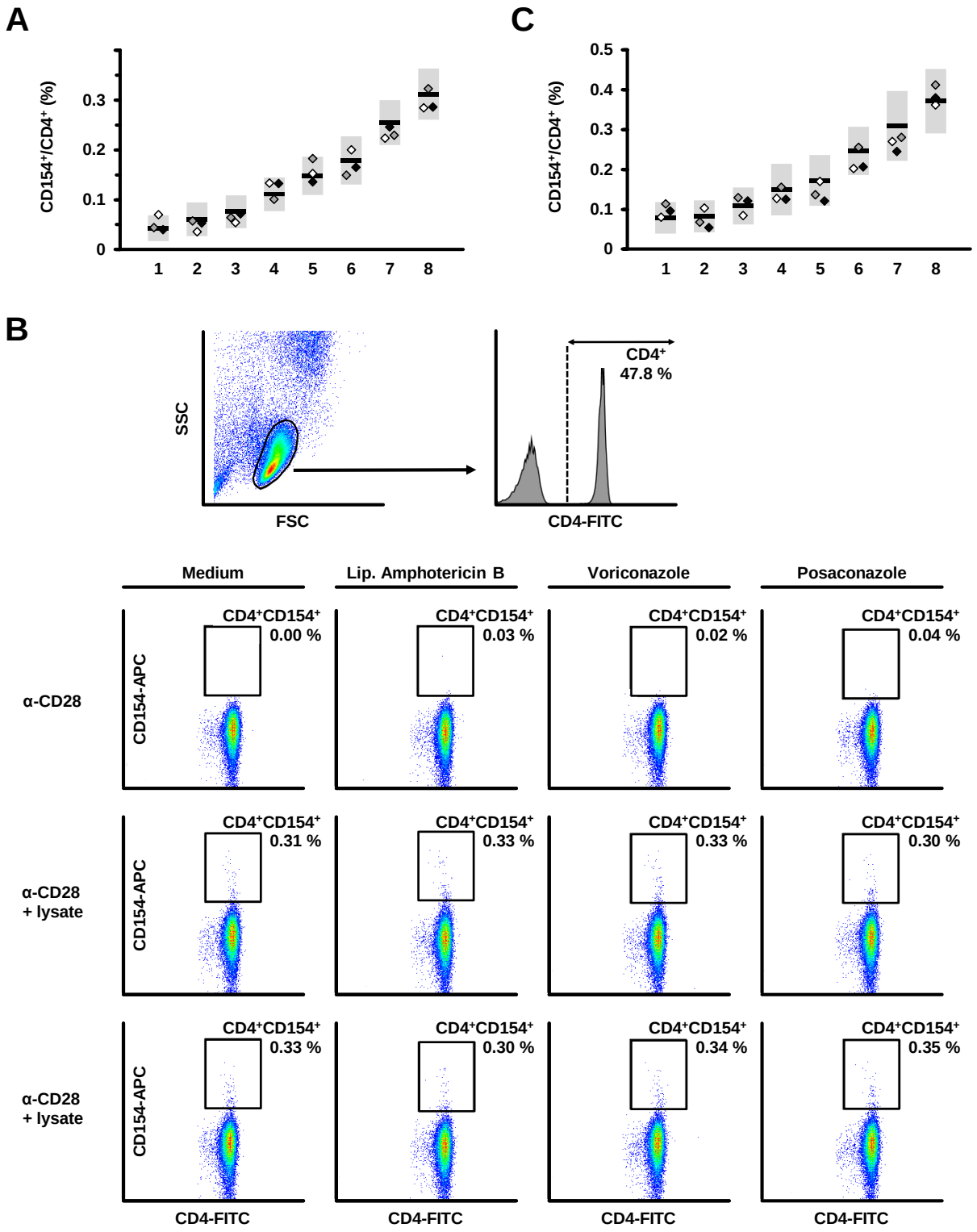

Figure 1. Liposomal amphotericin B, voriconazole, and posaconazole do not impair the performance of CD154⁺ *A. fumigatus* specific T-cell quantification.

(A and C) *A. fumigatus* specific CD154⁺/CD4⁺ T-cell frequencies of 8 healthy donors were quantified with and without prior exposure of PBMCs (A) or heparinized blood (C) to 50 µg/ml liposomal amphotericin B (white diamonds), 5 µg/ml voriconazole (grey diamonds), or 4 µg/ml posaconazole (black diamonds). Black bars indicate specific T-cell frequencies measured in the corresponding non-

drug-exposed controls and grey areas indicate their 95 % confidence intervals (CI). (B) $CD4^+/CD154^+$ plots of untreated PBMCs (Medium) and PBMC samples pre-treated with antifungals. Stimulation was performed with 0.1 µg α-CD28 (first line, unspecific background) or 0.1 µg α-CD28 + 5 µg *A. fumigatus* mycelial lysate (second and third line, analysis performed in duplicates). 50,000 lymphocytes, identified by FSC/SSC properties, were acquired. $CD4^+$ cells were gated in a CD4-FITC histogram plot and the percentage of $CD154^+$ cells among $CD4^+$ cells was quantified in a 2D pseudocolour plot. These data are derived from donor 8 in panel (A).

Comparing technical assay parameters depending on sample pre-treatment with antifungals, slightly elevated unspecific background values were found after exposure of PBMCs to the studied antifungals (Table 1). In the whole blood-based setting, only PCZ led to a minor elevation of unspecific background compared with untreated samples (Table 2). These observations, however, did not reach the level of statistical significance, and all parameters met the quality control requirements outlined in Appendix 1, irrespective of exposure to antifungals.

3.2 Impact of immunosuppressive and antifungal drugs on PBMC- and whole blood-based flow cytometric CD154+ Aspergillus fumigatus specific T-cell quantification

	untreated	AMB	VRC	PCZ
Lymphocytes acquired (mean ± SD)	50115 ± 334	50107 ± 401	50048 ± 362	49923 ± 415
$CD4^+$ cells acquired (mean ± SD)	23097 ± 1900	23059 ± 1534	22870 ± 1895	22979 ± 1874
Unspecific background (% $CD154^+/CD4^+$, mean ± SD)	0.013 ± 0.008	0.024 ± 0.008	0.024 ± 0.010	0.025 ± 0.015
Lysate reactive T-cells (% $CD154^+/CD4^+$, mean ± SD)	0.161 ± 0.087	0.168 ± 0.089	0.168 ± 0.088	0.167 ± 0.088
Specific T-cells after deduction of background (% $CD154^+/CD4^+$, mean ± SD)	0.148 ± 0.090	0.144 ± 0.083	0.144 ± 0.091	0.141 ± 0.083
Inter-replicate variation (% CV, mean ± SD)	11.2 ± 14.0	13.6 ± 12.2	12.7 ± 9.6	10.2 ± 9.2
Significant deviations (# out of 8, %)	n/a	1 (12.5 %)	0 (0 %)	0 (0 %)
Median signal-to-noise ratio [a]	11.75	6.71	7.99	6.91
Median relative detection rates of specific T-cell frequencies [b]	n/a	0.97	0.93	0.93
Coefficient of correlation [c]	n/a	0.97	0.98	0.99

Table 1. Influence of antifungal drugs on technical and statistical parameters of PBMC-based *A. fumigatus* specific T-cell quantification

[a] Median ratio of lysate-reactive T-cell frequencies divided by unspecific background

[b] Median ratio of individual test results in drug-exposed versus untreated samples

[c] Pearson's coefficient of correlation between test results in drug-exposed and untreated samples

3.2 Impact of immunosuppressive and antifungal drugs on PBMC- and whole blood-based flow cytometric CD154+ Aspergillus fumigatus specific T-cell quantification

	untreated	AMB	VRC	PCZ
Lymphocytes acquired (mean ± SD)	58389 ± 5911	59292 ± 7485	62399 ± 9751	56406 ± 5380
$CD4^+$ cells acquired (mean ± SD)	22836 ± 4258	23576 ± 3372	25015 ± 4009	23249 ± 3527
Unspecific background (% $CD154^+/CD4^+$, mean ± SD)	0.016 ± 0.015	0.015 ± 0.006	0.020 ± 0.020	0.024 ± 0.019
Lysate reactive T-cells (% $CD154^+/CD4^+$, mean ± SD)	0.206 ± 0.099	0.190 ± 0.094	0.213 ± 0.105	0.192 ± 0.093
Specific T-cells after deduction of background (% $CD154^+/CD4^+$, mean ± SD)	0.190 ± 0.102	0.175 ± 0.093	0.194 ± 0.106	0.168 ± 0.098
Significant deviations (# out of 8, %)	n/a	0 (0 %)	0 (0 %)	0 (0 %)
Median signal-to-noise ratio [a]	10.32	10.29	9.38	7.79
Median relative detection rates of specific T-cell frequencies [b]	n/a	0.92	1.04	0.84
Coefficient of correlation [c]	n/a	0.98	0.97	0.96

Table 2. Influence of antifungal drugs on technical and statistical parameters of whole blood-based *A. fumigatus* specific T-cell quantification

[a] Median ratio of lysate-reactive T-cell frequencies divided by unspecific background

[b] Median ratio of individual test results in drug-exposed versus untreated samples

[c] Pearson's coefficient of correlation between test results in drug-exposed and untreated samples

In stark contrast, mean *A. fumigatus* specific T-helper cell detection rates considerably declined after CsA (-42 %) or prednisolone (-21 %) pre-treatment of PBMCs (Figure 2A). Combined treatment with CsA and prednisolone further reduced the number of detected cells (-57 % vs. untreated PBMCs, $p = 0.016$). Importantly, striking inter-individual differences in PBMC susceptibility to the studied drugs were observed. Depending on the combination of drugs, three (prednisolone) to five (CsA + prednisolone) out of eight individual test results significantly deviated from the corresponding baseline measurements using non-immunosuppressed PBMCs. A representative example of strongly reduced CD154 response in one individual donor is provided in Figure 2B. Poor correlation of specific T-cell frequencies in immunosuppressed and untreated samples was found, especially when cells were exposed to CsA (coefficient of correlation 0.29, Table 3). The declined CD154 response of lysate stimulated samples (median fold change 0.50-076) was aggravated by increased inter-replicate variation of duplicate measurements upon CsA and prednisolone treatment (Table 3). These data highlight that both accuracy and assay precision are hampered in the presence of T-cell active immunosuppressive drugs.

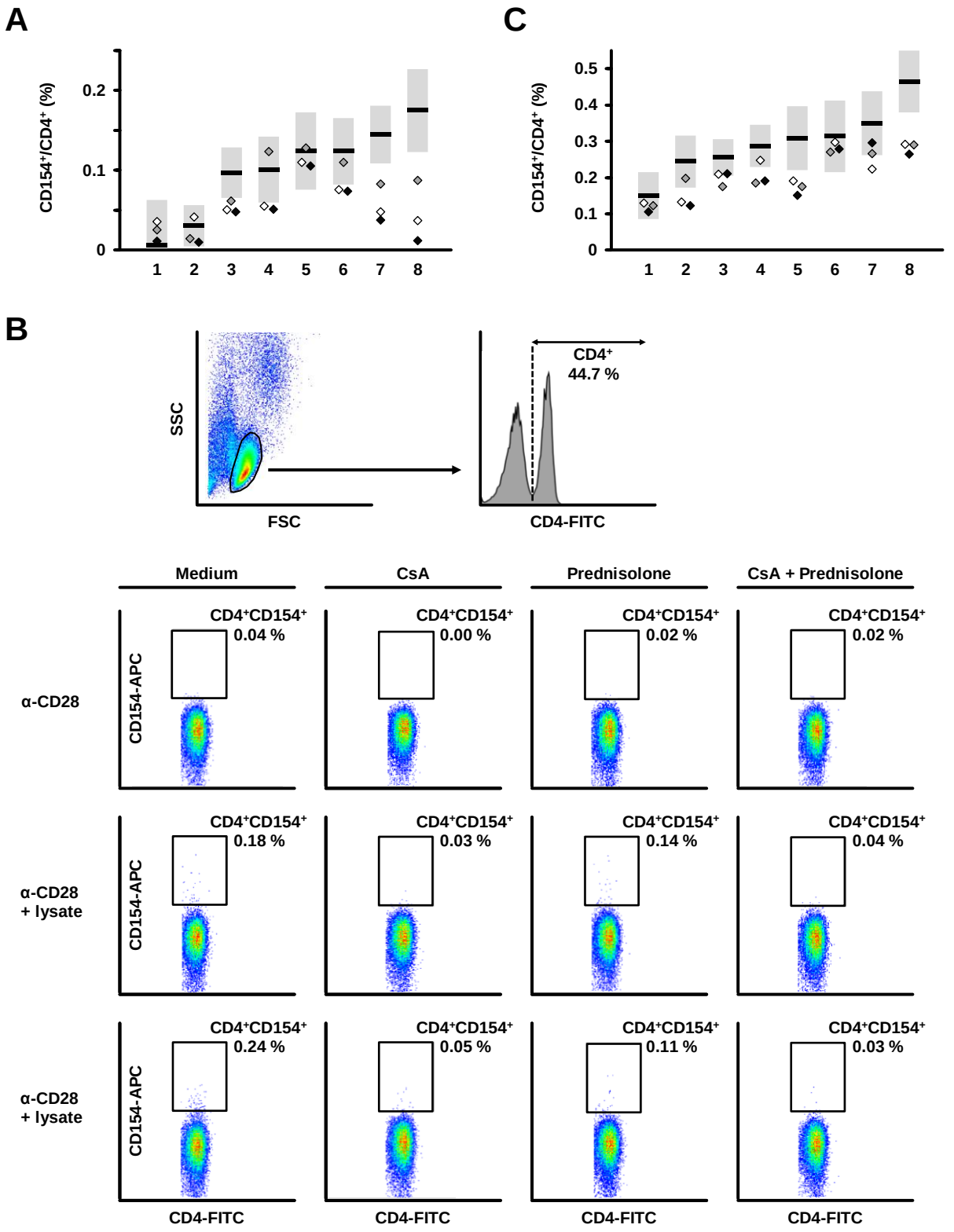

Figure 2. Detection rates of *A. fumigatus* specific T-cells are markedly lowered by cyclosporine A and prednisolone.

(A and C) *A. fumigatus* specific CD154⁺/CD4⁺ T-cell frequencies of 8 healthy donors were quantified with and without prior incubation of PBMCs (A) or heparinized blood (C) with 200 ng/ml cyclosporine A (white diamonds), 200 ng/ml prednisolone (grey diamonds), or a combination of both drugs (black diamonds). Black bars and grey areas indicate specific T-cell frequencies measured in the

corresponding non-immunosuppressed controls and their 95% CI, respectively. (B) $CD4^+/CD154^+$ plots of untreated PBMCs (Medium) and PBMC samples treated with 200 ng/ml CsA, 200 ng/ml prednisolone, or a combination of both drugs. Stimulation was performed with 0.1 µg α-CD28 (first line, unspecific background) or 0.1 µg α-CD28 + 5 µg *A. fumigatus* mycelial lysate (second and third line, analysis performed in duplicates). 50,000 lymphocytes, identified by FSC/SSC properties, were acquired. $CD4^+$ cells were gated in a CD4-FITC histogram plot and the percentage of $CD154^+$ cells among $CD4^+$ cells was quantified in a 2D pseudocolour plot. These data are derived from donor 8 in panel (A).

	untreated	CsA	prednisolone	CsA + prednisolone
Lymphocytes acquired (mean ± SD)	42999 ± 10181	42768 ± 10875	43823 ± 9454	42674 ± 11645
$CD4^+$ cells acquired (mean ± SD)	19418 ± 5239	19290 ± 5331	19925 ± 4606	19517 ± 5626
Unspecific background (% $CD154^+/CD4^+$, mean ± SD)	0.021 ± 0.012	0.000 ± 0.000	0.009 ± 0.011	0.005 ± 0.005
Lysate reactive T-cells (% $CD154^+/CD4^+$, mean ± SD)	0.121 ± 0.050	0.057 ± 0.023	0.089 ± 0.044	0.048 ± 0.029
Specific T-cells after deduction of background (% $CD154^+/CD4^+$, mean ± SD)	0.100 ± 0.053	0.057 ± 0.023	0.079 ± 0.040	0.044 ± 0.032
Inter-replicate variation (% CV, mean ± SD)	10.6 ± 9.2	25.0 ± 18.7	17.4 ± 18.7	26.3 ± 31.7
Significant deviations (# out of 8, %)	n/a	5 (62.5 %)	3 (37.5 %)	5 (62.5 %)
Median signal-to-noise ratio [a]	6.07	nd	14.03	nd
Median relative detection rates of specific T-cell frequencies [b]	n/a	0.58	0.76	0.50
Coefficient of correlation [c]	n/a	0.29	0.73	0.37

Table 3. Influence of immunosuppressive agents on technical and statistical parameters of PBMC-based *A. fumigatus* specific T-cell quantification

[a] Median ratio of lysate-reactive T-cell frequencies divided by unspecific background

[b] Median ratio of individual test results in immunosuppressed versus untreated samples

[c] Pearson's coefficient of correlation between test results in immunosuppressed and untreated samples

nd = not defined (≥ 4 measurements with 0 $CD154^+/CD4^+$ events in the unspecific background control)

Compared with untreated whole blood samples, CsA, prednisolone, and their combination led to a decline of mean *A. fumigatus* reactive T-cell frequencies from 0.297 % to 0.215 % (p = 0.008), 0.210 % (p = 0.008), and 0.202 % (p = 0.008), respectively (Figure 2C). Four significant deviations of individual test results were caused by both drugs individually as well as their combination. However, both median fold changes (0.68-0.73) and coefficients of correlation between treated and untreated samples (0.74 to 0.87) were less profoundly impacted by CsA and prednisolone in the whole blood-based assay compared with PBMC stimulation (Table 4).

	untreated	CsA	prednisolone	CsA + prednisolone
Lymphocytes acquired (mean ± SD)	48560 ± 5421	47585 ± 8681	48029 ± 7071	47707 ± 6667
$CD4^+$ cells acquired (mean ± SD)	17806 ± 3187	17325 ± 6482	19018 ± 3559	18620 ± 3787
Unspecific background (% $CD154^+/CD4^+$, mean ± SD)	0.009 ± 0.006	0.010 ± 0.011	0.014 ± 0.007	0.009 ± 0.006
Lysate reactive T-cells (% $CD154^+/CD4^+$, mean ± SD)	0.306 ± 0.088	0.225 ± 0.058	0.224 ± 0.055	0.212 ± 0.066
Specific T-cells after deduction of background (% $CD154^+/CD4^+$, mean ± SD)	0.297 ± 0.085	0.215 ± 0.060	0.210 ± 0.055	0.202 ± 0.068
Significant deviations (# out of 8, %)	n/a	4 (50 %)	4 (50 %)	4 (50 %)
Median signal-to-noise ratio [a]	51.57	33.39	14.36	35.92
Median relative detection rates of specific T-cell frequencies [b]	n/a	0.73	0.72	0.68
Coefficient of correlation [c]	n/a	0.77	0.87	0.74

Table 4. Influence of immunosuppressive agents on technical and statistical parameters of whole blood-based *A. fumigatus* specific T-cell quantification

[a] Median ratio of lysate-reactive T-cell frequencies divided by unspecific background

[b] Median ratio of individual test results in immunosuppressed versus untreated samples

[c] Pearson's coefficient of correlation between test results in immunosuppressed and untreated samples

Individual optimization of assay conditions for both matrices in a previous study (15) resulted in different co-stimulation protocols, using α-CD49d only for the whole blood assay. Therefore, we sought to test whether addition of α-CD49d can improve the assay performance in PBMCs pre-exposed to CsA and prednisolone. In line with our earlier findings (15), *A. fumigatus* specific T-cell frequencies did not significantly differ in non-immunosuppressed cells co-stimulated with α-CD28 and α-CD28+α-CD49d (0.115 % vs. 0.117 %, Figure 3A-B). Without α-CD49d, 7 out of 16 test results in immunosuppressed PBMCs (2 with CsA and 5 with prednisolone) significantly deviated from the corresponding untreated samples. On average, α-CD49d addition alleviated the CsA and prednisolone impact on *A. fumigatus* specific T-cell detection rates by 86 % and 90 %, respectively, and all significantly deviating individual measurements were mitigated by α-CD49d co-stimulation (Figure 3A-B).

To cover a broader range of specific T-helper cell frequencies that could be encountered in acutely infected patients and to assess the effect of α-CD49d co-stimulation in a second antigen-reactive $CD4^+$ T-cell population, we used a cytomegalo-, parainfluenza-, and influenza virion antigen pool (CPI) serving as universal functional positive control (28). In the absence of α-CD49d, CPI-specific T-cell detection rates were significantly reduced by CsA ($p = 0.008$, Figure 3C) and prednisolone ($p = 0.016$, Figure 3D). While not altering detection rates in non-immunosuppressed cells, addition of α-CD49d attenuated the decline of mean detectable CPI-specific T-cell frequencies in PBMCs pre-exposed to CsA and prednisolone by 53 and 78 %, respectively (Figure 3C-D). Furthermore, with α-CD49d co-stimulation, only 7 (5 with CsA and 2 with prednisolone) instead of 12 (7 with CsA and 5 with prednisolone) out of 16 individual results in immunosuppressed samples violated the 95% CI of the corresponding untreated reference measurements (Figure 3C-D).

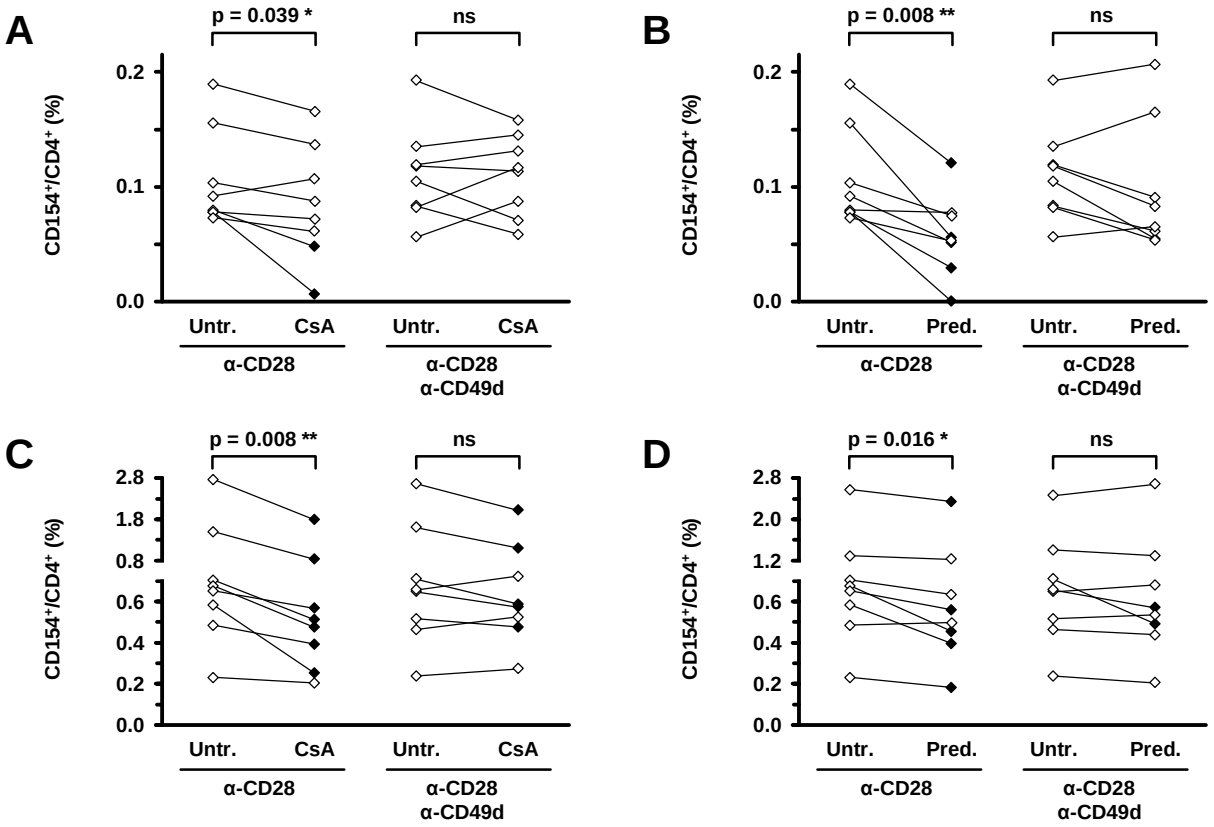

Figure 3. Co-stimulation with α-CD49d attenuates the susceptibility of PBMCs to CsA and prednisolone.

A. fumigatus (A-B) and CPI (cytomegalo-, parainfluenza-, and influenza virion antigen pool, C-D) specific $CD154^+/CD4^+$ T-cell frequencies of 8 healthy donors were quantified with and without prior exposure of PBMCs to 200 ng/ml CsA (A, C) or 200 ng/ml prednisolone (Pred., B, D). PBMCs were either stimulated in the presence of α-CD28 or α-CD28+α-CD49d. The paired Wilcoxon signed rank test was used for significance testing (ns: $p > 0.05$). Black diamonds indicate individual test results violating the 95% CI of untreated (Untr.) baseline measurements.

Due to the considerable susceptibility of the PBMC-based protocol to pre-analytic delays complicating drug treatment prior to cell isolation (11, 14), all experiments presented in Fig. 1-3 were based on drug exposure of isolated PBMCs. Aiming to validate these findings, venous blood from three occupationally mould-exposed subjects was pre-treated with CsA or prednisolone for 2 h. Thereafter, a portion of the blood was injected into whole blood stimulation tubes (15) while the remainder was used to isolate PBMCs that were subsequently stimulated with *A. fumigatus* mycelial lysate or CPI plus either α-CD28 or combined α-CD28+α-CD49d co-stimulation (Fig. 4A). Expectedly, *A. fumigatus* specific T-cell frequencies detectable by the PBMC-based protocol were very low, even in the control sample stored for 2 h without drug exposure. Nonetheless, a > 30 % reduction in *A. fumigatus* specific T-cell counts was

seen in all immunosuppressed samples (Fig. 4B). While addition of α-CD49d had no impact on the baseline detection efficacy after 2 h of blood storage, α-CD49d largely mitigated the CsA- and prednisolone-induced drop in specific T-cell detection rates (Fig. 4B). Similarly, the whole blood-based protocol showed no significant deviations of *A. fumigatus*-specific T-cell frequencies after CsA or prednisolone treatment compared with the corresponding non-drug-exposed samples (Fig. 4B). A similar trend was seen for CPI stimulation after immunosuppression, with 4, 0, and 2 out of 6 significant deviations for PBMCs, PBMCs with α-CD49d, and whole blood, respectively (Fig. 4C).

Interestingly, we found inhomogeneous susceptibility of *Aspergillus*-specific $CD4^+CD154^+$ sub-populations in the conventional PBMC-based protocol. The proportion of $CCR7^+$ subsets (naïve and central memory cells) among *A. fumigatus*-specific T-cells declined from 38.5 % in non-drug-exposed samples to 7.4 % and 21.5 %, respectively, after CsA and prednisolone treatment (Fig. 4D). Although less pronounced, this trend was confirmed for CPI-reactive T-cells, with 29.2 % $CCR7^+$ cells in the untreated sample versus 15.6 % (CsA) and 22.8 % (prednisolone) after immunosuppression, whereas the CCR7/CD45RA phenotypes of CPI-specific cells were highly stable in α-CD49-co-stimulated PBMCs and whole blood (Fig. 4E).

The IFN-γ^+ and IL-2^+ portion of the $CD154^+$ T-helper cell repertoire remained largely unaffected by the immunosuppressive treatments, whereas CsA and prednisolone caused a precipitous drop in $CD154^+CD69^+$ double-positive *A. fumigatus*- and CPI-specific T-cells detected by the conventional PBMC-based protocol (Fig. 4F-G). In contrast, both α-CD49-supplemented PBMC stimulation and the (α-CD49-containing) whole blood assay showed markedly greater stability of the $CD154^+CD69^+$ antigen-reactive subset, a marker that has been used in earlier studies (6, 10). Collectively, these data support that α-CD49d co-stimulation enhances the robustness of flow cytometric mould reactive T-cell quantification in the setting of immunosuppressive drug exposure.

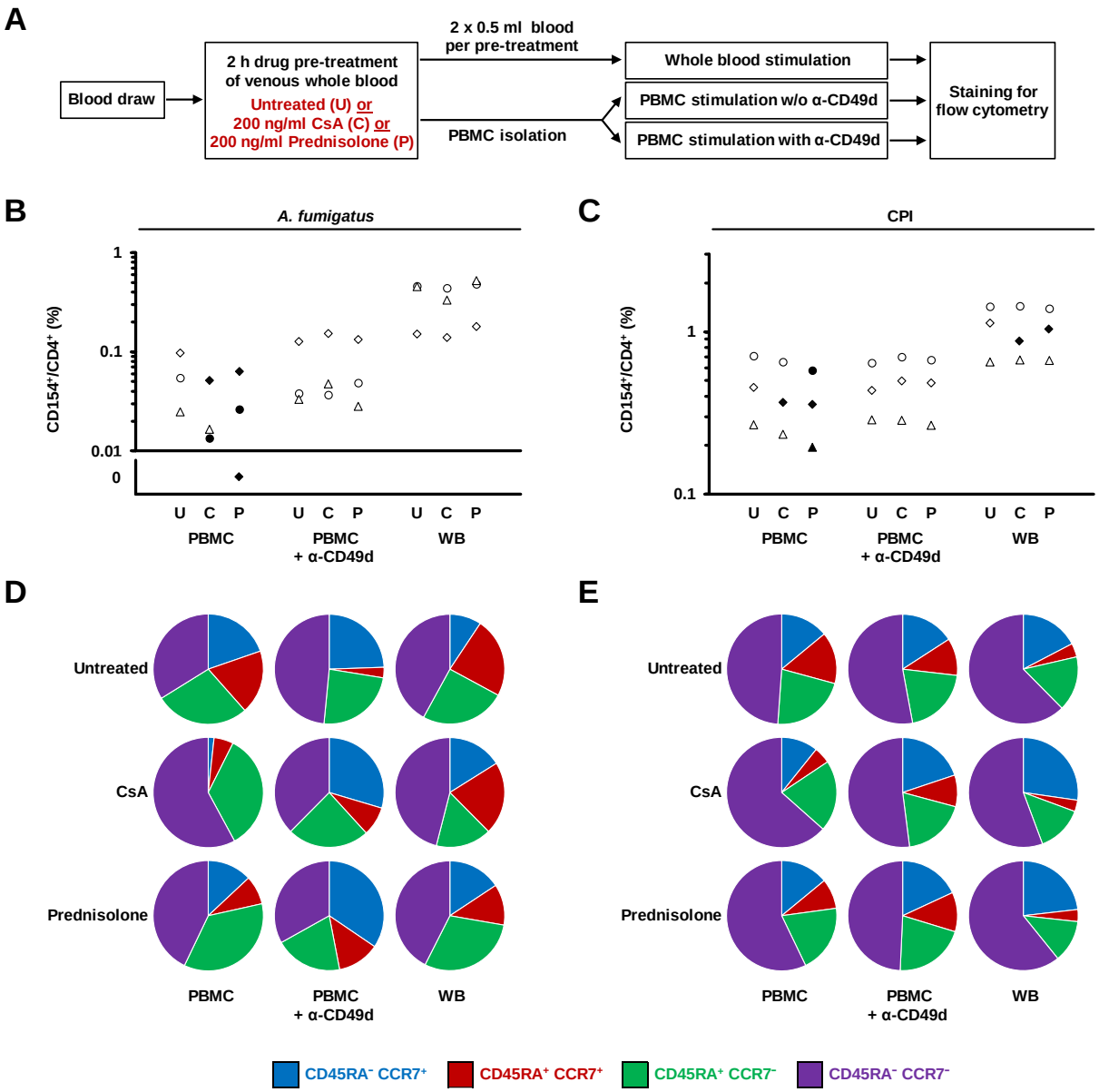

F

		PBMC	PBMC + α-CD49d	WB
CD154+ IL2+	U	0.030 %	0.037 %	0.223 %
	C	0.030 %	0.037 %	0.157 %
	P	0.022 %	0.029 %	0.186 %
CD154+ CD69+	U	0.029 %	0.030 %	0.132 %
	C	0.001 %	0.039 %	0.151 %
	P	0.009 %	0.041 %	0.178 %
CD154+ IFN-γ+	U	0.019 %	0.030 %	0.097 %
	C	0.021 %	0.027 %	0.086 %
	P	0.014 %	0.021 %	0.076 %

G

		PBMC	PBMC + α-CD49d	WB
CD154+ IL2+	U	0.314 %	0.331 %	0.493 %
	C	0.349 %	0.369 %	0.480 %
	P	0.296 %	0.368 %	0.473 %
CD154+ CD69+	U	0.144 %	0.104 %	0.540 %
	C	0.059 %	0.109 %	0.426 %
	P	0.062 %	0.123 %	0.466 %
CD154+ IFN-γ+	U	0.228 %	0.208 %	0.424 %
	C	0.235 %	0.258 %	0.416 %
	P	0.211 %	0.245 %	0.405 %

Figure 4. α-CD49d-supplemented protocols display improved resilience to CsA and prednisolone pre-treatment.

(A) Schematic of the experiment setup. Whole blood of three occupationally mould-exposed healthy donors was pre-treated with 200 ng/ml CsA (**C**) or prednisolone (**P**) for 2 h or kept for 2 h without drug exposure (untreated, **U**). Thereafter, PBMCs were isolated and stimulated with *A. fumigatus* mycelial

lysate or CPI (cytomegalo-, parainfluenza-, and influenza virion antigen pool) in the presence of α-CD28 or α-CD28+α-CD49d. In addition, the (α-CD28+α-CD49d-containing) whole blood-based protocol (WB) was performed. The gating strategy for flow cytometric analysis is detailed in Appendix 2. (B-C) Individual $CD154^+/CD4^+$ *A. fumigatus*- (B) and CPI-specific (C) T-helper cell frequencies were calculated for each protocol and pre-treatment after subtraction of unspecific background. Black diamonds indicate individual test results violating the 95% CI of untreated (**U**) baseline measurements. (D-E) Pie charts of CCR7/CD45RA phenotypes among detectable $CD154^+/CD4^+$ *A. fumigatus*- (D) and CPI-specific (E) T-helper cells. Mean values for each stimulus, protocol, and pre-treatment are shown. (F-G) Mean frequencies of $CD154^+/CD4^+$ *A. fumigatus*- (F) and CPI-specific (G) T-helper cells that are positive for additional activation markers IL-2, IFN-γ, and CD69.

Discussion

Flow cytometric or immunospot assays for specific T-cell enumeration are widely employed in the diagnosis and monitoring of infectious diseases, immunological trials, and vaccinology. Recent studies established mould specific T-cell frequencies as a supportive biomarker in invasive mycoses (6-10). For clinical application in patients undergoing allogenic haematological stem cell or solid organ transplantation, interference of immunosuppressive regimes with assay performance remains a concern. A recently published study reported applicability limitations in myelosuppressed patients, with almost two thirds of individual measurements not meeting technical acceptance criteria (10).

While data specifically addressing the influence of individual immunosuppressive agents on flow cytometric mould specific T-cell assays are yet scarce, our findings are in line with previous evidence that drugs modulating T-cell activation and metabolism can hamper diagnostic lymphocyte assays. For example, several reports suggested an increased number of indeterminate or false negative results of *Mycobacterium tuberculosis* interferon gamma release assays (IGRA) in patients receiving CsA, prednisolone or other T-cell active therapies (16-18, 29-30). In another study, enriched human *Aspergillus* specific T-helper cells showed reduced viability, impaired proliferative capacity, and increased apoptosis rates upon exposure to CsA, mycophenolic acid, prednisolone, or sirolimus (31). Contrary to our data, IFN-γ-producing and $CD154^+$ T-cell frequencies were only strongly lowered by CsA, whereas even supra-therapeutic concentrations of prednisolone had a limited effect (31). Focussing on the impact of these drugs on adoptive T-cell transfer approaches, however, the authors used an expanded, IL-2-pulsed, and restimulated

T-cell preparation. Hence, comparability with our study mimicking the diagnostic setting of freshly isolated cells is limited.

The striking effect of the calcineurin inhibitor CsA on $CD154^+$ specific T-cell detection is not surprising, as NF-AT, a downstream target of calcineurin, serves as a transcriptional activator of the CD154 (CD40L) promoter, driving mRNA and surface expression of CD154 (32-33). The effects of corticosteroids on the CD154 biosynthesis are more controversially discussed in the literature. Jabara and colleagues observed an induction of CD154 transcription and surface expression in PBMCs and purified T-cells (34), whereas others found a reversibly inhibited CD154 response to PMA and ionomycin in dexamethasone exposed $CD4^+$ cells (35).

Unexpectedly, our data revealed a stronger impact of CsA and prednisolone on the PBMC-based protocol than the whole blood assay, although the drugs were removed from PBMCs by a washing step prior to stimulation, recapitulating their elimination during cell isolation from patients' blood samples. As the detection power of the assay diminishes with increasing pre-analytic storage time (11, 14), most experiments in this study were based on drug treatment of PBMCs after isolation instead of adding a pre-incubation step immediately after blood collection. This setup presents an unavoidable limitation to this study and may hamper direct comparability of the protocols, e.g. due to the absence of blood cell subsets absorbing immunosuppressive agents (36) and a lower serum concentration in PBMC cultures compared with whole blood. Therefore, our experimental conditions may not fully reflect the *in vivo* situation. However, greater susceptibility of PBMCs to CsA and prednisolone was confirmed by direct comparison of both protocols after drug pre-treatment of collected blood prior to cell isolation despite very low detection efficacy of the PBMC-based protocol in this setting.

This led to the question whether differences in co-stimulatory factors used for the individually optimized protocols (15) modulate the susceptibility to immunosuppressive drugs. Leitner and colleagues found that CsA blocked T-cell proliferation and IFN-γ production without co-stimulation, whereas the susceptibility of CD28-costimulated cells to CsA was markedly attenuated (37). The authors and others hypothesized that downstream mediators of calcineurin are activated by alternative, CD28-dependent signalling pathways (38). While both the PBMC and whole blood stimulation setup in our study contained α-CD28, co-stimulation with α-

CD49d has been uniquely added to our enhanced whole blood assay and was crucial for its reliable performance (15). Co-stimulation with α-CD49d has not been evaluated in published diagnostic trials of mould-reactive T-cell testing but has been shown to improve T-cell viability and assay performance in related fields (39-40). Suggesting that α-CD49d can partially attenuate the adverse effect of CsA and prednisolone on antigen-reactive T-cell detection rates, our findings would encourage further evaluation of its influence on the diagnostic performance in the clinical setting. Such an investigation should also extend to cytokine secretion assays, which are often conducted without addition of any co-stimulatory reagents.

While only peripherally touched in this study, our results also revisit the question of differential robustness of antigen-reactive T-helper cell subsets under suboptimal assay conditions including immunosuppressive drug exposure. Specifically, we observed that the $CCR7^+$ subsets (naïve and central memory cells) were more strongly affected by CsA and prednisolone than $CCR7^-$ cells (effector memory and effector cells) in the conventional PBMC-based protocol without α-CD49d. This matches previous experimental evidence suggesting increased susceptibility of $CCR7^+$ cells to a freeze-thaw cycle (41), another major stress event for *ex vivo* immune cells and source of variation complicating multi-centre studies of PBMC-based functional T-cell assays. In addition, our findings suggest that the IFN-γ^+ (T_H1) portion of the *A. fumigatus* reactive T-helper cell repertoire may be more resilient to immunosuppressive agents. This hypothesis would be in line with the previously described relative robustness of IFN-γ^+ *A. fumigatus* reactive T-cells after pre-analytic delays and cryopreservation (14).

There is a possibility that our study overestimates the assay's susceptibility to immunosuppressive agents and the protective effect of α-CD49d due to differences in the *A. fumigatus*-reactive T-cell repertoire between healthy donors and acutely infected patients. The response to *A. fumigatus* in healthy individuals is dominated by regulatory T-cells (42), naïve $CD4^+$ cells and memory cells (43-44). During invasive aspergillosis, effector T-helper cells are induced (45), which tend to be more resilient to immunosuppressive drugs (Fig. 4D) and other confounding factors (41). Nonetheless, given the low incremental cost when adding α-CD49d to the stimulation cocktail and critical need for more robust protocols, enhanced co-stimulation would warrant further studies in the clinical setting.

Besides immunosuppressive compounds, several studies reported altered leukocyte in vitro functionality in the presence of antifungal agents. For example, mononuclear cell proliferation, leukotriene synthesis, and toll-like receptor signalling are influenced by AMB (19-23). Both increased and decreased proliferation of lymphocytes upon exposure to AMB have been described (24-25), whereas VRC did not affect mitogen- or antigen-driven murine T-cell proliferation (46) but stimulated PBMC proliferation and cytokine secretion (26). In our study, no evidence for impairment of $CD154^+$ *A. fumigatus* specific T-cell quantification by the studied antifungals was found, even if therapeutic doses were present for a prolonged period during cell stimulation in the whole blood system. These results match a report by Tramsen and colleagues demonstrating that therapeutic concentrations of commonly administered antifungal compounds do not significantly affect proliferation or cytokine secretion of enriched antifungal TH1-cells (47).

An important limitation of our *in vitro* examination in healthy donors is the lacking consideration of indirect antifungal drug effects on the *in vivo* immunopathology. Antifungal prophylaxis has been repeatedly described to interfere with the performance of various biomarkers employed in diagnostic mycology (48-49). Fungal proliferation and cell wall composition are influenced by antifungal drugs, in turn modulating PRR expression profiles and activation of human leukocytes (50-54). The influence of antifungals on the *in vivo* T-cell biology is hardly characterized and results have been heterogeneous. One study revealed marked differences in IL-2, IL-4, and IFN-γ serum levels upon AMB treatment of murine invasive aspergillosis, which indicated an altered TH1/TH2 balance (55), whereas others did not see an influence of antifungal therapy on systemic TNF-α, IL-1β or IFN-γ levels (56). Therefore, future clinical data addressing the sensitivity and specificity of mould specific T-cell quantification in the setting of antifungal prophylaxis and therapy are required.

In conclusion, our findings reiterate the importance of concomitant immunosuppressive medication when interpreting antigen-reactive T-cell assays. While antifungals had no impact on stimulation efficacy and technical assay properties in our study, increased numbers of inconclusive or false-negative measurements are to be expected in patients receiving T-cell active immunosuppression (e.g. GvHD prophylaxis). While experimental limitations

complicate direct compatibility, the whole blood stimulation approach tends to be less susceptible to immunosuppressive agents despite prolonged drug exposure in the test tube, further encouraging the exploitation of its logistical advantages and high detection sensitivity. Our findings also suggest a role of α-CD49d co-stimulation to increase the robustness of antigen-reactive T-cell quantification, inviting further clinical studies of the under-investigated impact of co-stimulation schemes on test reliability in an effort to overcome current applicability boundaries of T-cell assays in invasive mycoses.

Footnote Page

Compliance with ethical standards

Informed consent, approved by the ethics committee of the University of Wuerzburg (105/15 and 42/17), was obtained from all blood donors.

Author contributions

AJU, JL, and SW conceived and planned the experiments. LP, CDL, JH, PW, ML, and SW carried out the experiments. LP, CDL, PW, and SW analysed the data. LP and SW wrote the paper. HE contributed to project supervision and manuscript preparation. All authors provided revisions and approved the final version of the manuscript.

Acknowledgement

This work was supported by the Interdisciplinary Centre for Clinical Research (IZKF) Wuerzburg (grant number Z-3/56, SW), by the “Deutsche Forschungsgemeinschaft” (Collaborative Research Center / Transregio 124 “Pathogenic fungi and their human host: Networks of interaction – FungiNet”; project A2 to HE and JL), and by the Bavarian Ministry of Economics, Media, Energy and Technology (grant number BayBIO-1606-003, “T-cell based diagnostic monitoring of invasive aspergillosis in haematological patients” to JL). We would like to thank Dr. Markus Kredel (University Hospital of Wuerzburg) for providing valuable feedback and critical discussion of our data.

Disclosure of potential conflicts of interests

The authors have no conflicts of interest related to this study.

Meetings where the information has previously been presented

Parts of this study have been presented at the European Congress of Clinical Microbiology and Infectious Diseases 2016, Amsterdam, the Netherlands.

References

1. Park SJ, Mehrad B. 2009. Innate immunity to Aspergillus species. Clin Microbiol Rev 22:535-551.

2. Fukuda T, Boeckh M, Carter RA, Sandmaier BM, Maris MB, Maloney DG, Martin PJ, Storb RF, Marr KA. 2003. Risks and outcomes of invasive fungal infections in recipients of allogeneic hematopoietic stem cell transplants after nonmyeloablative conditioning. Blood 102:827-833.

3. Chamilos G, Lewis RE, Kontoyiannis DP. 2008. Delaying amphotericin B-based frontline therapy significantly increases mortality among patients with hematologic malignancy who have zygomycosis. Clin Infect Dis 47:503-509.

4. Cornely OA, Arikan-Akdagli S, Dannaoui E, Groll AH, Lagrou K, Chakrabarti A, Lanternier F, Pagano L, Skiada A, Akova M, Arendrup MC, Boekhout T, Chowdhary A, Cuenca-Estrella M, Freiberger T, Guinea J, Guarro J, de Hoog S, Hope W, Johnson E, Kathuria S, Lackner M, Lass-Florl C, Lortholary O, Meis JF, Meletiadis J, Munoz P, Richardson M, Roilides E, Tortorano AM, Ullmann AJ, van Diepeningen A, Verweij P, Petrikkos G, European Society of Clinical M, Infectious Diseases Fungal Infection Study G, European Confederation of Medical M. 2014. ESCMID and ECMM joint clinical guidelines for the diagnosis and management of mucormycosis 2013. Clin Microbiol Infect 20 Suppl 3:5-26.

5. Johnson G, Ferrini A, Dolan SK, Nolan T, Agrawal S, Doyle S, Bustin SA. 2014. Biomarkers for invasive aspergillosis: the challenges continue. Biomark Med 8:429-451.

6. Bacher P, Steinbach A, Kniemeyer O, Hamprecht A, Assenmacher M, Vehreschild MJ, Vehreschild JJ, Brakhage AA, Cornely OA, Scheffold A. 2015. Fungus-specific CD4(+) T cells for rapid identification of invasive pulmonary mold infection. Am J Respir Crit Care Med 191:348-352.

7. Potenza L, Vallerini D, Barozzi P, Riva G, Forghieri F, Beauvais A, Beau R, Candoni A, Maertens J, Rossi G, Morselli M, Zanetti E, Quadrelli C, Codeluppi M, Guaraldi G, Pagano L, Caira M, Del Giovane C, Maccaferri M, Stefani A, Morandi U, Tazzioli G, Girardis M, Delia M, Specchia G, Longo G, Marasca R, Narni F, Merli F, Imovilli A, Apolone G, Carvalho A, Comoli P, Romani L, Latge JP, Luppi M. 2013. Characterization of specific immune responses to different Aspergillus antigens during the course of invasive Aspergillosis in hematologic patients. PLoS One 8:e74326.

8. Potenza L, Vallerini D, Barozzi P, Riva G, Gilioli A, Forghieri F, Candoni A, Cesaro S, Quadrelli C, Maertens J, Rossi G, Morselli M, Codeluppi M, Mussini C, Colaci E, Messerotti A, Paolini A, Maccaferri M, Fantuzzi V, Del Giovane C, Stefani A, Morandi U, Maffei R, Marasca R, Narni F, Fanin R, Comoli P, Romani L, Beauvais A, Viale PL, Latge JP, Lewis RE, Luppi M.

2016. Mucorales-Specific T Cells in Patients with Hematologic Malignancies. PloS One 11:e0149108.

9. Koehler FC, Cornely OA, Wisplinghoff H, Schauss AC, Salmanton-Garcia J, Ostermann H, Ziegler M, Bacher P, Scheffold A, Alex R, Richter A, Koehler P. 2018. Candida-Reactive T Cells for the Diagnosis of Invasive Candida Infection-A Prospective Pilot Study. Front Microbiol. 9:1381.

10. Steinbach A, Cornely OA, Wisplinghoff H, Schauss AC, Vehreschild JJ, Rybniker J, Hamprecht A, Richter A, Bacher P, Scheffold A, Koehler P. 2019. Mould-reactive T cells for the diagnosis of invasive mould infection-A prospective study. Mycoses 62(7):562-569.

11. Wurster S, Weis P, Page L, Lazariotou M, Einsele H, Ullmann AJ. 2017. Quantification of A. fumigatus-specific CD154+ T-cells-preanalytic considerations. Med Mycol 55:223-227.

12. Afonso G, Scotto M, Renand A, Arvastsson J, Vassilieff D, Cilio CM, Mallone R. 2010. Critical parameters in blood processing for T-cell assays: validation on ELISpot and tetramer platforms. J Immunol Methods 359:28-36.

13. Mallone R, Mannering SI, Brooks-Worrell BM, Durinovic-Bello I, Cilio CM, Wong FS, Schloot NC, T-Cell Workshop Committee IoDS. 2011. Isolation and preservation of peripheral blood mononuclear cells for analysis of islet antigen-reactive T cell responses: position statement of the T-Cell Workshop Committee of the Immunology of Diabetes Society. Clin Exp Immunol 163:33-49.

14. Lauruschkat CD, Wurster S, Page L, Lazariotou M, Dragan M, Weis P, Ullmann AJ, Einsele H, Löffler J. 2018. Susceptibility of A. fumigatus-specific T-cell assays to pre-analytic blood storage and PBMC cryopreservation greatly depends on readout platform and analytes. Mycoses 61(8):549-560.

15. Weis P, Helm J, Page L, Lauruschkat CD, Lazariotou M, Einsele H, Loeffler J, Ullmann AJ, Wurster S. 2019. Development and evaluation of a whole blood-based approach for flow cytometric quantification of CD154+ mould-reactive T cells. Med Mycol pii: myz038. [Epub ahead of print]

16. Sester U, Wilkens H, van Bentum K, Singh M, Sybrecht GW, Schafers HJ, Sester M. 2009. Impaired detection of Mycobacterium tuberculosis immunity in patients using high levels of immunosuppressive drugs. Eur Respir J 34:702-710.

17. Helwig U, Muller M, Hedderich J, Schreiber S. 2012. Corticosteroids and immunosuppressive therapy influence the result of QuantiFERON TB Gold testing in inflammatory bowel disease patients. J Crohns Colitis 6:419-424.

18. Ndzi EN, Nkenfou CN, Gwom LC, Fainguem N, Fokam J, Pefura Y. 2016. The pros and cons of the QuantiFERON test for the diagnosis of tuberculosis, prediction of disease progression, and treatment monitoring. Int J Mycobacteriol 5:177-184.

19. Hedges JF, Mitchell AM, Jones K, Kimmel E, Ramstead AG, Snyder DT, Jutila MA. 2015. Amphotericin B stimulates gammadelta T and NK cells, and enhances protection from Salmonella infection. Innate Immun 21:598-608.

20. Rogers PD, Jenkins JK, Chapman SW, Ndebele K, Chapman BA, Cleary JD. 1998. Amphotericin B activation of human genes encoding for cytokines. J Infect Dis 178:1726-1733.

21. Shindo K, Fukumura M, Ito A. 1998. Inhibitory effect of amphotericin B on leukotriene B4 synthesis in human neutrophils in vitro. Prostaglandins Leukot Essent Fatty Acids 58:105-109.

22. Sau K, Mambula SS, Latz E, Henneke P, Golenbock DT, Levitz SM. 2003. The antifungal drug amphotericin B promotes inflammatory cytokine release by a Toll-like receptor- and CD14-dependent mechanism. J Biol Chem 278:37561-37568.

23. Choi JH, Kwon EY, Park CM, Choi SM, Lee DG, Yoo JH, Shin WS, Stevens DA. 2010. Immunomodulatory effects of antifungal agents on the response of human monocytic cells to Aspergillus fumigatus conidia. Med Mycol 48:704-709.

24. Boggs JM, Chang NH, Goundalkar A. 1991. Liposomal amphotericin B inhibits in vitro T-lymphocyte response to antigen. Antimicrob Agents Chemother 35:879-885.

25. Reyes E, Cardona J, Prieto A, Bernstein ED, Rodriguez-Zapata M, Pontes MJ, Alvarez-Mon M. 2000. Liposomal amphotericin B and amphotericin B-deoxycholate show different immunoregulatory effects on human peripheral blood mononuclear cells. J Infect Dis 181:2003-2010.

26. Fidan I, Yesilyurt E, Kalkanci A, Aslan SO, Sahin N, Ogan MC, Dizbay M. 2014. Immunomodulatory effects of voriconazole and caspofungin on human peripheral blood mononuclear cells stimulated by Candida albicans and Candida krusei. Am J Med Sci 348:219-223.

27. Britten CM, Janetzki S, Butterfield LH, Ferrari G, Gouttefangeas C, Huber C, Kalos M, Levitsky HI, Maecker HT, Melief CJ, O'Donnell-Tormey J, Odunsi K, Old LJ, Ottenhoff TH, Ottensmeier C, Pawelec G, Roederer M, Roep BO, Romero P, van der Burg SH, Walter S, Hoos A, Davis MM. 2012. T cell assays and MIATA: the essential minimum for maximum impact. Immunity 37:1-2.

28. Schiller A, Zhang T, Li R, Duechting A, Sundararaman S, Przybyla A, Kuerten S, Lehmann PV. 2017. A Positive Control for Detection of Functional CD4 T Cells in PBMC: The CPI Pool. Cells6(4). Pii: E47.

29. Belard E, Semb S, Ruhwald M, Werlinrud AM, Soborg B, Jensen FK, Thomsen H, Brylov A, Hetland ML, Nordgaard-Lassen I, Ravn P. 2011. Prednisolone treatment affects the performance of the QuantiFERON gold in-tube test and the tuberculin skin test in patients with autoimmune disorders screened for latent tuberculosis infection. Inflamm Bowel Dis 17:2340-2349.

30. Hewitt RJ, Singanayagam A, Sridhar S, Wickremasinghe M, Min Kon O. 2015. Screening for latent tuberculosis before tumour necrosis factor antagonist therapy. Eur Respir J 45:1510-1512.

31. Tramsen L, Schmidt S, Roeger F, Schubert R, Salzmann-Manrique E, Latge JP, Klingebiel T, Lehrnbecher T. 2014. Immunosuppressive compounds exhibit particular effects on functional properties of human anti-Aspergillus Th1 cells. Infect Immun 82:2649-2656.

32. Fuleihan R, Ramesh N, Horner A, Ahern D, Belshaw PJ, Alberg DG, Stamenkovic I, Harmon W, Geha RS. 1994. Cyclosporin A inhibits CD40 ligand expression in T lymphocytes. J Clin Invest 93:1315-1320.

33. Schubert LA, King G, Cron RQ, Lewis DB, Aruffo A, Hollenbaugh D. 1995. The human gp39 promoter. Two distinct nuclear factors of activated T cell protein-binding elements contribute independently to transcriptional activation. J Biol Chem 270:29624-29627.

34. Jabara HH, Brodeur SR, Geha RS. 2001. Glucocorticoids upregulate CD40 ligand expression and induce CD40L-dependent immunoglobulin isotype switching. J Clin Invest 107:371-378.

35. Bischof F, Melms A. 1998. Glucocorticoids inhibit CD40 ligand expression of peripheral CD4+ lymphocytes. Cell Immunol 187:38-44.

36. Dasgupta A. 2016. Limitations of Immunoassays Used for Therapeutic Drug Monitoring of Immunosuppressants. In: Oellerich & Dasgupta (eds) Personalized Immunosuppression in Transplantation, Elsevier, Amsterdam, pp. 29-56.

37. Leitner J, Drobits K, Pickl WF, Majdic O, Zlabinger G, Steinberger P. 2011. The effects of Cyclosporine A and azathioprine on human T cells activated by different costimulatory signals. Immunol Lett 140:74-80.

38. Ghosh P, Sica A, Cippitelli M, Subleski J, Lahesmaa R, Young HA, Rice NR. 1996. Activation of nuclear factor of activated T cells in a cyclosporin A-resistant pathway. J Biol Chem 271:7700-7704.

39. Gauduin MC. 2006. Intracellular cytokine staining for the characterization and quantitation of antigen-specific T lymphocyte responses. Methods 38(4):263-73.

40. Waldrop SL, Davis KA, Maino VC, Picker LJ. 1998. Normal human CD4+ memory T cells display broad heterogeneity in their activation threshold for cytokine synthesis. J Immunol 161: 5284–5295.

41. Lemieux J, Jobin C, Simard C, Neron S. A global look into human T cell subsets before and after cryopreservation using multiparametric flow cytometry and two-dimensional visualization analysis. J Immunol Methods. 2016; 434:73-82.

42. Bacher P, Heinrich F, Stervbo U, Nienen M, Vahldieck M, Iwert C, Vogt K, Kollet J, Babel N, Sawitzki B, Schwarz C, Bereswill S, Heimesaat MM, Heine G, Gadermaier G, Asam C, Assenmacher M, Kniemeyer O, Brakhage AA, Ferreira F, Wallner M, Worm M, Scheffold A. Regulatory T Cell Specificity Directs Tolerance versus Allergy against Aeroantigens in Humans. Cell. 2016; 167(4):1067-1078.e16.

43. Bacher P, Kniemeyer O, Teutschbein J, Thön M, Vödisch M, Wartenberg D, Scharf DH, Koester-Eiserfunke N, Schütte M, Dübel S, Assenmacher M, Brakhage AA, Scheffold A. Identification of immunogenic antigens from Aspergillus fumigatus by direct multiparameter characterization of specific conventional and regulatory CD4+ T cells. J Immunol. 2014; 193(7):3332-43.

44. Page L, Weis P, Müller T, Dittrich M, Lazariotou M, Dragan M, Waaga-Gasser AM, Helm J, Dandekar T, Einsele H, Löffler J, Ullmann AJ, Wurster S. Evaluation of Aspergillus and Mucorales specific T-cells and peripheral blood mononuclear cell cytokine signatures as biomarkers of environmental mold exposure. Int J Med Microbiol. 2018; 308(8):1018-1026.

45. Thakur R, Anand R, Tiwari S, Singh AP, Tiwary BN, Shankar J. Cytokines induce effector T-helper cells during invasive aspergillosis; what we have learned about T-helper cells? Front Microbiol. 2015; 6:429.

46. Van Epps HL, Feldmesser M, Pamer EG. 2003. Voriconazole inhibits fungal growth without impairing antigen presentation or T-cell activation. Antimicrob Agents Chemother 47:1818-1823.

47. Tramsen L, Schmidt S, Koehl U, Huenecke S, Latge JP, Roeger F, Schubert R, Klingebiel T, Lehrnbecher T. 2013. No effect of antifungal compounds on functional properties of human antifungal T-helper type 1 cells. Transpl Infect Dis 15:430-434.

48. Marr KA, Laverdiere M, Gugel A, Leisenring W. 2005. Antifungal therapy decreases sensitivity of the Aspergillus galactomannan enzyme immunoassay. Clin Infect Dis 40:1762-1769.

49. Reinwald M, Hummel M, Kovalevskaya E, Spiess B, Heinz WJ, Vehreschild JJ, Schultheis B, Krause SW, Claus B, Suedhoff T, Schwerdtfeger R, Reuter S, Kiehl MG, Hofmann WK, Buchheidt D. 2012. Therapy with antifungals decreases the diagnostic performance of PCR for diagnosing invasive aspergillosis in bronchoalveolar lavage samples of patients with haematological malignancies. J Antimicrob Chemother 67:2260-2267.

50. Bellocchio S, Gaziano R, Bozza S, Rossi G, Montagnoli C, Perruccio K, Calvitti M, Pitzurra L, Romani L. 2005. Liposomal amphotericin B activates antifungal resistance with reduced

toxicity by diverting Toll-like receptor ignaling from TLR-2 to TLR-4. J Antimicrob Chemother 55:214-222.

51. Hohl TM, Feldmesser M, Perlin DS, Pamer EG. 2008. Caspofungin modulates inflammatory responses to Aspergillus fumigatus through stage-specific effects on fungal beta-glucan exposure. J Infect Dis 198:176-185.

52. Simitsopoulou M, Roilides E, Paliogianni F, Likartsis C, Ioannidis J, Kanellou K, Walsh TJ. 2008. Immunomodulatory effects of voriconazole on monocytes challenged with Aspergillus fumigatus: differential role of Toll-like receptors. Antimicrob Agents Chemother 52:3301-3306.

53. Salvenmoser S, Seidler MJ, Dalpke A, Muller FM. 2010. Effects of caspofungin, Candida albicans and Aspergillus fumigatus on toll-like receptor 9 of GM-CSF-stimulated PMNs. FEMS Immunol Med Microbiol 60:74-77.

54. Cramer RA, Rivera A, Hohl TM. 2011. Immune responses against Aspergillus fumigatus: what have we learned? Curr Opin Infect Dis 24:315-322.

55. Saxena S, Bhatnagar PK, Ghosh PC, Sarma PU. 1999. Effect of amphotericin B lipid formulation on immune response in aspergillosis. Int J Pharm 188:19-30.

56. Becker MJ, de Marie S, Fens MH, Verbrugh HA, Bakker-Woudenberg IA. 2003. Effect of amphotericin B treatment on kinetics of cytokines and parameters of fungal load in neutropenic rats with invasive pulmonary aspergillosis. J Antimicrob Chemother 52:428-434.

Supplementary Materials

Appendix 1. MIATA reporting modules according to http://miataproject.org

Module 1: Sample		
1.1	Essential donor info	Healthy volunteers aged 22 to 33, 34 male, 11 female. Exclusion criteria: Signs and symptoms of acute or chronic infections, antimicrobial therapy within past 4 weeks, immunosuppressive treatment within past 12 weeks, diabetes mellitus, and pregnancy.
1.2	Source of cell material	Venous whole blood
1.3	Collection methodology	Monovette® blood collection system + 19 G butterfly needle
1.4	Anti-coagulant	NH_4-Heparin (for whole blood), EDTA for PBMC isolation
1.5	Transportation / storage conditions for unprocessed samples	Venipuncture was performed in the laboratory and samples were processed within 30 min (no storage).
1.6	Cell processing methodology	PBMC isolation by ficoll gradient centrifugation
1.7	Median time and ranges from sample collection until end of cell processing	Time from blood collection until plating of isolated PBMCs ranged from 75 to 100 min (Median: 85 min). Time from blood draw to begin of whole blood incubation ranged from 3 to 19 min (Median: 9 min).
1.8	Cut-offs	Periods from blood draw to begin of gradient centrifugation and completion of plating must not exceed 30 min and 180 min, respectively. Whole blood must be injected and incubation must be initiated within 30 min after blood draw.
1.9	Fresh or cryopreserved	Fresh
	1.10 – 1.14 not applicable (no cryopreservation)	
1.15	Median cell yield and viability	Median yield of PBMC isolation: 1.2 x 10^7 PBMCs / 10 ml EDTA whole blood, median viability 99 % (determined by trypan blue exclusion).
	1.16 – 1.18 not applicable (no cryopreservation)	
1.19	Cut-offs	Viability after PBMC isolation > 95 %.
1.20	Cell counting methodology	PBMCs were counted microscopically using a modified Neubauer chamber.
1.21	Additional assessments	n/a
Module 2: Assay		
2.1	Medium and serum details	RPMI 1640 + GlutaMAX™ (Gibco) + 5 % autologous heat-

		inactivated, sterile-filtered serum was used for PBMC culture and stimulation. No serum was added to whole blood cultures.
2.2	Pre-testing information	As sterile-filtered autologous serum was used, pre-testing was not required.
2.3	Treatment procedures of cells prior to assay	Described in the Materials & Methods section
2.4	Sufficient assay details	
2.5	Internal assay controls	Mock-stimulation with 1 µg/ml α-CD28 ± α-CD49d was used as an unspecific background control and reactive T-cell frequencies were deduced from all specific measurements.
2.6	Acceptance criteria	Unspecific background of $CD154^+/CD4^+$ cells < 0.07 %.
2.7	External reference samples	n/a
2.8	Assay acceptance criteria	n/a
Module 3: Data acquisition		
3.1	Equipment and software	Figure 1-3: FACS Calibur & Cell Quest Pro software (BD) Figure 4: CytoFLEX & CytExpert software (Beckman-Coulter)
3.2	Basic equipment settings	<u>FACS Calibur</u> Acquisition: Accept all events, acquisition will stop when 50000 in G1=R1 (lymphocyte gate according to FSC/SSC properties), resolution: 1024. Channels: P1: FSC-Height, P2: SSC-Height, P3: CD4-FITC, P7: CD154-APC. Detector / Amplitudes: P1 FSC E00 1.30-1.50 Lin, P2 SSC 455 1.00 Lin, P3 FL1 705 Log, P7 FL4 850 Log.
		<u>CytoFLEX</u> Acquisition: Accept all events, acquisition will stop when 200000 7-AAD-negative lymphocytes are acquired. Channels: FSC-H, SSC-H, FITC-H: CD197 (CCR7)-FITC, PE-H: IL-2-PE, PC5.5-H: 7-AAD, PC7-H: CD154-PE-Vio 770, APC-H: IFN-γ-APC, APC-A750-H: CD45RA-APC-Vio 770, PB450-H: CD69-VioBlue, KO525-H: CD4-VioGreen. Gain: FSC 490 (Lin), SSC 930 (Lin), FITC 182 (Log), PE 153 (Log), PC5.5 373 (Log), PC7 537 (Log), APC 850 (Log), APC-A750 476 (Log), PB450 42 (Log), KO525 29 (Log).
3.3	Detailed gating strategy	Fig. 1B, Fig. 2B, Appendix 2
3.4	Representative data set	
3.5	Mean, median, ranges of event counts for relevant populations	Relevant populations and statistical details are summarized in Tables 1-4.
3.6	Unusual strategies explained	n/a

3.2 Impact of immunosuppressive and antifungal drugs on PBMC- and whole blood-based flow cytometric CD154+ Aspergillus fumigatus specific T-cell quantification

3.7	Review of raw data	Raw data were reviewed by at least two authors.
Module 4: Results		
4.1	Background and ag-specific reactivity levels	Background and antigen specific responses are summarized in Tables 1-4.
4.2	Cut-off specifications	Unspecific background of $CD154^+/CD4^+$ cells < 0.07 %.
4.3	Accessibility of raw data	Donor record forms, flow cytometry files, and data printouts are stored onsite and were carefully reviewed by at least two authors.
4.4	Definition of positive reactivity (above background) including tests applied	As mould-reactive T-cells are detectable in most healthy donors, no cut-off specifications for reactivity were applied. 95 % confidence intervals for antigen reactive T-cell levels were determined as described in Appendix 2.
4.5	Parameters, software and version used for response determination	$CD154^+/CD4^+$ values were quantified using FlowJo vX.0.7.
4.6	Response definition predefined or post-hoc	n/a, since no cut-off was used.
4.7	Definition of response induced by treatment	n/a
4.8	Any data excluded and why	Two data set were excluded and data acquisition was repeated with a new blood sample due to an insufficient amount of acquired $CD4^+$ cells. One data set was excluded due to > 0.07 % $CD154^+/CD4^+$ cells in the unspecific background sample.
4.9	Why test was used	Mould reactive T-cells were proposed as a diagnostic biomarker. This study aimed to evaluate and improve protocol robustness and clinical applicability of CD154-based T-cell detection.
Module 5: Laboratory		
5.1	Guidance of lab operations	Experiments were conducted under GLP principles. SOPs were prepared by SW and reviewed by all authors. Lab members were trained thoroughly. Process related parameters were documented in case report forms.
5.2	Laboratory accreditions and certifications	n/a
5.3	Details on audits	n/a
5.4	Status of protocols	Monocentric study with SOPs followed by all authors.
5.5	Status of assays	The study was performed using qualified assays. Comparative assessment of different stimulation schemes was performed and published (S1).
5.6	Specific performance criteria	Specified in the Results section of this manuscript and Tables 1-4.

Appendix 2. Gating strategy for Figure 4 and representative data set.

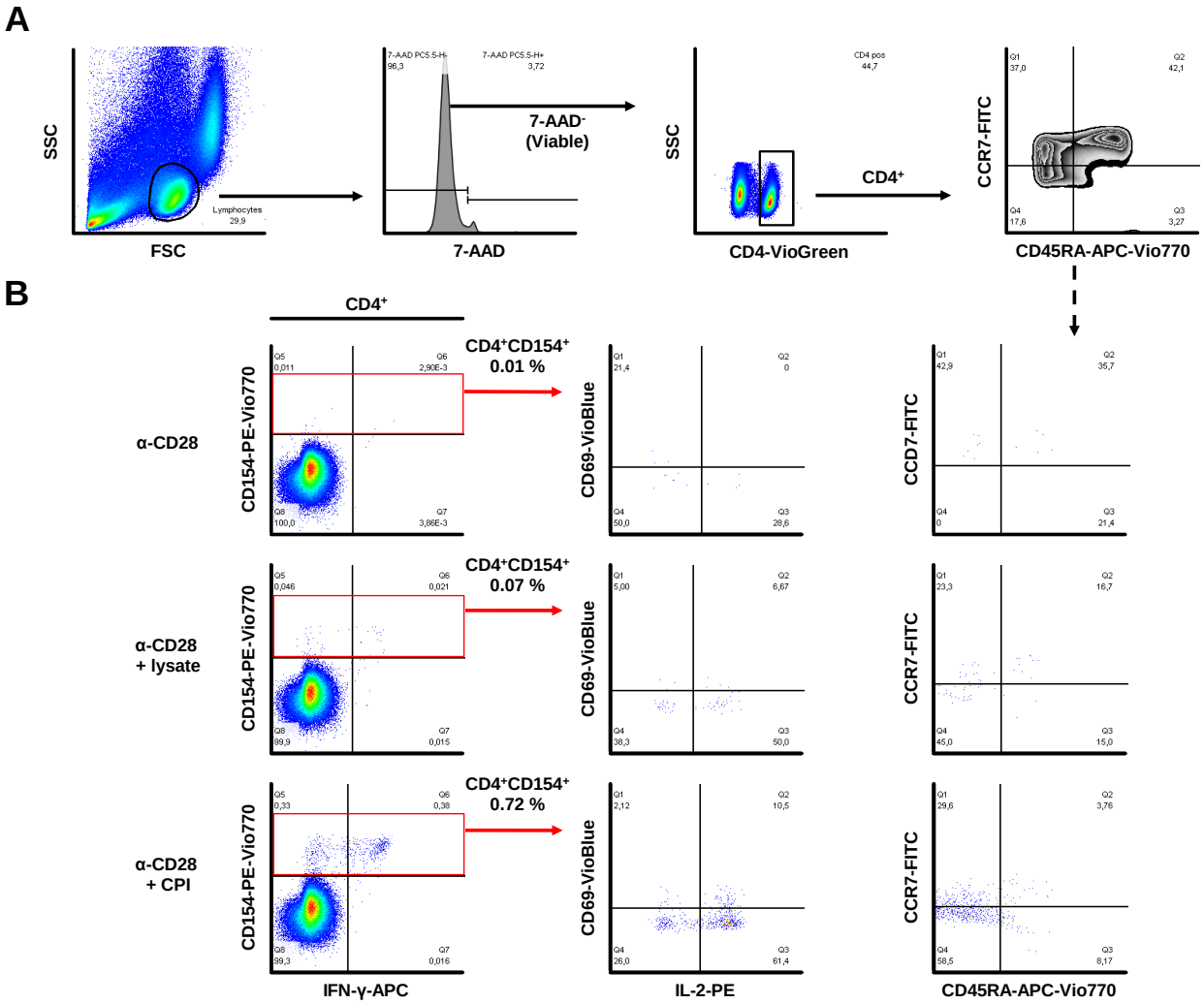

(A) 200000 lymphocytes were acquired according to forward and side scatter (FSC/SSC) properties. Using FlowJo software, the lymphocyte gate was adjusted precisely. Viable, 7-AAD-negative cells were identified on a histogram plot. Among viable lymphocytes, $CD4^+$ cells were gated using a CD4/SSC pseudocolour plot. A CD45RA/CCR7 quadrant gate (Q1-Q4) was adjusted on a zebra plot applied to $CD4^+$ events. (B) A quadrant gate (Q5-Q8) was adjusted on an IFN-γ/CD154 pseudocolour plot applied to $CD4^+$ cells in order to quantify $CD4^+CD154^+$ cells (Q5+Q6) and $CD4^+CD154^+IFN\text{-}\gamma^+$ events (Q6). Thereafter, an IL-2/CD69 quadrant gate was applied to $CD4^+CD154^+$ cells to identify $CD4^+CD154^+CD69^+$ (Q1+Q2) and $CD4^+CD154^+IL\text{-}2^+$ (Q2+Q3) events. In addition, the CD45RA/CCR7 gate adjusted to $CD4^+$ cells before was transferred to the $CD4^+CD154^+$ population to identify their memory/effector phenotypes. For each protocol, stimulus, and subset of interest, the event count/CD4 ratio of the unspecific control (co-stimulation only) was subtracted from the event count/CD4 ratio of antigen-stimulated samples. The representative data set is based on the conventional PBMC-based protocol without α-CD49d or immunosuppressive drugs and is derived from the donor depicted by the ○ symbol in Fig. 4B and 4C.

Appendix 3. Approximation of the confidence intervals of antigen-specific T-cell frequencies.

The coefficient of variation (CV) for flow cytometric quantification of rare antigen specific cell subsets can be estimated by the following formula (S2)

$$CV = \frac{1}{\sqrt{n\,[\text{antigen-specific cells acquired}]}}$$

Using a single measurement for unspecific background determination, the standard deviation has been calculated according to the following formula:

$$SD_{\text{unsp}} = \frac{f\,[\text{CD154}^+/\text{CD4}^+]}{\sqrt{n\,[\text{CD154}^+/\text{CD4}^+]}}$$

As duplicate measurement was used for *A. fumigatus*- or CPI-stimulated wells (antigen-reactive T-cells), the following adapted formula was applied to determine the standard deviation:

$$SD_{\text{stim}} = \frac{0.5\,x\,(f\,[\text{CD154}^+/\text{CD4}^+]_{\text{Well 1}} + f\,[\text{CD154}^+/\text{CD4}^+]_{\text{Well 2}})}{\sqrt{(n\,[\text{CD154}^+/\text{CD4}^+]_{\text{Well 1}} + n\,[\text{CD154}^+/\text{CD4}^+]_{\text{Well 2}})}}$$

These values result in a combined standard deviation calculated according to the following formula (Gaussian error propagation):

$$SD_{\text{total}} = \sqrt{(SD_{\text{unsp}}{}^2 + SD_{\text{stim}}{}^2)}$$

The 1.96-fold standard deviation was calculated to approximate the 95 % confidence interval.

Supplementary References

S1) Weis P, Helm J, Page L, Lauruschkat CD, Lazariotou M, Einsele H, Loeffler J, Ullmann AJ, Wurster S. 2019. Development and evaluation of a whole blood-based approach for flow cytometric quantification of CD154+ mould-reactive T cells. Med Mycol pii: myz038. [Epub ahead of print]

S2) Allan AL, Keeney M. 2010. Circulating tumor cell analysis: technical and statistical considerations for application to the clinic. J Oncol 2010:426218.4

3.3 Comparative analysis of inflammatory cytokine release and alveolar epithelial barrier invasion in a Transwell® bilayer model of mucormycosis

Running Title: Mucormycosis Alveolar Model

Revised manuscript 427808

Stanislav Belic[1,#], Lukas Page[1,#], Maria Lazariotou[1], Ana Maria Waaga-Gasser[2], Mariola Dragan[2], Jan Springer[1], Juergen Loeffler[1], Charles Oliver Morton[3], Hermann Einsele[1], Andrew J. Ullmann[1], Sebastian Wurster[1,4,*]

1) University Hospital of Wuerzburg, Department of Internal Medicine II, Division of Infectious Diseases, Wuerzburg, Germany

2) University Hospital of Wuerzburg, Department of Surgery I, Wuerzburg, Germany

3) Western Sydney University, School of Science and Health, Sydney, Australia

4) The University of Texas MD Anderson Cancer Center, Department of Infectious Diseases, Houston (TX), United States of America

# Contributed equally to this study

* Corresponding author:

University Hospital of Wuerzburg, Department of Internal Medicine II

Josef-Schneider-Str. 2, C11, Room 0.205, 97080 Wuerzburg, Germany

Present Contact Address:

The University of Texas MD Anderson Cancer Center, Department of Infectious Diseases

1515 Holcombe Boulevard, Y5.5725, Houston, TX 77030, United States of America

Email address: stwurster@mdanderson.org, Phone: 1-713-745-1371

Abstract

Understanding the mechanisms of early invasion and epithelial defense in opportunistic mold infections is crucial for the evaluation of diagnostic biomarkers and novel treatment strategies. Recent studies revealed unique characteristics of the immunopathology of mucormycoses. We therefore adapted an alveolar Transwell® A549/HPAEC bilayer model for the assessment of epithelial barrier integrity and cytokine response to *Rhizopus arrhizus*, *Rhizomucor pusillus*, and *Cunninghamella bertholletiae*. Hyphal penetration of the alveolar barrier was validated by 18S ribosomal DNA detection in the endothelial compartment. Addition of dendritic cells (moDCs) to the alveolar compartment led to reduced fungal invasion and strongly enhanced pro-inflammatory cytokine response, whereas epithelial CCL2 and CCL5 release was reduced. Despite their phenotypic heterogeneity, the studied Mucorales species elicited the release of similar cytokine patterns by epithelial and dendritic cells. There were significantly elevated lactate dehydrogenase concentrations in the alveolar compartment and epithelial barrier permeability for dextran blue of different molecular weights in Mucorales-infected samples compared to *Aspergillus fumigatus* infection. Addition of monocyte-derived dendritic cells further aggravated LDH release and epithelial barrier permeability, highlighting the influence of the inflammatory response in mucormycosis-associated tissue damage. An important focus of this study was the evaluation of the reproducibility of readout parameters in independent experimental runs. Our results revealed consistently low coefficients of variation for cytokine concentrations and transcriptional levels of cytokine genes and cell integrity markers. As additional means of model validation, we confirmed that our bilayer model captures key principles of Mucorales biology such as accelerated growth in a hyperglycemic or ketoacidotic environment or reduced epithelial barrier invasion upon epithelial growth factor receptor blockade by gefitinib. Our findings indicate that the Transwell® bilayer model provides a reliable and reproducible tool for assessing host response in mucormycosis.

Keywords: Mucormycosis, alveolar epithelium, *in vitro* model, cytokines, dendritic cells

Introduction

Invasive mycoses are responsible for significant morbidity and mortality in immuno-compromised patients. While *Aspergillus fumigatus* remains the most common cause of opportunistic mold infections, emerging fungal pathogens including those of the order Mucorales are observed with an increasing incidence (Roden et al., 2005). Invasive mucormycosis poses a serious clinical challenge, but its pathogenesis and immunopathology are still poorly understood (Roilides et al., 2014, Roilides & Simitsopoulou, 2017).

Humans are exposed to thousands of airborne mold spores every day and thus epithelial barriers of the respiratory tract, especially the 0.5 – 2 µm thin alveolar-capillary barrier with its over 100 m² surface, commonly represent the primary site of interaction (Croft et al., 2016). In addition to their anatomical barrier function, airway epithelia demonstrably contribute to a fined-tuned immunological balance, which is required to control fungal invasiveness while preventing hypersensitivity, hyperinflammation, and excessive tissue damage (Park & Mehrad, 2009). Epithelial cells recognize fungal pathogens by TLR and C-type-lectin-receptor dependent pathways (Sun et al., 2012), which in turn triggers transcriptional changes including the upregulation of genes associated with inflammatory responses and damage repair (Cortez et al., 2006, Osherov, 2012). Infected airway epithelial cells release a broad array of antimicrobial peptides, enzymes, and cytokines, and thereby contribute to both fungal clearance and orchestration of their micro-environment through cytokine signaling (Osherov, 2012, Park & Mehrad, 2009).

Understanding the mechanisms of early fungal invasion and epithelial defense is a key to the development of novel treatment strategies, but also to the evaluation of diagnostic biomarkers (Hope, 2009, Kniemeyer et al., 2016). Increasingly complex *in vitro* models have been established in *Candida* and *Aspergillus* research to characterize host-pathogen interplay at epithelial barriers (Croft et al., 2016, Hope, 2009). Most commonly, an alveolar bilayer model has been employed in different studies of invasive aspergillosis to monitor invasion, host response, and diagnostic biomarkers (Gregson et al., 2012, Hope et al., 2007, Morton et al., 2014). This model consists of monolayers of human lung adenocarcinoma epithelial cells (A549) and human pulmonary artery endothelial cells (HPAEC) cultured on both sides of a

Transwell® membrane, allowing for separate analysis of cellular responses (e. g. transcriptional profiles) or soluble markers (e. g. cytokine concentrations) in each compartment. Refinement of the model was achieved by addition of different immune cell subsets (Morton et al., 2014), facilitating assessment of the interplay between epithelial cells and innate immunity. Particular focus was placed on the role of dendritic cells (Morton et al., 2014), as they serve as an important crosslink with the T-helper cell system and contribute to shaping adaptive immune response (Lass-Florl et al., 2013).

Recent reports revealed striking differences in innate immune response to *Aspergillus* and Mucorales (Chamilos et al., 2008, Warris et al., 2005, Wurster et al., 2017). For example, a strong pro-inflammatory response to Mucorales spores was observed, whereas resting *Aspergillus* conidia, covered by an immunologically inert hydrophobin layer, induce little inflammation (Wurster et al., 2017). The biological and clinical implications of these differences remain largely unexplored. To characterize the inflammatory response to Mucorales in the alveolar context, this study aimed to adapt and validate the alveolar bilayer Transwell® model for Mucorales research, evaluate its technical reliability, and compare cytokine response, and epithelial barrier invasion upon infection with three common human pathogenic Mucorales species.

Material and Methods

Pre-analytical methods

PBMC isolation and generation of monocyte-derived dendritic cells (moDC)

Peripheral blood mononuclear cells (PBMC) were obtained by ficoll gradient centrifugation of leukocyte reduction systems kindly provided by the Institute for Transfusion Medicine and Immunohematology Wuerzburg. Subsequent monocyte isolation was conducted using MACS CD14 positive selection (Miltenyi Biotec). moDC maturation was induced by incubation with 20 ng/ml IL-4 and 100 ng/ml GM-CSF for 6 days at 37 °C, 5 % CO_2.

Preparation of molds

Aspergillus fumigatus ATCC 46645, *Rhizopus arrhizus* CBS 110.17, *Rhizomucor pusillus* CBS 245.58, and *Cunninghamella bertholletiae* CBS 187.84 were cultured

on beer wort agar plates. Conidia were harvested by gently scraping cultures with a cotton swab, diluted in distilled water, and passed through a 40 µm cell strainer to remove residual mycelium. Spores were diluted at a concentration of 5 x 10^6 cells per ml in endothelial cell basal medium 2 (EBM2) + 10 % fetal calf serum (FCS) + endothelial cell growth medium 2 SingleQuots™ without gentamicin/amphotericin B (GA-1000), hereinafter called “human pulmonary artery endothelial cell (HPAEC) medium”.

Preparation of fungal culture supernatants

To obtain supernatants of fungal cultures, 1 x 10^7 fungal spores were cultured in 2 ml EBM2 medium (Lonza) + 10 % FCS in 6-well-plates for 30 hours. Supernatants were sterile-filtered (0.2 µm) and cryopreserved at -20 °C until further use. Thawed supernatants were diluted 1:1 with fresh medium before addition to the alveolar model.

Construction of Transwell® bilayer model

An alveolar bilayer model was constructed as previously described (Hope, 2009, Hope et al., 2007). Briefly, human pulmonary artery endothelial cells (HPAEC, Lonza) and adenocarcinoma human alveolar basal epithelial cells (A549, Lonza) were cultured in 75 cm^2 flasks in HPAEC medium + 0.1 % GA-1000 at 37 °C, 5 % CO_2. 1 x 10^5 HPAECs were seeded on the lower side of a 6.5 mm diameter 3 µm pore Transwell® membrane (Corning). After 2 h incubation, inserts were placed in HPAEC medium in a 24 well plate overnight. Subsequently, 5 x 10^4 A549 cells suspended in 100 µl HPAEC medium were added to the upper compartment. Incubation of the assembly was performed in 24 well plates containing 600 µl HPAEC medium per well at 37 °C, 5 % CO_2. Media changes were performed every other day. 50 µl moDC solution (2.5 x 10^5 cells in HPAEC medium) or plain medium were added on day 5. Afterwards, inserts were infected by adding 50 µl fungal solution (2.5 x 10^5 spores in HPAEC medium), followed by another 30 h incubation period at 37 °C, 5 % CO_2. For selected experiments, 50 µg/ml gefitinib (Santa Cruz Biotechnology), 8 mg/ml D-(+)-glucose (Sigma-Aldrich), or 1 mg/ml betahydroxybuyrate (Sigma-Aldrich) were added to the endothelial compartment.

Analytical methods

Gene expression analyses

Endothelial cells and residual mycelium were removed from the lower side of the membrane using a cell scraper. After washing membranes in Hank's Balanced Salt Solution (HBSS), inserts were transferred to wells containing 600 µl RNAprotect Cell Reagent (Qiagen) to preserve the total RNA of A549 cells ± moDCs. RNA isolation and cDNA synthesis were performed using the RNAeasy Mini Kit (Qiagen) and High Capacity cDNA Reverse Transcription Kit (Applied Biosystems) according to the manufacturer's instructions.

Quantitative PCR

RT-qPCR was performed on a StepOne Plus PCR Cycler (Applied Biosystems) using the iTaq Universal SYBR Green Supermix (Bio-Rad) according to the manufacturer's instructions. Initial denaturation (30 s at 95 °C) was followed by 40 cycles of denaturation (3 s at 95 °C) and annealing / elongation steps (30 s at 60 °C). Melting curves were obtained at +0.5 °C / 15 s. The following primer sequences were used: *Cas3*: 5'-CTCTGGTTTTCGGTGGGTGT-3' and 5'-TCCAGAGTCCATTGATTCGCT-3'; *Cas9*: 5'-CAGGCCCCATATGATCGAGG-3' and 5'-TCGACAACTTTGCTGCTTGC-3'; *ICAM-1*: 5'-ACCCCGTTGCCTAAAAAGGA-3' and 5'-AGGGTAAGGTTCTTGCCCAC-3'; *IL-6*: 5'-AAAGAGGCACTGGCAGAGAAAAC-3' and 5'-AAAGCTGCGCAGAATGAGATG-3'; *IL-8*: 5'-AAGAAACCACCGGAAGGAAC-3' and 5'-ACTCCTTGGCAAAACTGCAC-3'; *CCL2*: 5'-CCCCAGTCACCTGCTGTTAT-3' and 5'-AGATCTCCTTGGCCACAATG-3'; *CCL5*: 5'-TCATTGCTACTGCCCTCTGC-3' and 5'- TACTCCTTGATGTGGGCACG-3'; *Alas1* (house-keeping gene / reference gene): 5'-GGCAGCACAGATGAATCAGA-3', and 5'-CCTCCATCGGTTTTCACACT-3'. Relative mRNA expression levels normalized to Alas1 were calculated using the ΔΔCt method.

Cytokine analyses

Culture medium from both compartments was collected, centrifuged at 7000 g for 5 min, and supernatants were frozen at -20 °C until analysis. After 1:1 dilution with fresh HPAEC medium, cytokine concentrations in the culture supernatant were determined using a magnetic bead-based cytokine assay (13-plex HCYTOMAG,

Merck Millipore) or TNF-α / IL-1β ELISA (ELISA Max Deluxe Kits, BioLegend) according to the manufacturer's instructions.

18S ribosomal DNA PCR assay

A Mucorales-specific real-time PCR assay (Muc18S) was used for semi-quantitative Mucorales DNA analysis as described before (Springer et al., 2016a und b). 0.5 ml of supernatant supplemented by 0.5 ml PBS was used for DNA extraction as described before (Springer et al., 2016b).

LDH quantification

Culture supernatants from the upper compartment were diluted 1:5 in 0.9 % NaCl. Lactate dehydrogenase (LDH) concentrations were determined by the central laboratory of the University Hospital of Wuerzburg using a diagnostic LDHI2 assay on a Cobas Integra analyzer.

Dextran blue assay

The alveolar model was assembled as described above and 1 µg dextran blue (5 kDa, 20 kDa, or 70 kDa) was added to the upper compartment. Inserts were placed in 600 µl HPAEC medium and incubated at 37 °C, 5 % CO_2. After 30 min, 90 min, 5 h, 10 h, 20 h, and 30 h, inserts were transferred to a new well containing fresh HPAEC medium to prevent back-diffusion. Dextran blue concentrations in the previously used wells were quantified photometrically at 622 nm by comparison with standard dilutions.

Statistical analysis

Unless otherwise stated, significance testing was performed using the paired or unpaired two-sided Student's t-test. * $p < 0.05$, ** $p < 0.01$, *** $p < 0.001$. Though not considered significant, we provided an additional indication of $p < 0.1$ (■).

Results

Validation of an alveolar bilayer model for mucormycosis research

An alveolar bilayer model was set up as described in the Methods section and infected with three common human pathogenic Mucorales species to assess cytokine

response and epithelial barrier integrity (**Figure 1**). A semi-quantitative 18S DNA assay was performed to evaluate epithelial barrier invasion by the studied Mucorales species, resulting in trans-epithelial growth. A constant increase in Mucorales DNA content in the lower compartment was detected over time (**Figure 2A**). Consistent with the macroscopic observation of more rapid and abundant mycelium formation, *R. arrhizus* and *C. bertholletiae* showed earlier and stronger increase in DNA content compared to *R. pusillus*. Addition of moDCs to the upper compartment effectively suppressed fungal invasion of the lower compartment, indicated by reduced Mucorales DNA content. To ensure sufficient fungal penetration of the alveolar barrier even in the presence of moDCs, an incubation period of 30 hours was selected for subsequent experiments. Evaluating the inter-experiment reproducibility of endothelial compartment invasion in 3 independent experiments, coefficients of variation (CVs) were 11.8-21.6 % (**Figure 2B**).

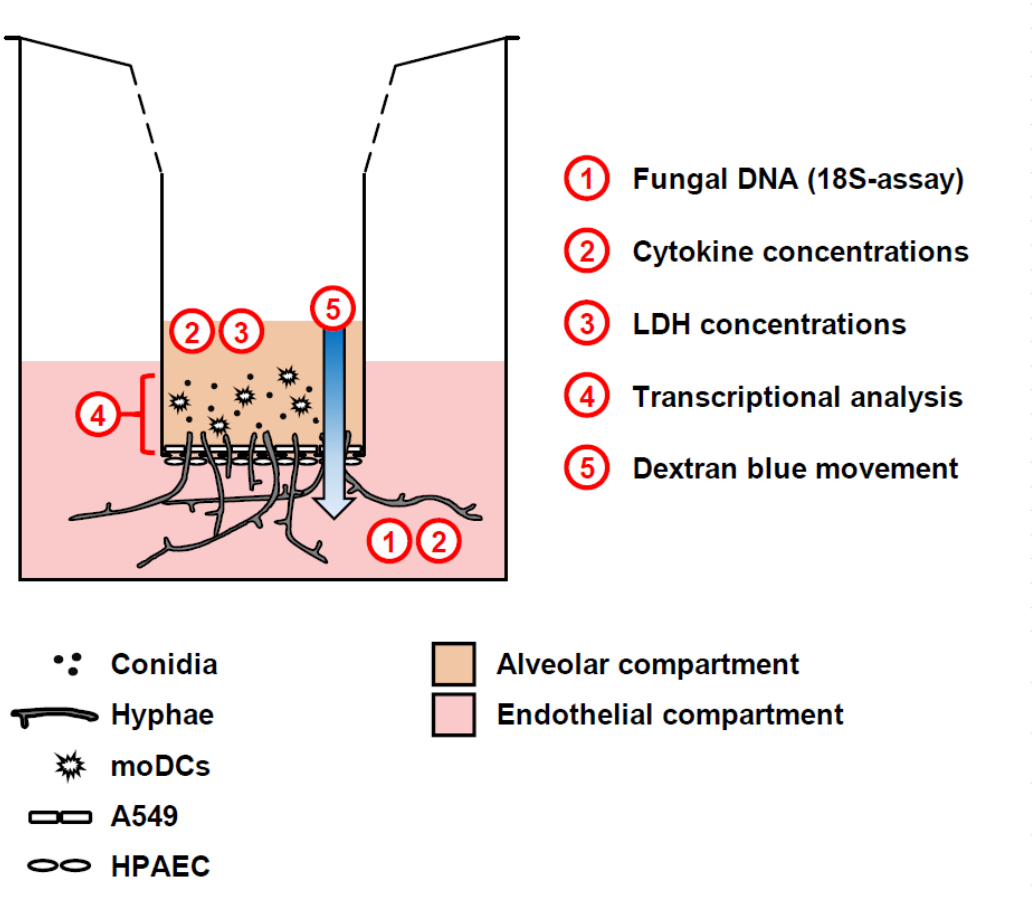

Figure 1: Schematic representation of the alveolar model.

Human pulmonary endothelial cells (HPAEC, lower part) and type 2 pneumocytes (A549, upper part) were cultivated on a 3 µm Transwell® membrane. Fungal cells and/or moDCs were added to the upper

compartment. For selected experiments, additional agents (e. g. glucose) were added to the endothelial environment. The scheme summarizes readouts from each compartment.

As an additional means of validation, we assessed *C. bertholletiae*, the most invasive isolate in our selection, to determine whether our bilayer model can recapitulate the finding of epithelial growth factor receptor (EGFR)-dependent A549 cell invasion recently described by others (Watkins et al., 2018). Addition of 50 µg/ml gefitinib, an FDA-approved EGFR inhibitor, to the endothelial chamber significantly reduced *C. bertholletiae* DNA content in the lower compartment after 30 h (**Figure 2C**, 86 % versus 44 % of positive control, p = 0.047). Moreover, enhanced endothelial invasion by *Rhizopus* in a hyperglycemic or ketoacidotic environment was previously shown in endothelial cell monolayers (Gebremariam et al., 2016). To validate the recapitulation of these findings in our model, we added 8 mg/ml glucose or 1 mg/ml beta-hydroxybutyrate to the endothelial compartment. Both treatments strongly and significantly ($p < 0.01$) increased the *R. arrhizus* DNA content in the endothelial compartment 30 h after inoculation of the alveolar chamber (**Figure 2D**).

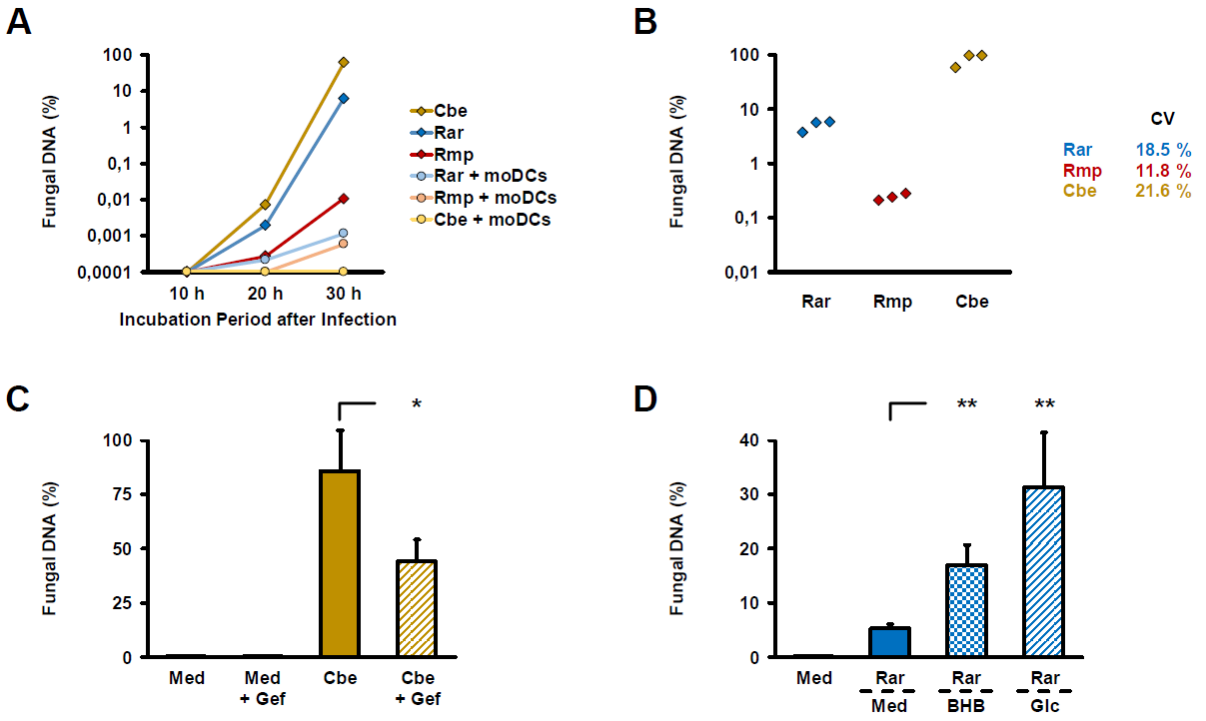

Figure 2: Validation of endothelial compartment invasion and its reproducibility

(**A**) The bilayer model was assembled as described in the methods section. 2.5 x 10^5 spores of different Mucorales species ± 2.5 x 10^5 moDCs were added to the upper compartment. Mucorales DNA in the lower compartment was quantified using an 18S ribosomal RNA assay. The diagram

shows the percentage of detected DNA in the lower compartment depending on incubation time after infection of the upper compartment. The percent scale refers to a positive control (= 100 %) incubated for 30 hours after addition of the same number of fungal spores directly to the lower compartment. Mean values based on technical duplicates from one representative run are shown. Rar = *R. arrhizus*, Rmp = *R. pusillus*, Cbe = *C. bertholletiae.* (**B**) To document the reproducibility of endothelial compartment invasion, the model was assembled and infected with spores of each pathogen in three independent experiments. Mucorales DNA was quantified after 30 h and compared with positive controls as described in (**A**). Mean values of technical duplicates in each run are shown and inter-assay CVs are provided. Intra-assay CVs were consistently < 10 %. (**C**) Endothelial compartment invasion by *C. bertholletiae* was assessed in the presence or absence of 50 µg/ml gefitinib (Gef) in the lower chamber. Uninfected inserts (medium control, Med) with and without gefitinib served as negative controls. Mucorales DNA was quantified after 30 h and compared with positive controls as described in (**A**). Three independent experiments were performed. Mean values and standard deviations are shown. (**D**) Prior to infection with *R. arrhizus* (Rar), transwell inserts assembled as described in the methods section were transferred to new wells containing either regular HPAEC medium (Med, glucose concentration: 1 mg/ml) or HPAEC medium supplemented with 8 mg/ml glucose (Glc) or 1 mg/ml beta-hydroxybutyrate (BHB). Mucorales DNA in the lower compartment was quantified 30 h post-infection normalized to a positive control (= 100 %) as described above. Mean values from four independent experiments and standard deviations are shown. The two-sided Student's t-test was used for significance testing in panel (**C**) and (**D**). * $p < 0.05$, ** $p < 0.01$.

Mucorales stimulate a strong pro-inflammatory cytokine response by moDCs, but cause reduced chemokine release from A549 cells

Next, we studied the cytokine response of epithelial cells and moDCs to Mucorales infection by applying a magnetic multiplex cytokine assay to culture supernatants from the alveolar (upper) compartment. Compared to uninfected samples, the secretion of pro-inflammatory cytokines IL-1β (161-335-fold), IL-6 (13-24-fold), IL-8 (12-23-fold), IL-12 p70 (78-289-fold), and TNF-α (54-89-fold) was strongly stimulated by the studied Mucorales species in the presence of moDCs (**Figure 3**).

3.3 Comparative analysis of inflammatory cytokine release and alveolar epithelial barrier invasion in a Transwell® bilayer model of mucormycosis

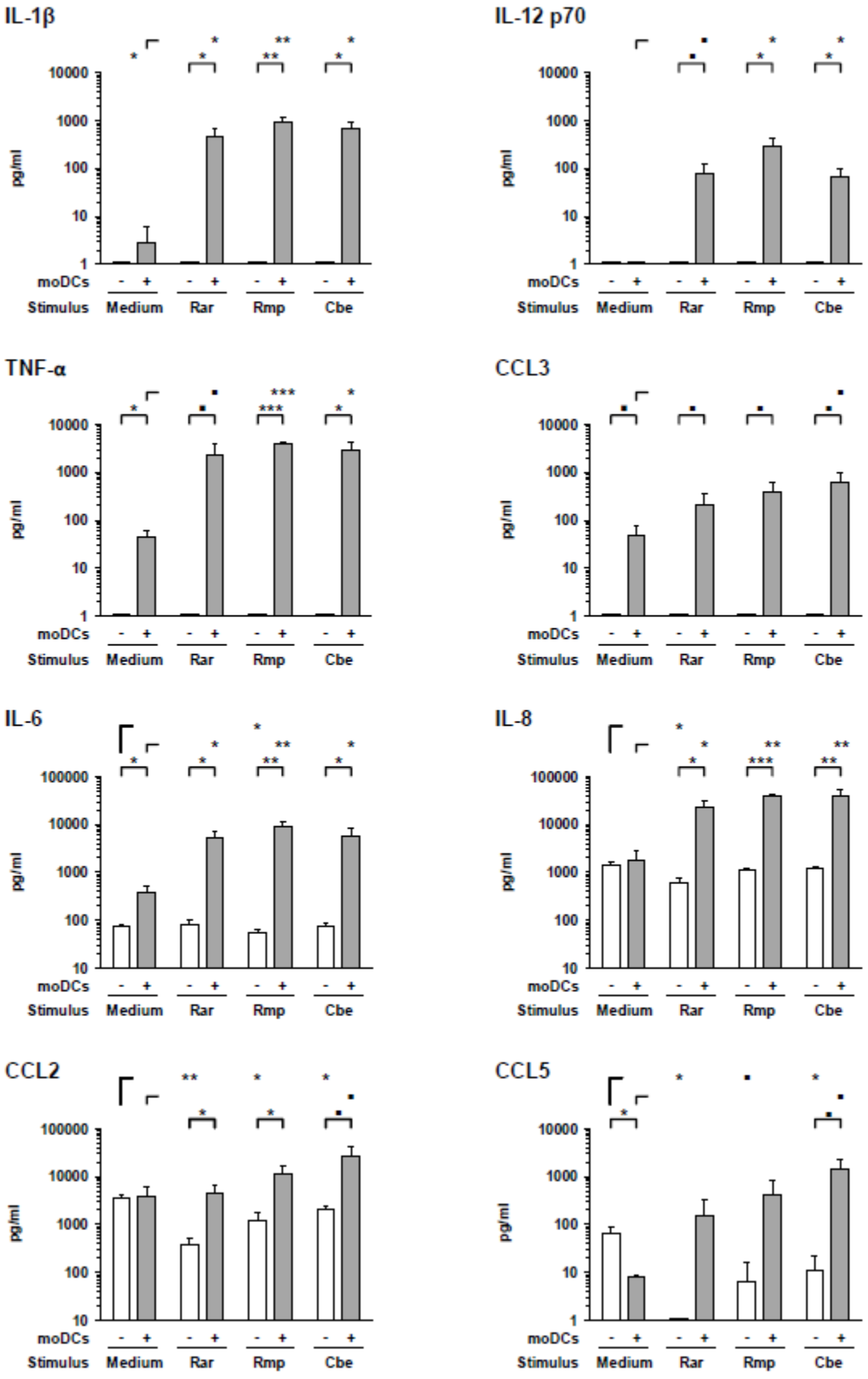

Figure 3: Mucorales stimulate strong pro-inflammatory cytokine response of moDCs

Concentrations of selected cytokines and chemokines were determined in the upper compartment using a 13-plex assay after 30 hours of incubation with 2.5 x 10^5 resting Mucorales spores or mock infection with medium (Med) in the presence or absence of moDCs. Mean values and standard deviations of four independent experimental runs using moDCs from different donors are shown. Two-sided Student's t-test was used for significance testing. ■ $p < 0.1$, * $p < 0.05$, ** $p < 0.01$, *** $p < 0.001$. Rar = *R. arrhizus*, Rmp = *R. pusillus*, Cbe = *C. bertholletiae*.

In samples lacking moDCs, IL-6 and IL-8 were also secreted by epithelial cells and remained largely unaffected by Mucorales exposure, except minor reductions of IL-6 and IL-8 secretion upon *R. arrhizus* and *R. pusillus* infection, respectively (**Figure 3**). Inversely, mRNA expression of IL-8 in A549 was significantly stimulated in infected samples (2.9-4.1, **Figure 4**). Mucorales infection also caused 2.1-2.9-fold induction of *Icam1* transcription in A549 and 5.9-8-4-fold upregulation in the presence of moDCs (**Figure 4**).

In inserts containing moDCs, CCL5 (RANTES) mRNA expression (26-92-fold) and secretion (19-180-fold) was stimulated by all tested pathogens compared to uninfected controls, though statistical significance was not attained for some of the treatments due to considerable inter-individual variation (**Figure 4**). In the absence of moDCs, the release of chemokines CCL2 and CCL5 from A549 cells was markedly reduced in Mucorales-infected samples (CCL2: 0.11-0.60-fold, CCL5: 0.02-0.17-fold, **Figure 3**). This observation was most pronounced for *R. arrhizus*, although transcriptional levels of *CCL2* and *CCL5* in A549 cells remained unaltered (**Figure 4**).

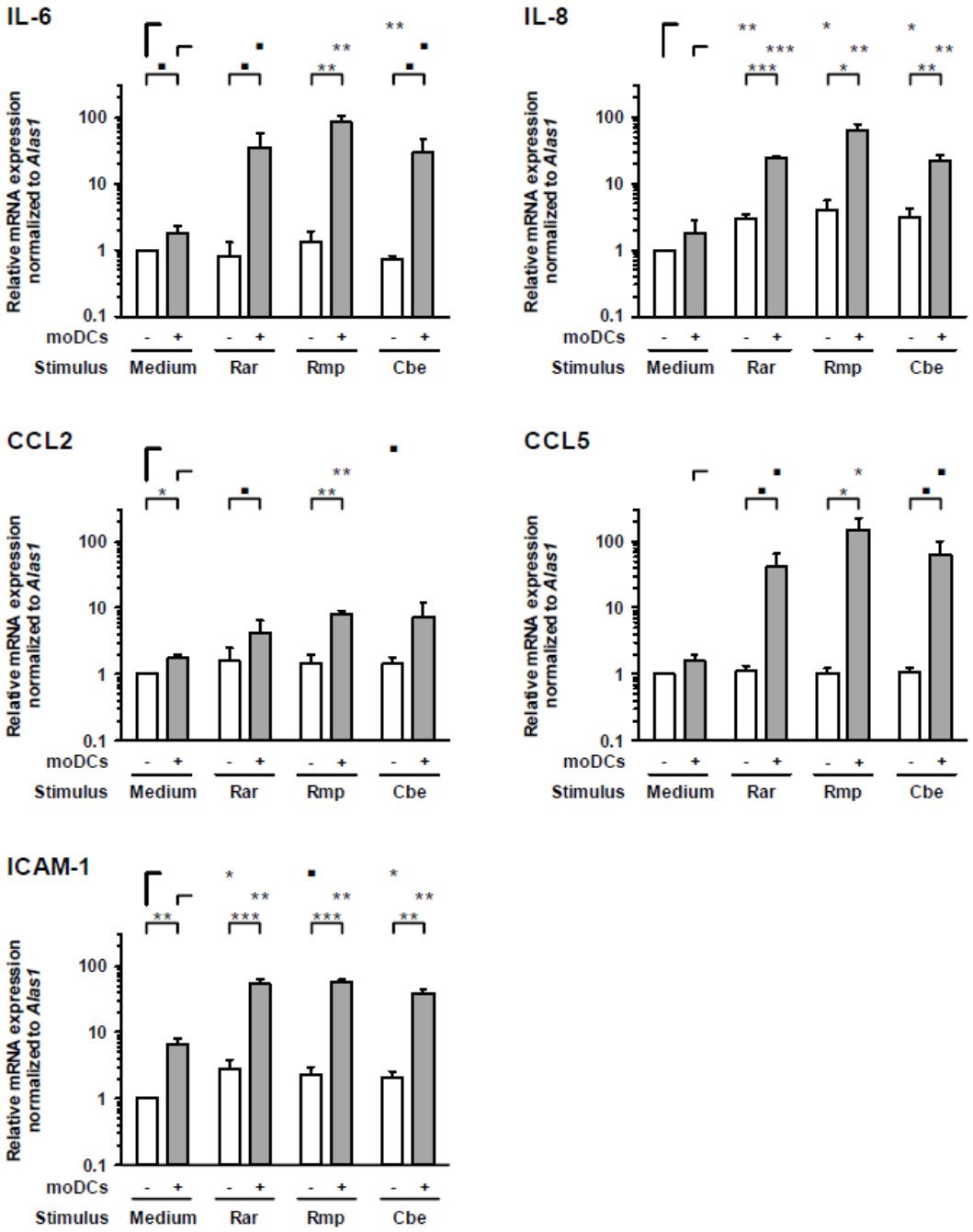

Figure 4: Transcription of epithelial cytokines, chemokines, and adhesion molecules

Relative mRNA expression of *IL-6*, *IL-8*, *CCL2*, *CCL5*, and *ICAM-1* in A549 ± moDCs was analyzed by RT-qPCR after 30 hours of incubation with Mucorales spores or mock infection with cell-free medium (Med). Relative expression levels were normalized to *Alas1* using the ΔΔCt method. Mean values and standard deviations of four independent experimental runs using moDCs from different donors are shown. Two-sided Student's t-test was used for significance testing. ■ $p < 0.1$, * $p < 0.05$, ** $p < 0.01$, *** $p < 0.001$. Rar = *R. arrhizus*, Rmp = *R. pusillus*, Cbe = *C. bertholletiae*.

Pro-inflammatory cytokine response aggravates alveolar barrier dysfunction caused by Mucorales infection

To evaluate epithelial cell damage caused by Mucorales infection, LDH concentrations were quantified in culture supernatants of the upper compartment. Compared to uninfected control samples, upper chamber LDH levels in Mucorales-infected inserts were significantly increased (4.1-8.3-fold, **Figure 5A**). Addition of moDCs led to further enhancement of LDH release, though statistical significance was not reached for this observation. While *R. arrhizus* and *C. bertholletiae* caused greater LDH release in the absence of moDCs, the strongest increase in cytotoxicity was observed when moDCs were added to *R. pusillus* infected inserts (2.2-fold increase). By contrast, transcription of *Cas3* was suppressed in Mucorales exposed A549 cells compared to uninfected samples regardless of moDC addition, whereas *Cas9* mRNA expression was only significantly reduced in the presence of moDCs (**Figure 5B**).

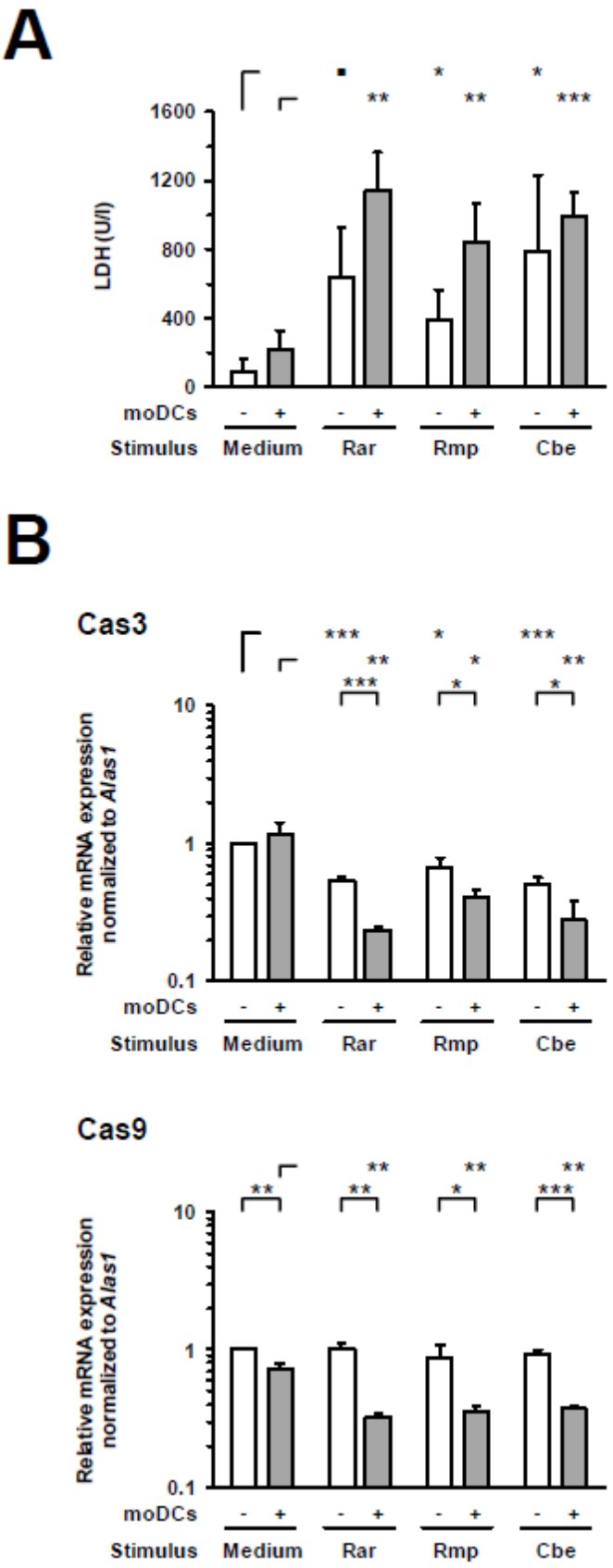
A
LDH (U/l)
1600
1200
800
400
0
moDCs
Stimulus
Medium
Rar
Rmp
Cbe
B
Cas3
Relative mRNA expression normalized to Alas1
10
1
0.1
Cas9

Figure 5: Lactate dehydrogenase concentrations and caspase expression in the epithelial compartment

(**A**) LDH concentrations in the upper compartment were quantified after 30 hours of incubation with or without moDCs and/or Mucorales spores. (**B**) Relative mRNA expression of *Cas3* and *Cas9* in A549 ± moDCs was analyzed by RT-qPCR after 30 hours of incubation with Mucorales spores or mock infection with cell-free medium (Med). Relative expression levels were normalized to *Alas1* using the ΔΔCt method. For both readouts, mean values and standard deviations of four independent experimental runs using moDCs from different donors are shown. Two-sided Student's t-test was used for significance testing. ■ $p < 0.1$, * $p < 0.05$, ** $p < 0.01$, *** $p < 0.001$. Rar = *R. arrhizus*, Rmp = *R. pusillus*, Cbe = *C. bertholletiae*.

For further assessment of epithelial barrier dysfunction, we performed a time-course analysis of membrane permeability using a dextran blue assay (**Figure 6**). Both uninfected inserts and those exposed to *A. fumigatus* showed minor trans-epithelial movement of dextran blue, reaching 9 % (70 kDa) to 15 % (5 kDa) after 30 hours. Greater epithelial permeability was observed in the presence of Mucorales (10 to 17 % for 70 kDa, 20 to 24 % for 5 kDa). Among the studied Mucorales species, *R. arrhizus* caused the earliest and strongest increase in epithelial barrier permeability, most prominently for 70 kDa dextran blue.

3.3 Comparative analysis of inflammatory cytokine release and alveolar epithelial barrier invasion in a Transwell® bilayer model of mucormycosis

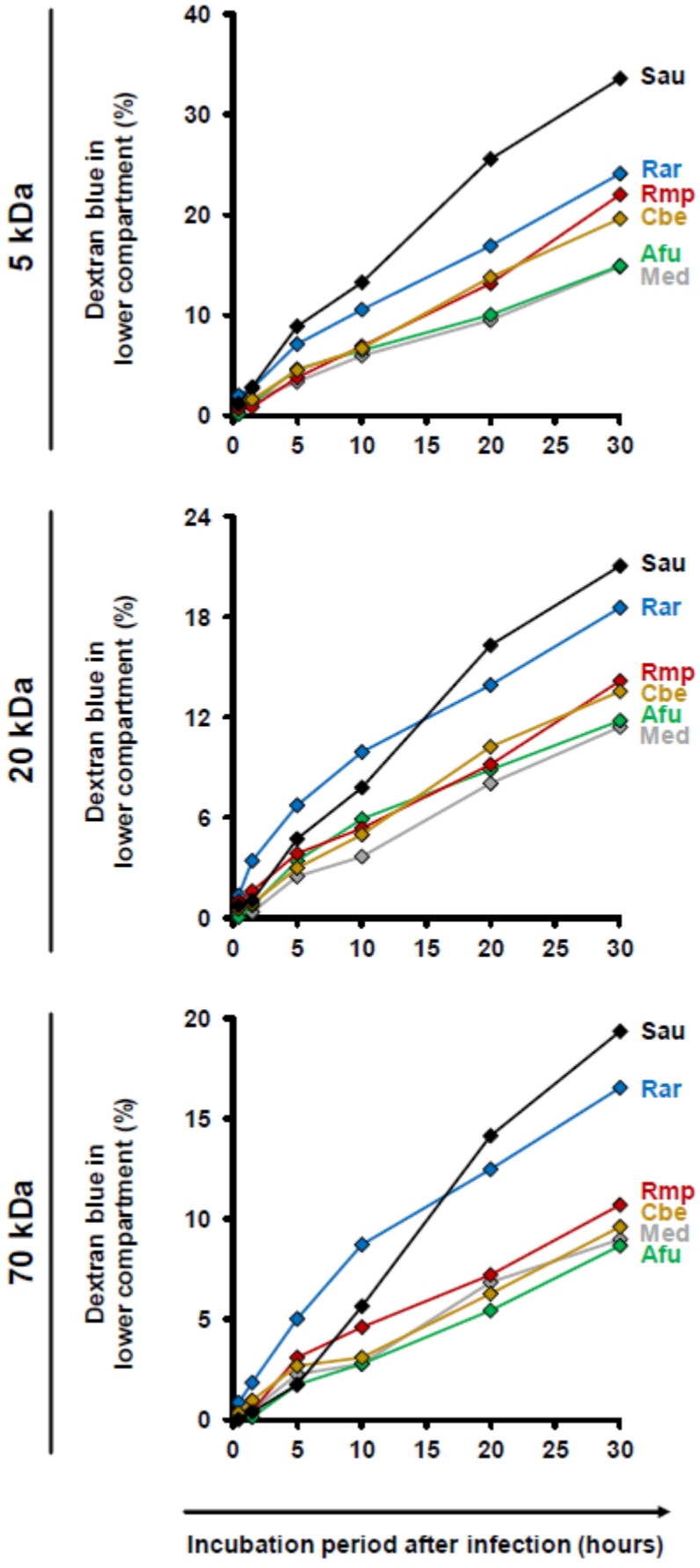

Figure 6: Impact of fungal infection on alveolar barrier permeability for macro-molecules

Culture inserts were prepared and infected as described in the Methods section. 1 µg dextran blue (5 kDa, 20 kDa or 70 kDa, diluted in HPAEC medium) was added to the upper compartment. Inserts were placed in 24 well plates containing 600 µl pre-warmed HPAEC medium per well. After 30 min, 90 min, 5 h, 10 h, 20 h, and 30 h inserts were transferred to a new well with fresh HPAEC medium to prevent back-diffusion. 100 µl medium from the previously used well were transferred to a 96 well microplate and absorbance was determined at 622 nm. Dextran blue concentrations were calculated by comparison of absorbance (OD) values with a standard curve of different dextran blue concentrations. The figure shows the percentage (cumulated over time) of dextran blue passing through the epithelial barrier (100 % = 1 µg). The following stimuli were used: Medium (Med), *A. fumigatus* conidia (Afu), *S. aureus* cells (Sau, clinical isolate), and Mucorales spores (Rar = *R. arrhizus*, Rmp = *R. pusillus*, Cbe = *C. bertholletiae*). Technical duplicates were analyzed and mean values are shown in the figure (CVs consistently < 15 %).

To assess the impact of moDC-mediated inflammation, trans-epithelial movement of dextran blue was comparatively quantified in the presence and absence of moDCs (**Figure 7A**). *R. arrhizus* infection caused a 65 % (5 kDa) to 88 % (70 kDa) increase in dextran blue movement after 30 hours compared to uninfected treatments and epithelial leakage was further aggravated by moDCs (+27 to +44 %, **Figure 7A**). For *C. bertholletiae*, a more heterogeneous impact of moDCs was found, with an early increase in 5kDa and 70kDa permeability, whereas trans-epithelial movement of 20 kDa dextran blue was only increased for one of the two donors tested (**Sup. Figure 1**). While epithelial permeability was not affected by *A. fumigatus* alone (-3 to +9 %), combined presence of the pathogen and moDCs resulted in minor elevations of trans-epithelial dextran blue movement (+10 to +46 %, **Figure 7A**). TNF-α and IL-1β concentrations in both chambers were determined by ELISA (**Figure 7B**). Concordant with data presented in **Figure 3**, TNF-α and IL-1β release by moDCs was strongly increased in *R. arrhizus*-infected samples, whereas concentrations of these cytokines were 28-55 % lower in *A. fumigatus*-infected samples.

3.3 Comparative analysis of inflammatory cytokine release and alveolar epithelial barrier invasion in a Transwell® bilayer model of mucormycosis

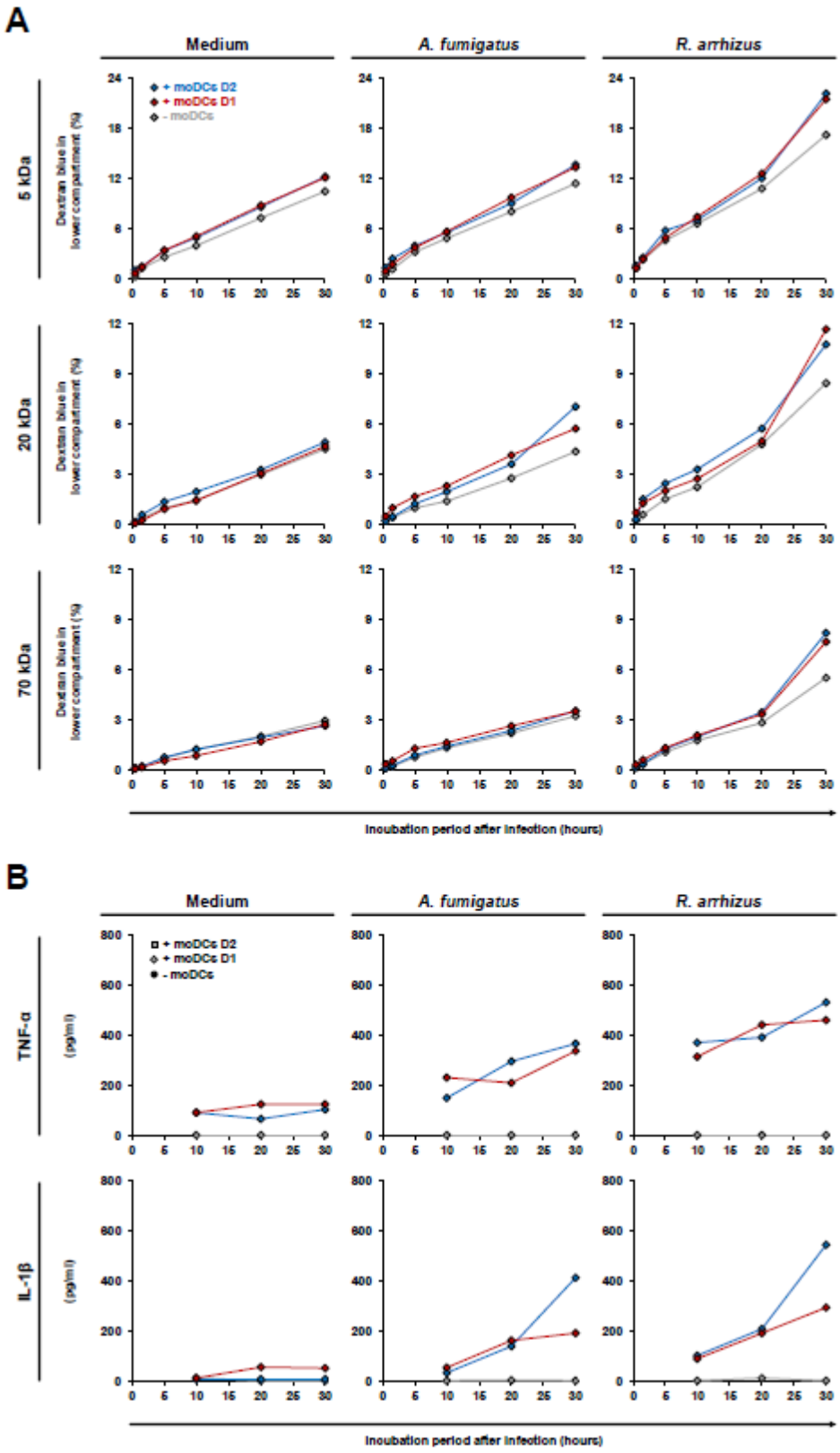

Figure 7: Influence of dendritic cells on alveolar barrier dysfunction caused by *A. fumigatus* and *R. arrhizus*

(**A**) Dextran blue assays were performed as described in the Methods section and figure legend 6. 2.5 x 10^5 moDCs from two healthy donors (red and blue diamonds) or plain medium (grey diamonds) were added to the dextran blue solution. Medium (left column), *A. fumigatus* conidia (central column), and *R. arrhizus* spores (right column) were used for infection. (**B**) In parallel, concentrations of TNF-α and IL-1β were determined in inserts without dextran blue 10, 20, and 30 hours after infection. (**A+B**) Dextran blue assays and ELISA were performed in technical duplicates, and mean values are shown in the figure (CVs consistently < 20 %).

To directly link inflammatory cytokines and epithelial damage, 1 ng/ml TNF-α and IL-1β were added to the upper chamber medium of Transwell® inserts containing A549 and HPAEC, but neither fungal pathogens nor moDCs. Comparing trans-epithelial movement of dextran blue with control inserts not supplemented with cytokines, 23 to 37 % higher concentrations of dextran blue were detected in the lower chamber after 30 hours (**Sup. Figure 2**). We also assessed whether secreted fungal metabolites contribute to epithelial damage. Addition of sterile-filtered supernatants from 30 h Mucorales cultures to the upper chamber of alveolar model inserts led to minimal LDH release (**Sup. Figure 3**), suggesting that Mucorales-related epithelial damage is mostly due to rapid fungal invasion, aggravated by strong pro-inflammatory response of mononuclear cells.

The alveolar bilayer model is a highly reproducible in vitro system for mucormycosis research

Apart from immunological research, the alveolar bilayer model was proposed as an *in vitro* tool for pharmacokinetic studies, antifungal drug screening, and investigation of new biomarkers (Hope et al., 2007). As these applications require highly reproducible experimental conditions, intra-assay, inter-assay, and inter-individual coefficients of variation of selected readout parameters were determined over a course of four independent experimental runs (**Table 1**). In the absence of Mucorales infection, median intra-assay CVs and inter-assay CVs for cytokine concentrations in the upper compartment ranged from 11.0 to 18.1 % and 8.7 to 27.0 %, respectively. Addition of fungal spores did not significantly influence intra-assay CVs, indicating excellent reproducibility of Mucorales infection in technical duplicates. While *C. bertholletiae* infection did not lead to elevated inter-assay CVs, there was a tendency towards slightly greater variability of A549 cytokine response to *R. arrhizus* and *R. pusillus* in independent experimental runs. Relative mRNA expression levels of epithelial cytokines showed higher inter-assay CVs than cytokine concentrations. For all three

fungal pathogens, however, at least 8 out of 10 studied parameters reached an inter-assay CV of less than 40 %. Predictably, for most studied parameters, inter-individual CVs using moDCs from four different donors exceeded technical variability of the assay.

Median intra-assay CV (w/o moDCs)				
	Medium	*R. arrhizus*	*R. pusillus*	*C. bertholletiae*
IL-6 concentration in upper compartment	17.0 %	16.3 %	13.4 %	18.1 %
IL-8 concentration in upper compartment	18.1 %	19.7 %	4.5 %	5.2 %
CCL2 concentration in upper compartment	14.9 %	26.3 %	21.0 %	15.8 %
Inter-assay CV (w/o moDCs)				
	Medium	*R. arrhizus*	*R. pusillus*	*C. bertholletiae*
IL-6 concentration in upper compartment	8.7 %	26.4 %	17.0 %	17.7 %
IL-8 concentration in upper compartment	19.5 %	22.9 %	6.2 %	9.1 %
CCL2 concentration in upper compartment	24.4 %	39.6 %	52.2 %	15.6 %
IL-6 mRNA expression comp. to Medium	n/a	58.8 %	43.1 %	9.2 %
IL-8 mRNA expression comp. to Medium	n/a	17.6 %	35.0 %	33.3 %
CCL2 mRNA expression comp. to Medium	n/a	57.7 %	39.4 %	22.8 %
CCL5 mRNA expression comp. to Medium	n/a	18.8 %	17.4 %	14.4 %
ICAM-1 mRNA expression comp. to Medium	n/a	33.9 %	31.7 %	22.7 %
Cas3 mRNA expression comp. to Medium	n/a	6.2 %	18.5 %	13.0 %
Cas9 mRNA expression comp. to Medium	n/a	13.1 %	20.9 %	5.7 %
Inter-individual CV (with moDCs from four different donors)				
	Medium	*R. arrhizus*	*R. pusillus*	*C. bertholletiae*
IL-6 concentration in upper compartment	38.8 %	48.4 %	23.3 %	42.3 %
IL-8 concentration in upper compartment	57.0 %	38.2 %	11.8 %	27.8 %
CCL2 concentration in upper compartment	67.3 %	41.8 %	53.7 %	59.3 %
IL-6 mRNA expression comp. to Medium	n/a	62.6 %	34.6 %	67.1 %
IL-8 mRNA expression comp. to Medium	n/a	66.2 %	61.4 %	88.9 %
CCL2 mRNA expression comp. to Medium	n/a	41.8 %	25.0 %	58.6 %
CCL5 mRNA expression comp. to Medium	n/a	66.5 %	54.1 %	66.2 %
ICAM-1 mRNA expression comp. to Medium	n/a	32.5 %	20.3 %	34.2 %
Cas3 mRNA expression comp. to Medium	n/a	18.4 %	28.0 %	15.6 %
Cas9 mRNA expression comp. to Medium	n/a	16.5 %	9.3 %	13.6 %

Table 1

The table summarizes median intra-assay (two inserts per condition in each experimental run), inter-assay (four independent experiments without moDCs), and inter-individual (moDCs obtained from four different donors) coefficients of variation for selected readout markers depending on the fungal

stimulus. Relative mRNA expression refers to analyses of cell samples from the upper compartment (A549 ± moDCs). For CV determination of multiplex cytokine assay, only cytokines with concentrations consistently > 10 pg/ml (including samples without moDCs or fungi) were considered.

Discussion

Opportunistic mold pathogens of the order Mucorales account for an increasing share of invasive infections in immunocompromised patients (Roden et al., 2005; Ibrahim & Kontoyiannis, 2013). The most common site of invasive mucormycosis in patients with hematological malignancies is the lung (Roden et al., 2005). In contrast to invasive aspergillosis, knowledge of pathogen-host-interplay in mucormycosis is still very limited (Roilides et al., 2014). Direct interaction studies revealed striking differences in the immunopathology of aspergillosis and mucormycosis (Chamilos et al., 2008, Warris et al., 2005, Wurster et al., 2017), especially in the inflammatory response to resting spores. While such analyses provide basic insights into fungal immunopathology, more sophisticated models are required to mimic the complexity of respiratory epithelia as the primary site of fungal invasion.

On the example of invasive aspergillosis, bilayer (Gregson et al., 2012, Hope et al., 2007, Morton et al., 2014) or monolayer (Morton et al., 2018) Transwell® models of the human alveolus have been introduced to complement animal research and basic cell culture experiments (Gregson et al., 2012, Hope et al., 2007, Morton et al., 2014). Building upon the extensive characterization and validation of these models in aspergillosis research, this study employed the alveolar bilayer model to comparatively assess the host response and epithelial integrity upon infection with different Mucorales species. The tested species were selected from the top seven causative agents of invasive mucormycosis (Lanternier et al., 2012) due to their biological heterogeneity in terms of spore diameter and mycelial morphology (Ribes et al., 2000). Fungal invasion of the lower compartment was documented using an 18S ribosomal DNA assay, since previously employed biomarkers (Gregson et al., 2012, Hope, 2009, Hope et al., 2007, Morton et al., 2014) such as galactomannan are not capable of detecting Mucorales (Lackner et al., 2014). High reproducibility of endothelial barrier invasion was documented (**Figure 2B**). Moreover, we have validated that our model is able to capture important hallmarks of Mucorales immunopathology such as EGFR-dependent alveolar barrier invasion (Watkins et al.,

2018) and enhanced growth into the endothelial compartment in a hyperglycemic or ketoacidotic environment (Gebremariam et al., 2016), both previously demonstrated in monolayer studies and *in vivo* models.

In analogy with earlier, *A. fumigatus*-based studies (Gregson et al., 2012, Hope et al., 2007, Morton et al., 2014, Morton et al., 2018), fungal invasion of the lower chamber was significantly reduced upon addition of moDCs to the alveolar compartment. In planktonic culture, moDCs were found to phagocytose and kill a significant proportion of *A. fumigatus* spores (Morton et al., 2011; Waylnka et al., 2005). Though the knowledge of dendritic cell-Mucorales interplay is very limited, we have demonstrated that both resting spores and germinated stages of *R. arrhizus* induce maturation marker upregulation and pro-inflammatory cytokine response in moDCs (Wurster et al., 2017). Others have previously shown that germinated Mucorales activate pro-inflammatory responses by moDCs in a Dectin-1-dependent manner (Chamilos et al., 2010). In addition, T-helper cell activation in PBMC-Mucorales co-culture was found suggesting that both spores and germ tubes are efficiently taken up and phagolysosomally processed by mononuclear phagocytes (Wurster et al., 2017). Therefore, it is likely that, similar to *A. fumigatus*, moDCs possess the ability to contribute to the clearance of Mucorales and thereby reduce fungal burden in the endothelial compartment.

Assessing cytokine release in A549-moDC co-culture in the bilayer model, a broad range of pro-inflammatory cytokines and chemokines was detected in Mucorales-infected inserts. Compared to a previous report of *A. fumigatus*-A549 interactions (Morton et al., 2018), markedly greater levels of IL-1β, IL-8, and TNF-α were found in response to the studied Mucorales. Similarly, induction of IL-8 and ICAM-1 transcription in A549-moDC-co-cultures was decidedly stronger than in an aspergillosis bilayer model (Morton et al., 2014), indicative of a more robust induction of pro-inflammatory cascades including the NF-κB pathways (Melotti et al., 2001). Direct comparison of IL-1β and TNF-α release in the present study confirmed earlier and significantly stronger induction in inserts infected with *R. arrhizus* compared to *A. fumigatus*, corroborating our previous observation of an early and robust pro-inflammatory cytokine response to both resting and germinated stages of Mucorales in planktonic culture (Wurster et al., 2017). Minor and mostly non-significant interspecies differences in cytokine and chemokine response patterns of epithelial

cells and moDCs were observed between the studied Mucorales. While *R. pusillus* led to more prominent release of IL-6 and IL-12 p70, *C. bertholletiae* caused greater CCL2, CCL3, and CCL5 secretion from moDCs. This observation, which may be attributable to variable recognition of fungal cell wall constituents (Roilides et al., 2014), however, is outweighed by far more distinct differences between Mucorales and *Aspergillus* (Morton et al., 2018).

We employed moDCs for reasons of comparability with previous alveolar bilayer studies in invasive aspergillosis (Morton et al., 2014, Morton et al., 2018), their extensive characterization in mold immunopathology (Lother et al., 2014, Mezger et al., 2008, Morton et al., 2011), and availability in large quantities using standardized protocols. The pulmonary dendritic cell repertoire is, however, heterogeneous and its composition undergoes dynamic changes depending on the degree of inflammation (Kim et al., 2014). In the inflammatory state, moDCs are generated in the lung and are pivotal for pro-inflammatory cytokine response, phagocytosis of fungal spores, and T_H1 cell priming, whereas conventional and plasmacytoid DCs are the dominant subsets in the steady state (Kim & Lee, 2014). Planktonic *in vitro* culture revealed specific roles of these subsets in the interplay with *A. fumigatus*, driven by distinct repertoires of pattern recognition receptors (Lother et al., 2014). Moreover, Morton and colleagues (2014) described distinct differences in cytokine gene induction in conventional DCs and moDCs exposed to *A. fumigatus* in the alveolar bilayer model. Therefore, future studies on Mucorales immunopathology may aim to comparatively elucidate the functional role of different DC subsets in the alveolar context.

Expectably, some of the studied cytokines showed baseline secretion from uninfected epithelial cells (e. g. IL-6 and IL-8), suggesting sufficient viability of A549 cells at the time of assessment. Though IL-8 mRNA expression in A549 was stimulated, there was no enhanced release in response to Mucorales. This observation is in line with an earlier study reporting minor stimulation of IL-6 and IL-8 release from airway epithelial cells infected with *A. fumigatus* (Zhang et al., 2005). Interestingly, in the absence of moDCs, our results document reduced concentrations of epithelial cytokines CCL2 and CCL5 in the alveolar compartment of Mucorales infected Transwell® inserts, whereas transcriptional activity compared to a reference gene remained largely unaffected and proper ICAM-1 transcriptional response was observed. This may be suggestive of reduced numbers of vital, cytokine-producing

epithelial cells upon infection. Accordingly, assessment of LDH, released from the cytosolic compartment of injured or dead cells (Chan et al., 2013), revealed significantly elevated concentrations upon Mucorales infection, whereas *A. fumigatus* caused minimal LDH release into the alveolar compartment. However, reduced expression of the key pro-apoptotic mediator *Cas3* in Mucorales-challenged A549 was observed, despite induction of apoptosis-driving cytokines (e. g. TNF-α). These findings may indicate active suppression of apoptosis in the presence of Mucorales, a mechanism previously described in *A. fumigatus* infected A549 and tracheal epithelial cells (Berkova et al., 2006).

Importantly, addition of moDCs led to strongly elevated LDH levels and epithelial barrier permeability, indicating aggravation of cellular stress due to inflammatory cytokines and mononuclear cell metabolites. In particular, TNF-α and IL-1β, strongly upregulated in Mucorales-exposed moDCs (Wurster et al., 2017), have been described to contribute to alveolar barrier dysfunction and A549 permeability (Cox et al., 2015, Tang et al., 2014). In the present study, time course experiments affirmed the link and temporal relationship between mononuclear cell cytokine secretion and a stronger moDC-associated increase in epithelial barrier disruption caused by infection with *R. arrhizus* compared to *A. fumigatus*.

Even in the absence of moDCs the studied Mucorales species caused stronger epithelial barrier disruption than *A. fumigatus*. Increased trans-epithelial movement of dextran blue was not only observed for *R. arrhizus*, known to rapidly produce abundant mycelium, but to a lesser extend also for *R. pusillus* despite its less extensive mycelial morphology (Ribes et al., 2000). While interstitial penetration upon adhesion of conidia to the basal lamina contributes to alveolar barrier invasion by both *A. fumigatus* (Croft et al., 2016, Wasylnka & Moore, 2000) and Mucorales (Bouchara et al., 1996), distinct means of invasion upon conidial attachment to epithelial cells have been described (Filler & Sheppard, 2006). Microscopic studies documented that *A. fumigatus* mostly grows horizontal to the epithelium (Escobar et al., 2016). *A. fumigatus* conidia internalized by A549 enter the phagolysosomal pathway, but some conidia germinate within epithelial cells, penetrate the cell membrane, and invade the extracellular space (Wasylnka et al., 2005, Wasylnka & Moore, 2000). Moreover, a recent study found that *A. fumigatus* hyphae traversed the bronchial epithelium through reorganization of the host actin exoskeleton, forming a

tunnel that allows hyphae to enter the cells without disturbing their integrity (Fernandez et al., 2018). These mechanisms apparently foster immune evasion and fungal survival in the alveolar environment (Escobar et al., 2016, Margalit & Kavanagh, 2015). By contrast, destructive invasive growth and rapid induction of cell damage are hallmarks of mucormycosis (Filler & Sheppard, 2006, Ibrahim et al. 2005). Though the pathogens' ability to produce an array of cytotoxic metabolites and lytic enzymes is well established (Binder et al., 2014, Ghuman & Voelz, 2017), our data did not reveal a prominent contribution of soluble mediators to epithelial cytolysis, suggesting that rapid mycelial growth of Mucorales, combined with an early and strong pro-inflammatory response by mononuclear cells, result in more pronounced epithelial cell damage and trans-epithelial movement of macromolecules.

An important limitation of this study is the continued use of A549 adenocarcinoma cells to mimic the alveolar side of the epithelial barrier. While this approach facilitates comparability with previous studies on *A. fumigatus* (Morton et al., 2014, Morton et al., 2018) and a recent Mucorales pathogenicity study in A549 monolayers (Watkins et al., 2018), specific properties of cancerous cells need to be considered, for example when assessing apoptosis markers (Croft et al., 2016, Gazdar et al., 2010). The use of cell lines also does not reflect the morphologic and genetic heterogeneity of respiratory epithelia. For this reason, the development of a perfused dynamic culture model with primary cells was recently reported and applied to study mold immunopathology (Chandorkar et al., 2017). On the other hand, the A549 cell line demonstrably contributes to highly reproducible performance of the model with intra- and inter-assay CVs for cytokine concentrations and RT-qPCR based readouts consistently below 40 %, allowing for the detection of inter-individual differences in innate immune response to the fungus, e. g. in studies assessing the influence of mutations in pathways associated with immune recognition of fungal pathogens.

In summary, this study presents a cost-effective and reliable *in vitro* model of mucormycosis, facilitating the screening of an array of pathogens, experimental conditions, or immune cell samples in parallel. Our findings reveal an early and strong pro-inflammatory response by dendritic cells, which aggravates epithelial barrier dysfunction. Due to its high reproducibility and ability to capture important hallmarks of Mucorales immunopathology, the alveolar bilayer model may become an

appealing tool for the *in vitro* screening of antifungal leads and biomarkers related to host immunity.

Footnote Page

Acknowledgement

We want to thank the Institute for Hygiene and Microbiology Wuerzburg for providing fungal and bacterial strains and Frank Ebel for critical discussion of the results. We would also like to thank Denise Michel for excellent technical assistance.

Funding

This work was supported by the Interdisciplinary Centre for Clinical Research (IZKF) Wuerzburg (grant number Z-3/56 to SW) and the DFG Transregio 124 “Funginet” (project A2 to HE and JL).

Disclosure of potential conflicts of interests

The authors have no conflicts of interest related to this study.

Meetings where the information has previously been presented

Preliminary data of this study have been presented at the European Congress of Clinical Microbiology and Infectious Diseases 2017, Vienna, Austria.

Author contributions

SB and LP performed experiments and data analysis and contributed to the manuscript. ML, MD and JS performed experiments. AMWG analyzed data. COM contributed to study design, data analysis, and manuscript preparation. HE, JL, and AJU provided discussions, and contributed to study supervision and manuscript preparation. SW designed and supervised the study, performed experiments and data analysis, and wrote the manuscript.

References

- Berkova N, Lair-Fulleringer S, Femenia F, et al. Aspergillus fumigatus conidia inhibit tumour necrosis factor- or staurosporine-induced apoptosis in epithelial cells. Int Immunol. 2006 Jan;18(1):139-50. doi: 10.1093/intimm/dxh356. PubMed PMID: 16357007.
- Binder U, Maurer E, Lass-Florl C. Mucormycosis--from the pathogens to the disease. Clin Microbiol Infect. 2014 Jun;20 Suppl 6:60-6. doi: 10.1111/1469-0691.12566. PubMed PMID: 24476149.
- Bouchara JP, Oumeziane NA, Lissitzky JC, et al. Attachment of spores of the human pathogenic fungus Rhizopus oryzae to extracellular matrix components. Eur J Cell Biol. 1996 May;70(1):76-83. PubMed PMID: 8738422.
- Chamilos G, Ganguly D, Lande R, et al. Generation of IL-23 producing dendritic cells (DCs) by airborne fungi regulates fungal pathogenicity via the induction of T(H)-17 responses. PLoS One. 2010;5(9):e12955. doi: 10.1371/journal.pone.0012955. PubMed PMID: 20886035.
- Chamilos G, Lewis RE, Lamaris G, et al. Zygomycetes hyphae trigger an early, robust proinflammatory response in human polymorphonuclear neutrophils through toll-like receptor 2 induction but display relative resistance to oxidative damage. Antimicrob Agents Chemother. 2008 Feb;52(2):722-4. doi: 10.1128/AAC.01136-07. PubMed PMID: 18025115.
- Chan FK, Moriwaki K, De Rosa MJ. Detection of necrosis by release of lactate dehydrogenase activity. Methods Mol Biol. 2013;979:65-70. doi: 10.1007/978-1-62703-290-2_7. PubMed PMID: 23397389.
- Chandorkar P, Posch W, Zaderer V, et al. Fast-track development of an in vitro 3D lung/immune cell model to study Aspergillus infections. Sci Rep. 2017;7(1):11644. doi: 10.1038/s41598-017-11271-4. PubMed PMID: 28912507.
- Cortez KJ, Lyman CA, Kottilil S, et al. Functional genomics of innate host defense molecules in normal human monocytes in response to Aspergillus fumigatus. Infect Immun. 2006 Apr;74(4):2353-65. doi: 10.1128/IAI.74.4.2353-2365.2006. PubMed PMID: 16552065.
- Cox R, Jr., Phillips O, Fukumoto J, et al. Resolvins Decrease Oxidative Stress Mediated Macrophage and Epithelial Cell Interaction through Decreased Cytokine Secretion. PLoS One. 2015;10(8):e0136755. doi: 10.1371/journal.pone.0136755. PubMed PMID: 26317859.
- Croft CA, Culibrk L, Moore MM, et al. Interactions of Aspergillus fumigatus Conidia with Airway Epithelial Cells: A Critical Review. Front Microbiol. 2016;7:472. doi: 10.3389/fmicb.2016.00472. PubMed PMID: 27092126.
- Escobar N, Ordonez SR, Wosten HA, et al. Hide, Keep Quiet, and Keep Low: Properties That Make Aspergillus fumigatus a Successful Lung Pathogen. Front Microbiol. 2016;7:438. doi: 10.3389/fmicb.2016.00438. PubMed PMID: 27092115.
- Fernandes J, Hamidi F, Beau R, et al. Penetration of the Human Pulmonary Epithelium by Aspergillus fumigatus Hyphae. J Infect Dis. 2018 May 26. doi: 10.1093/infdis/jiy298. [Epub ahead of print]. PubMed PMID: 29846638.

- Filler SG, Sheppard DC. Fungal invasion of normally non-phagocytic host cells. PLoS Pathog. 2006 Dec;2(12):e129. doi: 10.1371/journal.ppat.0020129. PubMed PMID: 17196036.
- Gazdar AF, Girard L, Lockwood WW, et al. Lung cancer cell lines as tools for biomedical discovery and research. J Natl Cancer Inst. 2010 Sep 8;102(17):1310-21. doi: 10.1093/jnci/djq279. PubMed PMID: 20679594.
- Gebremariam T, Lin L, Liu M, et al. Bicarbonate correction of ketoacidosis alters host-pathogen interactions and alleviates mucormycosis. J Clin Invest. 2016;126(6):2280-94. doi: 10.1172/JCI82744. PubMed PMID: 27159390.
- Ghuman H, Voelz K. Innate and Adaptive Immunity to Mucorales. J Fungi (Basel). 2017 Sep 5;3(3). doi: 10.3390/jof3030048. PubMed PMID: 29371565.
- Gregson L, Hope WW, Howard SJ. In vitro model of invasive pulmonary aspergillosis in the human alveolus. Methods Mol Biol. 2012;845:361-7. doi: 10.1007/978-1-61779-539-8_24. PubMed PMID: 22328387.
- Hope WW, Kruhlak MJ, Lyman CA, et al. Pathogenesis of Aspergillus fumigatus and the kinetics of galactomannan in an in vitro model of early invasive pulmonary aspergillosis: implications for antifungal therapy. J Infect Dis. 2007 Feb 1;195(3):455-66. doi: 10.1086/510535. PubMed PMID: 17205486.
- Hope WW. Invasion of the alveolar-capillary barrier by Aspergillus spp.: therapeutic and diagnostic implications for immunocompromised patients with invasive pulmonary aspergillosis. Med Mycol. 2009;47 Suppl 1:S291-8. doi: 10.1080/13693780802510232. PubMed PMID: 19306226.
- Ibrahim AS, Kontoyiannis DP. Update on mucormycosis pathogenesis. Curr Opin Infect Dis. 2013;26(6):508-15. doi: 10.1097/QCO.0000000000000008. PubMed PMID: 24126718
- Ibrahim AS, Spellberg B, Avanessian V, et al. Rhizopus oryzae adheres to, is phagocytosed by, and damages endothelial cells in vitro. Infect Immun. 2005 Feb;73(2):778-83. doi: 10.1128/IAI.73.2.778-783.2005. PubMed PMID: 15664916.
- Kim TH, Lee HK. Differential roles of lung dendritic cell subsets against respiratory virus infection. Immune Netw. 2014 Jun;14(3):128-37. doi: 10.4110/in.2014.14.3.128. PubMed PMID: 24999309.
- Kniemeyer O, Ebel F, Kruger T, et al. Immunoproteomics of Aspergillus for the development of biomarkers and immunotherapies. Proteomics Clin Appl. 2016 Oct;10(9-10):910-921. doi: 10.1002/prca.201600053. PubMed PMID: 27312145.
- Lackner M, Caramalho R, Lass-Florl C. Laboratory diagnosis of mucormycosis: current status and future perspectives. Future Microbiol. 2014;9(5):683-95. doi: 10.2217/fmb.14.23. PubMed PMID: 24957094.
- Lanternier F, Dannaoui E, Morizot G, et al. A global analysis of mucormycosis in France: the RetroZygo Study (2005-2007). Clin Infect Dis. 2012 Feb;54 Suppl 1:S35-43. doi: 10.1093/cid/cir880. PubMed PMID: 22247443.
- Lass-Florl C, Roilides E, Loffler J, et al. Minireview: host defence in invasive aspergillosis. Mycoses. 2013 Jul;56(4):403-13. doi: 10.1111/myc.12052. PubMed PMID: 23406508.

- Lother J, Breitschopf T, Krappmann S, et al. Human dendritic cell subsets display distinct interactions with the pathogenic mould Aspergillus fumigatus. Int J Med Microbiol. 2014 Nov;304(8):1160-8. doi: 10.1016/j.ijmm.2014.08.009. PubMed PMID: 25200858.
- Margalit A, Kavanagh K. The innate immune response to Aspergillus fumigatus at the alveolar surface. FEMS Microbiol Rev. 2015 Sep;39(5):670-87. doi: 10.1093/femsre/fuv018. PubMed PMID: 25934117.
- Melotti P, Nicolis E, Tamanini A, et al. Activation of NF-kB mediates ICAM-1 induction in respiratory cells exposed to an adenovirus-derived vector. Gene Ther. 2001;8(18):1436-42. PubMed PMID: 11571584
- Mezger M, Kneitz S, Wozniok I, et al. Proinflammatory response of immature human dendritic cells is mediated by dectin-1 after exposure to Aspergillus fumigatus germ tubes. J Infect Dis. 2008 Mar 15;197(6):924-31. doi: 10.1086/528694. PubMed PMID: 18279049.
- Morton CO, Fliesser M, Dittrich M, et al. Gene expression profiles of human dendritic cells interacting with Aspergillus fumigatus in a bilayer model of the alveolar epithelium/endothelium interface. PLoS One. 2014;9(5):e98279. doi: 10.1371/journal.pone.0098279. PubMed PMID: 24870357.
- Morton CO, Varga JJ, Hornbach A, et al. The temporal dynamics of differential gene expression in Aspergillus fumigatus interacting with human immature dendritic cells in vitro. PLoS One. 2011 Jan 14;6(1):e16016. doi: 10.1371/journal.pone.0016016. PubMed PMID: 21264256.
- Morton CO, Wurster S, Fliesser M, et al. Validation of a simplified in vitro Transwell® model of the alveolar surface to assess host immunity induced by different morphotypes of Aspergillus fumigatus. Int J Med Microbiol. 2018. [Epub ahead of print] PubMed PMID: 30197238.
- Osherov N. Interaction of the pathogenic mold Aspergillus fumigatus with lung epithelial cells. Front Microbiol. 2012;3:346. doi: 10.3389/fmicb.2012.00346. PubMed PMID: 23055997.
- Park SJ, Mehrad B. Innate immunity to Aspergillus species. Clin Microbiol Rev. 2009 Oct;22(4):535-51. doi: 10.1128/CMR.00014-09. PubMed PMID: 19822887.
- Ribes JA, Vanover-Sams CL, Baker DJ. Zygomycetes in human disease. Clin Microbiol Rev. 2000 Apr;13(2):236-301. PubMed PMID: 10756000.
- Roden MM, Zaoutis TE, Buchanan WL, et al. Epidemiology and outcome of zygomycosis: a review of 929 reported cases. Clin Infect Dis. 2005 Sep 1;41(5):634-53. doi: 10.1086/432579. PubMed PMID: 16080086.
- Roilides E, Antachopoulos C, Simitsopoulou M. Pathogenesis and host defence against Mucorales: the role of cytokines and interaction with antifungal drugs. Mycoses. 2014 Dec;57 Suppl 3:40-7. doi: 10.1111/myc.12236. PubMed PMID: 25175306.
- Roilides E, Simitsopoulou M. Immune responses to Mucorales growth forms: Do we know everything? Virulence. 2017 Nov 17;8(8):1489-1491. doi: 10.1080/21505594.2017.1368942. PubMed PMID: 28820315.
- Springer J, Goldenberger D, Schmidt F, et al. Development and application of two independent real-time PCR assays to detect clinically relevant Mucorales species. J Med Microbiol. 2016a Mar;65(3):227-34. doi: 10.1099/jmm.0.000218. PubMed PMID: 26743820.

- Springer J, Lackner M, Ensinger C, et al. Clinical evaluation of a Mucorales-specific real-time PCR assay in tissue and serum samples. J Med Microbiol. 2016b Dec;65(12):1414-1421. doi: 10.1099/jmm.0.000375. PubMed PMID: 27902424.
- Sun WK, Lu X, Li X, et al. Dectin-1 is inducible and plays a crucial role in Aspergillus-induced innate immune responses in human bronchial epithelial cells. Eur J Clin Microbiol Infect Dis. 2012 Oct;31(10):2755-64. doi: 10.1007/s10096-012-1624-8. PubMed PMID: 22562430.
- Tang M, Tian Y, Li D, et al. TNF-alpha mediated increase of HIF-1alpha inhibits VASP expression, which reduces alveolar-capillary barrier function during acute lung injury (ALI). PLoS One. 2014;9(7):e102967. doi: 10.1371/journal.pone.0102967. PubMed PMID: 25051011.
- Warris A, Netea MG, Verweij PE, et al. Cytokine responses and regulation of interferon-gamma release by human mononuclear cells to Aspergillus fumigatus and other filamentous fungi. Med Mycol. 2005 Nov;43(7):613-21. PubMed PMID: 16396246.
- Wasylnka JA, Hissen AH, Wan AN, et al. Intracellular and extracellular growth of Aspergillus fumigatus. Med Mycol. 2005 May;43 Suppl 1:S27-30. PubMed PMID: 16110789.
- Wasylnka JA, Moore MM. Adhesion of Aspergillus species to extracellular matrix proteins: evidence for involvement of negatively charged carbohydrates on the conidial surface. Infect Immun. 2000 Jun;68(6):3377-84. PubMed PMID: 10816488.
- Watkins TN, Gebremariam T, Swidergall M, et al. Inhibition of EGFR Signaling Protects from Mucormycosis. MBio. 2018;9(4). doi: 10.1128/mBio.01384-18. PubMed PMID: 30108171.
- Wurster S, Thielen V, Weis P, et al. Mucorales spores induce a proinflammatory cytokine response in human mononuclear phagocytes and harbor no rodlet hydrophobins. Virulence. 2017 Nov 17;8(8):1708-1718. doi: 10.1080/21505594.2017.1342920. PubMed PMID: 28783439.
- Zhang Z, Liu R, Noordhoek JA, et al. Interaction of airway epithelial cells (A549) with spores and mycelium of Aspergillus fumigatus. J Infect. 2005 Dec;51(5):375-82. doi: 10.1016/j.jinf.2004.12.012. PubMed PMID: 16321648.

Supplementary Materials

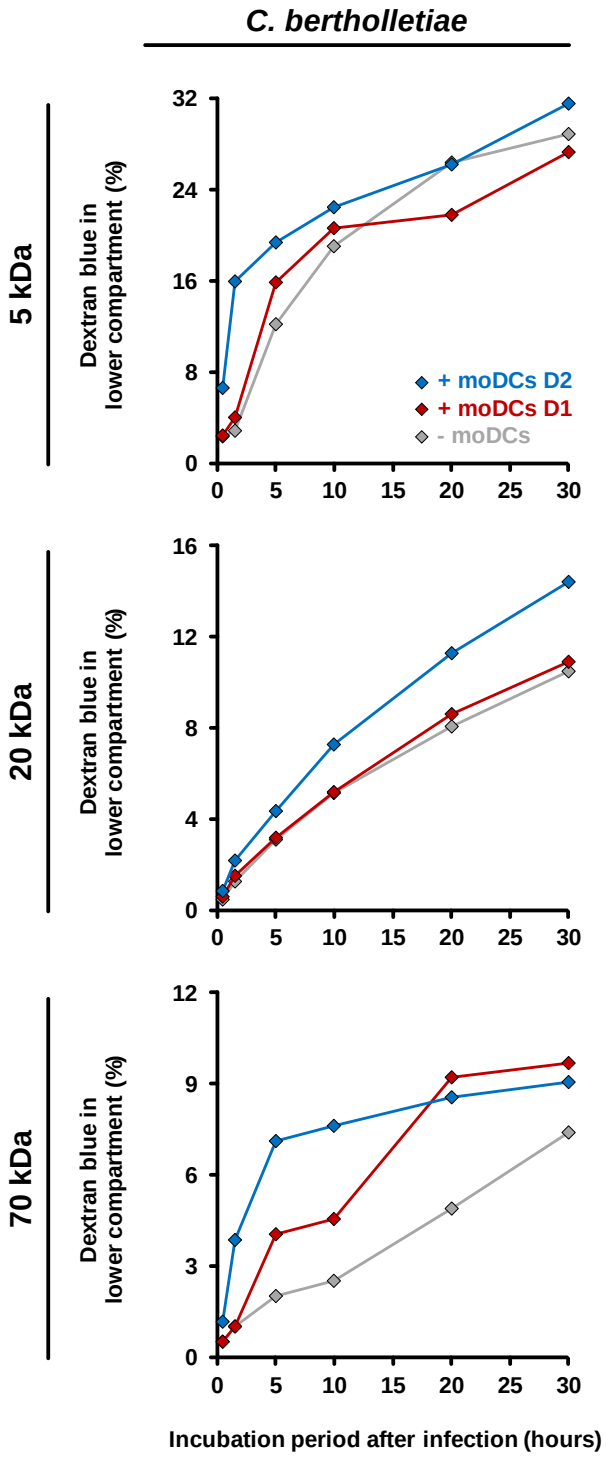

Supplementary Figure 1

Dextran blue assays were performed as described in the Methods section and figure legend 6 and inserts were infected with 2.5 x 10^5 *C. bertholletiae* spores. 2.5 x 10^5 moDCs from two healthy donors (red and blue diamonds) or plain medium (grey diamonds) were added to the dextran blue solution. Technical duplicates were performed, and mean values are shown. CVs were consistently below 25 %.

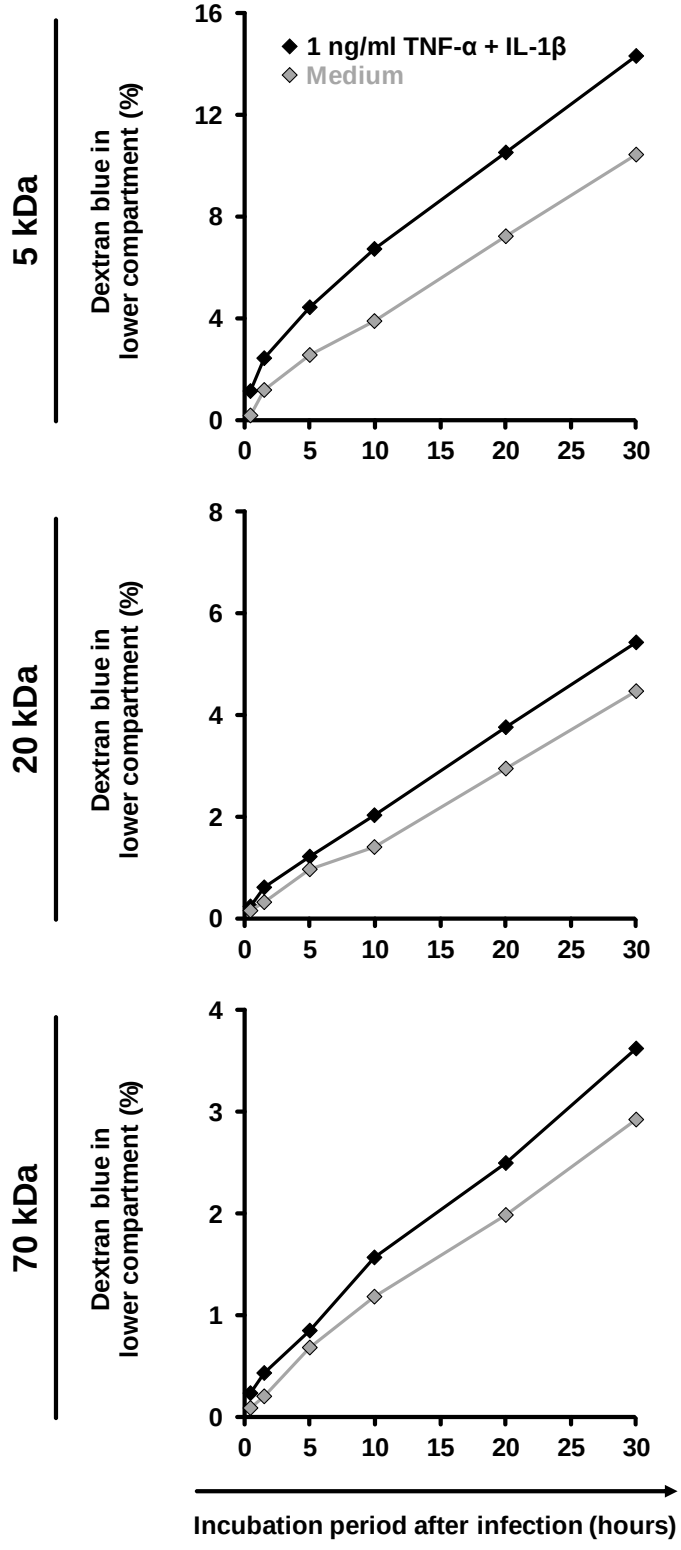

Supplementary Figure 2

Trans-epithelial dextran blue movement was assessed as described in the methods section. Dextran blue was dissolved either in plain HPAEC medium (grey diamonds) or medium supplemented with 1 ng/ml TNF-α and IL-1β (black diamonds). The analysis was performed in duplicates, and mean values are shown. CVs were consistently below 10 %.

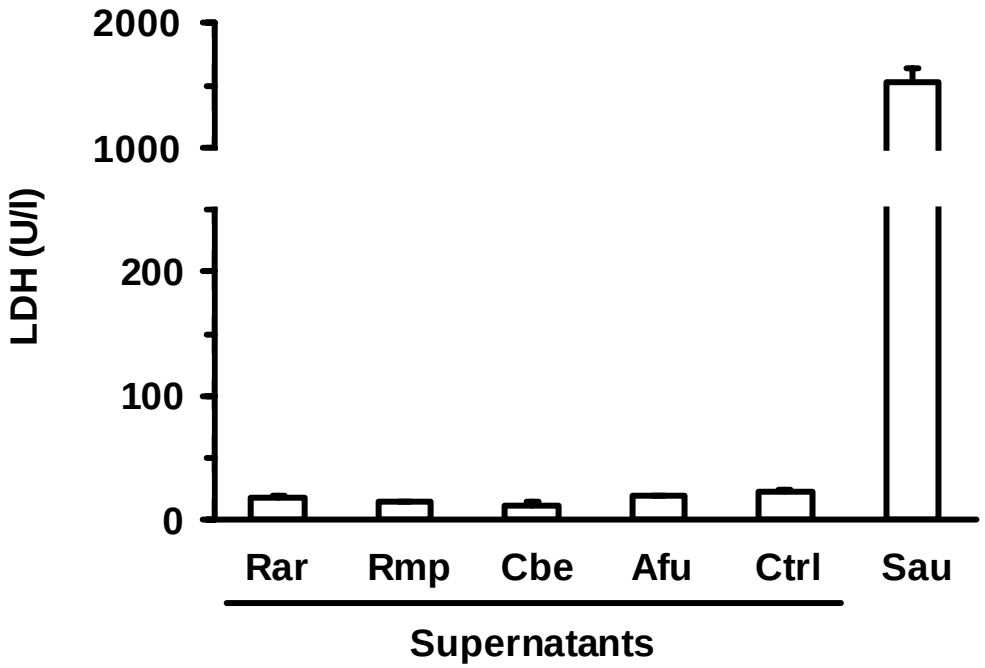

Supplementary Figure 3

Supernatants of fungal cultures (Rar = *R. arrhizus*, Rmp = *R. pusillus*, Cbe = *C. bertholletiae*, Afu = *A. fumigatus*) were generated and diluted as described in the methods section. Control supernatants (Ctrl) did not contain fungal pathogens. 100 µl of diluted supernatants were added to 100 µl A549 culture supernatants in the upper chamber. LDH concentrations in the upper compartment were quantified after 30 hours of incubation. Mean values and standard deviations based on two independent experimental runs are shown. *S. aureus* infected inserts were used as positive control (Sau).

3.4 *In Vitro* Evaluation of Radiolabeled Amphotericin B for Molecular Imaging of Mold Infections

Running Title: Radiolabeled Amphotericin B Tracers

Lukas Page[1], Andrew J. Ullmann[1], Fabian Schadt[2], Sebastian Wurster[1,3,‡,#], Samuel Samnick[2,‡]

1) Department of Internal Medicine II, Division of Infectious Diseases, University Hospital of Wuerzburg, Wuerzburg, Germany

2) Department of Nuclear Medicine, University Hospital of Wuerzburg, Wuerzburg, Germany

3) Department of Infectious Diseases, University of Texas MD Anderson Cancer Center, Houston, Texas, United States of America

‡ These authors contributed equally.

Corresponding author: Sebastian Wurster, MD

Department of Internal Medicine II, Division of Infectious Diseases, University Hospital of Wuerzburg

Josef-Schneider-Str. 2, 97080 Wuerzburg, Germany

Present contact address for correspondence:

The University of Texas MD Anderson Cancer Center

Department of Infectious Diseases, Infection Control and Employee Health

6565 MD Anderson Boulevard, Sheikh Zayed Building Z8.3002

Houston, TX 77030, United States of America

Email address: stwurster@mdanderson.org

Phone: +1-713-563-1753

Word count: 3563 words

Abstract: 242 words

Abstract

Invasive pulmonary aspergillosis and mucormycosis are life-threatening complications in immunocompromised patients. A rapid diagnosis followed by early antifungal treatment is essential for patient survival. Given the limited spectrum of biomarkers for invasive mold infections, recent studies have proposed radiolabeled siderophores or antibodies as molecular probes to increase the specificity of radiological findings by nuclear imaging modalities. While holding enormous diagnostic potential, most of the currently available molecular probes are tailored to the detection of *Aspergillus* species and their cost-intensive and sophisticated implementation restrict the accessibility at less specialized centers. In order to develop cost-efficient and broadly applicable tracers for pulmonary mold infections, this study established streamlined and high-yielding protocols to radiolabel amphotericin B (AMB) with the gamma-emitter technetium-99m (^{99m}Tc-AMB) and the positron-emitter gallium-68 (^{68}Ga-AMB). Radiochemical purity of the resulting tracers consistently exceeded 99 % and both probes displayed excellent stability in human serum (> 98 % after 60-240 min at 37 °C). The uptake kinetics by representative mold pathogens were assessed in an *in vitro* Transwell® assay using infected endothelial cell layers. Both tracers accumulated intensively and specifically Transwell® inserts infected with *Aspergillus fumigatus*, *Rhizopus arrhizus*, and other clinically relevant mold pathogens as compared with uninfected and bacterial controls. Inoculum-dependent enrichment was confirmed by gamma-counting and autoradiographic imaging. Taken together, this pilot *in vitro* study proposes ^{99m}Tc-AMB and ^{68}Ga-AMB as facile, stable, and specific probes meriting further pre-clinical *in vivo* evaluation of radiolabeled amphotericin B for molecular imaging in invasive mycoses.

Keywords

Antifungals, aspergillosis, mucormycosis, biomarker, nuclear imaging, tracer

Introduction

Invasive pulmonary mold infections (IPMI) pose a major threat to an expanding at-risk population, including patients with prolonged neutropenia, solid organ or allogeneic hematopoietic stem cell transplantation, and corticosteroid therapy (1). *Aspergillus* species remain the predominant cause of IPMI, but emerging pathogens such as Mucorales are increasingly observed (2-5). A rapid diagnosis and prompt initiation of antifungal treatment crucially impact patient survival (6, 7). However, the diagnosis of IPMI remains challenging and the likelihood is determined on a scale of probability according to a constellation of host factors, clinical and microbiological criteria (7).

While imaging techniques play a crucial role in the diagnostic work-up, with thin-section chest computed tomography as the modality of choice (8), radiological findings are often unspecific or transient in early stages of IPMI and frequently absent in non-neutropenic patients (9, 10). In addition, radiological characteristics such as the halo sign have limited specificity as other infections, neoplastic or inflammatory processes can cause comparable manifestations. Similarly, ^{18}F-fluorodesoxyglucose-based positron emission tomography (FDG-PET) can efficiently visualize fungal infections but struggles to discriminate different infectious etiologies, neoplasia, and inflammation (10-12). Therefore, recent studies tested further investigational PET imaging strategies using radiolabeled fungal siderophores and antibodies (13, 14) to improve the diagnostic accuracy in IPMI. The *Aspergillus*-derived siderophores ^{68}Ga-TAFC and ^{68}Ga-FOXE reliably distinguished fungal from bacterial infection *in vivo* but showed unspecific enrichment in sterile inflamed tissue (15). Tracking mannoprotein targets of the *Aspergillus* cell wall, antibody-guided immuno-PET combined with magnetic resonance tomography showed a promising potential in murine pulmonary aspergillosis and is about to enter first-in-human trials (10, 12, 14). However, the cost-intensiveness and the challenging implementation of this approach in the clinical setting limit its applicability in less-specialized regional institutions (10). Moreover, most published probes for molecular imaging of IPMI were designed to detect selected *Aspergillus* species and would thus require additional probes to support the diagnostic workup of mucormycosis or other emerging mold infections.

To meet the need for cost-effective and facile molecular probes with broad applicability in IPMI, this study established streamlined protocols to radiolabel amphotericin B (AMB). Using a simplified monolayer version of a previously established alveolar Transwell® *in vitro* model mimicking IPMI (16-18), we demonstrate that AMB labeled with the positron-emitter gallium-68 (^{68}Ga) for PET imaging or the gamma-emitting technetium-99m (^{99m}Tc) for single photon emission computed tomography (SPECT) imaging allows for sensitive and reproducible detection of low-inoculum mold infection and reliably distinguishes fungal and bacterial etiologies.

Material and Methods

Preparation of ^{99m}Tc-AMB

Sodium pertechnetate, derived from a ^{99}Mo/^{99m}Tc generator (Curium, Netherlands) with an initial activity of 1000 MBq ± 100 MBq in 200 ± 50 µL saline, was added to a vial containing 50 µg of pure AMB powder (European Pharmacopoeia reference standard, Sigma-Aldrich Y0000005) dissolved in 100 µL Hanks Balanced Salt Solution (HBSS, Sigma-Aldrich). After adding 20 µL of a solution consisting of 10 mg $SnCl_2$ / mL 0.1 N HCl and 20 min incubation at room temperature, the resulting ^{99m}Tc-AMB solution was diluted with 3 mL PBS (pH = 7.0) and passed through a 0.22 µm sterile filter (Millipore, USA) into a sterile vial.

Preparation of ^{68}Ga-AMB

Gallium-68 (^{68}Ga) for radiolabeling was eluted in the form of $^{68}GaCl_3$ in 1.0 mL HCl (0.1N) from a ^{68}Ge/^{68}Ga-generator (Eckert & Ziegler, Germany) into a vial containing 50 µg of AMB and 350 µL of 0.1 N sodium acetate (pH = 3.4). After a 10 min incubation period at 90 °C, the resulting ^{68}Ga-AMB solution was neutralized with 1.5 mL PBS (pH = 7.0) and filter-sterilized as described above.

Determination of radiochemical yield and purity

The quality of ^{99m}Tc-AMB and ^{68}Ga-AMB was assessed by gradient high-performance liquid chromatography (HPLC, Scintomics, Germany) and by thin layer chromatography (TLC) as described before (19). The mobile phase for gradient HPLC analysis consisted of solvent mixtures of MeCN/0.1 % trifluoroacetic acid

(TFA) and water/0.1 % TFA at a flow rate of 0.7 mL/min. TLC analysis was performed on ITLC-SG stripes (Varian, USA), using 0.1 M ammonium acetate/methanol (1:1) as mobile phase. The strips were imaged with a TLC-scanner (mini-GITA®, Raytest, Germany) for quantification.

In vitro stability studies

5 MBq of ^{99m}Tc-AMB or 20 MBq of ^{68}Ga-AMB (in up to 50 µL injectable solution) were added to 950 µL human serum previously equilibrated in a 5 % CO_2 environment at 37 °C. The mixtures were maintained at 37 °C in a 5 % CO_2 humidified incubator for 60, 120, or 240 min. 10 µL aliquots were applied to TLC analysis (ITLC-SG stripes, 1 M ammonium acetate/MeOH [1:1] as eluent) and compared with sodium pertechnetate and ^{99m}Tc-AMB or $^{68}GaCl_3$ and ^{68}Ga-AMB, respectively. In addition, 500 µL of the mixtures were diluted with 1 mL EtOH and centrifuged at 14000 rpm for 15 min. The supernatants were subsequently analyzed by HPLC using a Nucleosil 100-5 C_{18} column (125 x 4.6 mm) and a gamma-detector for radioactivity as previously described (20).

Preparation of fungal spores

Mold isolates were obtained from reference collections (American Type Culture Collection and Westerdijk Fungal Biodiversity Institute). Identification numbers and culture conditions are summarized in **Table S1**. Spores were harvested by gently scraping cultures with a cotton swab, washed with PBS, passed through a 40 µm cell strainer to remove residual mycelium, and quantified with a hemocytometer.

Amphotericin B susceptibility testing

Minimal inhibitory concentrations (MIC) of amphotericin B were determined using the EUCAST method for susceptibility testing of molds, version 9.3.1 (21). MICs were read after an incubation period of 24 h for Mucorales and 48 h for Ascomycetes and are summarized in **Table S1**.

Construction of Transwell® model

Human pulmonary artery endothelial cells (HPAECs, Lonza, Switzerland) were grown to confluency in a 75 cm^2 cell culture flask in EGM-2 medium (EBM-2 medium + EGM-2 single quots, Lonza, Switzerland). HPAECs were harvested using Trypsin-

EDTA (Lonza, Switzerland) according to the manufacturer's instructions and suspended in EGM-2 medium at a final concentration of 1 x 10^6/mL. 1 x 10^5 cells (100 µL) were seeded on the lower side of a Transwell® membrane insert (6.5 mm diameter, 3 µm pore size, Corning, USA) and incubated for 2 h at 37 °C. The inserts were subsequently transferred to 24-well-plates and incubated at 37 °C in 600 µL EGM-2 medium without gentamicin/amphotericin B (GA-1000). The medium was exchanged every other day. After 6 days of culture, the lower sides of the Transwell® inserts were inoculated with fungal spores (2.5 x 10^5 in 12.5 µL EGM-2, unless indicated otherwise) and incubated upside-down for 2 h at 37 °C. Inserts were then placed in 24-well-plates containing 600 µL EGM-2 without GA-1000 and incubated for another 15 h at 37 °C. The latter incubation step was omitted for the assessment of tracer uptake by dormant spores. HPAEC layers inoculated with plain medium or a *Staphylococcus aureus* suspension (2.5 x 10^5 in 12.5 µL, clinical isolate from the Institute for Hygiene and Microbiology Wuerzburg) served as sterile and bacterial controls.

Uptake experiments, gamma-counting, and autoradiographic imaging (**Fig. 1**)

^{99m}Tc-AMB and ^{68}Ga-AMB were diluted in EGM-2 to a final concentration of 50 and 5 ng/mL, respectively. Transwell® inserts prepared and infected as described above were incubated in 600 µL tracer solution for up to 240 min at 37 °C. Incubation periods for each experiment are specified in the figure legends. Experiments comparing multiple incubation periods are based on independent sets of inserts for each time point. Inserts were washed 5 times for 1 minute each with 1 mL cold HBSS to terminate tracer uptake and to remove unbound tracer solution. Thereafter, radioactivity accumulation in the infected Transwell® inserts was quantified with a calibrated WIZARD2 gamma-counter (Perkin-Elmer, Germany) as previously described (19, 22). To determine uptake percentages, the mean activity of three vials each containing 600 µL of tracer solution served as a 100 % standard. Additional inserts generated in independent experiments were washed five times with HBSS. After drying, the inserts were exposed on phosphor image plates (Biostep, Germany) for 30 min. The image plates were analyzed using an image plate scanner (Dürr Medical, Germany) and the corresponding AIDA Image Data Analyzing Software (Raytest, Germany) as previously described (23).

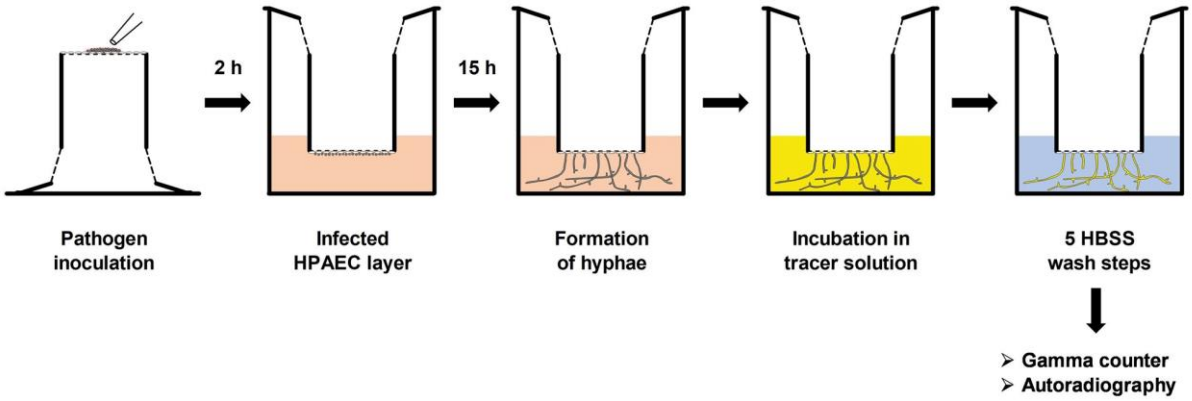

Figure 1: *In vitro* model to study tracer uptake by infected HPAEC monolayers

Statistics

For quantitative *in vitro* tracer uptake studies, mean values and standard deviations were determined based on three independent replicate experiments using freshly prepared HPAEC layers, pathogen inoculums, and tracer solutions. Depending on the data format, the two-sided t-test, one-way ANOVA, or two-way ANOVA was used for significance testing (specified in the figure legends). Significance levels are denoted by asterisks: * $p < 0.05$, ** $p < 0.01$, *** $p < 0.001$.

For inoculum-dependent tracer uptake studies, the minimum inoculum resulting in differential tracer enrichment (limit of detection) was determined based on relative uptake compared with the uninfected control, with the following three conditions to be met: 1.) The lower end of the standard deviation range has exceeded the background in uninfected samples (= fold change 1.0). 2.) None of the individual measurements in mold-infected samples has been below the corresponding medium control. 3.) At least 2-fold mean uptake compared with either the medium control or the highest value in *S. aureus*-infected samples (whatever was higher) has been achieved.

Results

Radiochemistry

^{99m}Tc-AMB and ^{68}Ga-AMB were obtained in an overall decay-corrected reaction yield of 95 ± 5 %, following a reaction of 50 µg of AMB with pertechnetate ($^{99m}TcO_4^-$) in saline at room temperature or with $^{68}GaCl_3$ in acetate buffer (pH 3.4) at 90 °C. The total synthesis time including purification and quality control was 30-40 min. The resulting ^{99m}Tc-AMB or ^{68}Ga-AMB solutions were analyzed by TLC for radiochemical

purity, which was greater than 99 %. ^{99m}Tc-AMB and ^{68}Ga-AMB exhibited an excellent *in vitro* stability in human serum (**Fig. 2A-B**) and in the chosen injectable solution (PBS, **Fig. 2C-D**), as only the intact ^{99m}Tc-AMB and ^{68}Ga-AMB were identified chromatographically in the investigated samples following a 60 to 240 min incubation period.

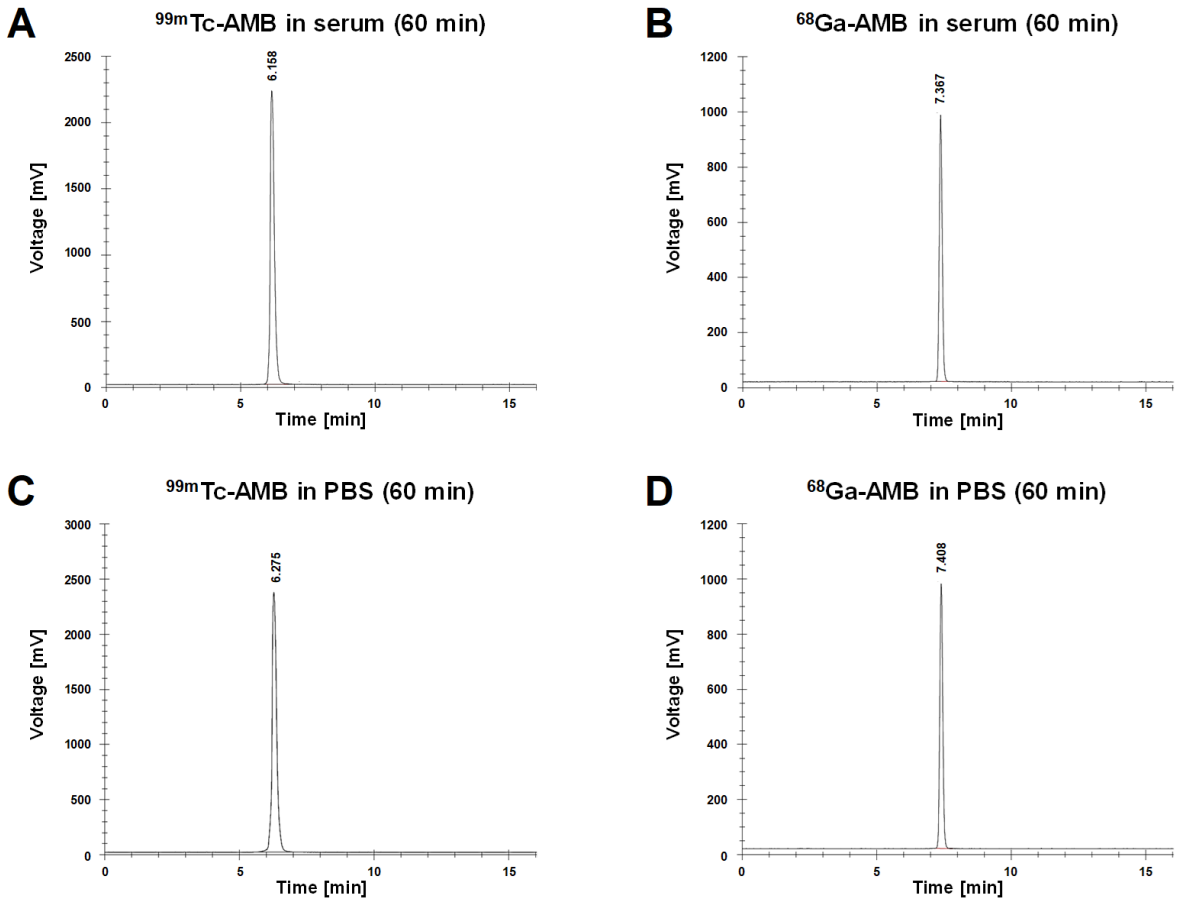

Figure 2: *In vitro* stability of ^{99m}Tc-AMB and ^{68}Ga-AMB in human serum

The stability of the radiolabeled AMB in human serum as assessed chromatographically by HPLC after 1 h incubation of ^{99m}Tc-AMB (**A**) and ^{68}Ga-AMB (**B**) in human serum at 37 °C. The corresponding HPLC chromatographs of the initial aliquots of ^{99m}Tc-AMB and ^{68}Ga-AMB (in PBS) analyzed in parallel are shown in (**C**) and (**D**). The main radioactivity peaks (> 98 %) represent ^{99m}Tc-AMB and ^{68}Ga-AMB, respectively.

In vitro evaluation of tracer uptake by infected HPAEC layers

The *in vitro* uptake kinetics of the gamma-emitter ^{99m}Tc-AMB were determined over a period of 240 min (**Fig. 3A**). Minimal tracer uptake by uninfected HPAECs and *S. aureus* infected samples was found for all exposure periods tested (maximum uptake

at 240 min < 0.1 %). The mean uptake of ^{99m}Tc-AMB was consistently higher in *A. fumigatus* than in *R. arrhizus* infected inserts. Percent uptake of ^{99m}Tc-AMB by *A. fumigatus* and relative tracer enrichment compared with the uninfected control peaked at 60 min (fold change 52.1 ± 14.8, **Fig. 3B**), whereas binding of ^{99m}Tc-AMB to *R. arrhizus* infected samples remained relatively constant over time (**Fig. 3A-B**). While both percent uptakes and fold changes significantly distinguished the type of infection, the impact of the tracer exposure period on relative uptake kinetics did not reach the level significance (**Fig. 3B**). Therefore, we considered the reproducibility of tracer uptake to prioritize the optimal exposure period. Across all conditions, the lowest variation in relative tracer enrichment was found at 120 min of incubation (median coefficient of variation 0.18) and thus a tracer exposure period of 120 min was selected for all subsequent ^{99m}Tc-AMB *in vitro* experiments.

To determine the limit of detection, Transwell® inserts were infected with various pathogen inoculums ranging from 2.5 x 10^1 to 2.5 x 10^6 spores per insert and uptakes of ^{99m}Tc-AMB were measured by gamma-counting (**Fig. 3C**). The limit of detection was determined based on relative tracer uptakes (**Fig. 3D**) as described in the Materials & Methods section. The lowest spore inoculum yielding differential tracer uptake by the resulting mycelium was at 2.5 x 10^4 *A. fumigatus* conidia and 2.5 x 10^2 *R. arrhizus* spores, respectively (**Fig. 3D**). A steady inoculum-dependent increase in tracer uptake was observed for *A. fumigatus*, whereas *R. arrhizus* infected samples showed no further incremental uptake once inoculums exceeded 2.5 x 10^4 spores. Negligible enrichment was found for all *S. aureus* concentrations (mean relative uptake 1.0-1.1). Autoradiographic imaging of independently prepared samples incubated with ^{99m}Tc-AMB confirmed both the inoculum-dependent enrichment in mold-infected inserts and the breakpoints for differential detection determined for *A. fumigatus* in the gamma-counting assay. For *R. arrhizus* infected inserts, the limit of detection in the autoradiography was one 10-fold dilution higher (2.5 x 10^3 spores) than in the gamma-counting assay (**Fig. 3E**).

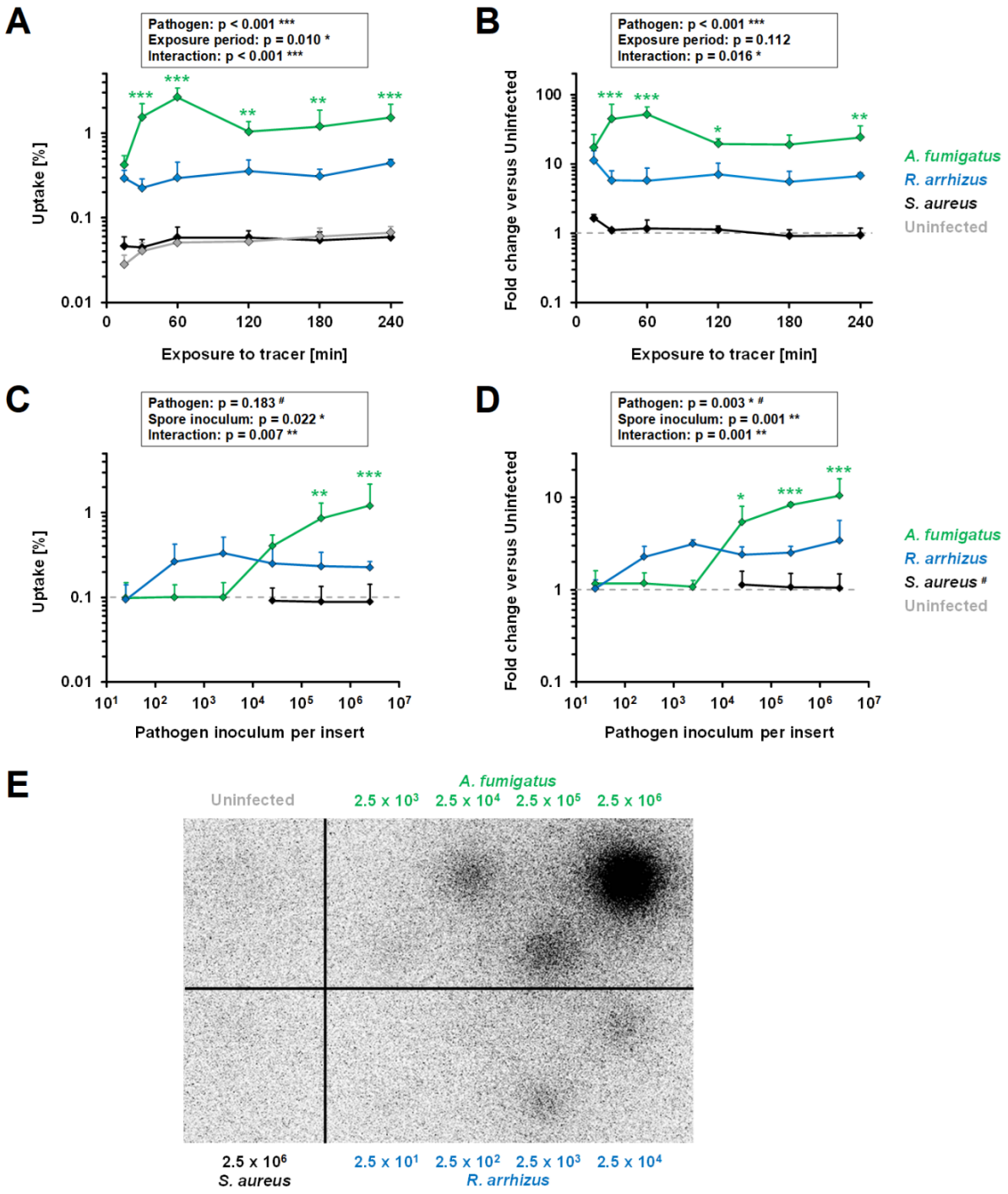

Figure 3: Evaluation of time- and inoculum-dependent ^{99m}Tc-AMB uptake in an alveolar IPMI model

(**A-B**) Percent uptakes (**A**) and fold enrichment (**B**) of ^{99m}Tc-AMB in HPAEC monolayers infected with 2.5 x 10^5 *A. fumigatus* conidia (green), *R. arrhizus* spores (blue), or *S. aureus* cells (black) were compared with uninfected HPAECs (grey, dashed line in panel **B**) depending on the tracer exposure period (15-240 min). Two-way ANOVA (variables: pathogen, exposure period) was used for significance testing. For each tracer exposure period, Dunnett's multiple comparison test was applied to compare the results of pathogen-infected samples with the uninfected control. (**C-D**) Percent

uptakes (**C**) and fold enrichment (**D**) of ^{99m}Tc-AMB in HPAEC layers infected with 10-fold serial dilutions (2.5 x 10^1 – 2.5 x 10^6) of *A. fumigatus* conidia (green), *R. arrhizus* spores (blue), or *S. aureus* cells (black) were compared with uninfected HPAECs monolayers (dashed grey line). Tracer exposure period: 120 min. Two-way ANOVA (variables: pathogen, spore inoculum per insert) was used for significance testing. # As no increased tracer uptake was found in preceding experiments, only the three highest inoculums (2.5 x 10^4 – 2.5 x 10^6) were tested for *S. aureus* and were not considered for significance testing. For each fungal pathogen, Dunnett's multiple comparison test was applied to compare spore concentrations above the limit of detection with the highest inoculum below the detection threshold. (**E**) Autoradiographic image of ^{99m}Tc-AMB-exposed HPAEC layers infected with 10-fold serial dilutions of *A. fumigatus* conidia and *R. arrhizus* spores, or 2.5 x 10^6 *S. aureus* cells. Tracer exposure period: 120 min. Three independent experiments were performed to confirm reproducible limits of detection. One representative image is shown.

Next, we assessed the differential uptake kinetics of ^{99m}Tc-AMB by 2.5 x 10^5 dormant *A. fumigatus* (**Fig. 4A**) or *R. arrhizus* (**Fig. 4B**) spores and the mycelium formed thereof. HPAEC layers infected with spores of either pathogen showed non-significantly increased ^{99m}Tc-AMB uptake compared with the uninfected control, whereas inserts with hyphal growth displayed significantly increased tracer enrichment. In line with the results presented above, both absolute and relative hyphal uptake of ^{99m}Tc-AMB were markedly higher in *A. fumigatus* than in *R. arrhizus*. Remarkably, for either pathogen, mean hyphal tracer uptake after 120 min relative to the uninfected control (**Fig. 4C-D**) was essentially identical to the initial time course experiment (**Fig. 3B**), further underscoring the high reproducibility of both the endothelial infection model and tracer enrichment.

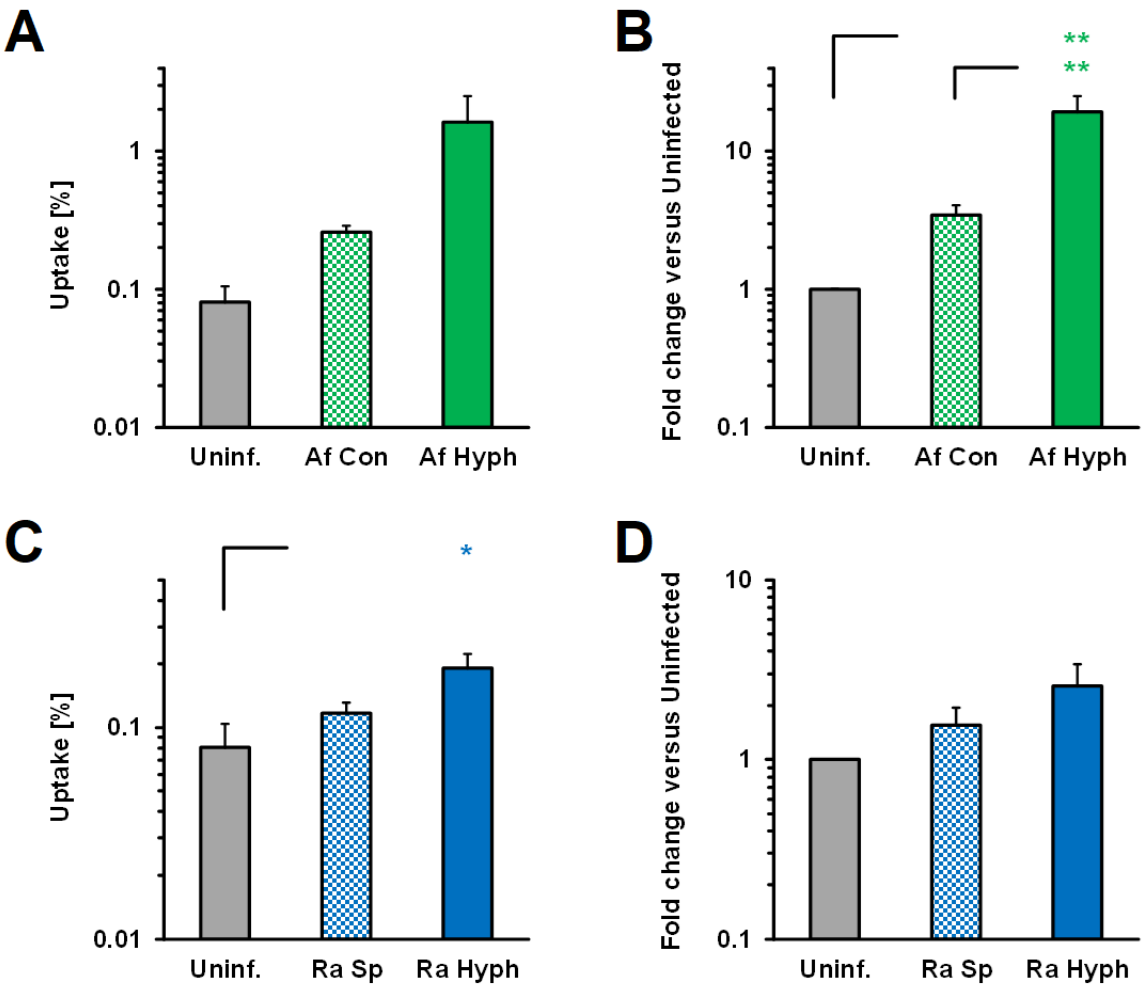

Figure 4: Discrimination of resting and invasive stages of *A. fumigatus* and *R. arrhizus* stages by ^{99m}Tc-AMB enrichment

HPAEC monolayers were infected with 2.5 x 10^5 *A. fumigatus* conidia (**A-B**, Af Con) or *R. arrhizus* spores (**C-D**, Ra Sp) and inverted inserts were allowed to rest for 2 h to attain adequate spore attachment. The infected HPAEC monolayers were either exposed to ^{99m}Tc-AMB for 120 min immediately or after a 15 h incubation period to facilitate formation of hyphae (Hyph). Percent uptakes (**A, C**) and fold enrichment (**B, D**) of ^{99m}Tc-AMB compared with uninfected inserts were determined by gamma-counting. One-way ANOVA with Tukey's multiple comparison test was used for significance testing.

Furthermore, we tested 120 min uptakes of ^{99m}Tc-AMB by mycelia derived from 2.5 x 10^5 spores of additional pulmonary mold pathogens. With the exception of *Fusarium solani*, all isolates tested showed at least 3-fold ^{99m}Tc-AMB enrichment compared with the uninfected control and displayed low inter-assay variation (CV 35.0%, **Fig. S1A**). Remarkably, even isolates that are resistant to AMB (e.g., *Aspergillus terreus* or *Cunninghamella berthollatiae* isolates with an AMB MIC of 4 µg/mL, **Table S1**) significantly accumulated ^{99m}Tc-AMB (**Fig. S1A**).

In additional experiments, we evaluated the fungal uptake kinetics of ^{68}Ga-AMB, a beta-emitting tracer that was developed for future PET imaging applications. Due to the short half-life of ^{68}Ga (68 min), the analysis was terminated after 120 min. While a time-dependent increase in tracer uptake was found for all conditions (**Fig. 5A**), relative uptakes compared with the uninfected control were nearly constant over time (**Fig. 5B**), with fold changes of 4.2-4.8 for *A. fumigatus* and 3.3-4.4 for *R. arrhizus* (**Fig. 5B**). Inoculum-dependent ^{68}Ga-AMB enrichment in the studied molds was confirmed by autoradiography (**Fig. 5C**). The threshold spore inoculum for differential tracer uptake by the resulting mycelium was at 2.5 x 10^3 spores for both pathogens (**Fig. 5C**). No enrichment in *S. aureus* infection was found in the gamma-counting assay (mean relative uptake 0.84-1.08, **Fig. 5B**) or autoradiography (**Fig. 5C**). Testing ^{68}Ga-AMB enrichment in additional Ascomycetes and Mucorales species, all pathogens had at least 5-fold mean relative uptakes (**Fig. S1B**). Variation of uptake was very low, with a median CV of 14.5% (**Fig. S1B**).

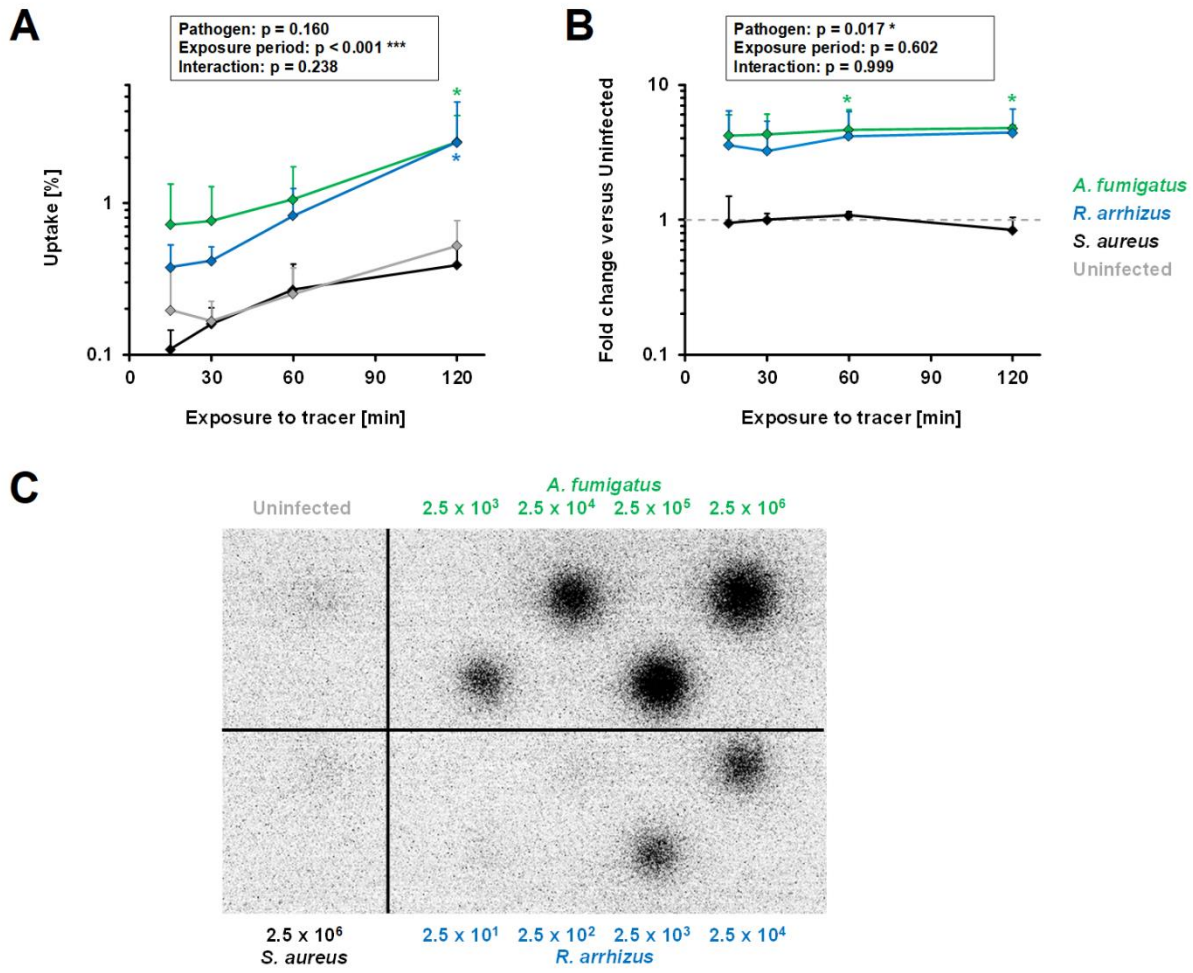

Figure 5: Evaluation of ^{68}Ga-AMB uptake by infected HPAEC monolayers

(**A-B**) Percent uptake (**A**) and fold enrichment (**B**) of ^{68}Ga-AMB in HPAEC layers infected with 2.5 x 10^5 *A. fumigatus* conidia (green), *R. arrhizus* spores (blue), or *S. aureus* cells (black) were compared with uninfected HPAECs (grey, dashed line in panel **B**) depending on the tracer exposure period (15-120 min). Two-way ANOVA (variables: pathogen, exposure period) was used for significance testing. For each tracer exposure period, Dunnett's multiple comparison test was applied to compare the results for individual pathogens with the uninfected control. **C**) Autoradiographic image of ^{68}Ga-AMB-exposed HPAEC layers infected with 10-fold serial dilutions of *A. fumigatus* conidia and *R. arrhizus* spores, or 2.5 x 10^6 *S. aureus* cells. Tracer exposure period: 60 min. Three independent experiments were performed to confirm reproducible limits of detection. One representative image is shown.

Discussion

In an effort to establish supportive diagnostic modalities for IPMI by molecular imaging, previous studies have mainly focused on radiolabeled siderophores and mannoprotein antibodies (12-14). While the concept of antifungal-derived tracers for molecular imaging of invasive mycoses is *per se* not novel (24-26), this study presents a streamlined, time- and resource-efficient methodology to label AMB with ^{68}Ga and ^{99m}Tc for nuclear imaging by PET and SPECT. The rationale for selecting AMB is, on one hand, its wide therapeutic activity against various classes of fungal pathogens including Mucorales. On the other hand, AMB displays an advantageous molecular structure for radiolabeling. Specifically, the high amount of hydroxyl groups in the molecule allows for efficient complexation with metal ions. Importantly, our radiosynthesis approach is suitable for routine clinical applications in every nuclear medicine department and differs from previous protocols to label AMB (26) by omitting major lengthy reaction steps required in the synthesis of tricarbonyl precursors and amphotericin derivatives. While it is not easily feasible to define a specific isotope binding site due to the resulting mixture of complexes, thin layer chromatography confirmed consistent and near-optimal radiochemical yield and purity of our tracer solutions. ^{99m}Tc-AMB and ^{68}Ga-AMB also showed high stability in aqueous injectable solutions as well as human serum (**Fig. 2**), which is an important prerequisite for potential clinical applications.

Providing an *in vitro* environment to mimic fungal invasion of epithelial barriers, alveolar Transwell® mono- and bilayer models have been repeatedly proposed as tools to evaluate antifungal compounds or novel biomarkers (16-18, 27). Here, we opted for an HPAEC monolayer model facilitating highly reproducible infection and establishment of a mycelial biofilm in the endothelial compartment that can be easily

exposed to the tracer, washed, and analyzed in a standardized manner. The low technical variation of this system (18) contributed to the high consistency of temporal uptake kinetics and inoculum-dependent detection thresholds. While the small membrane diameter (6.5 mm) and low fungal inoculums used in this study underscore the efficacy of tracer enrichment, the restricted space in the endothelial compartment of the Transwell® chamber has likely been attributable for the lack of incremental tracer uptake at high inoculums of *R. arrhizus*, a mold that is known to rapidly form abundant mycelium (28).

In line with the broad antifungal activity of AMB (29), our *in vitro* results suggest that both AMB-based tracers display intensive accumulation in representative Ascomycetes and Mucorales species at AMB concentrations markedly below therapeutic serum exposures (30). Interestingly, considerable *in vitro* uptake was even seen in strains with reduced AMB susceptibility. Based on prior experience with tracers for lung infections (31-33), we hypothesize that minimal, sub-therapeutic uptakes are sufficient to yield significantly differential enrichment compared with unspecific background noise. Furthermore, AMB resistance of molds is mediated by a multitude of molecular mechanisms and isolates with reduced susceptibility do not necessarily show reduced ergosterol content or significantly reduced AMB uptake (34, 35).

Complementing our data and corroborating the relatively broad application potential of radiolabeled AMB in invasive mycoses, an exploratory *in vivo* study showed significant enrichment of AMB-based molecular probes in mice with subcutaneous *Candida albicans* and *A. niger* infection (26). By contrast, ^{99m}Tc-fluconazole successfully detected *Candida albicans* but not *A. fumigatus* infection in a murine model (24). ^{99m}Tc-tricarbonyl-caspofungin showed potential for scintigraphic imaging of *C. albicans* and *Aspergillus niger* infections in mice (25), whereas its suitability in the diagnostic workup of mucormycosis remains unclear, given the relative inefficacy of echinocandins against Mucorales (36, 37). Similarly, most previously reported siderophore- or antibody-based molecular imaging strategies are restricted to pathogens of the *Aspergillus* genus or even selected *Aspergillus* species and fail to detect Mucorales. The only notable exception is ^{68}Ga-FOXE, a probe that showed *in vitro* enrichment in *Rhizopus* (15). However, a potential drawback of siderophore-

derived tracers is their strongly disparate uptake efficacy depending on iron availability (10, 15).

Besides broad coverage of potential fungal agents, cross-reactivity with other etiologies of pneumonia presents an important criterion for the evaluation of IPMI imaging probes. For both AMB-derived tracers tested in our study, no differential enrichment was found in *S. aureus* and uninfected endothelial cell layers. *S. aureus* was selected as a bacterial control, since this pathogen was most difficult to discriminate from molds by siderophore-derived radiopharmaceuticals, especially under iron-deprived conditions (15). Furthermore, *S. aureus* is considered one of the most common causative pathogens of hospital-acquired pneumonia in the United States, Europe, and Asia (38, 39) and a frequent agent of community-acquired pneumonia in neutropenic patients (40).

In addition to the discrimination of bacterial and fungal etiologies, a previous study revealed the unique potential of JF5-antibody-based immuno-PET to distinguish active infection from dormant spores by detecting a signature molecule of invasive *Aspergillus* morphotypes (10, 14). The comparative susceptibility of resting and germinated stages of several clinically relevant molds to conventional amphotericin B has been controversially discussed, with mostly non-differential results (41-44). Nonetheless, our *in vitro* study revealed significantly greater uptake by hyphae than dormant spores, especially for *A. fumigatus*, likely due to the increased plasma membrane surface of the hyphal stage. Although unlikely based on previous work (26), *in vivo* studies would be needed to rule out relevant unspecific enrichment of the proposed tracers in fungal commensals or transiently colonized respiratory epithelia upon intravenous tracer administration. Such *in vivo* studies would also need to confirm that our streamlined radiochemical labeling strategy did not alter the previously described excellent tolerability and favorable urinary excretion kinetics of AMB-derived probes (26).

There are further potential limitations and questions to be addressed by future *in vivo* studies. The intrinsic specificity of AMB to fungal ergosterol is limited due to low-affinity binding to cholesterol in human cell membranes (45). Specifically, accumulation of AMB in cholesterol-rich renal tubule cells has been associated with the nephrotoxicity of conventional AMB (45). While a previous murine study revealed low accumulation of ^{99m}Tc-AMB in kidney cells (26), *in vivo* imaging studies would

need to evaluate whether potential noise due to unspecific uptake of AMB could interfere with the sensitivity of SPECT or PET imaging in a real-life setting. Although we observed no significant reduction in fungal tracer uptake upon pre-exposure to sub-inhibitory concentrations of AMB (data not shown), there is a possibility that heavily AMB-saturated fungal membranes would enrich ^{99m}Tc-AMB and ^{68}Ga-AMB less efficiently. Furthermore, as seen with other biomarkers of invasive mold infections (46, 47), indirect effects of antifungal pre-treatment on fungal biomass could reduce the sensitivity of tracer-guided imaging.

Despite these limitations and need for confirmatory preclinical studies, our pilot *in vitro* evaluation suggests that radiolabeled AMB could provide an easily producible and cost-efficient alternative for nuclear imaging in invasive mycoses. The advantageous stability of ^{99m}Tc-AMB and ^{68}Ga-AMB, their high accumulation in aspergillosis and mucormycosis, and their ability to distinguish fungal and bacterial infection etiologies encourage clinical translation after thorough *in vivo* evaluation. Our streamlined and high-yielding synthesis protocol would position ^{99m}Tc-AMB and ^{68}Ga-AMB as particularly facile probes for diagnostic applications in smaller, regional hospitals with a ^{99}Mo/^{99m}Tc or ^{68}Ge/^{68}Ga generator for daily in-house radio-preparation.

Footnote Page

Acknowledgement

We want to thank Dr. Ina Israel and Dr. Maria Lazariotou for assisting in sample preparation and analysis. We also thank the Institute of Hygiene and Microbiology (IHM) Wuerzburg for providing fungal strains, plates, and reagents. Furthermore, we want to thank Prof. Dimitrios P. Kontoyiannis and Prof. Ulrike Holzgrabe for providing valuable feedback and discussion of our results. This work was supported by the Interdisciplinary Centre for Clinical Research (IZKF) Wuerzburg (grant number Z-3/56 to SW). The funder had no role in study design, data collection and interpretation, or the decision to submit the work for publication.

Author Contribution Statement

AJU, SW, and SaS conceived and planned the experiments. LP, FS, SW, and SaS carried out the experiments. LP, FS, and SW performed data analysis. LP, SW, and SaS wrote the paper. All authors provided revisions and approved the final version of the manuscript.

Disclosure of potential conflicts of interests

The authors have no conflicts of interest related to this study.

Meetings where the information has previously been presented

Preliminary data of this study have been presented at 9th Trends in Medical Mycology 2019, Nice, France.

Ethics statement

This study employed a commercially available endothelial cell line and de-identified (anonymized) remainders from diagnostic serum specimens and was therefore exempt from IRB review.

References

1. Patterson TF, Thompson GR, 3rd, Denning DW, Fishman JA, Hadley S, Herbrecht R, Kontoyiannis DP, Marr KA, Morrison VA, Nguyen MH, Segal BH, Steinbach WJ, Stevens DA, Walsh TJ, Wingard JR, Young JA, Bennett JE. 2016. Practice Guidelines for the Diagnosis and Management of Aspergillosis: 2016 Update by the Infectious Diseases Society of America. Clin Infect Dis 63:e1-e60.

2. Bitar D, Van Cauteren D, Lanternier F, Dannaoui E, Che D, Dromer F, Desenclos JC, Lortholary O. 2009. Increasing incidence of zygomycosis (mucormycosis), France, 1997-2006. Emerg Infect Dis 15:1395-401.

3. Goncalves SS, Souza ACR, Chowdhary A, Meis JF, Colombo AL. 2016. Epidemiology and molecular mechanisms of antifungal resistance in Candida and Aspergillus. Mycoses 59:198-219.

4. Lanternier F, Dannaoui E, Morizot G, Elie C, Garcia-Hermoso D, Huerre M, Bitar D, Dromer F, Lortholary O, French Mycosis Study G. 2012. A global analysis of mucormycosis in France: the RetroZygo Study (2005-2007). Clin Infect Dis 54 Suppl 1:S35-43.

5. Roden MM, Zaoutis TE, Buchanan WL, Knudsen TA, Sarkisova TA, Schaufele RL, Sein M, Sein T, Chiou CC, Chu JH, Kontoyiannis DP, Walsh TJ. 2005. Epidemiology and outcome of zygomycosis: a review of 929 reported cases. Clin Infect Dis 41:634-53.

6. Chamilos G, Lewis RE, Kontoyiannis DP. 2008. Delaying amphotericin B-based frontline therapy significantly increases mortality among patients with hematologic malignancy who have zygomycosis. Clin Infect Dis 47:503-9.

7. Lamoth F, Calandra T. 2017. Early diagnosis of invasive mould infections and disease. J Antimicrob Chemother 72:i19-i28.

8. Ullmann AJ, Aguado JM, Arikan-Akdagli S, Denning DW, Groll AH, Lagrou K, Lass-Florl C, Lewis RE, Munoz P, Verweij PE, Warris A, Ader F, Akova M, Arendrup MC, Barnes RA, Beigelman-Aubry C, Blot S, Bouza E, Bruggemann RJM, Buchheidt D, Cadranel J, Castagnola E, Chakrabarti A, Cuenca-Estrella M, Dimopoulos G, Fortun J, Gangneux JP, Garbino J, Heinz WJ, Herbrecht R, Heussel CP, Kibbler CC, Klimko N, Kullberg BJ, Lange C, Lehrnbecher T, Loffler J, Lortholary O, Maertens J, Marchetti O, Meis JF, Pagano L, Ribaud P, Richardson M, Roilides E, Ruhnke M, Sanguinetti M, Sheppard DC, Sinko J, Skiada A, et al. 2018. Diagnosis and management of Aspergillus diseases: executive summary of the 2017 ESCMID-ECMM-ERS guideline. Clin Microbiol Infect 24 Suppl 1:e1-e38.

9. Huang L, He H, Ding Y, Jin J, Zhan Q. 2018. Values of radiological examinations for the diagnosis and prognosis of invasive bronchial-pulmonary aspergillosis in critically ill patients with chronic obstructive pulmonary diseases. Clin Respir J 12:499-509.

10. Thornton CR. 2018. Molecular Imaging of Invasive Pulmonary Aspergillosis Using ImmunoPET/MRI: The Future Looks Bright. Front Microbiol 9:691.

11. Sharma P, Mukherjee A, Karunanithi S, Bal C, Kumar R. 2014. Potential role of 18F-FDG PET/CT in patients with fungal infections. AJR Am J Roentgenol 203:180-9.

12. Rolle AM, Hasenberg M, Thornton CR, Solouk-Saran D, Mann L, Weski J, Maurer A, Fischer E, Spycher PR, Schibli R, Boschetti F, Stegemann-Koniszewski S, Bruder D, Severin GW, Autenrieth SE, Krappmann S, Davies G, Pichler BJ, Gunzer M, Wiehr S. 2016. ImmunoPET/MR imaging allows specific detection of Aspergillus fumigatus lung infection in vivo. Proc Natl Acad Sci U S A 113:E1026-33.

13. Haas H, Petrik M, Decristoforo C. 2015. An iron-mimicking, Trojan horse-entering fungi--has the time come for molecular imaging of fungal infections? PLoS Pathog 11:e1004568.

14. Davies G, Rolle AM, Maurer A, Spycher PR, Schillinger C, Solouk-Saran D, Hasenberg M, Weski J, Fonslet J, Dubois A, Boschetti F, Denat F, Gunzer M, Eichner M, Ryder LS, Jensen M, Schibli R, Pichler BJ, Wiehr S, Thornton CR. 2017. Towards Translational ImmunoPET/MR Imaging of Invasive Pulmonary Aspergillosis: The Humanised Monoclonal Antibody JF5 Detects Aspergillus Lung Infections In Vivo. Theranostics 7:3398-3414.

15. Petrik M, Haas H, Laverman P, Schrettl M, Franssen GM, Blatzer M, Decristoforo C. 2014. 68Ga-triacetylfusarinine C and 68Ga-ferrioxamine E for Aspergillus infection imaging: uptake specificity in various microorganisms. Mol Imaging Biol 16:102-8.

16. Hope WW, Kruhlak MJ, Lyman CA, Petraitiene R, Petraitis V, Francesconi A, Kasai M, Mickiene D, Sein T, Peter J, Kelaher AM, Hughes JE, Cotton MP, Cotten CJ, Bacher J, Tripathi S, Bermudez L, Maugel TK, Zerfas PM, Wingard JR, Drusano GL, Walsh TJ. 2007. Pathogenesis of Aspergillus fumigatus and the kinetics of galactomannan in an in vitro model of early invasive pulmonary aspergillosis: implications for antifungal therapy. J Infect Dis 195:455-66.

17. Morton CO, Fliesser M, Dittrich M, Mueller T, Bauer R, Kneitz S, Hope W, Rogers TR, Einsele H, Loeffler J. 2014. Gene expression profiles of human dendritic cells interacting with Aspergillus fumigatus in a bilayer model of the alveolar epithelium/endothelium interface. PLoS One 9:e98279.

18. Belic S, Page L, Lazariotou M, Waaga-Gasser AM, Dragan M, Springer J, Loeffler J, Morton CO, Einsele H, Ullmann AJ, Wurster S. 2018. Comparative Analysis of Inflammatory Cytokine Release and Alveolar Epithelial Barrier Invasion in a Transwell((R)) Bilayer Model of Mucormycosis. Front Microbiol 9:3204.

19. Li X, Bauer W, Israel I, Kreissl MC, Weirather J, Richter D, Bauer E, Herold V, Jakob P, Buck A, Frantz S, Samnick S. 2014. Targeting P-selectin by gallium-68-labeled fucoidan positron

emission tomography for noninvasive characterization of vulnerable plaques: correlation with in vivo 17.6T MRI. Arterioscler Thromb Vasc Biol 34:1661-7.

20. Samnick S, Hellwig D, Bader JB, Romeike BF, Moringlane JR, Feiden W, Kirsch CM. 2002. Initial evaluation of the feasibility of single photon emission tomography with p-[123 I]iodo-L-phenylalanine for routine brain tumour imaging. Nucl Med Commun 23:121-30.

21. Arendrup MC, Meletiadis J, Mouton JW, Lagrou K, Hamal P, Guinea J, Testing SoASTotEECfAS. 2017. EUCAST DEFINITIVE DOCUMENT E.DEF 9.3.1 Method for the determination of broth dilution minimum inhibitory concentrations of antifungal agents for conidia forming moulds. https://www.eucast.org/fileadmin/src/media/PDFs/EUCAST_files/AFST/Files/EUCAST_E_Def_9.3.2_Mould_testing_definitive_revised_2020.pdf. Accessed 2020/04/24.

22. Samnick S, Scheuer C, Munks S, El-Gibaly AM, Menger MD, Kirsch CM. 2004. Technetium-99m labeled 1-(4-fluorobenzyl)-4-(2-mercapto-2-methyl-4-azapentyl)-4-(2-mercapto-2-methylprop ylamino)-piperidine and iodine-123 metaiodobenzylguanidine for studying cardiac adrenergic function: a comparison of the uptake characteristics in vascular smooth muscle cells and neonatal cardiac myocytes, and an investigation in rats. Nucl Med Biol 31:511-22.

23. Israel I, Fluri F, Schadt F, Buck AK, Samnick S. 2018. Positron Emission Tomography and Autoradiography Imaging of P-selectin Activation Using 68Ga-Fucoidan in Photothrombotic Stroke. Curr Neurovasc Res 15:55-62.

24. Lupetti A, Welling MM, Pauwels EK, Nibbering PH. 2005. Detection of fungal infections using radiolabeled antifungal agents. Curr Drug Targets 6:945-54.

25. Reyes AL, Fernandez L, Rey A, Teran M. 2014. Development and evaluation of 99mTc-tricarbonyl-caspofungin as potential diagnostic agent of fungal infections. Curr Radiopharm 7:144-50.

26. Fernandez L, Teran M. 2017. Development and Evaluation of 99mTc-Amphotericin Complexes as Potential Diagnostic Agents in Nuclear Medicine. 4:e62150.

27. Morton CO, Wurster S, Fliesser M, Ebel F, Page L, Hunniger K, Kurzai O, Schmitt AL, Michel D, Springer J, Einsele H, Loeffler J. 2018. Validation of a simplified in vitro Transwell((R)) model of the alveolar surface to assess host immunity induced by different morphotypes of Aspergillus fumigatus. Int J Med Microbiol 308:1009-1017.

28. Omar IC, Lee SJPJST. 1993. Fungal Isolation and the production of its biomass in a palm oil medium. 1:209-24.

29. Stone NR, Bicanic T, Salim R, Hope W. 2016. Liposomal Amphotericin B (AmBisome((R))): A Review of the Pharmacokinetics, Pharmacodynamics, Clinical Experience and Future Directions. Drugs 76:485-500.

30. Hamill RJ. 2013. Amphotericin B formulations: a comparative review of efficacy and toxicity. Drugs 73:919-34.

31. Kim JY, Yoo JW, Oh M, Park SH, Shim TS, Choi YY, Ryu JS. 2013. (18)F-fluoro-2-deoxy-D-glucose positron emission tomography/computed tomography findings are different between invasive and noninvasive pulmonary aspergillosis. J Comput Assist Tomogr 37:596-601.

32. Kumar V, Boddeti DK. 2013. (68)Ga-radiopharmaceuticals for PET imaging of infection and inflammation. Recent Results Cancer Res 194:189-219.

33. Vorster M, Maes A, Jacobs A, Malefahlo S, Pottel H, Van de Wiele C, Sathekge MM. 2014. Evaluating the possible role of 68Ga-citrate PET/CT in the characterization of indeterminate lung lesions. Ann Nucl Med 28:523-30.

34. Posch W, Blatzer M, Wilflingseder D, Lass-Florl C. 2018. Aspergillus terreus: Novel lessons learned on amphotericin B resistance. Med Mycol 56:73-82.

35. Blum G, Perkhofer S, Haas H, Schrettl M, Wurzner R, Dierich MP, Lass-Florl C. 2008. Potential basis for amphotericin B resistance in Aspergillus terreus. Antimicrob Agents Chemother 52:1553-5.

36. Almyroudis NG, Sutton DA, Fothergill AW, Rinaldi MG, Kusne S. 2007. In vitro susceptibilities of 217 clinical isolates of zygomycetes to conventional and new antifungal agents. Antimicrob Agents Chemother 51:2587-90.

37. Isham N, Ghannoum MA. 2006. Determination of MICs of aminocandin for Candida spp. and filamentous fungi. J Clin Microbiol 44:4342-4.

38. Jones RN. 2010. Microbial etiologies of hospital-acquired bacterial pneumonia and ventilator-associated bacterial pneumonia. Clin Infect Dis 51 Suppl 1:S81-7.

39. Barbier F, Andremont A, Wolff M, Bouadma L. 2013. Hospital-acquired pneumonia and ventilator-associated pneumonia: recent advances in epidemiology and management. Curr Opin Pulm Med 19:216-28.

40. Evans SE, Ost DE. 2015. Pneumonia in the neutropenic cancer patient. Curr Opin Pulm Med 21:260-71.

41. van de Sande WW, Tavakol M, van Vianen W, Bakker-Woudenberg IA. 2010. The effects of antifungal agents to conidial and hyphal forms of Aspergillus fumigatus. Med Mycol 48:48-55.

42. Lass-Florl C, Nagl M, Gunsilius E, Speth C, Ulmer H, Wurzner R. 2002. In vitro studies on the activity of amphotericin B and lipid-based amphotericin B formulations against Aspergillus conidia and hyphae. Mycoses 45:166-9.

43. Espinel-Ingroff A. 2001. Germinated and nongerminated conidial suspensions for testing of susceptibilities of Aspergillus spp. to amphotericin B, itraconazole, posaconazole, ravuconazole, and voriconazole. Antimicrob Agents Chemother 45:605-7.

44. Gonzalez GM, Tijerina R, Sutton DA, Graybill JR, Rinaldi MG. 2002. In vitro activities of free and lipid formulations of amphotericin B and nystatin against clinical isolates of Coccidioides immitis at various saprobic stages. Antimicrob Agents Chemother 46:1583-5.

45. Lewis RE. 2011. Current concepts in antifungal pharmacology. Mayo Clin Proc 86:805-17.

46. Marr KA, Laverdiere M, Gugel A, Leisenring W. 2005. Antifungal therapy decreases sensitivity of the Aspergillus galactomannan enzyme immunoassay. Clin Infect Dis 40:1762-9.

47. Lass-Florl C, Gunsilius E, Gastl G, Bonatti H, Freund MC, Gschwendtner A, Kropshofer G, Dierich MP, Petzer A. 2004. Diagnosing invasive aspergillosis during antifungal therapy by PCR analysis of blood samples. J Clin Microbiol 42:4154-7.

Supplementary Information

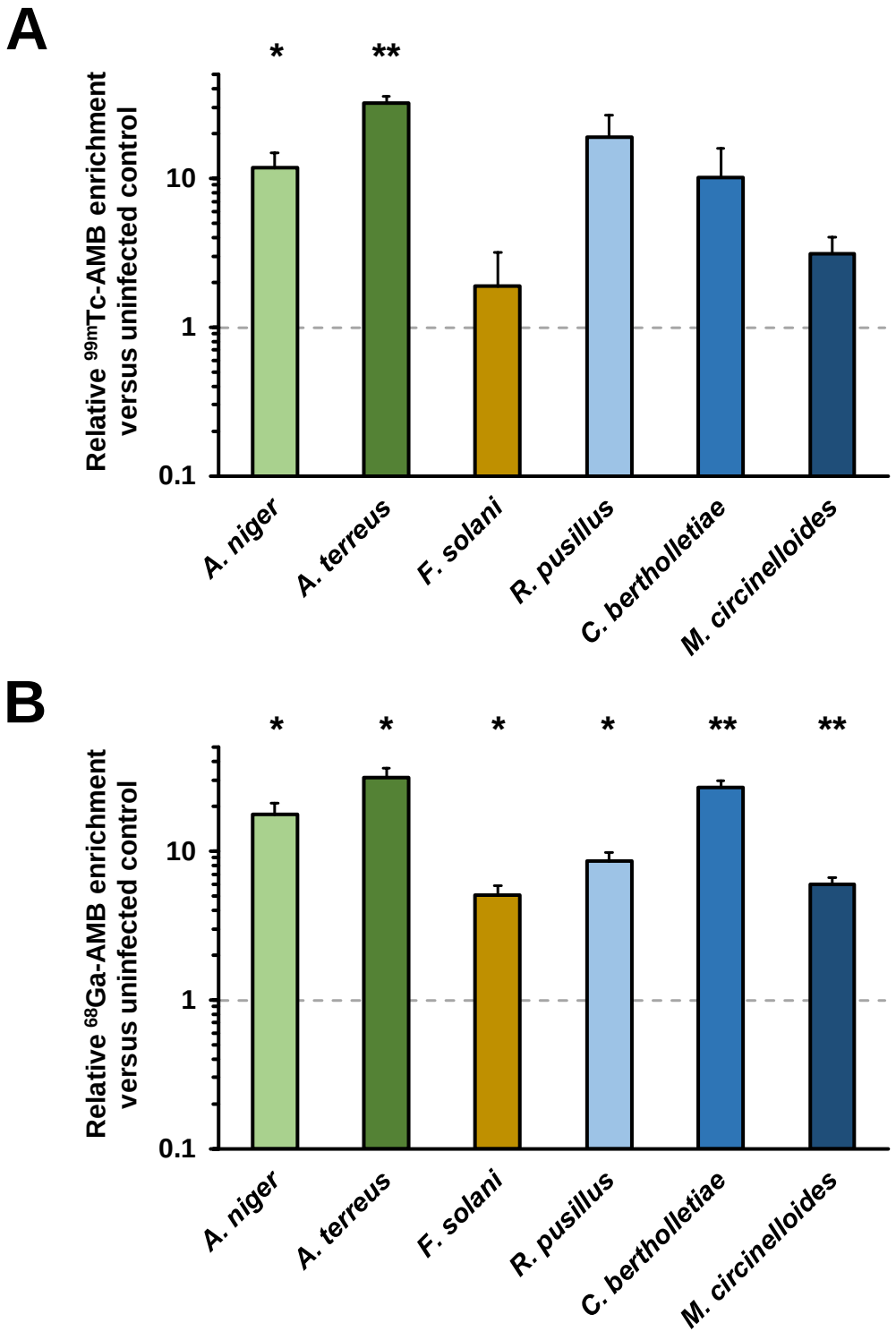

Figure S1: ^{99m}Tc-AMB and ^{68}Ga-AMB enrichment in HPAEC monolayers infected with a selection of additional pulmonary mold pathogens

(**A-B**) Fold enrichment of ^{99m}Tc-AMB (**A**) and ^{68}Ga-AMB (**B**) in HPAEC layers infected with 2.5 x 10^5 spores of various pulmonary mold pathogens. Uptakes by each isolate were compared with an uninfected control (grey dashed line) using the two-sided paired t-test.

Table S1. Culture conditions and amphotericin B MICs for mold isolates used in this study.

Species	Source	Culture conditions to obtain spores/conidia		Amphotericin B MIC (mg/L)
		Temp. (°C)	Incubation period (days)	
Aspergillus fumigatus	ATCC 46645	35	4	1
Aspergillus niger	CBS 553.65	35	5	1
Aspergillus terreus	CBS 594.65	35	5	4
Rhizopus arrhizus	CBS 110.17	35	5	0.25
Rhizomucor pusillus	CBS 245.58	35	5	1
Cunninghamella bertholletiae	CBS 187.84	35	4	4
Mucor circinelloides	CBS 192.68	21	8	0.5
Fusarium solani	CBS 181.29	21	8	4

4. DISKUSSION

4.1 Limitationen und Perspektiven Antigen-spezifischer T-Zell-Untersuchungen bei invasiven Mykosen und Schimmel-assoziierten hypersensitiven Erkrankungen

Es konnte gezeigt werden, dass Schimmelpilz-spezifische T-Zellen als potenzieller Biomarker für invasive Pilzinfektionen und Schimmelpilzexposition genutzt werden können (Bacher et al. 2015b, Koehler et al., 2018, Potenza et al., 2011, 2013 und 2016, Page et al., 2018, Wurster et al., 2017b). PBMC-basierte *Assays* leiden jedoch unter einer Anzahl technischer Limitationen, welche die klinische Anwendbarkeit dieses Biomarkers beeinträchtigen können. So muss das zu verwertende venöse Blut schnellstmöglich nach der Blutentnahme verarbeitet werden, da bereits nach 2 h Lagerung des Blutes ein signifikanter Funktionalitätsverlust der reaktiven T-Zellen eintritt (Wurster et al., 2017c). Im klinischen Alltag können sich derart zeitkritische Abläufe als impraktikabel erweisen, da im Zuge optimierter und effizienter Abläufe Proben bevorzugt gesammelt versandt werden. Zudem verfügt nicht jede regionale Klinik über die benötigte Ausrüstung um diese *Assays* durchzuführen zu können, etwa sterile Werkbänke oder Durchflusszytometer. Eine zentralisierte Verarbeitung und Analyse der Blutproben erfordert Transportwege, welche nicht immer innerhalb jenes präanalytischen Zeitfensters erbracht werden können, das eine vollständige Funktionalität der T-Zellen zum Zeitpunkt der Analysen garantieren kann.

Die Zugabe von RPMI Medium und Agitation konnten das präanalytische Zeitfenster leicht expandieren (Wurster et al., 2016, Kongress für Infektionskrankheiten und Tropenmedizin, Würzburg, Deutschland), eine Kühlung der Proben hatte sich hingegen als eher nachteilig herausgestellt (Wurster et al., 2017c). Es wird vermutet, dass insbesondere die Voraktivierung von neutrophilen Granulozyten zu Schwankungen der T-Zell-Funktionalität führen kann (McKenna et al., 2009, Wurster et al., 2017c). In mehreren T-Zell-basierten Tests zur Diagnostik von u. a. Tuberkulose (Doberne et al., 2011) basierend auf der adaptiven Immunantwort führen prolongierte Lagerungszeiten mitunter ebenfalls zu falsch negativen Ergebnissen. Im Falle des Cytomegalovirus werden T-Zell-*Assays* durchgeführt, um eine funktionale und potentiell protektive Immunreaktion gegen seropositive

Patienten nach HSZT zu verifizieren (Egli et al., 2012), im Falle dieser Anwendungsgebiete existieren bereits handelsübliche Möglichkeiten zur Erhöhung präanalytischer Zeitfenster. Dazu zählen BD *Vacutainer*® CPT (Becton Dickinson), die über einen semipermeablen Einsatz in zur Ficoll-Zentrifugation genutzten Glasröhrchen verfügen. Die Leukozyten werden so nach der Zentrifugation im autologen Serum suspendiert, während Neutrophile und Erythrozyten unterhalb des Einsatzes abgetrennt vorliegen (Bowen & Remaley, 2014, Gawria et al., 2019). Eine weitere Möglichkeit stellen die als *T-Cell Xtend*® bezeichneten Antikörper dar, der in Kombination mit dem klinisch etablierten T-SPOT zur Diagnostik von u. a. Tuberkulose und CMV-Infektionen vertrieben wird (Oxford Immunotec). Die Antikörper binden parallel an Erythrozyten und neutrophile Granulozyten, sodass während der Ficoll-Zentrifugation beide Zellfraktionen effizient von den Lymphozyten getrennt werden. Der Hersteller gibt an, dass mit *T-Cell Xtend*® präanalytische Zeitfenster von bis zu 32 h Lagerung der Blutproben ermöglicht werden (http://www.oxfordimmunotec.com/international/products-services/t-cell-xtend/, Aufrufdatum: 15.10.2019). So lassen sich die Immunreaktionen von Patienten bei bei Tuberkulose und CMV-Infektionen bei adäquater Probenverarbeitung zuverlässig in positiv bzw. negativ klassifizieren.

Beim Nachweis Schimmelpilz-spezifischer T-Zellen bestehen jedoch zusätzliche Besonderheiten, welche die Effizienz dieser Methoden gegenwärtig limitieren. So gibt es im Fall von Schimmelpilzassoziierenden Erkrankungen noch keine etablierten klinisch validierten Erfahrungswerte, um Patienten in positiv oder negativ für eine Infektion zu differenzieren. Im Fall von Tuberkulose und Virusinfektionen kann in der Regel anhand der adaptiven Immunantwort zudem klar zwischen exponierten bzw. infizierten und bislang nicht exponierten Personen differenziert werden. Schimmelpilze hingegen treten ubiquitär in der Umwelt auf (Park & Mehrad, 2009, Ribes et al., 2000) und führen so zu einer kontinuierlichen Exposition der Bevölkerung, die je nach Intensität der Exposition Schwankungen unterliegt (Wurster et al., 2017b, Page et al., 2018).

Für klinische Anwendungen muss demnach garantiert werden, dass das Ergebnis der Quantifizierung reaktiver T-Zellen präzise den Zustand der Exposition des Patienten wiederspiegelt bzw. auf eine Infektion zurückzuführen ist. Insbesondere die im Falle von Pilzen relevanten Th17- und Gedächtniszell-Populationen weisen im

Vergleich zu beispielsweise zytotoxischen T-Zellen jedoch eine erhöhte Sensitivität gegenüber Lagerungszeiten und Kryopräservation auf (Costantini et al., 2003, Jeurink et al., 2008b, Lemieux et al., 2016, Lauruschkat et al., 2018). Weder die *Vacutainer*® CPT-Röhrchen, noch *T-Cell Xtend*® konnte hier zufriedenstellende Ergebnisse nach präanalytischer Lagerzeit erzielen (Daten nicht gezeigt).

Isolierte PBMC könnten potenziell kryopräserviert versandt werden und so externen Zentren zur weiteren Verarbeitung durch ELISPOT oder Durchflusszytometrie zugeleitet werden. Hierzu wurde in unserem Labor systematisch evaluiert, PBMC nach der Isolation in unterschiedlichen Medien (RPMI + 20 % autologes Serum, RPMI + 40 % FCS und serumfreies AIM-V, + jeweils 10 % Dimethylsulfoxid, DMSO) zu kryopräservieren, nach 2 Wochen Lagerungszeit wieder aufzutauen und unterschiedliche T-Zell-*Assays* durchzuführen (ELISPOT, Durchflusszytometrie, Multiplex-Zytokinanalyse). Die Ergebnisse wurden mit frisch aufbereiteten Proben verglichen, wobei insbesondere Zytokin-basierte Tests nach Kryopräservation in keiner der untersuchten Konditionen zu verlässlichen Ergebnissen mehr geführt hatten, obwohl Zellviabilität und Lymphozytenkompositionen kaum von frisch verarbeiteten Proben abwichen (Lauruschkat et al., 2018). Durchflusszytometrische Analysen führten zumindest nach Einfrieren in 20 % autologem Serum zu mit frischen Proben vergleichbaren Ergebnissen (Lauruschkat et al., 2018, Wurster et al., 2017c). Dies löst allerdings nicht die Problematik, dass die PBMC vor der Kryopröservation weiterhin innerhalb eines engen Zeitfensters aufgereinigt werden müssen. Des Weiteren entsteht durch die Toxizität von DMSO und die nötigen Waschschritte nach dem Auftauprozess ein Zellverlust, der die Machbarkeit funktioneller T-Zell-*Assays* bei lymphopenischen Patienten weiter limitiert (Lauruschkat et al., 2018).

Um diesen Limitationen zu begegnen wurde ein Vollblut-basiertes System entwickelt, das potentiell in der Lage ist, den Aspekt der zeitkritischen Probenverarbeitung zu eliminieren: Monovetten® (Sarstedt) wurden mit den entsprechenden Stimulantien und kostimulatorischen Faktoren steril befüllt und konnten anschließend ohne Beeinflussung der späteren Messung für mindestens 4 Wochen gefroren gelagert werden (Weis et al., 2019). Hierdurch ist es möglich, die Testsysteme in größeren Mengen herzustellen, womit dieses Verfahren im Gegensatz zur PBMC-basierten Methode auch peripheren Zentren zugänglich sein könnte. Zum Zeitpunkt der

Probennahme können die Monovetten® dann auf Raumtemperatur gebracht und bettseitig analog der Vorbereitung von Blutkulturen mit dem Blut der Patienten beimpft werden (Weis et al., 2019). Innerhalb dieses Systems beträgt die mögliche Lagerungszeit der Proben bei Raumtemperatur 4 bis 6 Stunden, was neben logistischen Vorteilen auch Möglichkeiten zum Versand der Proben zu spezialisierteren Zentren mit Zugang zu durchflusszytometrischen Analysen bietet (Page et al., 2017, *8th Trends in Medical Mycology*, Belgrad, Serbien, Weis et al., 2019). Zusätzlich war dieser Ansatz in der Lage Schimmelpilz-reaktive T-Zellen reproduzierbar mit höherer Sensitivität zu detektieren, als das PBMC-basierte Protokoll. Das geringe hierfür benötigte Blutvolumen (500 µl je Probe im Vergleich zu mindestens 15-20 ml beim PBMC-basierten Verfahren) erleichtert zudem die Probennahme bei Patienten mit kritischem hämatologischem Status oder pädiatrischen Patienten. Die Anwendung an Patienten nach HSZT wurde von Weis et al. (2019) ebenfalls evaluiert, wobei die an gesunden Probanden ermittelte höhere Sensitivität reproduziert werden konnte. Angesichts dieser Vorteile im Vergleich zu konventionellen Protokollen wird auf Basis dessen das System in laufenden Studien unseres Labors für ELISA-Analysen adaptiert (analog bereits etablierter diagnostischer Tests wie *TruCulture*®, Brunet et al., 2016a). Durch gezielte Zugabe kostimulatorischer Faktoren sollen die von uns dargestellten Systeme hierbei vor allem optimierte Bedingungen zur Aktivierung von spezifischen T-Zellen liefern.

Allerdings besteht die Notwendigkeit, kritisch zu evaluieren, wo die Grenzen der klinischen Anwendbarkeit derartiger *Assays* in Patienten mit Risikoprofil für invasive Mykosen liegen. Beispielsweise besteht bei Patienten in der Phase der Neutropenie in den ersten Wochen nach einer HSZT ein hohes Risiko, an opportunistischen Infektionserkrankungen wie invasiven Mykosen zu erkranken. Zu frühen Zeitpunkten nach HSZT ist das System der Lymphozyten aber potentiell nicht ausreichend rekonstituiert, um robuste Analysen an deren $CD4^+$ Population durchführen zu können. So führten in einer prospektiven Studie zur Diagnostik von invasiven Mykosen mittels Durchflusszytometrie 38 % der Proben von 115 Patienten zu technisch nicht auswertbaren Ergebnissen (Steinbach et al., 2019). Das häufigste Ausschlusskriterium der dort analysierten Proben waren niedrige messbare Gesamt-T-Zell-Zahlen von < 4500 in 78 % der nicht auswertbaren Proben, gefolgt von nicht reagierenden Positivkontrollen (< 2 % aktivierte T-Zellen) in 16 % dieser Proben (Steinbach et al., 2019). Ein anderer wichtiger Einflussfaktor sind T-Zell-aktive

Immunsuppressiva, die zu einer weiteren variablen Beeinträchtigung der *Assays* führen (Page et al., 2020a). Es bestanden hohe intra-individuelle Schwankungen der Suszeptibilität gegenüber den Immunsuppressiva, der Zusatz von α-CD49d als weiteren kostimulatorischen Faktor konnte ihren Einfluss auf die Messergebnisse jedoch mindern. Dennoch lagen die Ergebnisse fernab klinisch verwertbarer Diagnostika, sodass bisher nicht zu einer Verwendung dieser *Assays* in immunsupprimierten Patientenkohorten geraten werden kann.

Aus diesem Grund liegt ein Schwerpunkt unserer Forschungen auf der Exploration weiterer Anwendungsgebiete funktioneller T-Zell-Analysen in Patientenkohorten ohne immunsupprimierende Therapien. Die in Lauruschkat et al. (2018) und Page et al. (2018) demonstrierten Möglichkeiten, Zytokin- und Populationsprofile der Lymphozyten Schimmelpilz-exponierter Probanden zu beschreiben, legen den Schluss nahe, dass sich die Polarisation der T-Zell-Antwort in Richtung Th1 oder Th2 ermitteln und diagnostisch als supportiver Marker bei Risikogruppen mit erhöhter beruflicher oder Umweltexposition nutzen ließe. Bei gesunden Probanden konnte gezeigt werden, dass sich die Schimmelpilz-reaktiven T-Zell-Populationen ohne deutliche Veränderung des Expositions- oder Immunstatus nicht signifikant verändern (Wurster et al., 2017b). Wechselnde Expositionsprofile oder temporäre Expositions-Ereignisse können jedoch sensitiv detektiert werden, sollte etwa durch Laborarbeiten eine Person kurzzeitig mit Pilzsporen in Kontakt treten (Wurster et al., 2016, *7th Advances against Aspergillosis*, Manchester, Großbritannien, Wurster et al., 2017b). Insbesondere unter beruflich exponierten Personengruppen wäre es daher denkbar, Pilz-spezifische T-Zell-Frequenzen und -Phänotypen als Bioeffekt-*Monitoring* einzusetzen, um mit Hypersensitivität assoziierte Th2-Polarisierungen frühzeitig detektieren zu können (Licona-Limòn et al., 2013).

Patienten mit ABPA weisen ein hyperaktives Th2-Profil mit paralleler Eosinophilie in der Lunge auf (Dewi et al., 2017, Moss, 2005), während CPA eher mit einer Th17-dominierten Immunantwort und damit einhergehender pulmonaler Neutrophilie korreliert (Dewi et al., 2017). Wir gehen davon aus, dass sich derartige Antigen-reaktive T-Zell-Profile im peripheren Blut effizient nachweisen lassen. Dies ist ein Gegenstand aktueller Studien unseres Labors, wobei verschiedene T-Zell-*Assays* mit dem bisherigen allergologischen Goldstandard, der serologischen Bestimmung *Aspergillus*-spezifischer IgG und IgE (Greenberger et al., 2014, Knutsen et al., 2012,

Ullmann et al., 2018), verglichen werden. Dies beinhaltet einen Serum-basierten Zytokin-*Assay*, der analog des beschriebenen Protokolls für durchflusszytometrische Analysen (Kap. 2.2.9) in mit Vollblut befüllten Monovetten® durchgeführt werden kann.

Derzeit wird zudem untersucht, ob T-Zell-basierte *Assays* in umwelt- und arbeitsmedizinischen Kontext die Schimmelpilzexposition einer Person adäquat verifizieren können. Landwirte aus biologischen/ökologischen Einrichtungen stellen hierbei eine ideale Berufsgruppe dar, da sie während ihrer Arbeiten zwangsläufig mit den in ihrem Umfeld auftretenden Schimmelpilzsporen in Kontakt treten und eine Risikogruppe für die sog. Farmerlunge darstellen, die medizinisch als Hypersensitivitätspneumonitis klassifiziert wird (Kotimaa et al., 1984, Liu et al., 2015). Der verringerte Einsatz von Fungiziden in der ökologischen Landwirtschaft bedingt das Auftreten größerer Pilzreservate im Umfeld der Anlagen, welche in der konventionellen Landwirtschaft zu einem Teil eradiziert werden würden (Adak et al., 2019, Meyer & Hausbeck, 2013), was die Exposition der dort arbeitenden Personen reduziert. Die Evaluation der Quantifizierung reaktiver T-Zellen und deren Zytokinprofile anhand dieser Probandengruppe kann ein weiterer Hinweis auf dessen Nutzbarkeit in der Arbeitsmedizin sein.

Weitere Risikogruppen stellen Patienten mit cystischer Fibrose, Tuberkulose und Asthma dar (Dhooria et al., 2014, Ghosh et al., 2015, King et al., 2016). Die finale Prämisse dieser *Assays* im allergologischen Kontext wäre, die adaptiven Immunantworten von Patienten mit ABPA, CPA und allergischer Alveolitis differenzieren oder gar vor dem Auftreten klinischer Symptome detektieren zu können. Letzteres wäre bei den meist chronifizierenden Erkrankungen bedeutend, da die pathophysiologischen Reaktionen bereits lange Zeit vor der Diagnosestellung mit den aktuell verfügbaren Verfahren vorhanden sein können (Barac et al., 2019, Greenberger et al., 2014).

Mixturen von Lysaten unterschiedlicher Pilze könnten dabei die Bandbreite detektierbarer Spezies und somit die Sensitivität der Diagnostik möglicher invasiver Mykosen erhöhen. In der Allergologie wäre es hingegen bedeutsamer, präzise die Spezies der im Einzelfall sensitivierenden Schimmelpilze ermitteln zu können. Im Vergleich zu den in T-Zell-Studien bisher zumeist verwendeten fungalen Zelllysaten (Bacher et al., 2015a und b, Potenza et al., 2011, 2013 und 2016, Steinbach et al., 200

2019) könnten sich hier einzelne Proteinantigene als alternative Stimulantien anbieten. Lysate unterliegen wie alle Naturprodukte biologischer Variabilität, rekombinant produzierte Antigene können reproduzierbarer hergestellt werden und lieferten unter Umständen noch geringere intraindividuelle Schwankungen in reaktiven T-Zell-Frequenzen, als dies mit Lysaten der Fall war. Bei Verwendung einzelner Antigene besteht jedoch die Möglichkeit einer verminderten Präzision der Messergebnisse aufgrund geringerer Absolutzahlen korrespondierender antigen-spezifischer T-Zellen (siehe Kap. 2.2.21.2 zur Bestimmung von Konfidenzintervallen, Allan & Keeney, 2010) gegenüber den einzelnen Proteinen verglichen mit der Varietät unterschiedlicher Antigene in einem Ganzzell-Lysat. Proteinmischungen könnten dies kompensieren, wobei im Vorfeld evaluiert werden muss, welche Antigene die immunogen dominantesten darstellen. Kandidaten für *A. fumigatus* wären auf Basis vorhergehender Studien u. a. Aspf4 (Jolink et al., 2015, Knutsen et al., 2012), Aspf6 (Jolink et al., 2015), CatB (Jolink et al., 2013 und 2015) und Crf1 (Jolink et al., 2013). Laufende Studien zeigen hingegen, dass bei Stimulation mittels dieser rekombinanten Antigene stattdessen höhere spezifische T-Zell-Zahlen detektiert werden als bei Stimulation mit *Aspergillus*-Lysat (Daten nicht gezeigt). Aufgrund der geringeren Komplexität der Antigene würde dabei eventuell auch die Prozessierung und Präsentation der Peptide über MHC II der APC beschleunigt, sodass sich die Aktivierung der T-Zellen möglicherweise weniger anfällig gegenüber präanalytischer oder pharmazeutischer Beeinträchtigung zeigen könnte (Kaveh et al., 2012, Meier et al., 2008).

Lysate von Pilzzellen können zudem mit Kreuzreaktivitäten gegenüber anderer Pilzspezies als dem originär lysierten Organismus in Verbindung gebracht werden (Deo et al., 2016). Ein weiterer Hinweis liefern die in Page et al. (2018) dargestellten Korrelationen zwischen reaktiven T-Zell-Frequenzen von Gesunden gegenüber mehreren Schimmelpilz-Spezies, welche neben in der Umwelt vorkommenden Mischkulturen auch auf Kreuzreaktivität der T-Zellen zurückzuführen sein könnten. Es wird zudem vermutet, dass ein großer Anteil der gegen Pilze gerichteten adaptiven Immunantwort auf Kreuzreaktivitäten gegenüber *C. albicans* zurückzuführen ist (Bacher et al., 2019). So wird davon ausgegangen, dass sich im Mikrobiom von 89 % aller Menschen kommensalische *Candida spp.* befinden (Hoffmann et al., 2013). Diese führen zu einer konstanten benignen Aktivierung von Th17-Populationen, welche sich im Organismus verbreiten und so auch die pulmonal

in den Körper eintretenden Pilze detektieren (Bacher et al., 2019). Der Anteil der kreuzreagierenden T-Zellen ließe sich durch Isolation aktivierter T-Zellen über Positivselektion der CD154-exprimierenden T-Zellen nach Stimulation, Expansion und Restimulation ermitteln (Schmidt et al., 2012). So geartete Experimente erfordern allerdings eine weitaus größere Anzahl aktivierter T-Zellen, als es durch die Stimulation mit fungalen Antigenen und Lysaten für gewöhnlich zu erwarten ist. Die erforderlichen Blutvolumina ließen sich nur aus LZRS gewinnen, unterliefen dabei jedoch einem Aufreinigungsprozess, welcher aufgrund des verlängerten zeitlichen Aufwands und zusätzlichem Stress der Zellen mit den etablierten Kriterien zum Erhalt verlässlicher Ergebnisse aus T-Zell-basierten Studien nur schwer vereinbar ist (Britten et al., 2012, Lauruschkat et al., 2018, Wurster et al., 2017c). Da somit gegenwärtig keine klinisch praktikablen Verfahren zur Verfügung stehen, derartige Kreuzreaktivitäten aus einem diagnostischen Assay zu bestimmen, wäre die Verwendung definierter Antigene mit hoher Genus- oder Spezies-Spezifität eine Möglichkeit, Schimmelpilz-spezifische T-Zell-*Assays* in Abhängigkeit der Patientenkohorte zu optimieren.

In weiterführenden klinischen Machbarkeitsstudien soll nun evaluiert werden, welche der existierenden bzw. in der Entwicklung befindlichen T-Zell-basierten *Assays* für welche Patientenkohorte zu bevorzugen ist. Nachfolgende klinische Studien an Risikopatienten mit HSZT (Mellinghoff et al., 2018), prädisponierenden Infektionen wie CMV, HIV oder Influenza (Camargo & Komanduri, 2017, Denis et al., 2015, Shah et al., 2018) oder exazerbierenden COPD (Bao et al., 2017) oder Diabetes mellitus (Petrikkos et al., 2012) können in Zukunft potentiell dazu beitragen, Durchflusszytometrie als supportiven diagnostischen Biomarker invasiver Mykosen zu validieren. Analog zu der Anwendung spezifischer T-Zellen als prognostischer Biomarker bei Infektionen mit Cytomegalievirus (Ashokkumar et al., 2019, Schachtner et al., 2017) könnten auch Schimmelpilz-spezifische T-Zellen zur Prognose und Therapie-*Monitoring* bei Mykosen genutzt werden (Bacher et al., 2015b). Aufgrund der geringen Fallzahlen von Schimmelpilzinfektionen werden allerdings multizentrische Studien benötigt, welche bislang durch die beschriebene präanalytische Suszeptibilität und fehlende Standardisierung insbesondere der PBMC-basierten Durchflusszytometrie erschwert werden. Unsere Weiterentwicklung in Form eines Vollblut-basierten Protokolls mit optimierter Kostimulation hat ein signifikantes Potenzial, die Machbarkeit und Standardisierung multizentrischer

Studien zu katalysieren und damit einen wichtigen Schritt zu einer diagnostischen und prognostischen Verwendung funktioneller T-Zell-Assays in der medizinischen Mykologie zu gehen.

4.2 Untersuchung der Wirt-Pathogen-Interaktion und Antimykotika-basierter nuklearmedizinischer *Tracer* in optimierten Alveolarmodellen invasiv-pulmonaler Pilzinfektionen

Während Tiermodelle zwar den Goldstandard präklinischer Forschung zu neuen Biomarkern, Diagnostik und Pharmaka darstellen, sind diese Modelle mitunter kostenintensiv und mit logistischen und ethischen Hürden verbunden. Zellkulturen stellen dabei ein ressourceneffizientes Mittel zur Generation präliminärer Ergebnisse dar, wobei versucht wird, durch Kombination multipler Zell-Populationen zur Abbildung relevanter Zell-Zell-Interaktionen möglichst physiologische Bedingungen zu simulieren. Das von Hope et al. (2007) entworfene *Transwell*®-Alveolarmodell wurde bereits wiederholt zu pathophysiologischen und pharmakologischen Studien der pulmonalen invasiven Aspergillose herangezogen und variiert (Colley et al., 2019, Lestner et al., 2010, Morton et al., 2014, Morton et al., 2018).

In der vorliegenden Studie wurde das *Bilayer*-Modell für Mucorales adaptiert und validiert. Das invasive Wachstum von Mucorales wie v. a. *R. arrhizus* und *C. bertholletiae* unterscheidet sich zu dem von *A. fumigatus* dahingehend sehr stark, dass Mucorales ein rapides, extensives Myzelwachstum , das zu massiver Gewebedestruktion führt (Belic et al., 2019, Ibrahim et al., 2005, Ibrahim & Kontoyiannis, 2013), während das von *A. fumigatus* geringeres Volumen in Anspruch nimmt und in seinem Wachstumsverhalten die Integrität des Wirtsgewebes zunächst weitgehend intakt hält (Escobar et al., 2016, Morton et al., 2018).

Die Konidien von *A. fumigatus* verfügen über eine hydrophobe *Rodlet*-Schicht über ihrer Zellwand, welche immunogene Strukturen vor dem Immunsystem verdeckt und die Phagozytose ruhender Konidien erschwert. Erst beim Auskeimen wird diese *Rodlet*-Schicht abgelegt, und die freiliegenden Zellwandbestandteile wie α-Mannan und β-Glucan der entstehenden Keimschläuche können von PRR der innaten Immunzellen wie v. a. Neutrophilen detektiert werden (Aimanianda et al., 2009, Lass-Flörl et al., 2013). Sporen der Mucorales verfügen über keine *Rodlet*-Hydrophobine

und führen somit auch in ruhender Form zu einer proinflammatorischen Immunantwort (Wurster et al., 2017a). Mikroskopisch konnte erkannt werden, dass die Hyphen von *A. fumigatus* primär an humanen Epithelzellen an *Tight Junction* Verbindungen vorbei oder durch Actin-Tunnel wachsen, ohne das Gewebe zu zerstören (Escobar et al., 2016, Fernandes et al., 2018). Hier wird ein Mechanismus zur Immunevasion vermutet, diese schonende Art der Penetration der infizierten Epithelzellen erhält deren Integrität, sodass keine inflammatorischen oder mit Zelltod assoziierten Faktoren wie Lactatdehydrogenase sezerniert werden (Fernandes et al., 2018).

Die von dendritischen und epithelialen Zellen freigesetzten Zytokinprofile decken sich qualitativ mit denen aus vorangegangenen Studien zu Mucorales (Chamilos et al., 2008b, Warris et al. 2005, Wurster et al., 2017a). Die quantitativ erhöhten proinflammatorischen Reaktionen über die sezernierten Zytokine IL-1β, IL-8 und TNF-α von Seiten der Epithelzellen und moDCs bei einer Infektion mit sowohl Keimschläuchen als auch ruhenden Sporen von Mucorales im Vergleich zu *A. fumigatus* bestätigen ebenfalls frühere Studien (Morton et al., 2014, Wurster et al., 2017a, Zhang et al., 2005). Da sich auch die Transkription von insbesondere IL-8 und ICAM-1 bei Mucorales-infizierten Proben verglichen mit *A. fumigatus* stark erhöhte (Belic et al., 2019, Morton et al., 2014), deutet dies auf eine stärkere Stimulation des damit assoziierten NF-κB-Signalwegs durch Mucorales hin (Melotti et al., 2001).

Klinisch fällt zudem der Unterschied auf, dass Mucorales neben immunkompromittierten Patienten auch immunkompetente Personen betreffen kann, u. a. mit Diabetes mellitus als prädisponierende Vorerkrankung (Skiada et al., 2018). Hier konnte gezeigt werden, dass sich die Risikofaktoren Hyperglykämie und Ketoazidose, wie sie bei schlecht eingestellten Diabetes-Patienten vorkommen, *in vitro* in unserem Modell rekonstruieren lassen und zu einem signifikant erhöhtem Biomassezuwachs von Mucorales im endothelialen Kompartiment führen (Belic et al., 2019). Auch die im Mausmodell dokumentierte Inhibition des invasiven Wachstums mithilfe des EGFR Inhibitors Gefitinib ließ sich reproduzieren, was die Anwendbarkeit des Modells in der Erprobung neuer Pharmaka unterstreicht (Belic et al., 2019, Watkins et al., 2018).

Ein optimales Zellkulturmodell pulmonaler Infektionen müsste jedoch weitere Faktoren aufgreifen. Hier wurden während der Infektion des alveolären Kompartiments die Zellen der Epithelschicht mit Medium überschichtet, während ein realistischerer Mechanismus die Infektion mit Sporen über einen Luftstrom darstellen würde (Fernandes et al., 2018). Anstelle der auf Polyester basierenden Membranen der *Transwell*®-Einsätze wären potenziell aus Kollagen konstruierte Matrizes einer physiologischen Umgebung der Zellen zuträglich (Miller & Spence, 2017). Rekonstituierte oder *ex vivo* erhaltene Gewebeproben stellen ebenfalls näher an *in vivo* Situationen gelegene Bedingungen dar als die mitunter immortalisierten Zelllinien, welche aufgrund der Langzeitbehandlungen in Laboren anders auf externe Stimuli reagieren könnten als primäre Zellen (Fernandes et al., 2018, Miller & Spence, 2017, Maciel Quatrin et al., 2019). *Airway-on-a-Chip*-Modelle erlauben zudem neben einem Epithel-Endothel-*Interface* die Simulation eines Blutkreislaufsystems, inklusive der Präsenz von Leukozyten, mittels Mikrofluidik (Benam et al., 2017).

Dreidimensionale Organoide werden gegenwärtig vermehrt als *in vitro* Modellierung von sowohl pulmonaler Erkrankungen (Tan et al., 2017, Wilkinson et al., 2017), als auch ausgewählter bakterieller und viraler Infektionen angewandt (Dutta & Clevers, 2017), bisher jedoch nicht für Mykosen. Perfundierte 3D-Modelle wurden in Bioreaktoren hingegen bereits für *A. fumigatus*-Infektionen etabliert (Chandorkar et al., 2017). Dezellularisierte Lungen können ebenfalls als Gerüst zur Kultur und Generation eines dreidimensionalen multizellulären pulmonalen Modells genutzt werden (Gilpin & Wagner, 2018, Miller & Spence, 2017). Da insbesondere bei Letzterem allerdings die biologische Variabilität der Ursprungsorganismen, sowie die der multiplen Arbeitsschritte in der Versuchsdurchführung Rechnung getragen muss, kann hierbei jedoch kaum dieselbe Reproduzierbarkeit verglichen mit der Verwendung von Zelllinien erreicht werden (Miller & Spence, 2017).

Im Gegensatz dazu erreichten im hier optimierten *Transwell*®-Modell 8 von 10 auf Zytokinsekretion und Transkription basierende Analysen Mucorales-infizierter Proben CVs von weniger als 40 %, womit eine hohe Reproduzierbarkeit dokumentiert wird, weswegen es sich auch in der Evaluation potenzieller Biomarker nutzen ließe (Belic et al., 2019). Diagnostisch angewandte fungale Biomarker wie Galactomannan und DNA konnten bereits in diesem Modell gezeigt werden (Hope et al., 2007, Belic et al.,

2019). Analog ließe sich dieser Schritt invertieren und mithilfe des Modells könnten neuartige Biomarker für Blut- oder BAL-basierte Diagnostik invasiver Mykosen entwickelt werden. Zudem könnten Immunzellpopulationen mit *Single Nucleotide Polymorphisms*, welche mit invasiven Mykosen in Verbindung gebracht werden (Fisher et al., 2017, Grube et al., 2013, Ok et al., 2011), anhand des Modells auf ihre Fähigkeit hin, Pilzsporen effizient zu eliminieren, überprüft werden.

Im Rahmen dieser Arbeit sollte die vorteilhafte Balance des Modells aus physiologischer Relevanz und technischer Reproduzierbarkeit genutzt werden, um die Eignung neuer nuklearmedizinischer *Tracer* bei invasiv-pulmonalen Mykosen zu prüfen. Die Detektion von Schimmelpilzen wurde bisher anhand von markierten Siderophoren, Antikörpern und Oligonukleotiden erfolgreich gezeigt (Petrik et al., 2014, Rolle et al., 2016, Thornton, 2018, Wang et al., 2014). Die Herstellung dieser ist jedoch sehr kosten- und zeitintensiv und erfordert mitunter hohe Investitionen in die benötigte Ausrüstung. Dies gilt ebenfalls für die zu ihrer Evaluation genutzten Tiermodelle, zumal aufgrund der Kombination von infektiösen Agenzien und Radiopharmaka ein hoher logistischer Aufwand zur Genehmigung und Durchführung dieser Studien erforderlich ist.

Die Durchführung präliminärer Studien in einem adäquaten *in vitro* Modell lässt sich hingegen in kurzer Zeit durchführen und kann ungeeignete Wirkstoffe ohne den Aufwand eines Tiermodells exkludieren, während vielversprechende Substanzen präliminär validiert werden können. So konnte das in Page et al. (2020b, in Druck) als HPAEC-*Monolayer* genutzte *Transwell*®-Modell zeigen, dass mit ^{99m}Tc und ^{68}Ga markiertes AMB das Potential aufweist, mykologische von bakteriellen Infektionen reproduzierbar zu unterscheiden. Hierbei wurde in einem ersten Schritt neben *A. fumigatus* mit *R. arrhizus* ein Erreger der Mucorales untersucht, in beiden Fällen konnte eine vom Sporen-Inokulum abhängige Aufnahme anhand zweier unterschiedlicher *Assays* gezeigt werden (*Gamma Counting* und Autoradiografie, Page et al., 2020b, in Druck). Dadurch, dass AMB gegenüber einer Vielzahl unterschiedlicher Pilzinfektionen therapeutisch wirksam ist (Hamill, 2013), wurde ein breiteres Spektrum pathogener Schimmelpilze untersucht, bestehend aus *A. niger*, *A. terreus*, *R. pusillus*, *C. bertholletiae*, *M. circinelloides* und *F. solani*. Es konnte jedoch kein Zusammenhang zwischen minimaler inhibitorischer Konzentrationen der Pilze und deren *Tracer*-Aufnahme beobachtet werden (Page et al., 2020b, in Druck).

Für die Markierung stünden potenziell mehrere radioaktive Isotope zur Verfügung. Die hier beschriebene Methodik basiert auf der Komplexierung dreiwertiger geladener Metall-Kationen an mehreren der Hydroxygruppen des AMB-Moleküls. Neben ^{99m}Tc und ^{68}Ga könnten je nach Ausrüstung und Erfahrungen der jeweiligen nuklearmedizinischen Einrichtungen potenziell weitere Isotope für analoge Markierungen für Anwendungen in Szintigrafie, SPECT oder PET infrage kommen, insofern sie ausreichend stabile elektrostatische Wechselwirkungen ausüben. Während PET-Geräte zwar zu hochauflösender Bildgebung in der Lage sind, stellen sie jedoch kostspielige Investitionen dar (Slomka et al., 2015). Gamma-Kameras und SPECT sind hingegen ubiquitär in nuklearmedizinischen Kliniken verfügbar und diese könnten auch aufgrund der vergleichsweise einfachen Markierung des patentfrei zu erwerbenden AMB diesen *Tracer* anwenden. Neben den genannten Applikationen zur Diagnostik erlaubt die parallele Markierung diagnostischer *Tracer* mit z. B. dem Beta-Strahler ^{177}Lu aufgrund ihrer höheren Äquivalentdosis als Gamma-Strahlung auch theranostische Anwendungen. Bei höheren Dosierungen können so beispielsweise Tumorzellen aufgrund ihrer erhöhten Anreicherung der *Tracer* direkt geschädigt werden, während die Aufnahme des *Tracers* in gesundem Gewebe minimal ist (Filippi et al., 2020).

Aufgrund der komplexen kardiovaskulären Systeme und vollständigen Organe kann *in vivo* jedoch eine Anreicherung der *Tracer* außerhalb infizierten Gewebes vorkommen. Außerdem müssen neben bakteriellen Infektionen auch sterile Inflammationen differenziert werden können, da diese ebenfalls Zellmembran-kompositionen verändern und so zu erhöhter AMB-Aufnahme führen könnten (De Groot & Burgas, 2015, Sunshine & Iruela-Arispe, 2017). Wenngleich Fernandez et al. (2017) für einen anderen AMB-basierten *Tracer* bereits eine gute Verträglichkeit, spezifische Anreicherung und rapide Exkretion im Mausmodell zeigten, könnte aufgrund erhöhter Mitoseaktivität und Stoffwechselleistung, analog zu FDG, Tumorzellen auch auf Antimykotika basierte *Tracer* unspezifisch aufnehmen. Aufgrund der Lipophilität von AMB wäre eine Anreicherung in Fettgewebe ebenfalls möglich. Akkumulationen in den Exkretionsorganen Leber und Niere müssen ebenfalls ausgeschlossen werden, sobald das Risiko besteht, mit der spezifischen Detektion einer Mykose zu interferieren. Zusätzlich birgt AMB aufgrund seiner hohen Toxizität das Risiko von Nebenwirkungen (Hamill, 2013), welches aber aufgrund der hier verringerten Dosis verglichen mit üblichen therapeutischen Dosen minimiert wird

(die therapeutische Dosis von AMB gegenüber *A. fumigatus* liegt in der Regel bei 0,5 – 4 µg/ml, Meletiadis et al., 2007).

Wenngleich diese Fragen abschließend nur im Tiermodell untersucht werden können, lieferte das Alveolarmodell eine Möglichkeit, unter annähernd physiologischen Bedingungen zeit- und dosisabhängige Aufnahmen der *Tracer* zu dokumentieren. Bedingt durch die hohe Reproduzierbarkeit der Konstruktion und Infektion des Modells konnten präzise Kinetiken der Aufnahmen unterschiedlicher Erreger untersucht werden, während *in vivo* durch interindividuelle Variation der Tiere, sowie die technische Variabilität der geläufigen Infektionsmethoden (intratracheale oder intranasale Applikation von Sporen) mit höheren Variationskoeffizienten gerechnet werden muss. *In vitro*-Zellkultursysteme stellen stets eine Balance aus technischer Reproduzierbarkeit und physiologischer Bedingungen. Die erfolgreiche Detektion von Schimmelpilzen mittels markiertem AMB im *Transwell*®-Modell stellt ein Beispiel für die Eignung dieser Systeme zur präliminären Evaluation neuer Biomarker dar.

5. ZUSAMMENFASSUNG

5.1 Deutsche Zusammenfassung

Schimmelpilze können in Abhängigkeit des Immunstatus und der Vorerkrankungen betroffener Patienten unterschiedliche Krankheitsbilder wie Hypersensitivitäts-erkrankungen oder lebensbedrohliche invasive Infektionen hervorrufen. Da die Diagnosestellung dieser Erkrankungen mitunter komplex und insensitiv ist, sollten im Rahmen dieser Arbeit unterschiedliche Ansätze neuer diagnostischer *Assays* untersucht werden.

In den letzten Jahren wurden *Assays* entwickelt, die auf Basis durchflusszytometrisch quantifizierter Pilz-spezifischer T-Zellen aus peripherem Blut einen supportiven Biomarker zur Diagnostik invasiver Mykosen liefern könnten. Da die hierfür isolierten T-Zellen anfällig gegenüber präanalytischer Lagerzeiten und immunsuppressiver Medikation sind, wurden hier Protokolloptimierungen vorgenommen, um anhand eines Vollblut-basierten *Assays* mit zusätzlicher CD49d-Kostimulation diesen Limitationen entgegen zu wirken. In einer Studie an gesunden Probanden konnte dabei gezeigt werden, dass die Kombination der Durchflusszytometrie mit ausgewählten Zytokin-Messungen (IL-5, IL-10 und IL-17) zu einer verbesserten Erkennung vermehrt Schimmelpilz-exponierter Personen beitragen könnte. Neben Infektionen könnten dabei im umwelt- und arbeitsmedizinischen Kontext Polarisationen der T-Zell-Populationen detektiert werden, welche mit Sensibilisierungen und Hypersensitivität assoziiert werden.

Zusätzlich wurde ein *in vitro Transwell*® Alveolarmodell zur Simulation pulmonaler Pilzinfektionen für Erreger der Ordnung Mucorales adaptiert, durch Reproduktion wichtiger Merkmale der Pathogenese von Mucormykosen validiert, und für Untersuchungen der Immunpathologie und Erreger-Invasion verwendet. Das Modell wurde anschließend zur *in vitro* Evaluation von radioaktiv markiertem Amphotericin B mit ^{99m}Tc oder ^{68}Ga als nuklearmedizinischen *Tracer* verwendet. Die untersuchten Schimmelpilze zeigten dabei eine zeit- und dosis-abhängige Aufnahme der *Tracer*, während bakteriell infizierte Proben nicht detektiert wurden. Die erhobenen Daten dokumentieren ein vielversprechendes Potenzial von Amphotericin B-basierten *Tracer*, das in zukünftigen *in vivo* Studien weiter evaluiert werden sollte.

5.2 English Summary

Depending on the immune constitution and predisposing illnesses, moulds can cause a variety of diseases ranging from hypersensitivity syndromes to life-threatening invasive infections. As the diagnosis of mould-associated diseases remains challenging, this work aimed to refine immunological assays and to develop molecular imaging protocols for pulmonary mould infections.

Recently, a flow cytometric assay for mould specific T cell quantification has been proposed as a novel supportive biomarker to diagnose invasive mycoses. As these assays are susceptible to pre-analytic delays and immunosuppressive drugs, a whole blood-based protocol with enhanced CD28 plus CD49d co-stimulation was developed and was shown to be less prone to these limitations. In addition, a study on healthy volunteers demonstrated the applicability of flow cytometric antigen-reactive T cell quantification as a surrogate of environmental mould exposure, especially when combined with T-cellular cytokine measurements (specifically, IL-5, IL-10, and IL-17). Therefore, these assays could potentially be used to detect polarizations of T-cell populations associated with sensitization and hypersensitivity, e. g. in allergology and occupational medicine.

Moreover, an *in vitro Transwell*® alveolar model of invasive pulmonary mould infections has been adapted to study mucormycoses, validated by recapitulation of known pathogenicity factors, and used to characterize the immunopathology and epithelial invasion of Mucorales. The *Transwell*® model was subsequently used to evaluate radioactively labelled Amphotericin B with either ^{99m}Tc or ^{68}Ga as a potential nuclear medical tracer. Time- and dose-dependent enrichment of the tracers was found in both *Aspergillus* and Mucorales, whereas samples infected with bacteria showed negligible uptake. These *in vitro* data document a promising potential of radiolabeled amphotericin B for molecular imaging of invasive mycoses and encourage further evaluation in animal models.

6. REFERENZEN

(2017). 8th Trends in Medical Mycology, Organised under the auspices of EORTC-IDG and ECMM, 6-9 October 2017, Belgrade, Serbia. Mycoses 60 Suppl 2, 3-238.

Abbas, A.K., Lichtman, A.H., Pillai, S., Baker, D.L., and Baker, A. (2018a). Cellular and molecular immunology, Ninth edition. edn (Philadelphia, PA: Elsevier).

Abbas, A.K., Trotta, E., D, R.S., Marson, A., and Bluestone, J.A. (2018b). Revisiting IL-2: Biology and therapeutic prospects. Sci Immunol 3.

Adak, T., Mukherjee, A.K., J, B., Pokhare, S.S., Yadav, M.K., Bag, M.K., Lenka, S., Munda, S., and Jena, M. (2019). Target and non-target effect of commonly used fungicides on microbial properties in rhizospheric soil of rice. International Journal of Environmental Analytical Chemistry, 1-12.

Afonso, G., Scotto, M., Renand, A., Arvastsson, J., Vassilieff, D., Cilio, C.M., and Mallone, R. (2010). Critical parameters in blood processing for T-cell assays: validation on ELISpot and tetramer platforms. J Immunol Methods 359, 28-36.

Agarwal, R., Chakrabarti, A., Shah, A., Gupta, D., Meis, J.F., Guleria, R., Moss, R., Denning, D.W., and group, A.c.a.I.w. (2013). Allergic bronchopulmonary aspergillosis: review of literature and proposal of new diagnostic and classification criteria. Clin Exp Allergy 43, 850-873.

Agarwal, R., Sehgal, I.S., Dhooria, S., and Aggarwal, A.N. (2016). Developments in the diagnosis and treatment of allergic bronchopulmonary aspergillosis. Expert Rev Respir Med 10, 1317-1334.

Aimanianda, V., Bayry, J., Bozza, S., Kniemeyer, O., Perruccio, K., Elluru, S.R., Clavaud, C., Paris, S., Brakhage, A.A., Kaveri, S.V., et al. (2009). Surface hydrophobin prevents immune recognition of airborne fungal spores. Nature 460, 1117-1121.

Allan, A.L., and Keeney, M. (2010). Circulating tumor cell analysis: technical and statistical considerations for application to the clinic. J Oncol 2010, 426218.

Almyroudis, N.G., Sutton, D.A., Fothergill, A.W., Rinaldi, M.G., and Kusne, S. (2007). In vitro susceptibilities of 217 clinical isolates of zygomycetes to conventional and new antifungal agents. Antimicrob Agents Chemother 51, 2587-2590.

Arendrup, M.C., Meletiadis, J., Mouton, J.W., Lagrou, K., Hamal, P., Guinea, J., and Testing, S.o.A.S.T.o.t.E.E.C.f.A.S. (2017). EUCAST DEFINITIVE DOCUMENT E.DEF 9.3.1 Method for the determination of broth dilution minimum inhibitory concentrations of antifungal agents for conidia forming moulds.

Ashokkumar, C., Green, M., Soltys, K., Michaels, M., Mazariegos, G., Reyes-Mugica, M., Higgs, B.W., Spishock, B., Zaccagnini, M., Sethi, P., et al. (2019). CD154-expressing CMV-specific T cells

associate with freedom from DNAemia and may be protective in seronegative recipients after liver or intestine transplantation. Pediatr Transplant, e13601.

Bacher, P., Heinrich, F., Stervbo, U., Nienen, M., Vahldieck, M., Iwert, C., Vogt, K., Kollet, J., Babel, N., Sawitzki, B., et al. (2016). Regulatory T Cell Specificity Directs Tolerance versus Allergy against Aeroantigens in Humans. Cell 167, 1067-1078 e1016.

Bacher, P., Hohnstein, T., Beerbaum, E., Rocker, M., Blango, M.G., Kaufmann, S., Rohmel, J., Eschenhagen, P., Grehn, C., Seidel, K., et al. (2019). Human Anti-fungal Th17 Immunity and Pathology Rely on Cross-Reactivity against Candida albicans. Cell 176, 1340-1355 e1315.

Bacher, P., Jochheim-Richter, A., Mockel-Tenbrink, N., Kniemeyer, O., Wingenfeld, E., Alex, R., Ortigao, A., Karpova, D., Lehrnbecher, T., Ullmann, A.J., et al. (2015a). Clinical-scale isolation of the total Aspergillus fumigatus-reactive T-helper cell repertoire for adoptive transfer. Cytotherapy 17, 1396-1405.

Bacher, P., Kniemeyer, O., Teutschbein, J., Thon, M., Vodisch, M., Wartenberg, D., Scharf, D.H., Koester-Eiserfunke, N., Schutte, M., Dubel, S., et al. (2014). Identification of immunogenic antigens from Aspergillus fumigatus by direct multiparameter characterization of specific conventional and regulatory CD4+ T cells. J Immunol 193, 3332-3343.

Bacher, P., and Scheffold, A. (2013). Flow-cytometric analysis of rare antigen-specific T cells. Cytometry A 83, 692-701.

Bacher, P., and Scheffold, A. (2015). New technologies for monitoring human antigen-specific T cells and regulatory T cells by flow-cytometry. Curr Opin Pharmacol 23, 17-24.

Bacher, P., Schink, C., Teutschbein, J., Kniemeyer, O., Assenmacher, M., Brakhage, A.A., and Scheffold, A. (2013). Antigen-reactive T cell enrichment for direct, high-resolution analysis of the human naive and memory Th cell repertoire. J Immunol 190, 3967-3976.

Bacher, P., Steinbach, A., Kniemeyer, O., Hamprecht, A., Assenmacher, M., Vehreschild, M.J., Vehreschild, J.J., Brakhage, A.A., Cornely, O.A., and Scheffold, A. (2015b). Fungus-specific CD4(+) T cells for rapid identification of invasive pulmonary mold infection. Am J Respir Crit Care Med 191, 348-352.

Baehner, R.L. (1980). Neutrophil dysfunction associated with states of chronic and recurrent infection. Pediatr Clin North Am 27, 377-401.

Bao, Z., Chen, H., Zhou, M., Shi, G., Li, Q., and Wan, H. (2017). Invasive pulmonary aspergillosis in patients with chronic obstructive pulmonary disease: a case report and review of the literature. Oncotarget 8, 38069-38074.

Barac, A., Kosmidis, C., Alastruey-Izquierdo, A., Salzer, H.J.F., and Cpanet (2019). Chronic pulmonary aspergillosis update: A year in review. Med Mycol 57, S104-S109.

Barbier, F., Andremont, A., Wolff, M., and Bouadma, L. (2013). Hospital-acquired pneumonia and ventilator-associated pneumonia: recent advances in epidemiology and management. Curr Opin Pulm Med 19, 216-228.

Barnes, P.J. (2017). Glucocorticosteroids. Handb Exp Pharmacol 237, 93-115.

Baron, F., and Nagler, A. (2017). Novel strategies for improving hematopoietic reconstruction after allogeneic hematopoietic stem cell transplantation or intensive chemotherapy. Expert Opin Biol Ther 17, 163-174.

Becker, K.L., Gresnigt, M.S., Smeekens, S.P., Jacobs, C.W., Magis-Escurra, C., Jaeger, M., Wang, X., Lubbers, R., Oosting, M., Joosten, L.A., et al. (2015). Pattern recognition pathways leading to a Th2 cytokine bias in allergic bronchopulmonary aspergillosis patients. Clin Exp Allergy 45, 423-437.

Becker, M.J., de Marie, S., Fens, M.H., Verbrugh, H.A., and Bakker-Woudenberg, I.A. (2003). Effect of amphotericin B treatment on kinetics of cytokines and parameters of fungal load in neutropenic rats with invasive pulmonary aspergillosis. J Antimicrob Chemother 52, 428-434.

Belard, E., Semb, S., Ruhwald, M., Werlinrud, A.M., Soborg, B., Jensen, F.K., Thomsen, H., Brylov, A., Hetland, M.L., Nordgaard-Lassen, I., et al. (2011). Prednisolone treatment affects the performance of the QuantiFERON gold in-tube test and the tuberculin skin test in patients with autoimmune disorders screened for latent tuberculosis infection. Inflamm Bowel Dis 17, 2340-2349.

Belic, S., Page, L., Lazariotou, M., Waaga-Gasser, A.M., Dragan, M., Springer, J., Loeffler, J., Morton, C.O., Einsele, H., Ullmann, A.J., et al. (2018). Comparative Analysis of Inflammatory Cytokine Release and Alveolar Epithelial Barrier Invasion in a Transwell((R)) Bilayer Model of Mucormycosis. Front Microbiol 9, 3204.

Bellanger, A.P., Reboux, G., Murat, J.B., Bex, V., and Millon, L. (2010). Detection of Aspergillus fumigatus by quantitative polymerase chain reaction in air samples impacted on low-melt agar. Am J Infect Control 38, 195-198.

Bellocchio, S., Gaziano, R., Bozza, S., Rossi, G., Montagnoli, C., Perruccio, K., Calvitti, M., Pitzurra, L., and Romani, L. (2005). Liposomal amphotericin B activates antifungal resistance with reduced toxicity by diverting Toll-like receptor signalling from TLR-2 to TLR-4. J Antimicrob Chemother 55, 214-222.

Benam, K.H., Mazur, M., Choe, Y., Ferrante, T.C., Novak, R., and Ingber, D.E. (2017). Human Lung Small Airway-on-a-Chip Protocol. Methods Mol Biol 1612, 345-365.

Benedict, K., and Park, B.J. (2014). Invasive fungal infections after natural disasters. Emerg Infect Dis 20, 349-355.

Berkova, N., Lair-Fulleringer, S., Femenia, F., Huet, D., Wagner, M.C., Gorna, K., Tournier, F., Ibrahim-Granet, O., Guillot, J., Chermette, R., et al. (2006). Aspergillus fumigatus conidia inhibit tumour necrosis factor- or staurosporine-induced apoptosis in epithelial cells. Int Immunol 18, 139-150.

Binder, U., Maurer, E., and Lass-Florl, C. (2014). Mucormycosis--from the pathogens to the disease. Clin Microbiol Infect 20 Suppl 6, 60-66.

Bischof, F., and Melms, A. (1998). Glucocorticoids inhibit CD40 ligand expression of peripheral CD4+ lymphocytes. Cell Immunol 187, 38-44.

Bitar, D., Van Cauteren, D., Lanternier, F., Dannaoui, E., Che, D., Dromer, F., Desenclos, J.C., and Lortholary, O. (2009). Increasing incidence of zygomycosis (mucormycosis), France, 1997-2006. Emerg Infect Dis 15, 1395-1401.

Boggs, J.M., Chang, N.H., and Goundalkar, A. (1991). Liposomal amphotericin B inhibits in vitro T-lymphocyte response to antigen. Antimicrob Agents Chemother 35, 879-885.

Bouchara, J.P., Oumeziane, N.A., Lissitzky, J.C., Larcher, G., Tronchin, G., and Chabasse, D. (1996). Attachment of spores of the human pathogenic fungus Rhizopus oryzae to extracellular matrix components. Eur J Cell Biol 70, 76-83.

Bowen, R.A., and Remaley, A.T. (2014). Interferences from blood collection tube components on clinical chemistry assays. Biochem Med (Zagreb) 24, 31-44.

Britten, C.M., Janetzki, S., Butterfield, L.H., Ferrari, G., Gouttefangeas, C., Huber, C., Kalos, M., Levitsky, H.I., Maecker, H.T., Melief, C.J., et al. (2012). T cell assays and MIATA: the essential minimum for maximum impact. Immunity 37, 1-2.

Britton, K.E., Wareham, D.W., Das, S.S., Solanki, K.K., Amaral, H., Bhatnagar, A., Katamihardja, A.H., Malamitsi, J., Moustafa, H.M., Soroa, V.E., et al. (2002). Imaging bacterial infection with (99m)Tc-ciprofloxacin (Infecton). J Clin Pathol 55, 817-823.

Brown, G.D., Taylor, P.R., Reid, D.M., Willment, J.A., Williams, D.L., Martinez-Pomares, L., Wong, S.Y., and Gordon, S. (2002). Dectin-1 is a major beta-glucan receptor on macrophages. J Exp Med 196, 407-412.

Brunet, L.R., LaBrie, S., and Hagemann, T. (2016a). Immune monitoring technology primer: immunoprofiling of antigen-stimulated blood. J Immunother Cancer 4, 18.

Brunet, M., Millan Lopez, O., and Lopez-Hoyos, M. (2016b). T-Cell Cytokines as Predictive Markers of the Risk of Allograft Rejection. Ther Drug Monit 38 Suppl 1, S21-28.

Bush, R.K., Portnoy, J.M., Saxon, A., Terr, A.I., and Wood, R.A. (2006). The medical effects of mold exposure. J Allergy Clin Immunol 117, 326-333.

Camargo, J.F., and Komanduri, K.V. (2017). Emerging concepts in cytomegalovirus infection following hematopoietic stem cell transplantation. Hematol Oncol Stem Cell Ther 10, 233-238.

Cano-Jimenez, E., Rubal, D., Perez de Llano, L.A., Mengual, N., Castro-Anon, O., Mendez, L., Golpe, R., Sanjuan, P., Martin, I., and Veres, A. (2017). Farmer's lung disease: Analysis of 75 cases. Med Clin (Barc) 149, 429-435.

Cenci, E., Mencacci, A., Del Sero, G., Bacci, A., Montagnoli, C., d'Ostiani, C.F., Mosci, P., Bachmann, M., Bistoni, F., Kopf, M., et al. (1999). Interleukin-4 causes susceptibility to invasive pulmonary aspergillosis through suppression of protective type I responses. J Infect Dis 180, 1957-1968.

Cenci, E., Mencacci, A., Fe d'Ostiani, C., Del Sero, G., Mosci, P., Montagnoli, C., Bacci, A., and Romani, L. (1998). Cytokine- and T helper-dependent lung mucosal immunity in mice with invasive pulmonary aspergillosis. J Infect Dis 178, 1750-1760.

Chamilos, G., Ganguly, D., Lande, R., Gregorio, J., Meller, S., Goldman, W.E., Gilliet, M., and Kontoyiannis, D.P. (2010). Generation of IL-23 producing dendritic cells (DCs) by airborne fungi regulates fungal pathogenicity via the induction of T(H)-17 responses. PLoS One 5, e12955.

Chamilos, G., Lewis, R.E., and Kontoyiannis, D.P. (2008a). Delaying amphotericin B-based frontline therapy significantly increases mortality among patients with hematologic malignancy who have zygomycosis. Clin Infect Dis 47, 503-509.

Chamilos, G., Lewis, R.E., Lamaris, G., Walsh, T.J., and Kontoyiannis, D.P. (2008b). Zygomycetes hyphae trigger an early, robust proinflammatory response in human polymorphonuclear neutrophils through toll-like receptor 2 induction but display relative resistance to oxidative damage. Antimicrob Agents Chemother 52, 722-724.

Chamilos, G., Luna, M., Lewis, R.E., Bodey, G.P., Chemaly, R., Tarrand, J.J., Safdar, A., Raad, II, and Kontoyiannis, D.P. (2006). Invasive fungal infections in patients with hematologic malignancies in a tertiary care cancer center: an autopsy study over a 15-year period (1989-2003). Haematologica 91, 986-989.

Chan, F.K., Moriwaki, K., and De Rosa, M.J. (2013). Detection of necrosis by release of lactate dehydrogenase activity. Methods Mol Biol 979, 65-70.

Chandorkar, P., Posch, W., Zaderer, V., Blatzer, M., Steger, M., Ammann, C.G., Binder, U., Hermann, M., Hortnagl, P., Lass-Florl, C., et al. (2017). Fast-track development of an in vitro 3D lung/immune cell model to study Aspergillus infections. Sci Rep 7, 11644.

Chen, K., Wang, Q., Pleasants, R.A., Ge, L., Liu, W., Peng, K., and Zhai, S. (2017). Empiric treatment against invasive fungal diseases in febrile neutropenic patients: a systematic review and network meta-analysis. BMC Infect Dis 17, 159.

Choi, J.H., Kwon, E.Y., Park, C.M., Choi, S.M., Lee, D.G., Yoo, J.H., Shin, W.S., and Stevens, D.A. (2010). Immunomodulatory effects of antifungal agents on the response of human monocytic cells to Aspergillus fumigatus conidia. Med Mycol 48, 704-709.

Colley, T., Sharma, C., Alanio, A., Kimura, G., Daly, L., Nakaoki, T., Nishimoto, Y., Bretagne, S., Kizawa, Y., Strong, P., et al. (2019). Anti-fungal activity of a novel triazole, PC1244, against emerging azole-resistant Aspergillus fumigatus and other species of Aspergillus. J Antimicrob Chemother 74, 2950-2958.

Cornely, O.A., Arikan-Akdagli, S., Dannaoui, E., Groll, A.H., Lagrou, K., Chakrabarti, A., Lanternier, F., Pagano, L., Skiada, A., Akova, M., et al. (2014). ESCMID and ECMM joint clinical guidelines for the diagnosis and management of mucormycosis 2013. Clin Microbiol Infect 20 Suppl 3, 5-26.

Cortez, K.J., Lyman, C.A., Kottilil, S., Kim, H.S., Roilides, E., Yang, J., Fullmer, B., Lempicki, R., and Walsh, T.J. (2006). Functional genomics of innate host defense molecules in normal human monocytes in response to Aspergillus fumigatus. Infect Immun 74, 2353-2365.

Costantini, A., Mancini, S., Giuliodoro, S., Butini, L., Regnery, C.M., Silvestri, G., and Montroni, M. (2003). Effects of cryopreservation on lymphocyte immunophenotype and function. J Immunol Methods 278, 145-155.

Cote, J., Chan, H., Brochu, G., and Chan-Yeung, M. (1991). Occupational asthma caused by exposure to neurospora in a plywood factory worker. Br J Ind Med 48, 279-282.

Cox, R., Jr., Phillips, O., Fukumoto, J., Fukumoto, I., Tamarapu Parthasarathy, P., Mandry, M., Cho, Y., Lockey, R., and Kolliputi, N. (2015). Resolvins Decrease Oxidative Stress Mediated Macrophage and Epithelial Cell Interaction through Decreased Cytokine Secretion. PLoS One 10, e0136755.

Cramer, R.A., Rivera, A., and Hohl, T.M. (2011). Immune responses against Aspergillus fumigatus: what have we learned? Curr Opin Infect Dis 24, 315-322.

Croft, C.A., Culibrk, L., Moore, M.M., and Tebbutt, S.J. (2016). Interactions of Aspergillus fumigatus Conidia with Airway Epithelial Cells: A Critical Review. Front Microbiol 7, 472.

Cui, N., Wang, H., Su, L.X., Zhang, J.H., Long, Y., and Liu, D.W. (2017). Role of Triggering Receptor Expressed on Myeloid Cell-1 Expression in Mammalian Target of Rapamycin Modulation of CD8(+) T-cell Differentiation during the Immune Response to Invasive Pulmonary Aspergillosis. Chin Med J (Engl) 130, 1211-1217.

Darling, B.A., and Milder, E.A. (2018). Invasive Aspergillosis. Pediatr Rev 39, 476-478.

Daschner, A. (2016). An Evolutionary-Based Framework for Analyzing Mold and Dampness-Associated Symptoms in DMHS. Front Immunol 7, 672.

Davies, G., Rolle, A.M., Maurer, A., Spycher, P.R., Schillinger, C., Solouk-Saran, D., Hasenberg, M., Weski, J., Fonslet, J., Dubois, A., et al. (2017). Towards Translational ImmunoPET/MR Imaging of Invasive Pulmonary Aspergillosis: The Humanised Monoclonal Antibody JF5 Detects Aspergillus Lung Infections In Vivo. Theranostics 7, 3398-3414.

de Groot, N.S., and Burgas, M.T. (2015). Is membrane homeostasis the missing link between inflammation and neurodegenerative diseases? Cell Mol Life Sci 72, 4795-4805.

Denis, B., Guiguet, M., de Castro, N., Mechai, F., Revest, M., Melica, G., Costagliola, D., Lortholary, O., French Hospital Database on, H.I.V.N.A.f.R.o.A., and Viral Hepatitis, F.C.O. (2015). Relevance of EORTC Criteria for the Diagnosis of Invasive Aspergillosis in HIV-Infected Patients, and Survival Trends Over a 20-Year Period in France. Clin Infect Dis 61, 1273-1280.

Denning, D.W., Cadranel, J., Beigelman-Aubry, C., Ader, F., Chakrabarti, A., Blot, S., Ullmann, A.J., Dimopoulos, G., Lange, C., European Society for Clinical, M., et al. (2016). Chronic pulmonary aspergillosis: rationale and clinical guidelines for diagnosis and management. Eur Respir J 47, 45-68.

Denning, D.W., Pashley, C., Hartl, D., Wardlaw, A., Godet, C., Del Giacco, S., Delhaes, L., and Sergejeva, S. (2014). Fungal allergy in asthma-state of the art and research needs. Clin Transl Allergy 4, 14.

Deo, S.S., Virassamy, B., Halliday, C., Clancy, L., Chen, S., Meyer, W., Sorrell, T.C., and Gottlieb, D.J. (2016). Stimulation with lysates of Aspergillus terreus, Candida krusei and Rhizopus oryzae maximizes cross-reactivity of anti-fungal T cells. Cytotherapy 18, 65-79.

Dewi, I.M.W., van de Veerdonk, F.L., and Gresnigt, M.S. (2017). The Multifaceted Role of T-Helper Responses in Host Defense against Aspergillus fumigatus. J Fungi (Basel) 3.

Dhooria, S., Kumar, P., Saikia, B., Aggarwal, A.N., Gupta, D., Behera, D., Chakrabarti, A., and Agarwal, R. (2014). Prevalence of Aspergillus sensitisation in pulmonary tuberculosis-related fibrocavitary disease. Int J Tuberc Lung Dis 18, 850-855.

Doberne, D., Gaur, R.L., and Banaei, N. (2011). Preanalytical delay reduces sensitivity of QuantiFERON-TB gold in-tube assay for detection of latent tuberculosis infection. J Clin Microbiol 49, 3061-3064.

Dogan, I.S., Sarac, S., Sari, S., Kart, D., Essiz Gokhan, S., Vural, I., and Dalkara, S. (2017). New azole derivatives showing antimicrobial effects and their mechanism of antifungal activity by molecular modeling studies. Eur J Med Chem 130, 124-138.

Douglas, A., Lau, E., Thursky, K., and Slavin, M. (2017). What, where and why: exploring fluorodeoxyglucose-PET's ability to localise and differentiate infection from cancer. Curr Opin Infect Dis 30, 552-564.

Dudakov, J.A., Hanash, A.M., and van den Brink, M.R. (2015). Interleukin-22: immunobiology and pathology. Annu Rev Immunol 33, 747-785.

Dutta, D., and Clevers, H. (2017). Organoid culture systems to study host-pathogen interactions. Curr Opin Immunol 48, 15-22.

Edmondson, D.A., Barrios, C.S., Brasel, T.L., Straus, D.C., Kurup, V.P., and Fink, J.N. (2009). Immune response among patients exposed to molds. Int J Mol Sci 10, 5471-5484.

Eduard, W., Sandven, P., and Levy, F. (1992). Relationships between exposure to spores from Rhizopus microsporus and Paecilomyces variotii and serum IgG antibodies in wood trimmers. Int Arch Allergy Immunol 97, 274-282.

Egli, A., Humar, A., and Kumar, D. (2012). State-of-the-art monitoring of cytomegalovirus-specific cell-mediated immunity after organ transplant: a primer for the clinician. Clin Infect Dis 55, 1678-1689.

Elgueta, R., Benson, M.J., de Vries, V.C., Wasiuk, A., Guo, Y., and Noelle, R.J. (2009). Molecular mechanism and function of CD40/CD40L engagement in the immune system. Immunol Rev 229, 152-172.

England, A.C., 3rd, Weinstein, M., Ellner, J.J., and Ajello, L. (1981). Two cases of rhinocerebral zygomycosis (mucormycosis) with common epidemiologic and environmental features. Am Rev Respir Dis 124, 497-498.

Escobar, N., Ordonez, S.R., Wosten, H.A., Haas, P.J., de Cock, H., and Haagsman, H.P. (2016). Hide, Keep Quiet, and Keep Low: Properties That Make Aspergillus fumigatus a Successful Lung Pathogen. Front Microbiol 7, 438.

Esensten, J.H., Helou, Y.A., Chopra, G., Weiss, A., and Bluestone, J.A. (2016). CD28 Costimulation: From Mechanism to Therapy. Immunity 44, 973-988.

Espinel-Ingroff, A. (2001). Germinated and nongerminated conidial suspensions for testing of susceptibilities of Aspergillus spp. to amphotericin B, itraconazole, posaconazole, ravuconazole, and voriconazole. Antimicrob Agents Chemother 45, 605-607.

Evans, S.E., and Ost, D.E. (2015). Pneumonia in the neutropenic cancer patient. Curr Opin Pulm Med 21, 260-271.

Faerden, K., Lund, M.B., Mogens Aalokken, T., Eduard, W., Sostrand, P., Langard, S., and Kongerud, J. (2014). Hypersensitivity pneumonitis in a cluster of sawmill workers: a 10-year follow-up of exposure, symptoms, and lung function. Int J Occup Environ Health 20, 167-173.

Fellman, C.L., Stokes, J.V., Archer, T.M., Pinchuk, L.M., Lunsford, K.V., and Mackin, A.J. (2011). Cyclosporine A affects the in vitro expression of T cell activation-related molecules and cytokines in dogs. Vet Immunol Immunopathol 140, 175-180.

Fernandes, J., Hamidi, F., Leborgne, R., Beau, R., Castier, Y., Mordant, P., Boukkerou, A., Latge, J.P., and Pretolani, M. (2018). Penetration of the Human Pulmonary Epithelium by Aspergillus fumigatus Hyphae. J Infect Dis 218, 1306-1313.

Fernandez, L., and Teran, M. (2017). Development and Evaluation of 99mTc-Amphotericin Complexes as Potential Diagnostic Agents in Nuclear Medicine. 4, e62150.

Fidan, I., Yesilyurt, E., Kalkanci, A., Aslan, S.O., Sahin, N., Ogan, M.C., and Dizbay, M. (2014). Immunomodulatory effects of voriconazole and caspofungin on human peripheral blood mononuclear cells stimulated by Candida albicans and Candida krusei. Am J Med Sci 348, 219-223.

Filippi, L., Chiaravalloti, A., Schillaci, O., Cianni, R., and Bagni, O. (2020). Theranostic approaches in nuclear medicine: current status and future prospects. Expert Rev Med Devices, 1-13.

Filler, S.G., and Sheppard, D.C. (2006). Fungal invasion of normally non-phagocytic host cells. PLoS Pathog 2, e129.

Fisher, C.E., Hohl, T.M., Fan, W., Storer, B.E., Levine, D.M., Zhao, L.P., Martin, P.J., Warren, E.H., Boeckh, M., and Hansen, J.A. (2017). Validation of single nucleotide polymorphisms in invasive aspergillosis following hematopoietic cell transplantation. Blood 129, 2693-2701.

Fukuda, T., Boeckh, M., Carter, R.A., Sandmaier, B.M., Maris, M.B., Maloney, D.G., Martin, P.J., Storb, R.F., and Marr, K.A. (2003). Risks and outcomes of invasive fungal infections in recipients of allogeneic hematopoietic stem cell transplants after nonmyeloablative conditioning. Blood 102, 827-833.

Fuleihan, R., Ramesh, N., Horner, A., Ahern, D., Belshaw, P.J., Alberg, D.G., Stamenkovic, I., Harmon, W., and Geha, R.S. (1994). Cyclosporin A inhibits CD40 ligand expression in T lymphocytes. J Clin Invest 93, 1315-1320.

Gafa, V., Remoli, M.E., Giacomini, E., Gagliardi, M.C., Lande, R., Severa, M., Grillot, R., and Coccia, E.M. (2007). In vitro infection of human dendritic cells by Aspergillus fumigatus conidia triggers the secretion of chemokines for neutrophil and Th1 lymphocyte recruitment. Microbes Infect 9, 971-980.

Gamboa, P.M., Urbaneja, F., Olaizola, I., Boyra, J.A., Gonzalez, G., Antepara, I., Urrutia, I., Jauregui, I., and Sanz, M.L. (2005). Specific IgG to Thermoactynomices vulgaris, Micropolyspora faeni and Aspergillus fumigatus in building workers exposed to esparto grass (plasterers) and in patients with esparto-induced hypersensitivity pneumonitis. J Investig Allergol Clin Immunol 15, 17-21.

Garcia-Cela, E., Crespo-Sempere, A., Gil-Serna, J., Porqueres, A., and Marin, S. (2015). Fungal diversity, incidence and mycotoxin contamination in grapes from two agro-climatic Spanish regions with emphasis on Aspergillus species. J Sci Food Agric 95, 1716-1729.

Garzoni, C., Emonet, S., Legout, L., Benedict, R., Hoffmeyer, P., Bernard, L., and Garbino, J. (2005). Atypical infections in tsunami survivors. Emerg Infect Dis 11, 1591-1593.

Gauduin, M.C. (2006). Intracellular cytokine staining for the characterization and quantitation of antigen-specific T lymphocyte responses. Methods 38, 263-273.

Gawria, G., Tillmar, L., and Landberg, E. (2019). A comparison of stability of chemical analytes in plasma from the BD Vacutainer((R)) Barricor tube with mechanical separator versus tubes containing gel separator. J Clin Lab Anal, e23060.

Gazdar, A.F., Girard, L., Lockwood, W.W., Lam, W.L., and Minna, J.D. (2010). Lung cancer cell lines as tools for biomedical discovery and research. J Natl Cancer Inst 102, 1310-1321.

Gazendam, R.P., van de Geer, A., Roos, D., van den Berg, T.K., and Kuijpers, T.W. (2016). How neutrophils kill fungi. Immunol Rev 273, 299-311.

Gebremariam, T., Lin, L., Liu, M., Kontoyiannis, D.P., French, S., Edwards, J.E., Jr., Filler, S.G., and Ibrahim, A.S. (2016). Bicarbonate correction of ketoacidosis alters host-pathogen interactions and alleviates mucormycosis. J Clin Invest 126, 2280-2294.

Ghosh, P., Sica, A., Cippitelli, M., Subleski, J., Lahesmaa, R., Young, H.A., and Rice, N.R. (1996). Activation of nuclear factor of activated T cells in a cyclosporin A-resistant pathway. J Biol Chem 271, 7700-7704.

Ghosh, S., Hoselton, S.A., and Schuh, J.M. (2015). Allergic Inflammation in Aspergillus fumigatus-Induced Fungal Asthma. Curr Allergy Asthma Rep 15, 59.

Ghuman, H., and Voelz, K. (2017). Innate and Adaptive Immunity to Mucorales. J Fungi (Basel) 3.

Gilpin, S.E., and Wagner, D.E. (2018). Acellular human lung scaffolds to model lung disease and tissue regeneration. Eur Respir Rev 27.

Goncalves, S.S., Souza, A.C.R., Chowdhary, A., Meis, J.F., and Colombo, A.L. (2016). Epidemiology and molecular mechanisms of antifungal resistance in Candida and Aspergillus. Mycoses 59, 198-219.

Gonzalez, G.M., Tijerina, R., Sutton, D.A., Graybill, J.R., and Rinaldi, M.G. (2002). In vitro activities of free and lipid formulations of amphotericin B and nystatin against clinical isolates of Coccidioides immitis at various saprobic stages. Antimicrob Agents Chemother 46, 1583-1585.

Gowrishankar, G., Namavari, M., Jouannot, E.B., Hoehne, A., Reeves, R., Hardy, J., and Gambhir, S.S. (2014). Investigation of 6-[(1)(8)F]-fluoromaltose as a novel PET tracer for imaging bacterial infection. PLoS One 9, e107951.

Greenberger, P.A., Bush, R.K., Demain, J.G., Luong, A., Slavin, R.G., and Knutsen, A.P. (2014). Allergic bronchopulmonary aspergillosis. J Allergy Clin Immunol Pract 2, 703-708.

Gregson, L., Hope, W.W., and Howard, S.J. (2012). In vitro model of invasive pulmonary aspergillosis in the human alveolus. Methods Mol Biol 845, 361-367.

Grube, M., Loeffler, J., Mezger, M., Kruger, B., Echtenacher, B., Hoffmann, P., Edinger, M., Einsele, H., Andreesen, R., and Holler, E. (2013). TLR5 stop codon polymorphism is associated with invasive aspergillosis after allogeneic stem cell transplantation. Med Mycol 51, 818-825.

Guermonprez, P., Valladeau, J., Zitvogel, L., Thery, C., and Amigorena, S. (2002). Antigen presentation and T cell stimulation by dendritic cells. Annu Rev Immunol 20, 621-667.

Guinea, J., Torres-Narbona, M., Gijon, P., Munoz, P., Pozo, F., Pelaez, T., de Miguel, J., and Bouza, E. (2010). Pulmonary aspergillosis in patients with chronic obstructive pulmonary disease: incidence, risk factors, and outcome. Clin Microbiol Infect 16, 870-877.

Guzera, M., Szulc-Dabrowska, L., Cywinska, A., Archer, J., and Winnicka, A. (2016). In Vitro Influence of Mycophenolic Acid on Selected Parameters of Stimulated Peripheral Canine Lymphocytes. PLoS One 11, e0154429.

Haas, H., Petrik, M., and Decristoforo, C. (2015). An iron-mimicking, Trojan horse-entering fungi--has the time come for molecular imaging of fungal infections? PLoS Pathog 11, e1004568.

Halpin, D.M., Graneek, B.J., Turner-Warwick, M., and Newman Taylor, A.J. (1994). Extrinsic allergic alveolitis and asthma in a sawmill worker: case report and review of the literature. Occup Environ Med 51, 160-164.

Hamill, R.J. (2013). Amphotericin B formulations: a comparative review of efficacy and toxicity. Drugs 73, 919-934.

Hammond, S.M. (1977). Biological activity of polyene antibiotics. Prog Med Chem 14, 105-179.

Hedges, J.F., Mitchell, A.M., Jones, K., Kimmel, E., Ramstead, A.G., Snyder, D.T., and Jutila, M.A. (2015). Amphotericin B stimulates gammadelta T and NK cells, and enhances protection from Salmonella infection. Innate Immun 21, 598-608.

Helwig, U., Muller, M., Hedderich, J., and Schreiber, S. (2012). Corticosteroids and immunosuppressive therapy influence the result of QuantiFERON TB Gold testing in inflammatory bowel disease patients. J Crohns Colitis 6, 419-424.

Hewitt, R.J., Singanayagam, A., Sridhar, S., Wickremasinghe, M., and Min Kon, O. (2015). Screening for latent tuberculosis before tumour necrosis factor antagonist therapy. Eur Respir J 45, 1510-1512.

Hoffmann, C., Dollive, S., Grunberg, S., Chen, J., Li, H., Wu, G.D., Lewis, J.D., and Bushman, F.D. (2013). Archaea and fungi of the human gut microbiome: correlations with diet and bacterial residents. PLoS One 8, e66019.

Hohl, T.M. (2017). Immune responses to invasive aspergillosis: new understanding and therapeutic opportunities. Curr Opin Infect Dis 30, 364-371.

Hohl, T.M., Feldmesser, M., Perlin, D.S., and Pamer, E.G. (2008). Caspofungin modulates inflammatory responses to Aspergillus fumigatus through stage-specific effects on fungal beta-glucan exposure. J Infect Dis 198, 176-185.

Hope, W.W. (2009). Invasion of the alveolar-capillary barrier by Aspergillus spp.: therapeutic and diagnostic implications for immunocompromised patients with invasive pulmonary aspergillosis. Med Mycol 47 Suppl 1, S291-298.

Hope, W.W., Kruhlak, M.J., Lyman, C.A., Petraitiene, R., Petraitis, V., Francesconi, A., Kasai, M., Mickiene, D., Sein, T., Peter, J., et al. (2007). Pathogenesis of Aspergillus fumigatus and the kinetics of galactomannan in an in vitro model of early invasive pulmonary aspergillosis: implications for antifungal therapy. J Infect Dis 195, 455-466.

Huang, L., He, H., Ding, Y., Jin, J., and Zhan, Q. (2018). Values of radiological examinations for the diagnosis and prognosis of invasive bronchial-pulmonary aspergillosis in critically ill patients with chronic obstructive pulmonary diseases. Clin Respir J 12, 499-509.

Hulin, M., Moularat, S., Kirchner, S., Robine, E., Mandin, C., and Annesi-Maesano, I. (2013). Positive associations between respiratory outcomes and fungal index in rural inhabitants of a representative sample of French dwellings. Int J Hyg Environ Health 216, 155-162.

Ibrahim, A.S., and Kontoyiannis, D.P. (2013). Update on mucormycosis pathogenesis. Curr Opin Infect Dis 26, 508-515.

Ibrahim, A.S., Spellberg, B., Avanessian, V., Fu, Y., and Edwards, J.E., Jr. (2005). Rhizopus oryzae adheres to, is phagocytosed by, and damages endothelial cells in vitro. Infect Immun 73, 778-783.

Ibrahim-Granet, O., Philippe, B., Boleti, H., Boisvieux-Ulrich, E., Grenet, D., Stern, M., and Latge, J.P. (2003). Phagocytosis and intracellular fate of Aspergillus fumigatus conidia in alveolar macrophages. Infect Immun 71, 891-903.

Isham, N., and Ghannoum, M.A. (2006). Determination of MICs of aminocandin for Candida spp. and filamentous fungi. J Clin Microbiol 44, 4342-4344.

Jabara, H.H., Brodeur, S.R., and Geha, R.S. (2001). Glucocorticoids upregulate CD40 ligand expression and induce CD40L-dependent immunoglobulin isotype switching. J Clin Invest 107, 371-378.

Jacob, B., Ritz, B., Gehring, U., Koch, A., Bischof, W., Wichmann, H.E., and Heinrich, J. (2002). Indoor exposure to molds and allergic sensitization. Environ Health Perspect 110, 647-653.

Janetzki, S., Rueger, M., and Dillenbeck, T. (2014). Stepping up ELISpot: Multi-Level Analysis in FluoroSpot Assays. Cells 3, 1102-1115.

Jeurink, P.V., Noguera, C.L., Savelkoul, H.F., and Wichers, H.J. (2008a). Immunomodulatory capacity of fungal proteins on the cytokine production of human peripheral blood mononuclear cells. Int Immunopharmacol 8, 1124-1133.

Jeurink, P.V., Vissers, Y.M., Rappard, B., and Savelkoul, H.F. (2008b). T cell responses in fresh and cryopreserved peripheral blood mononuclear cells: kinetics of cell viability, cellular subsets, proliferation, and cytokine production. Cryobiology 57, 91-103.

Johnson, G., Ferrini, A., Dolan, S.K., Nolan, T., Agrawal, S., Doyle, S., and Bustin, S.A. (2014). Biomarkers for invasive aspergillosis: the challenges continue. Biomark Med 8, 429-451.

Jolink, H., de Boer, R., Hombrink, P., Jonkers, R.E., van Dissel, J.T., Falkenburg, J.H., and Heemskerk, M.H. (2017). Pulmonary immune responses against Aspergillus fumigatus are characterized by high frequencies of IL-17 producing T-cells. J Infect 74, 81-88.

Jolink, H., de Boer, R., Willems, L.N., van Dissel, J.T., Falkenburg, J.H., and Heemskerk, M.H. (2015). T helper 2 response in allergic bronchopulmonary aspergillosis is not driven by specific Aspergillus antigens. Allergy 70, 1336-1339.

Jolink, H., Hagedoorn, R.S., Lagendijk, E.L., Drijfhout, J.W., van Dissel, J.T., Falkenburg, J.H., and Heemskerk, M.H. (2014). Induction of A. fumigatus-specific CD4-positive T cells in patients recovering from invasive aspergillosis. Haematologica 99, 1255-1263.

Jolink, H., Meijssen, I.C., Hagedoorn, R.S., Arentshorst, M., Drijfhout, J.W., Mulder, A., Claas, F.H., van Dissel, J.T., Falkenburg, J.H., and Heemskerk, M.H. (2013). Characterization of the T-cell-mediated immune response against the Aspergillus fumigatus proteins Crf1 and catalase 1 in healthy individuals. J Infect Dis 208, 847-856.

Jones, R.N. (2010). Microbial etiologies of hospital-acquired bacterial pneumonia and ventilator-associated bacterial pneumonia. Clin Infect Dis 51 Suppl 1, S81-87.

Joshi, A.D., Fong, D.J., Oak, S.R., Trujillo, G., Flaherty, K.R., Martinez, F.J., and Hogaboam, C.M. (2009). Interleukin-17-mediated immunopathogenesis in experimental hypersensitivity pneumonitis. Am J Respir Crit Care Med 179, 705-716.

Kamperschroer, C., O'Donnell, L.M., Schneider, P.A., Li, D., Roy, M., Coskran, T.M., and Kawabata, T.T. (2014). Measuring T-cell responses against LCV and CMV in cynomolgus macaques using ELISPOT: potential application to non-clinical testing of immunomodulatory therapeutics. J Immunotoxicol 11, 35-43.

Karthaus, M., and Buchheidt, D. (2013). Invasive aspergillosis: new insights into disease, diagnostic and treatment. Curr Pharm Des 19, 3569-3594.

Kaveh, D.A., Whelan, A.O., and Hogarth, P.J. (2012). The duration of antigen-stimulation significantly alters the diversity of multifunctional CD4 T cells measured by intracellular cytokine staining. PLoS One 7, e38926.

Kawakami, Y., Tagami, T., Kusakabe, T., Kido, N., Kawaguchi, T., Omura, M., and Tosa, R. (2012). Disseminated aspergillosis associated with tsunami lung. Respir Care 57, 1674-1678.

Kim, S.H., Lee, H.J., Kim, S.M., Jung, J.H., Shin, S., Kim, Y.H., Sung, H., Lee, S.O., Choi, S.H., Kim, Y.S., et al. (2015). Diagnostic Usefulness of Cytomegalovirus (CMV)-Specific T Cell Immunity in Predicting CMV Infection after Kidney Transplantation: A Pilot Proof-of-Concept Study. Infect Chemother 47, 105-110.

Kim, T.H., and Lee, H.K. (2014). Differential roles of lung dendritic cell subsets against respiratory virus infection. Immune Netw 14, 128-137.

King, J., Brunel, S.F., and Warris, A. (2016). Aspergillus infections in cystic fibrosis. J Infect 72 Suppl, S50-55.

Klaric, M.S., and Pepeljnjak, S. (2005). [Beauvericin: chemical and biological aspects and occurrence]. Arh Hig Rada Toksikol 56, 343-350.

Kniemeyer, O., Ebel, F., Kruger, T., Bacher, P., Scheffold, A., Luo, T., Strassburger, M., and Brakhage, A.A. (2016). Immunoproteomics of Aspergillus for the development of biomarkers and immunotherapies. Proteomics Clin Appl 10, 910-921.

Knutsen, A.P., Bush, R.K., Demain, J.G., Denning, D.W., Dixit, A., Fairs, A., Greenberger, P.A., Kariuki, B., Kita, H., Kurup, V.P., et al. (2012). Fungi and allergic lower respiratory tract diseases. J Allergy Clin Immunol 129, 280-291; quiz 292-283.

Koehler, F.C., Cornely, O.A., Wisplinghoff, H., Schauss, A.C., Salmanton-Garcia, J., Ostermann, H., Ziegler, M., Bacher, P., Scheffold, A., Alex, R., et al. (2018). Candida-Reactive T Cells for the Diagnosis of Invasive Candida Infection-A Prospective Pilot Study. Front Microbiol 9, 1381.

Kotimaa, M.H., Husman, K.H., Terho, E.O., and Mustonen, M.H. (1984). Airborne molds and actinomycetes in the work environment of farmer's lung patients in Finland. Scand J Work Environ Health 10, 115-119.

Kumaresan, P.R., da Silva, T.A., and Kontoyiannis, D.P. (2017). Methods of Controlling Invasive Fungal Infections Using CD8(+) T Cells. Front Immunol 8, 1939.

Lackner, M., Caramalho, R., and Lass-Florl, C. (2014). Laboratory diagnosis of mucormycosis: current status and future perspectives. Future Microbiol 9, 683-695.

Lahoz-Beneytez, J., Elemans, M., Zhang, Y., Ahmed, R., Salam, A., Block, M., Niederalt, C., Asquith, B., and Macallan, D. (2016). Human neutrophil kinetics: modeling of stable isotope labeling data supports short blood neutrophil half-lives. Blood 127, 3431-3438.

Lamoth, F., and Calandra, T. (2017). Early diagnosis of invasive mould infections and disease. J Antimicrob Chemother 72, i19-i28.

Lanternier, F., Dannaoui, E., Morizot, G., Elie, C., Garcia-Hermoso, D., Huerre, M., Bitar, D., Dromer, F., Lortholary, O., and French Mycosis Study, G. (2012). A global analysis of mucormycosis in France: the RetroZygo Study (2005-2007). Clin Infect Dis 54 Suppl 1, S35-43.

Lass-Florl, C., Nagl, M., Gunsilius, E., Speth, C., Ulmer, H., and Wurzner, R. (2002). In vitro studies on the activity of amphotericin B and lipid-based amphotericin B formulations against Aspergillus conidia and hyphae. Mycoses 45, 166-169.

Lass-Florl, C., Roilides, E., Loffler, J., Wilflingseder, D., and Romani, L. (2013). Minireview: host defence in invasive aspergillosis. Mycoses 56, 403-413.

Lauruschkat, C.D., Wurster, S., Page, L., Lazariotou, M., Dragan, M., Weis, P., Ullmann, A.J., Einsele, H., and Loffler, J. (2018). Susceptibility of A. fumigatus-specific T-cell assays to pre-analytic blood storage and PBMC cryopreservation greatly depends on readout platform and analytes. Mycoses 61, 549-560.

Leitner, J., Drobits, K., Pickl, W.F., Majdic, O., Zlabinger, G., and Steinberger, P. (2011). The effects of Cyclosporine A and azathioprine on human T cells activated by different costimulatory signals. Immunol Lett 140, 74-80.

Lemieux, J., Jobin, C., Simard, C., and Neron, S. (2016). A global look into human T cell subsets before and after cryopreservation using multiparametric flow cytometry and two-dimensional visualization analysis. J Immunol Methods 434, 73-82.

Lestner, J.M., Howard, S.J., Goodwin, J., Gregson, L., Majithiya, J., Walsh, T.J., Jensen, G.M., and Hope, W.W. (2010). Pharmacokinetics and pharmacodynamics of amphotericin B deoxycholate, liposomal amphotericin B, and amphotericin B lipid complex in an in vitro model of invasive pulmonary aspergillosis. Antimicrob Agents Chemother 54, 3432-3441.

Licona-Limon, P., Kim, L.K., Palm, N.W., and Flavell, R.A. (2013). TH2, allergy and group 2 innate lymphoid cells. Nat Immunol 14, 536-542.

Liu, S., Chen, D., Fu, S., Ren, Y., Wang, L., Zhang, Y., Zhao, M., He, X., and Wang, X. (2015). Prevalence and risk factors for farmer's lung in greenhouse farmers: an epidemiological study of 5,880 farmers from Northeast China. Cell Biochem Biophys 71, 1051-1057.

Lordan, J.L., Bucchieri, F., Richter, A., Konstantinidis, A., Holloway, J.W., Thornber, M., Puddicombe, S.M., Buchanan, D., Wilson, S.J., Djukanovic, R., et al. (2002). Cooperative effects of Th2 cytokines and allergen on normal and asthmatic bronchial epithelial cells. J Immunol 169, 407-414.

Lother, J., Breitschopf, T., Krappmann, S., Morton, C.O., Bouzani, M., Kurzai, O., Gunzer, M., Hasenberg, M., Einsele, H., and Loeffler, J. (2014). Human dendritic cell subsets display distinct interactions with the pathogenic mould Aspergillus fumigatus. Int J Med Microbiol 304, 1160-1168.

Lueg, E.A., Ballagh, R.H., and Forte, V. (1996). Analysis of the recent cluster of invasive fungal sinusitis at the Toronto Hospital for Sick Children. J Otolaryngol 25, 366-370.

Lupetti, A., de Boer, M.G., Erba, P., Campa, M., and Nibbering, P.H. (2011). Radiotracers for fungal infection imaging. Med Mycol 49 Suppl 1, S62-69.

Lupetti, A., Welling, M.M., Mazzi, U., Nibbering, P.H., and Pauwels, E.K. (2002). Technetium-99m labelled fluconazole and antimicrobial peptides for imaging of Candida albicans and Aspergillus fumigatus infections. Eur J Nucl Med Mol Imaging 29, 674-679.

Lupetti, A., Welling, M.M., Pauwels, E.K., and Nibbering, P.H. (2005). Detection of fungal infections using radiolabeled antifungal agents. Curr Drug Targets 6, 945-954.

Maciel Quatrin, P., Flores Dalla Lana, D., Andrzejewski Kaminski, T.F., and Meneghello Fuentefria, A. (2019). Fungal infection models: Current progress of ex vivo methods. 62, 860-873.

Madney, Y., Khedr, R., Al-Mahellawy, H., Adel, N., Taha, H., Zaki, I., Youssef, A., Taha, G., Hassanain, O., and Hafez, H. (2017). "Mucormycosis" the Emerging Global Threat; Overview and Treatment Outcome Among Pediatric Cancer Patients in Egypt. Blood 130, 4830-4830.

Maertens, J., Selleslag, D., Heinz, W.J., Saulay, M., Rahav, G., Giladi, M., Aoun, M., Kovanda, L., Kaufhold, A., Engelhardt, M., et al. (2018). Treatment outcomes in patients with proven/probable vs possible invasive mould disease in a phase III trial comparing isavuconazole vs voriconazole. Mycoses 61, 868-876.

Mallone, R., Mannering, S.I., Brooks-Worrell, B.M., Durinovic-Bello, I., Cilio, C.M., Wong, F.S., Schloot, N.C., and T-Cell Workshop Committee, I.o.D.S. (2011). Isolation and preservation of peripheral blood mononuclear cells for analysis of islet antigen-reactive T cell responses: position statement of the T-Cell Workshop Committee of the Immunology of Diabetes Society. Clin Exp Immunol 163, 33-49.

Margalit, A., and Kavanagh, K. (2015). The innate immune response to Aspergillus fumigatus at the alveolar surface. FEMS Microbiol Rev 39, 670-687.

Marr, K.A., Carter, R.A., Boeckh, M., Martin, P., and Corey, L. (2002a). Invasive aspergillosis in allogeneic stem cell transplant recipients: changes in epidemiology and risk factors. Blood 100, 4358-4366.

Marr, K.A., Carter, R.A., Crippa, F., Wald, A., and Corey, L. (2002b). Epidemiology and outcome of mould infections in hematopoietic stem cell transplant recipients. Clin Infect Dis 34, 909-917.

Marr, K.A., Laverdiere, M., Gugel, A., and Leisenring, W. (2005). Antifungal therapy decreases sensitivity of the Aspergillus galactomannan enzyme immunoassay. Clin Infect Dis 40, 1762-1769.

Martiniova, L., Palatis, L., Etchebehere, E., and Ravizzini, G. (2016). Gallium-68 in Medical Imaging. Curr Radiopharm 9, 187-207.

Maschmeyer, G., Haas, A., and Cornely, O.A. (2007). Invasive aspergillosis: epidemiology, diagnosis and management in immunocompromised patients. Drugs 67, 1567-1601.

Matsuda, S., and Koyasu, S. (2000). Mechanisms of action of cyclosporine. Immunopharmacology 47, 119-125.

McKenna, K.C., Beatty, K.M., Vicetti Miguel, R., and Bilonick, R.A. (2009). Delayed processing of blood increases the frequency of activated CD11b+ CD15+ granulocytes which inhibit T cell function. J Immunol Methods 341, 68-75.

Meier, S., Stark, R., Frentsch, M., and Thiel, A. (2008). The influence of different stimulation conditions on the assessment of antigen-induced CD154 expression on CD4+ T cells. Cytometry A 73, 1035-1042.

Meletiadis, J., Antachopoulos, C., Stergiopoulou, T., Pournaras, S., Roilides, E., and Walsh, T.J. (2007). Differential fungicidal activities of amphotericin B and voriconazole against Aspergillus species determined by microbroth methodology. Antimicrob Agents Chemother 51, 3329-3337.

Mellinghoff, S.C., Panse, J., Alakel, N., Behre, G., Buchheidt, D., Christopeit, M., Hasenkamp, J., Kiehl, M., Koldehoff, M., Krause, S.W., et al. (2018). Primary prophylaxis of invasive fungal infections in patients with haematological malignancies: 2017 update of the recommendations of the Infectious Diseases Working Party (AGIHO) of the German Society for Haematology and Medical Oncology (DGHO). Ann Hematol 97, 197-207.

Melotti, P., Nicolis, E., Tamanini, A., Rolfini, R., Pavirani, A., and Cabrini, G. (2001). Activation of NF-kB mediates ICAM-1 induction in respiratory cells exposed to an adenovirus-derived vector. Gene Ther 8, 1436-1442.

Mendell, M.J., Mirer, A.G., Cheung, K., Tong, M., and Douwes, J. (2011). Respiratory and allergic health effects of dampness, mold, and dampness-related agents: a review of the epidemiologic evidence. Environ Health Perspect 119, 748-756.

Mengoli, C., Cruciani, M., Barnes, R.A., Loeffler, J., and Donnelly, J.P. (2009). Use of PCR for diagnosis of invasive aspergillosis: systematic review and meta-analysis. Lancet Infect Dis 9, 89-96.

Merad, M., Sathe, P., Helft, J., Miller, J., and Mortha, A. (2013). The dendritic cell lineage: ontogeny and function of dendritic cells and their subsets in the steady state and the inflamed setting. Annu Rev Immunol 31, 563-604.

Meyer, M.D., and Hausbeck, M.K. (2013). Using Soil-Applied Fungicides to Manage Phytophthora Crown and Root Rot on Summer Squash. Plant Dis 97, 107-112.

Mezger, M., Kneitz, S., Wozniok, I., Kurzai, O., Einsele, H., and Loeffler, J. (2008). Proinflammatory response of immature human dendritic cells is mediated by dectin-1 after exposure to Aspergillus fumigatus germ tubes. J Infect Dis 197, 924-931.

Miller, A.J., and Spence, J.R. (2017). In Vitro Models to Study Human Lung Development, Disease and Homeostasis. Physiology (Bethesda) 32, 246-260.

Miller, S.G., Carnell, L., and Moore, H.H. (1992). Post-Golgi membrane traffic: brefeldin A inhibits export from distal Golgi compartments to the cell surface but not recycling. J Cell Biol 118, 267-283.

Miller-Kittrell, M., and Sparer, T.E. (2009). Feeling manipulated: cytomegalovirus immune manipulation. Virol J 6, 4.

Montagnoli, C., Fallarino, F., Gaziano, R., Bozza, S., Bellocchio, S., Zelante, T., Kurup, W.P., Pitzurra, L., Puccetti, P., and Romani, L. (2006). Immunity and tolerance to Aspergillus involve functionally distinct regulatory T cells and tryptophan catabolism. J Immunol 176, 1712-1723.

Morton, C.O., Fliesser, M., Dittrich, M., Mueller, T., Bauer, R., Kneitz, S., Hope, W., Rogers, T.R., Einsele, H., and Loeffler, J. (2014). Gene expression profiles of human dendritic cells interacting with Aspergillus fumigatus in a bilayer model of the alveolar epithelium/endothelium interface. PLoS One 9, e98279.

Morton, C.O., Varga, J.J., Hornbach, A., Mezger, M., Sennefelder, H., Kneitz, S., Kurzai, O., Krappmann, S., Einsele, H., Nierman, W.C., et al. (2011). The temporal dynamics of differential gene expression in Aspergillus fumigatus interacting with human immature dendritic cells in vitro. PLoS One 6, e16016.

Morton, C.O., Wurster, S., Fliesser, M., Ebel, F., Page, L., Hunniger, K., Kurzai, O., Schmitt, A.L., Michel, D., Springer, J., et al. (2018). Validation of a simplified in vitro Transwell((R)) model of the alveolar surface to assess host immunity induced by different morphotypes of Aspergillus fumigatus. Int J Med Microbiol 308, 1009-1017.

Moss, R.B. (2005). Pathophysiology and immunology of allergic bronchopulmonary aspergillosis. Med Mycol 43 Suppl 1, S203-206.

Muller, U., Stenzel, W., Kohler, G., Werner, C., Polte, T., Hansen, G., Schutze, N., Straubinger, R.K., Blessing, M., McKenzie, A.N., et al. (2007). IL-13 induces disease-promoting type 2 cytokines, alternatively activated macrophages and allergic inflammation during pulmonary infection of mice with Cryptococcus neoformans. J Immunol 179, 5367-5377.

Murdock, B.J., Falkowski, N.R., Shreiner, A.B., Sadighi Akha, A.A., McDonald, R.A., White, E.S., Toews, G.B., and Huffnagle, G.B. (2012). Interleukin-17 drives pulmonary eosinophilia following repeated exposure to Aspergillus fumigatus conidia. Infect Immun 80, 1424-1436.

Nanjappa, S.G., Heninger, E., Wuthrich, M., Sullivan, T., and Klein, B. (2012). Protective antifungal memory CD8(+) T cells are maintained in the absence of CD4(+) T cell help and cognate antigen in mice. J Clin Invest 122, 987-999.

Ndzi, E.N., Nkenfou, C.N., Gwom, L.C., Fainguem, N., Fokam, J., and Pefura, Y. (2016). The pros and cons of the QuantiFERON test for the diagnosis of tuberculosis, prediction of disease progression, and treatment monitoring. Int J Mycobacteriol 5, 177-184.

Neblett Fanfair, R., Benedict, K., Bos, J., Bennett, S.D., Lo, Y.C., Adebanjo, T., Etienne, K., Deak, E., Derado, G., Shieh, W.J., et al. (2012). Necrotizing cutaneous mucormycosis after a tornado in Joplin, Missouri, in 2011. N Engl J Med 367, 2214-2225.

Nielsen, O.L., Afzelius, P., Bender, D., Schonheyder, H.C., Leifsson, P.S., Nielsen, K.M., Larsen, J.O., Jensen, S.B., and Alstrup, A.K. (2015). Comparison of autologous (111)In-leukocytes, (18)F-FDG,

(11)C-methionine, (11)C-PK11195 and (68)Ga-citrate for diagnostic nuclear imaging in a juvenile porcine haematogenous staphylococcus aureus osteomyelitis model. Am J Nucl Med Mol Imaging 5, 169-182.

Nimmo, G.R., Whiting, R.F., and Strong, R.W. (1988). Disseminated mucormycosis due to Cunninghamella bertholletiae in a liver transplant recipient. Postgraduate medical journal 64, 82-84.

Oellerich, M., and DasGupta, A. (2016). Personalized immunosuppression in transplantation : role of biomarker monitoring and therapeutic drug monitoring (Amsterdam ; Boston: Elsevier).

Ok, M., Einsele, H., and Loeffler, J. (2011). Genetic susceptibility to Aspergillus fumigatus infections. Int J Med Microbiol 301, 445-452.

Omar, I.C., and Lee, S.J.P.J.S.T. (1993). Fungal Isolation and the production of its biomass in a palm oil medium. 1, 209-224.

Osherov, N. (2012). Interaction of the pathogenic mold Aspergillus fumigatus with lung epithelial cells. Front Microbiol 3, 346.

Page, I.D., Byanyima, R., Hosmane, S., Onyachi, N., Opira, C., Richardson, M., Sawyer, R., Sharman, A., and Denning, D.W. (2019). Chronic pulmonary aspergillosis commonly complicates treated pulmonary tuberculosis with residual cavitation. Eur Respir J 53.

Page, L., Lauruschkat, C.D., Helm, J., Weis, P., Lazariotou, M., Einsele, H., Ullmann, A.J., Loeffler, J., and Wurster, S. (2020a). Impact of immunosuppressive and antifungal drugs on PBMC- and whole blood-based flow cytometric CD154(+)Aspergillus fumigatus specific T-cell quantification. Med Microbiol Immunol. https://doi.org/10.1007/s00430-020-00665-3

Page L., Ullmann A.J., Schadt F., Einsele H., Wurster S., Samnick S. (2020b). In vitro evaluation of radiolabeled Amphotericin B for molecular imaging of mold infections. Antimicrob Agents Chemother. doi:10.1128/AAC.02377-19

Page, L., Weis, P., Muller, T., Dittrich, M., Lazariotou, M., Dragan, M., Waaga-Gasser, A.M., Helm, J., Dandekar, T., Einsele, H., et al. (2018). Evaluation of Aspergillus and Mucorales specific T-cells and peripheral blood mononuclear cell cytokine signatures as biomarkers of environmental mold exposure. Int J Med Microbiol 308, 1018-1026.

Paiva, J.A., Mergulhao, P., and Pereira, J.M. (2018). Aspergillus and other respiratory fungal infections in the ICU: diagnosis and management. Curr Opin Infect Dis 31, 187-193.

Pant, H., and Macardle, P. (2014). CD8(+) T cells implicated in the pathogenesis of allergic fungal rhinosinusitis. Allergy Rhinol (Providence) 5, 146-156.

Papagiannopoulou, D. (2017). Technetium-99m radiochemistry for pharmaceutical applications. J Labelled Comp Radiopharm 60, 502-520.

Park, S.J., and Mehrad, B. (2009). Innate immunity to Aspergillus species. Clin Microbiol Rev 22, 535-551.

Patel, G., and Greenberger, P.A. (2019). Allergic bronchopulmonary aspergillosis. Allergy Asthma Proc 40, 421-424.

Patil, A., and Majumdar, S. (2017). Echinocandins in antifungal pharmacotherapy. J Pharm Pharmacol 69, 1635-1660.

Patino, J.F., Castro, D., Valencia, A., and Morales, P. (1991). Necrotizing soft tissue lesions after a volcanic cataclysm. World J Surg 15, 240-247.

Patterson, T.F., Thompson, G.R., 3rd, Denning, D.W., Fishman, J.A., Hadley, S., Herbrecht, R., Kontoyiannis, D.P., Marr, K.A., Morrison, V.A., Nguyen, M.H., et al. (2016). Practice Guidelines for the Diagnosis and Management of Aspergillosis: 2016 Update by the Infectious Diseases Society of America. Clin Infect Dis 63, e1-e60.

Petrik, M., Haas, H., Laverman, P., Schrettl, M., Franssen, G.M., Blatzer, M., and Decristoforo, C. (2014). 68Ga-triacetylfusarinine C and 68Ga-ferrioxamine E for Aspergillus infection imaging: uptake specificity in various microorganisms. Mol Imaging Biol 16, 102-108.

Petrikkos, G., Skiada, A., Lortholary, O., Roilides, E., Walsh, T.J., and Kontoyiannis, D.P. (2012). Epidemiology and clinical manifestations of mucormycosis. Clin Infect Dis 54 Suppl 1, S23-34.

Potenza, L., Vallerini, D., Barozzi, P., Riva, G., Forghieri, F., Beauvais, A., Beau, R., Candoni, A., Maertens, J., Rossi, G., et al. (2013). Characterization of specific immune responses to different Aspergillus antigens during the course of invasive Aspergillosis in hematologic patients. PLoS One 8, e74326.

Potenza, L., Vallerini, D., Barozzi, P., Riva, G., Forghieri, F., Zanetti, E., Quadrelli, C., Candoni, A., Maertens, J., Rossi, G., et al. (2011). Mucorales-specific T cells emerge in the course of invasive mucormycosis and may be used as a surrogate diagnostic marker in high-risk patients. Blood 118, 5416-5419.

Potenza, L., Vallerini, D., Barozzi, P., Riva, G., Gilioli, A., Forghieri, F., Candoni, A., Cesaro, S., Quadrelli, C., Maertens, J., et al. (2016). Mucorales-Specific T Cells in Patients with Hematologic Malignancies. PLoS One 11, e0149108.

Prabhu, R.M., and Patel, R. (2004). Mucormycosis and entomophthoramycosis: a review of the clinical manifestations, diagnosis and treatment. Clin Microbiol Infect 10 Suppl 1, 31-47.

Punsmann, S., Liebers, V., Stubel, H., Bruning, T., and Raulf-Heimsoth, M. (2013). Determination of inflammatory responses to Aspergillus versicolor and endotoxin with human cryo-preserved blood as a suitable tool. Int J Hyg Environ Health 216, 402-407.

Quirce, S., Vandenplas, O., Campo, P., Cruz, M.J., de Blay, F., Koschel, D., Moscato, G., Pala, G., Raulf, M., Sastre, J., et al. (2016). Occupational hypersensitivity pneumonitis: an EAACI position paper. Allergy 71, 765-779.

Ratanatharathorn, V., Ayash, L., Lazarus, H.M., Fu, J., and Uberti, J.P. (2001). Chronic graft-versus-host disease: clinical manifestation and therapy. Bone Marrow Transplant 28, 121-129.

Reinwald, M., Hummel, M., Kovalevskaya, E., Spiess, B., Heinz, W.J., Vehreschild, J.J., Schultheis, B., Krause, S.W., Claus, B., Suedhoff, T., et al. (2012). Therapy with antifungals decreases the diagnostic performance of PCR for diagnosing invasive aspergillosis in bronchoalveolar lavage samples of patients with haematological malignancies. J Antimicrob Chemother 67, 2260-2267.

Reyes, A.L., Fernandez, L., Rey, A., and Teran, M. (2014). Development and evaluation of 99mTc-tricarbonyl-caspofungin as potential diagnostic agent of fungal infections. Curr Radiopharm 7, 144-150.

Reyes, E., Cardona, J., Prieto, A., Bernstein, E.D., Rodriguez-Zapata, M., Pontes, M.J., and Alvarez-Mon, M. (2000). Liposomal amphotericin B and amphotericin B-deoxycholate show different immunoregulatory effects on human peripheral blood mononuclear cells. J Infect Dis 181, 2003-2010.

Ribes, J.A., Vanover-Sams, C.L., and Baker, D.J. (2000). Zygomycetes in human disease. Clin Microbiol Rev 13, 236-301.

Richardson, M. (2009). The ecology of the Zygomycetes and its impact on environmental exposure. Clin Microbiol Infect 15 Suppl 5, 2-9.

Rick, E.M., Woolnough, K., Pashley, C.H., and Wardlaw, A.J. (2016). Allergic Fungal Airway Disease. J Investig Allergol Clin Immunol 26, 344-354.

Roden, M.M., Zaoutis, T.E., Buchanan, W.L., Knudsen, T.A., Sarkisova, T.A., Schaufele, R.L., Sein, M., Sein, T., Chiou, C.C., Chu, J.H., et al. (2005). Epidemiology and outcome of zygomycosis: a review of 929 reported cases. Clin Infect Dis 41, 634-653.

Rogers, P.D., Jenkins, J.K., Chapman, S.W., Ndebele, K., Chapman, B.A., and Cleary, J.D. (1998). Amphotericin B activation of human genes encoding for cytokines. J Infect Dis 178, 1726-1733.

Rognon, B., Reboux, G., Roussel, S., Barrera, C., Dalphin, J.C., Fellrath, J.M., Monod, M., and Millon, L. (2015). Western blotting as a tool for the serodiagnosis of farmer's lung disease: validation with Lichtheimia corymbifera protein extracts. J Med Microbiol 64, 359-368.

Roilides, E., Antachopoulos, C., and Simitsopoulou, M. (2014). Pathogenesis and host defence against Mucorales: the role of cytokines and interaction with antifungal drugs. Mycoses 57 Suppl 3, 40-47.

Roilides, E., and Simitsopoulou, M. (2017). Immune responses to Mucorales growth forms: Do we know everything? Virulence 8, 1489-1491.

Rolle, A.M., Hasenberg, M., Thornton, C.R., Solouk-Saran, D., Mann, L., Weski, J., Maurer, A., Fischer, E., Spycher, P.R., Schibli, R., et al. (2016). ImmunoPET/MR imaging allows specific detection of Aspergillus fumigatus lung infection in vivo. Proc Natl Acad Sci U S A 113, E1026-1033.

Romagnani, S. (1991). Type 1 T helper and type 2 T helper cells: functions, regulation and role in protection and disease. Int J Clin Lab Res 21, 152-158.

Romani, L. (2011). Immunity to fungal infections. Nat Rev Immunol 11, 275-288.

Rosenblum Lichtenstein, J.H., Hsu, Y.H., Gavin, I.M., Donaghey, T.C., Molina, R.M., Thompson, K.J., Chi, C.L., Gillis, B.S., and Brain, J.D. (2015). Environmental mold and mycotoxin exposures elicit specific cytokine and chemokine responses. PLoS One 10, e0126926.

Rossi, D., and Zlotnik, A. (2000). The biology of chemokines and their receptors. Annu Rev Immunol 18, 217-242.

Salvenmoser, S., Seidler, M.J., Dalpke, A., and Muller, F.M. (2010). Effects of caspofungin, Candida albicans and Aspergillus fumigatus on toll-like receptor 9 of GM-CSF-stimulated PMNs. FEMS Immunol Med Microbiol 60, 74-77.

Sau, K., Mambula, S.S., Latz, E., Henneke, P., Golenbock, D.T., and Levitz, S.M. (2003). The antifungal drug amphotericin B promotes inflammatory cytokine release by a Toll-like receptor- and CD14-dependent mechanism. J Biol Chem 278, 37561-37568.

Saxena, S., Bhatnagar, P.K., Ghosh, P.C., and Sarma, P.U. (1999). Effect of amphotericin B lipid formulation on immune response in aspergillosis. Int J Pharm 188, 19-30.

Schachtner, T., Stein, M., and Reinke, P. (2017). CMV-Specific T Cell Monitoring Offers Superior Risk Stratification of CMV-Seronegative Kidney Transplant Recipients of a CMV-Seropositive Donor. Transplantation 101, e315-e325.

Schiller, A., Zhang, T., Li, R., Duechting, A., Sundararaman, S., Przybyla, A., Kuerten, S., and Lehmann, P.V. (2017). A Positive Control for Detection of Functional CD4 T Cells in PBMC: The CPI Pool. Cells 6.

Schmidt, S., Tramsen, L., Perkhofer, S., Lass-Florl, C., Roger, F., Schubert, R., and Lehrnbecher, T. (2012). Characterization of the cellular immune responses to Rhizopus oryzae with potential impact on immunotherapeutic strategies in hematopoietic stem cell transplantation. J Infect Dis 206, 135-139.

Schubert, L.A., King, G., Cron, R.Q., Lewis, D.B., Aruffo, A., and Hollenbaugh, D. (1995). The human gp39 promoter. Two distinct nuclear factors of activated T cell protein-binding elements contribute independently to transcriptional activation. J Biol Chem 270, 29624-29627.

Schwarz, C., Hartl, D., Eickmeier, O., Hector, A., Benden, C., Durieu, I., Sole, A., Gartner, S., Milla, C.E., and Barry, P.J. (2018). Progress in Definition, Prevention and Treatment of Fungal Infections in Cystic Fibrosis. Mycopathologia 183, 21-32.

Sellmyer, M.A., Lee, I., Hou, C., Weng, C.C., Li, S., Lieberman, B.P., Zeng, C., Mankoff, D.A., and Mach, R.H. (2017). Bacterial infection imaging with [(18)F]fluoropropyl-trimethoprim. Proc Natl Acad Sci U S A 114, 8372-8377.

Selman, M., Pardo, A., and King, T.E., Jr. (2012). Hypersensitivity pneumonitis: insights in diagnosis and pathobiology. Am J Respir Crit Care Med 186, 314-324.

Sester, U., Wilkens, H., van Bentum, K., Singh, M., Sybrecht, G.W., Schafers, H.J., and Sester, M. (2009). Impaired detection of Mycobacterium tuberculosis immunity in patients using high levels of immunosuppressive drugs. Eur Respir J 34, 702-710.

Shah, M.M., Hsiao, E.I., Kirsch, C.M., Gohil, A., Narasimhan, S., and Stevens, D.A. (2018). Invasive pulmonary aspergillosis and influenza co-infection in immunocompetent hosts: case reports and review of the literature. Diagn Microbiol Infect Dis 91, 147-152.

Sharma, P., Mukherjee, A., Karunanithi, S., Bal, C., and Kumar, R. (2014). Potential role of 18F-FDG PET/CT in patients with fungal infections. AJR Am J Roentgenol 203, 180-189.

Shelton, B.G., Kirkland, K.H., Flanders, W.D., and Morris, G.K. (2002). Profiles of airborne fungi in buildings and outdoor environments in the United States. Appl Environ Microbiol 68, 1743-1753.

Shindo, K., Fukumura, M., and Ito, A. (1998). Inhibitory effect of amphotericin B on leukotriene B4 synthesis in human neutrophils in vitro. Prostaglandins Leukot Essent Fatty Acids 58, 105-109.

Silveira, M.B.V., Ferrarini, M.A.G., Viana, P.O., Succi, R.C., Terreri, M.T., Costa-Carvalho, B., Carlesse, F., and de Moraes-Pinto, M.I. (2018). Contribution of the interferon-gamma release assay to tuberculosis diagnosis in children and adolescents. Int J Tuberc Lung Dis 22, 1172-1178.

Simitsopoulou, M., Roilides, E., Paliogianni, F., Likartsis, C., Ioannidis, J., Kanellou, K., and Walsh, T.J. (2008). Immunomodulatory effects of voriconazole on monocytes challenged with Aspergillus fumigatus: differential role of Toll-like receptors. Antimicrob Agents Chemother 52, 3301-3306.

Simms, E., Kjarsgaard, M., Denis, S., Hargreave, F.E., Nair, P., and Larche, M. (2013). Cytokine responses of peripheral blood mononuclear cells to allergen do not identify asthma or asthma phenotypes. Clin Exp Allergy 43, 1226-1235.

Simonian, P.L., Roark, C.L., Wehrmann, F., Lanham, A.K., Diaz del Valle, F., Born, W.K., O'Brien, R.L., and Fontenot, A.P. (2009). Th17-polarized immune response in a murine model of hypersensitivity pneumonitis and lung fibrosis. J Immunol 182, 657-665.

Skiada, A., Lass-Floerl, C., Klimko, N., Ibrahim, A., Roilides, E., and Petrikkos, G. (2018). Challenges in the diagnosis and treatment of mucormycosis. Med Mycol 56, 93-101.

Slomka, P.J., Pan, T., Berman, D.S., and Germano, G. (2015). Advances in SPECT and PET Hardware. Prog Cardiovasc Dis 57, 566-578.

Spagnolo, P., Rossi, G., Cavazza, A., Bonifazi, M., Paladini, I., Bonella, F., Sverzellati, N., and Costabel, U. (2015). Hypersensitivity Pneumonitis: A Comprehensive Review. J Investig Allergol Clin Immunol 25, 237-250; quiz follow 250.

Springer, J., Goldenberger, D., Schmidt, F., Weisser, M., Wehrle-Wieland, E., Einsele, H., Frei, R., and Loffler, J. (2016a). Development and application of two independent real-time PCR assays to detect clinically relevant Mucorales species. J Med Microbiol 65, 227-234.

Springer, J., Lackner, M., Ensinger, C., Risslegger, B., Morton, C.O., Nachbaur, D., Lass-Florl, C., Einsele, H., Heinz, W.J., and Loeffler, J. (2016b). Clinical evaluation of a Mucorales-specific real-time PCR assay in tissue and serum samples. J Med Microbiol 65, 1414-1421.

Springer, J., and Loffler, J. (2017). Genus- and Species-Specific PCR Detection Methods. Methods Mol Biol 1508, 267-279.

Springer, J., Walther, G., Rickerts, V., Hamprecht, A., Willinger, B., Teschner, D., Einsele, H., Kurzai, O., and Loeffler, J. (2019). Detection of Fusarium Species in Clinical Specimens by Probe-Based Real-Time PCR. J Fungi (Basel) 5.

Steele, C., Rapaka, R.R., Metz, A., Pop, S.M., Williams, D.L., Gordon, S., Kolls, J.K., and Brown, G.D. (2005). The beta-glucan receptor dectin-1 recognizes specific morphologies of Aspergillus fumigatus. PLoS Pathog 1, e42.

Steinbach, A., Cornely, O.A., Wisplinghoff, H., Schauss, A.C., Vehreschild, J.J., Rybniker, J., Hamprecht, A., Richter, A., Bacher, P., Scheffold, A., et al. (2019). Mould-reactive T cells for the diagnosis of invasive mould infection-A prospective study. Mycoses 62, 562-569.

Sterclova, M., Vasakova, M., and Metlicka, M. (2011). Significance of specific IgG against sensitizing antigens in extrinsic allergic alveolitis: serological methods in EAA. Rev Port Pneumol 17, 253-259.

Stone, N.R., Bicanic, T., Salim, R., and Hope, W. (2016). Liposomal Amphotericin B (AmBisome((R))): A Review of the Pharmacokinetics, Pharmacodynamics, Clinical Experience and Future Directions. Drugs 76, 485-500.

Stuehler, C., Nowakowska, J., Bernardini, C., Topp, M.S., Battegay, M., Passweg, J., and Khanna, N. (2015). Multispecific Aspergillus T cells selected by CD137 or CD154 induce protective immune responses against the most relevant mold infections. J Infect Dis 211, 1251-1261.

Sun, W.K., Lu, X., Li, X., Sun, Q.Y., Su, X., Song, Y., Sun, H.M., and Shi, Y. (2012). Dectin-1 is inducible and plays a crucial role in Aspergillus-induced innate immune responses in human bronchial epithelial cells. Eur J Clin Microbiol Infect Dis 31, 2755-2764.

Sunshine, H., and Iruela-Arispe, M.L. (2017). Membrane lipids and cell signaling. Curr Opin Lipidol 28, 408-413.

Taccone, F.S., Van den Abeele, A.M., Bulpa, P., Misset, B., Meersseman, W., Cardoso, T., Paiva, J.A., Blasco-Navalpotro, M., De Laere, E., Dimopoulos, G., et al. (2015). Epidemiology of invasive aspergillosis in critically ill patients: clinical presentation, underlying conditions, and outcomes. Crit Care 19, 7.

Tan, Q., Choi, K.M., Sicard, D., and Tschumperlin, D.J. (2017). Human airway organoid engineering as a step toward lung regeneration and disease modeling. Biomaterials 113, 118-132.

Tang, M., Tian, Y., Li, D., Lv, J., Li, Q., Kuang, C., Hu, P., Wang, Y., Wang, J., Su, K., et al. (2014). TNF-alpha mediated increase of HIF-1alpha inhibits VASP expression, which reduces alveolar-capillary barrier function during acute lung injury (ALI). PLoS One 9, e102967.

Tevyashova, A.N., Olsufyeva, E.N., Solovieva, S.E., Printsevskaya, S.S., Reznikova, M.I., Trenin, A.S., Galatenko, O.A., Treshalin, I.D., Pereverzeva, E.R., Mirchink, E.P., et al. (2013). Structure-antifungal activity relationships of polyene antibiotics of the amphotericin B group. Antimicrob Agents Chemother 57, 3815-3822.

Thakur, A., Riber, U., Davis, W.C., and Jungersen, G. (2013). Increasing the ex vivo antigen-specific IFN-gamma production in subpopulations of T cells and NKp46+ cells by anti-CD28, anti-CD49d and recombinant IL-12 costimulation in cattle vaccinated with recombinant proteins from Mycobacterium avium subspecies paratuberculosis. Vet Immunol Immunopathol 155, 276-283.

Thakur, R., Anand, R., Tiwari, S., Singh, A.P., Tiwary, B.N., and Shankar, J. (2015). Cytokines induce effector T-helper cells during invasive aspergillosis; what we have learned about T-helper cells? Front Microbiol 6, 429.

Thornton, C.R. (2018). Molecular Imaging of Invasive Pulmonary Aspergillosis Using ImmunoPET/MRI: The Future Looks Bright. Front Microbiol 9, 691.

Toniato, E., Frydas, I., Robuffo, I., Ronconi, G., Caraffa, A., Kritas, S.K., and Conti, P. (2017). Activation and inhibition of adaptive immune response mediated by mast cells. J Biol Regul Homeost Agents 31, 543-548.

Tramsen, L., Schmidt, S., Koehl, U., Huenecke, S., Latge, J.P., Roeger, F., Schubert, R., Klingebiel, T., and Lehrnbecher, T. (2013). No effect of antifungal compounds on functional properties of human antifungal T-helper type 1 cells. Transpl Infect Dis 15, 430-434.

Tramsen, L., Schmidt, S., Roeger, F., Schubert, R., Salzmann-Manrique, E., Latge, J.P., Klingebiel, T., and Lehrnbecher, T. (2014). Immunosuppressive compounds exhibit particular effects on functional properties of human anti-Aspergillus Th1 cells. Infect Immun 82, 2649-2656.

Tsiavou, A., Degiannis, D., Hatziagelaki, E., Koniavitou, K., and Raptis, S. (2002). Flow cytometric detection of intracellular IL-12 release: in vitro effect of widely used immunosuppressants. Int Immunopharmacol 2, 1713-1720.

Twaroch, T.E., Curin, M., Valenta, R., and Swoboda, I. (2015). Mold allergens in respiratory allergy: from structure to therapy. Allergy Asthma Immunol Res 7, 205-220.

Udagawa, T., Woodside, D.G., and McIntyre, B.W. (1996). Alpha 4 beta 1 (CD49d/CD29) integrin costimulation of human T cells enhances transcription factor and cytokine induction in the absence of altered sensitivity to anti-CD3 stimulation. J Immunol 157, 1965-1972.

Ullmann, A.J., Aguado, J.M., Arikan-Akdagli, S., Denning, D.W., Groll, A.H., Lagrou, K., Lass-Florl, C., Lewis, R.E., Munoz, P., Verweij, P.E., et al. (2018). Diagnosis and management of Aspergillus diseases: executive summary of the 2017 ESCMID-ECMM-ERS guideline. Clin Microbiol Infect 24 Suppl 1, e1-e38.

van de Sande, W.W., Tavakol, M., van Vianen, W., and Bakker-Woudenberg, I.A. (2010). The effects of antifungal agents to conidial and hyphal forms of Aspergillus fumigatus. Med Mycol 48, 48-55.

Van Epps, H.L., Feldmesser, M., and Pamer, E.G. (2003). Voriconazole inhibits fungal growth without impairing antigen presentation or T-cell activation. Antimicrob Agents Chemother 47, 1818-1823.

Vanderbeke, L., Spriet, I., Breynaert, C., Rijnders, B.J.A., Verweij, P.E., and Wauters, J. (2018). Invasive pulmonary aspergillosis complicating severe influenza: epidemiology, diagnosis and treatment. Curr Opin Infect Dis 31, 471-480.

Vandevyver, S., Dejager, L., Tuckermann, J., and Libert, C. (2013). New insights into the anti-inflammatory mechanisms of glucocorticoids: an emerging role for glucocorticoid-receptor-mediated transactivation. Endocrinology 154, 993-1007.

Verhoeff, A.P., and Burge, H.A. (1997). Health risk assessment of fungi in home environments. Ann Allergy Asthma Immunol 78, 544-554; quiz 555-546.

Vignali, D.A., Collison, L.W., and Workman, C.J. (2008). How regulatory T cells work. Nat Rev Immunol 8, 523-532.

Villar, A., Munoz, X., Sanchez-Vidaurre, S., Gomez-Olles, S., Morell, F., and Cruz, M.J. (2014). Bronchial inflammation in hypersensitivity pneumonitis after antigen-specific inhalation challenge. Respirology 19, 891-899.

Waldrop, S.L., Davis, K.A., Maino, V.C., and Picker, L.J. (1998). Normal human CD4+ memory T cells display broad heterogeneity in their activation threshold for cytokine synthesis. J Immunol 161, 5284-5295.

Walsh, T.J., Groll, A., Hiemenz, J., Fleming, R., Roilides, E., and Anaissie, E. (2004). Infections due to emerging and uncommon medically important fungal pathogens. Clin Microbiol Infect 10 Suppl 1, 48-66.

Wang, Y., Chen, L., Liu, X., Cheng, D., Liu, G., Liu, Y., Dou, S., Hnatowich, D.J., and Rusckowski, M. (2013). Detection of Aspergillus fumigatus pulmonary fungal infections in mice with (99m)Tc-labeled MORF oligomers targeting ribosomal RNA. Nucl Med Biol 40, 89-96.

Warris, A., Netea, M.G., Verweij, P.E., Gaustad, P., Kullberg, B.J., Weemaes, C.M., and Abrahamsen, T.G. (2005). Cytokine responses and regulation of interferon-gamma release by human mononuclear cells to Aspergillus fumigatus and other filamentous fungi. Med Mycol 43, 613-621.

Wasylnka, J.A., Hissen, A.H., Wan, A.N., and Moore, M.M. (2005). Intracellular and extracellular growth of Aspergillus fumigatus. Med Mycol 43 Suppl 1, S27-30.

Wasylnka, J.A., and Moore, M.M. (2000). Adhesion of Aspergillus species to extracellular matrix proteins: evidence for involvement of negatively charged carbohydrates on the conidial surface. Infect Immun 68, 3377-3384.

Watkins, T.N., Gebremariam, T., Swidergall, M., Shetty, A.C., Graf, K.T., Alqarihi, A., Alkhazraji, S., Alsaadi, A.I., Edwards, V.L., Filler, S.G., et al. (2018). Inhibition of EGFR Signaling Protects from Mucormycosis. MBio 9.

Wauters, J., Baar, I., Meersseman, P., Meersseman, W., Dams, K., De Paep, R., Lagrou, K., Wilmer, A., Jorens, P., and Hermans, G. (2012). Invasive pulmonary aspergillosis is a frequent complication of critically ill H1N1 patients: a retrospective study. Intensive Care Med 38, 1761-1768.

Weber, J., Illi, S., Nowak, D., Schierl, R., Holst, O., von Mutius, E., and Ege, M.J. (2015). Asthma and the hygiene hypothesis. Does cleanliness matter? Am J Respir Crit Care Med 191, 522-529.

Weis, P., Helm, J., Page, L., Lauruschkat, C.D., Lazariotou, M., Einsele, H., Loeffler, J., Ullmann, A.J., and Wurster, S. (2019). Development and evaluation of a whole blood-based approach for flow cytometric quantification of CD154+ mould-reactive T cells. Med Mycol.

Werner, J.L., Metz, A.E., Horn, D., Schoeb, T.R., Hewitt, M.M., Schwiebert, L.M., Faro-Trindade, I., Brown, G.D., and Steele, C. (2009). Requisite role for the dectin-1 beta-glucan receptor in pulmonary defense against Aspergillus fumigatus. J Immunol 182, 4938-4946.

Wilkinson, D.C., Alva-Ornelas, J.A., Sucre, J.M., Vijayaraj, P., Durra, A., Richardson, W., Jonas, S.J., Paul, M.K., Karumbayaram, S., Dunn, B., et al. (2017). Development of a Three-Dimensional Bioengineering Technology to Generate Lung Tissue for Personalized Disease Modeling. Stem Cells Transl Med 6, 622-633.

Woolnough, K., Fairs, A., Pashley, C.H., and Wardlaw, A.J. (2015). Allergic fungal airway disease: pathophysiologic and diagnostic considerations. Curr Opin Pulm Med 21, 39-47.

Worthley, D.L., Bardy, P.G., and Mullighan, C.G. (2005). Mannose-binding lectin: biology and clinical implications. Intern Med J 35, 548-555.

Wurster, S., Thielen, V., Weis, P., Walther, P., Elias, J., Waaga-Gasser, A.M., Dragan, M., Dandekar, T., Einsele, H., Loffler, J., et al. (2017a). Mucorales spores induce a proinflammatory cytokine response in human mononuclear phagocytes and harbor no rodlet hydrophobins. Virulence 8, 1708-1718.

Wurster, S., Weis, P., Page, L., Helm, J., Lazariotou, M., Einsele, H., and Ullmann, A.J. (2017b). Intra- and inter-individual variability of Aspergillus fumigatus reactive T-cell frequencies in healthy volunteers in dependency of mould exposure in residential and working environment. Mycoses 60, 668-675.

Wurster, S., Weis, P., Page, L., Lazariotou, M., Einsele, H., and Ullmann, A.J. (2017c). Quantification of A. fumigatus-specific CD154+ T-cells-preanalytic considerations. Med Mycol 55, 223-227.

Wuthrich, M., Filutowicz, H.I., Warner, T., Deepe, G.S., Jr., and Klein, B.S. (2003). Vaccine immunity to pathogenic fungi overcomes the requirement for CD4 help in exogenous antigen presentation to CD8+ T cells: implications for vaccine development in immune-deficient hosts. J Exp Med 197, 1405-1416.

Yamamoto, N., Shendell, D.G., and Peccia, J. (2011). Assessing allergenic fungi in house dust by floor wipe sampling and quantitative PCR. Indoor Air 21, 521-530.

Yong, M.K., Slavin, M.A., and Kontoyiannis, D.P. (2018). Invasive fungal disease and cytomegalovirus infection: is there an association? Curr Opin Infect Dis 31, 481-489.

Zawrotniak, M., and Rapala-Kozik, M. (2013). Neutrophil extracellular traps (NETs) - formation and implications. Acta Biochim Pol 60, 277-284.

Zelante, T., De Luca, A., Bonifazi, P., Montagnoli, C., Bozza, S., Moretti, S., Belladonna, M.L., Vacca, C., Conte, C., Mosci, P., et al. (2007). IL-23 and the Th17 pathway promote inflammation and impair antifungal immune resistance. Eur J Immunol 37, 2695-2706.

Zhang, S., Zhang, W., Wang, Y., Jin, Z., Wang, X., Zhang, J., and Zhang, Y. (2011). Synthesis and biodistribution of a novel ((9)(9)m)TcN complex of norfloxacin dithiocarbamate as a potential agent for bacterial infection imaging. Bioconjug Chem 22, 369-375.

Zhang, Z., Liu, R., Noordhoek, J.A., and Kauffman, H.F. (2005). Interaction of airway epithelial cells (A549) with spores and mycelium of Aspergillus fumigatus. J Infect 51, 375-382.

Zielinska-Jankiewicz, K., Kozajda, A., Piotrowska, M., and Szadkowska-Stanczyk, I. (2008). Microbiological contamination with moulds in work environment in libraries and archive storage facilities. Ann Agric Environ Med 15, 71-78.

Zielinski, C.E., Mele, F., Aschenbrenner, D., Jarrossay, D., Ronchi, F., Gattorno, M., Monticelli, S., Lanzavecchia, A., and Sallusto, F. (2012). Pathogen-induced human TH17 cells produce IFN-gamma or IL-10 and are regulated by IL-1beta. Nature 484, 514-518.

Konferenzbeiträge

Page, L., Wurster, S., Weis, P., Helm, J., Lazariotou, M., Einsele, H., Ullmann, A.J. (2017). Evaluation of a whole blood based approach for the determination of mould reactive T-cell quantification and its susceptibility to pre-analytic delays. 8th Trends in Medical Mycology, Belgrad, Serbien

Wurster, S., Morton, C.O., Page, L., Belic, S., Dragan, M., Loeffler, J. (2018). Alveolar immunopathology of Aspergillus and Mucorales compared in a highly reproducible transwell model. PEG Frühjahrstagung Sektion antimykotische Therapie, Bonn, Deutschland

Wurster, S., Page, L., Weis, P., Lazariotou, M., Einsele, H., Ullmann, A.J. (2017). Environmental mould exposure leads to elevated Mucorales specific T-helper and T-memory cell frequencies in healthy adults. 27th European Congress of Clinical Microbiology and Infectious Diseases, Wien, Österreich

Wurster, S., Weis, P., Helm, J., Page, L., Lazariotou, M., Einsele, H., Löffler, J., Ullmann, A.J. (2016). Agitation und Verdünnung von Blutproben mit RPMI-Medium verlängern das präanalytische Fenster bei der Quantifizierung Antigen-spezifischer T-Zellen über den Marker CD154. 13. Kongress für Infektionskrankheiten und Tropenmedizin, Würzburg, Deutschland

Internetquellen

EUCAST DEFINITIVE DOCUMENT E.DEF 9.3.1 Method for the determination of broth dilution minimum inhibitory concentrations of antifungal agents for conidia forming moulds:

https://www.eucast.org/fileadmin/src/media/PDFs/EUCAST_files/AFST/Files/EUCAST_E_Def_9.3.2_Mould_testing_definitive_revised_2020.pdf

(Aufrufdatum 24.04.2020)

P Value from Pearson (R) Calculator:

http://www.socscistatistics.com/pvalues/pearsondistribution.aspx

(Aufrufdatum: 19.11.2019)

T-Cell Xtend®:

http://www.oxfordimmunotec.com/international/products-services/t-cell-xtend/

(Aufrufdatum: 15.10.2019)

Wilcoxon-Mann-Whitney Test Calculator:

https://ccb-compute2.cs.uni-saarland.de/wtest/?id=www/www-ccb/html/software/wtest/

(Aufrufdatum: 19.11.2019)

7. ANHANG

7.1 Abkürzungsverzeichnis

7-AAD	7-Amino-Actinomycin D
A. fumigatus	*Aspergillus fumigatus*
A. niger	*Aspergillus niger*
A. terreus	*Aspergillus terreus*
Abb.	Abbildung
ABPA	Allergische broncho-pulmonale Aspergillose
Acc	Beschleunigung
Af	*Aspergillus fumigatus*
Afu	*Aspergillus fumigatus*
Alas1	δ-Aminolävulinatsynthase
AM	Alveolarmakrophage
AMB	Amphotericin B
AMP	Antimikrobielle Peptide
ANOVA	*Analysis of Variance*
APC	Allophycocyanin
APC	Antigenpräsentierende Zelle
Aspf	*Aspergillus fumigatus*-Allergen
ATCC	*American Type Culture Collection*
BAL	Bronchoalveoläre Lavage
BHB	Beta-Hydroxybutansäure
BrA	Brefeldin A
BSA	Bovines Serumalbumin
C	Kohlenstoff
C. albicans	*Candida albicans*
C. bertholletiae	*Cunninghamella bertholletiae*
Cas	CRISPR-assoziiertes Protein
CatB	Katalase B
Cbe	*Cunninghamella bertholletiae*
CBS	*Central Bureau of Fungal Cultures*
CCL	CC-Chemokin-Ligand

CCR	CC-Chemokin-Rezeptor
CD	*Cluster of Differentiation*
CD40L	CD40-Ligand
cDNA	Komplementäre Desoxyribonukleinsäure
CF	Zystische Fibrose
CI	Konfidenzintervall
cm	Zentimeter
CMV	Cytomegalievirus
Crf	*Chitin Ring Formation*
CO_2	Kohlenstoffdioxid
Con	Konidien
COPD	Chronisch-obstruktive Lungenerkrankung
CPA	Chronische pulmonale Aspergillose
CPI	Cytomegalie-/Parainfluenza-/Influenzavirus Positivkontrolllösung
CsA	Ciclosporin A
CT	Computertomografie
Ct	*Cycle threshold*
CTLA	Zytotoxisches T-Lymphozyten-Antigen
Ctrl	Kontrolle
CV	Variationskoeffizient
D	Donor
DC	Dendritische Zelle
Dec	Bremse
dH_2O	Destilliertes Wasser
DMSO	Dimethylsulfoxid
DNA	Desoxyribonukleinsäure
dNTP	Desoxyribonukleotidphosphat
EBM	*Endothelial Growth Basal Medium*
EC	Epithelzelle
EDTA	Ethylendiamintetraessigsäure
EGFR	*Epidermal Growth Factor Receptor*
EGM	*Endothelial Growth Medium*
ELISA	*Enzyme Linked Immunosorbent Assay*
ELISPOT	*Enzyme Linked Immuno Spot Assay*

EtOH	Ethanol
EU	*European Unit*
EUCAST	*European Committee on Antimicrobial Susceptibility Testing*
F	Fluor
f	Frequenz
F. solani	*Fusarium solani*
FACS	*Fluorescence Activated Cell Sorting*
F_c	Kristallisierbares Fragment
FCS	Fötales Kälberserum
FDG	Fluorodesoxyglucose
FITC	Fluorescein-Isothiocyanat
FOXE	Ferrioxamin E
FSC	*Forward Scatter*
fv	*Forward*
G	*Gauge*
g	Gravitationskraft
GA	Gentamicin-Amphotericin B-Lösung
Ga	Gallium
$GaCl_3$	Galliumtrichlorid
Ge	Germanium
Gef	Gefitinib
Glc	D-(+)-Glucose
GM-CSF	Granulozyten-Monozyten-Kolonie-stimulierender Faktor
GvHD	*Graft versus Host Disease*
H	Hoch exponiert
h	Stunde
HBSS	*Hank's Buffered Salt Solution*
$HBSS^{++}$	HBSS + 1 % FCS + 0,4 % EDTA
HCl	Salzsäure
HIV	Humanes Immundefizienzvirus
HLA	Humanes Leukozyten-Antigen
HPAEC	*Human Pulmonary Artery Endothelial Cells*
HPLC	Hochleistungsflüssigchromatografie
HSZT	Hämatopoietische Stammzelltransplantation

Hyph	Hyphen
ICAM	Interzelluläres Adhäsionsmolekül
IE	*Immediate Early*-Protein
IFN	Interferon
Ig	Immunglobulin
IHM	Institut für Hygiene und Mikrobiologie Würzburg
IL	Interleukin
IM	Invasive Mykose
IPMI	Invasiv-pulmonale Schimmelpilzinfektion
ITS	*Internal Transcribed Spacer*
Kap.	Kapitel
kDa	Kilodalton
km	Kilometer
Konz.	Konzentration
L	Gering exponiert
LAMB	Liposomales Amphotericin B
LDH	Lactatdehydrogenase
Lu	Lutetium
LZRS	Leukozytenreduktionssystem
M	Molar
M. circinelloides	*Mucor circinelloides*
MACS	*Magnetic Activated Cell Sorting*
MBq	Megabecquerel
MeCN	Acetonitril
Med	Mediumkontrolle
mg	Milligramm
MHC	Haupthistokompatibilitätskomplex
min	Minute
ml	Milliliter
mm	Millimeter
MMF	Mycophenolat Mofetil
Mo	Molybdän
moDC	*Monocyte-derived Dendritic Cell*
MORF	Phosphorodiamidat-Morpholino

mRNA	*Messenger*-Ribonukleinsäure
N	Normal
n	Anzahl
n/a	Nicht verfügbar
Na	Natrium
NaCl	Natriumchlorid
NF-AT	*Nuclear Factor of Activated T cells*
NF-κB	*Nuclear Factor κB*
ng	Nanogramm
NH_4	Ammonium
NK	Natürliche Killerzelle
nm	Nanometer
nMol	Nanomol
ns	Nicht significant
p	*Probability Value*
p-Wert	*Probability Value*
PAMP	*Pathogen Associated Molecular Pattern*
PBMC	*Peripheral Blood Mononuclear Cells*
PBS	*Phosphate Buffered Saline*
PCR	Polymerase-Kettenreaktion
PCZ	Posaconazol
PE	Phycoerythrin
PerCP	Peridinin-Chlorophyll-Protein
PET	Positronenemissionstomografie
pg	Pikogramm
PHA	Phytohemagglutinin
PMN	Polymorphkernige Leukozyten
pp	Phosphoprotein
Pred	Prednisolon
PRR	*Pattern Recognition Receptor*
qPCR	Quantitative Echtzeit-Polymerase-Kettenreaktion
r	Korrelationskoeffizient
R. arrhizus	*Rhizopus arrhizus*
R. pusillus	*Rhizomucor pusillus*

Ra	*Rhizopus arrhizus*
Rar	*Rhizopus arrhizus*
RANTES	*Regulated And Normal T cell Expressed and Secreted*
RF	Risikofaktor
Rmp	*Rhizomucor pusillus*
RNA	Ribonukleinsäure
rpm	Umdrehungen pro Minute
RPMI	*Roswell Park Memorial Institute*-Medium
RT	Reverse Transkriptase / Reverse Transkription
rv	*Reverse*
S. aureus	*Staphylococcus aureus*
SA	Standardabweichung
Sau	*Staphylococcus aureus*
SD	Standardabweichung
sec	Sekunde
spp.	Spezies
Sn	Zinn
$SnCl_2$	Zinndichlorid
Sp	Sporen
SPECT	Einzelphotonenemissionscomputertomografie
SSC	*Side Scatter*
Tab.	Tabelle
TAFC	Triacetylfusarinin C
Tc	Technetium
TCR	T-Zell-Rezeptor
TFA	Trifluoressigsäure
TGF	*Transforming Growth Factor*
T_H	T-Helfer-Zelle
Th	T-Helfer-Zelle
TLC	Dünnschichtchromatografie
TLR	*Toll-like*-Rezeptor
T_{Reg}	Regulatorische T-Zelle
TNF	Tumornekrosefaktor
U	*Unit*

uns	unstimuliert
VCAM	*Vascular Cell Adhesion Molecule*
VCZ	Voriconazol
VLA	*Very Late Antigen*
WB	Vollblut
α	Anti
µg	Mikrogramm
µl	Mikroliter
µM	Mikromolar
µm	Mikrometer
°C	Grad Celsius

7.2 Beiträge der Autoren

“Dissertation Based on Several Published Manuscripts“

Statement of individual author contributions and of legal second publication rights

(If required please use more than one sheet)

Publication (complete reference): Page L, Weis P, Müller T, Dittrich M, Lazariotou M, Dragan M, Waaga-Gasser AM, Helm J, Dandekar T, Einsele H, Löffler J, Ullmann AJ, Wurster S. Evaluation of Aspergillus and Mucorales specific T-cells and peripheral blood mononuclear cell cytokine signatures as biomarkers of environmental mold exposure, International Journal of Medical Microbiology, 2018, ISSN 1438-4221, https://doi.org/10.1016/j.ijmm.2018.09.002.

Participated in	**Author Initials,** Responsibility decreasing from left to right				
Study Design Methods Development	WS, PL	WP	UAJ	LJ	EH
Data Collection	PL	WS	WP, LM	DrM	HJ
Data Analysis and Interpretation	WS	PL	MT, DiM	DT, WP	UAJ, WGAM
Manuscript Writing					
Writing of Introduction	PL	WS			
Writing of Materials & Methods	PL	WS	DT	MT	DiM
Writing of Discussion	PL	WS			
Writing of First Draft	PL	WS			

Explanations (if applicable): The results shown in figures 1, 2, and 3 have been previously used in the Master thesis of PL (M.Sc. Biochemistry, Wuerzburg, 2016).

Publication (complete reference): Belic S*, Page L*, Lazariotou M, Waaga-Gasser AM, Dragan M, Springer J, Loeffler J, Morton CO, Einsele H, Ullmann AJ, Wurster S. Comparative analysis of inflammatory cytokine release and alveolar epithelial barrier invasion in a Transwell® bilayer model of mucormycosis. Frontiers in Microbiology, 2018, 9: 3204. doi: 10.3389/fmicb.2018.03204

Participated in	**Author Initials,** Responsibility decreasing from left to right				
Study Design Methods Development	WS, BS, PL	UAJ	LJ, LM	MCO	EH
Data Collection	PL, BS	WS	LM	DrM	SJ
Data Analysis and Interpretation	WS	PL, BS	UAJ, WGAM	LJ	MCO
Manuscript Writing					
Writing of Introduction	PL	BS	WS		
Writing of Materials & Methods	PL	BS	WS	SJ	
Writing of Discussion	WS	PL	BS	MCO	
Writing of First Draft	WS	PL	BS		

Explanations (if applicable): *contributed equally

The results shown in figures 2AB, 3, 4, and 5, as well as table 1, will be used in the monografic dissertation of BS (Dr. med., in preparation).

Publication (complete reference): Page L, Lauruschkat CD, Helm J, Weis P, Lazariotou M, Einsele H, Ullmann AJ, Loeffler J, Wurster S. Impact of immunosuppressive and antifungal drugs on PBMC- and whole blood-based flow cytometric CD154+ Aspergillus fumigatus specific T-cell quantification. Medical Microbiology and Immunology. https://doi.org/10.1007/s00430-020-00665-3					
Participated in	**Author Initials,** Responsibility decreasing from left to right				
Study Design Methods Development	WS	PL, WP	UAJ, HJ, LCD	LJ	EH
Data Collection	PL	HJ, LCD	WP	LM	WS
Data Analysis and Interpretation	PL	WS	HJ, LCD	WP	LJ, UAJ
Manuscript Writing Writing of Introduction Writing of Materials & Methods Writing of Discussion Writing of First Draft	 PL PL WS WS	 WS WP PL PL	 WS LCD WP		

Explanations (if applicable): The results shown in figure 2, as well as tables 3 and 4, have been previously used in the monografic dissertation of HJ (Dr. med., submitted).

Publication (complete reference): Page L, Ullmann AJ, Schadt F, Wurster S*, Samnick S*. In vitro evaluation of radiolabeled Amphotericin B for molecular imaging of mold infections. Antimicrobial Agents and Chemotherapy. doi:10.1128/AAC.02377-19					
Participated in	**Author Initials,** Responsibility decreasing from left to right				
Study Design Methods Development	WS	PL	UAJ	SaS	
Data Collection	PL	WS	SaS	SF	
Data Analysis and Interpretation	PL	WS	SaS	UAJ	SF
Manuscript Writing Writing of Introduction Writing of Materials & Methods Writing of Discussion Writing of First Draft	 PL PL WS PL	 WS SaS PL	 WS		

Explanations (if applicable): *contributed equally

The doctoral researcher confirms that she/he has obtained permission from both the publishers and the co-authors for legal second publication.

The doctoral researcher and the primary supervisor confirm the correctness of the above mentioned assessment.

Lukas Page

_____

Doctoral Researcher's Name Date Place Signature

Prof. Andrew J. Ullmann

_____

Primary Supervisor's Name Date Place Signature

“Dissertation Based on Several Published Manuscripts“

Statement of individual author contributions to figures/tables/chapters included in the manuscripts

(If required please use more than one sheet)

Publication (complete reference): Page L, Weis P, Müller T, Dittrich M, Lazariotou M, Dragan M, Waaga-Gasser AM, Helm J, Dandekar T, Einsele H, Löffler J, Ullmann AJ, Wurster S. Evaluation of Aspergillus and Mucorales specific T-cells and peripheral blood mononuclear cell cytokine signatures as biomarkers of environmental mold exposure, International Journal of Medical Microbiology, 2018, ISSN 1438-4221, https://doi.org/10.1016/j.ijmm.2018.09.002.

Figure	**Author Initials,** Responsibility decreasing from left to right				
1	PL	WP	WS	LM	HJ
2	PL	WP	WS	LM	HJ
3	PL	WP	WS	LM	HJ
4	PL	WS	LM		
5	WS	PL	LM		
6	PL	WS	WP	DrM	WGAM
7	WS, PL	WP, DrM	MT, DiM	WGAM, DT	ML
S1	WS	PL			
S2	WS	PL			
Table	**Author Initials,** Responsibility decreasing from left to right				
1	PL	WS	WP		
S1	PL	WS			
S2	PL	WS	LM		
S3	PL	WS	LM		
S4	WS	DrM	WGAM	PL	LM

Explanations (if applicable): The results shown in figures 1, 2, and 3 have been previously used in the Master thesis of PL (M.Sc. Biochemistry, Wuerzburg, 2016).

Publication (complete reference): Belic S*, Page L*, Lazariotou M, Waaga-Gasser AM, Dragan M, Springer J, Loeffler J, Morton CO, Einsele H, Ullmann AJ, Wurster S. Comparative analysis of inflammatory cytokine release and alveolar epithelial barrier invasion in a Transwell® bilayer model of mucormycosis. Frontiers in Microbiology, 2018, 9: 3204. doi: 10.3389/fmicb.2018.03204

Figure	**Author Initials,** Responsibility decreasing from left to right				
1	BS	WS			
2	PL	BS	JS	WS	LM
3	BS	WS	LM	WGAM	DrM
4	BS	WS	PL	LM	
5	BS	WS	PL	LM	
6	WS	PL			
7	WS	PL			
S1	PL	WS			
S2	PL	WS			
S3	PL	WS			
Table	**Author Initials,** Responsibility decreasing from left to right				
1	BS	WS	WGAM	DrM	LM

Explanations (if applicable): *contributed equally

The results shown in figures 2AB, 3, 4, and 5, as well as table 1, will be used in the monographic dissertation of BS (Dr. med., in preparation).

Publication (complete reference): Page L, Lauruschkat CD, Helm J, Weis P, Lazariotou M, Einsele H, Ullmann AJ, Loeffler J, Wurster S. Impact of immunosuppressive and antifungal drugs on PBMC- and whole blood-based flow cytometric CD154+ Aspergillus fumigatus specific T-cell quantification. Medical Microbiology and Immunology. https://doi.org/10.1007/s00430-020-00665-3

Figure	**Author Initials,** Responsibility decreasing from left to right				
1	PL	WS	LM	WP	
2	HJ	WS	PL	WP	LM
3	PL	LCD	WS		
4	PL	LCD	WS		
Table	**Author Initials,** Responsibility decreasing from left to right				
1	PL	WS	LM	WP	
2	PL	WS	LM	WP	
3	HJ	WS	WP	LM	PL
4	HJ	WS	PL	WP	LM
A1	PL	WS			
A2	PL	LCD	WS		
A3	WS				

Explanations (if applicable): The results shown in figure 2, as well as tables 3 and 4, have been previously used in the monographic dissertation of HJ (Dr. med., submitted).

Publication (complete reference): Page L, Ullmann AJ, Schadt F, Wurster S*, Samnick S*. In vitro evaluation of radiolabeled Amphotericin B for molecular imaging of mold infections. Antimicrobial Agents and Chemotherapy. doi:10.1128/AAC.02377-19

Figure	**Author Initials,** Responsibility decreasing from left to right				
1	WS	PL			
2	SaS				
3	PL	WS	SaS	SF	
4	PL	SaS	WS		
5	PL	SaS	WS	SF	
S1	PL	SaS	WS		
Table	**Author Initials,** Responsibility decreasing from left to right				
S1	PL	WS			

Explanations (if applicable): *contributed equally

I also confirm my primary supervisor's acceptance.

Lukas Page

_____

Doctoral Researcher's Name Date Place Signature

7.3 Lebenslauf

Der Lebenslauf wurde aus Gründen des Datenschutzes entfernt.

7.4 Publikationsverzeichnis

Originalarbeiten

Belic S, Page L, Lazariotou M, Waaga-Gasser AM, Dragan M, Springer J, Loeffler J, Morton CO, Einsele H, Ullmann AJ, Wurster S (2019). "Comparative Analysis of Inflammatory Cytokine Release and Alveolar Epithelial Barrier Invasion in a Transwell® Bilayer Model of Mucormycosis." Front Microbiol. **9**:3204.

Lauruschkat CD, Wurster S, Page L, Lazariotou M, Dragan M, Weis P, Ullmann AJ, Einsele H, Löffler J (2018). "Susceptibility of A. fumigatus specific T-cell assays to pre-analytic blood storage and PBMC cryopreservation greatly depends on readout platform and analytes." Mycoses. **61**(8):549-560.

Morton CO, Wurster S, Fliesser M, Ebel F, Page L, Hünniger K, Kurzai O, Schmitt AL, Michel D, Springer J, Einsele H, Loeffler J (2018). "Validation of a simplified in vitro Transwell® model of the alveolar surface to assess host immunity induced by different morphotypes of Aspergillus fumigatus." Int J Med Microbiol. **308**(8):1009-1017.

Page L, Lauruschkat CD, Helm J, Weis P, Lazariotou M, Einsele H, Ullmann AJ, Loeffler J, Wurster S (2020). "Impact of immunosuppressive and antifungal drugs on PBMC- and whole blood-based flow cytometric CD154+ Aspergillus fumigatus specific T-cell quantification" Med Microbiol Immunol. https://doi.org/10.1007/s00430-020-00665-3.

Page L, Ullmann AJ, Schadt F, Einsele H, Wurster S, Samnick S (2020). "In vitro evaluation of radiolabeled Amphotericin B for molecular imaging of mold infections." Antimicrob Agents Chemother. doi:10.1128/AAC.02377-19

Page L, Weis P, Müller T, Dittrich M, Lazariotou M, Dragan M, Waaga-Gasser AM, Helm J, Dandekar T, Einsele H, Löffler J, Ullmann AJ, Wurster S (2018). "Evaluation of Aspergillus and Mucorales specific T-cells and peripheral blood mononuclear cell cytokine signatures as biomarkers of environmental mold exposure." Int J Med Microbiol. **308**(8):1018-1026.

Seelbinder B, Wallstabe J, Marischen L, Weiss E, Wurster S, Page L, Löffler C, Bussemer L, Schmitt AL, Wolf T, Linde J, Cicin-Sain L, Becker J, Kalinke U, Vogel J,

Panagiotou G, Einsele H, Westermann A, Schäuble S, Loeffler J (2020). "A triple RNA-seq analysis reveals synergy in a human virus-fungus co-infection model." Cell Rep. (eingereicht Februar 2020, in Begutachtung seit April 2020)

Weis P, Helm J, Page L, Lauruschkat CD, Lazariotou M, Einsele H, Loeffler J, Ullmann AJ, Wurster S (2019). "Development and evaluation of a whole blood-based approach for flow cytometric quantification of CD154+ mould-reactive T cells." Med Mycol. **58**(2): 187-196.

Wurster S, Weis P, Page L, Helm J, Lazariotou M, Einsele H, Ullmann AJ (2017). "Intra- and inter-individual variability of Aspergillus fumigatus reactive T-cell frequencies in healthy volunteers in dependency of mould exposure in residential and working environment." Mycoses. **60**(10): 668-675.

Wurster S, Weis P, Page L, Lazariotou M, Einsele H, Ullmann AJ (2017). "Quantification of A. fumigatus-specific CD154+ T-cells-preanalytic considerations." Med Mycol. **55**(2): 223-227.

Konferenzbeiträge

Lauruschkat CD, Page L, Lazariotou M, Dragan M, Ullmann AJ, Einsele H, Löffler J, Wurster S (2018). "Optimal PBMC cryopreservation protocols for A. fumigatus specific T-cell quantification depend on downstream assay and analytes." 28th European Congress of Clinical Microbiology and Infectious Diseases, Madrid, Spanien

Page L, Ullmann AJ, Schadt F, Wurster S, Samnick S (2020). "Tc-99m-Amphotericin B zur Detektion pulmonaler Schimmelpilz-Infektionen: Evaluation anhand eines in vitro Transwell-Modells." 58. Jahrestagung der deutschen Gesellschaft für Nuklearmedizin, digital

Page L, Wurster S, Schadt F, Einsele H, Ullmann AJ, Samnick S (2019). "Evaluation of 99mTc-Amphotericin B for nuclear imaging of mould infections in a transwell in vitro system." 9th Trends in Medical Mycology, Nizza, Frankreich

Page L, Wurster S, Weis P, Helm J, Lazariotou M, Einsele H, Ullmann AJ (2017). "Evaluation of a whole blood based approach for the determination of mould reactive

T-cell quantification and its susceptibility to pre-analytic delays." 8th Trends in Medical Mycology, Belgrad, Serbien

Wurster S, Helm J, Weis P, Lazariotou M, Page L, Einsele H, Löffler J, Ullmann AJ (2016). "Etablierung eines hochsensitiven Vollblut-basierten Protokolls für die Quantifizierung A. fumigatus-spezifischer T-Zellen." 13. Kongress für Infektionskrankheiten und Tropenmedizin, Würzburg, Deutschland

Wurster S, Helm J, Weis P, Lazariotou M, Page L, Einsele H, Ullmann AJ (2016). "Ciclosporin A, MMF, and prednisolone lead to reduced sensitivity of the quantification of Aspergillus-specific T-cells." 26th European Congress of Clinical Microbiology and Infectious Diseases, Amsterdam, Niederlande

Wurster S, Morton CO, Page L, Belic S, Dragan M, Löffler J (2018). "Alveolar immunopathology of Aspergillus and Mucorales compared in a highly reproducible Transwell® model." PEG Frühjahrstagung Sektion antimykotische Therapie, Bonn, Deutschland

Wurster S, Page L, Weis P, Lazariotou M, Einsele H, Ullmann AJ (2017). "Environmental mould exposure leads to elevated Mucorales specific T-helper and T-memory cell frequencies in healthy adults." 27th European Congress of Clinical Microbiology and Infectious Diseases, Wien, Österreich

Wurster S, Page L, Weis P, Lazariotou M, Ullmann AJ (2017)." PBMC- und Vollblut-basierter Nachweis Aspergillus- und Mucorales-spezifischer T-Zellen unter dem Einfluss von Voriconazol, Posaconazol und liposomalem Amphotericin B." PEG Frühjahrstagung Sektion antimykotische Therapie, Bonn, Deutschland

Wurster S, Weis P, Helm J, Lazariotou M, Page L, Einsele H, Ullmann AJ (2015). "Aspergillus-spezifische T-Zellen – ein neuer Biomarker bei der invasiven Aspergillose." 7. Kooperationsforum Drug Development, Würzburg, Deutschland

Wurster S, Weis P, Helm J, Lazariotou M, Page L, Ullmann AJ (2016). "Aspergillus-spezifische T-Zellen in der Diagnostik invasiver Aspergillosen – Möglichkeiten und Grenzen in der klinischen Praxis." PEG Frühjahrstagung Sektion antimykotische Therapie, Bonn, Deutschland

Wurster S, Weis P, Helm J, Page L, Lazariotou M, Einsele H, Löffler J, Ullmann AJ (2016). "Agitation und Verdünnung von Blutproben mit RPMI-Medium verlängern das präanalytische Fenster bei der Quantifizierung Antigen-spezifischer T-Zellen über den Marker CD154." 13. Kongress für Infektionskrankheiten und Tropenmedizin, Würzburg, Deutschland

Wurster S, Weis P, Lazariotou M, Helm J, Hellmann AM, Page L, Einsele H, Ullmann AJ (2016). "Exposure to Aspergillus spores in a scientific laboratory is associated with elevated specific T-cell frequencies in laboratory personnel." 7th Advances against Aspergillosis, Manchester, Großbritannien

7.5 Danksagung

Mit dem Abschluss dieser Arbeit möchte ich nun allen danken, die mich auf diesem Weg begleitet und mich unterstützt haben.

Mein Dank gebührt dabei meinem Doktorvater Prof. Andrew J. Ullmann, der mir durch seinen Einsatz und sein Vertrauen diese vielseitigen interdisziplinären Projekte ermöglicht hat.

Zudem möchte ich Prof. Jürgen Löffler, Prof. Samuel Samnick und Prof. Ulrike Holzgrabe für ihre Betreuung und die erfolgreichen Kollaborationen im Rahmen dieser Arbeit danken.

Besonderer Dank geht an Dr. Sebastian Wurster für die exzellente Laborausbildung und durchgehende Unterstützung trotz räumlicher Entfernungen.

Chris D. Lauruschkat danke ich für die angenehme und produktive Zusammenarbeit während unserer gemeinsamen Doktorandenzeit. Dabei möchte ich ebenfalls Fabian Schadt, Philipp Weis und Stanislav Belic für ihre engagierte Mitwirkung danken.

Außerdem bedanke ich mich bei Dr. Maria Lazariotou für ihre überaus präzise und effiziente Assistenz bei unseren Experimenten.

Natürlich danke ich auch allen freiwilligen Blutspendern, ohne die ein großer Teil unserer Arbeiten nicht möglich gewesen wäre.

Ich danke Margit und Rainer Pachl für die großzügige finanzielle Unterstützung während meines Studiums, sodass ich dieses sorgenfrei absolvieren konnte.

Zuletzt danke ich meiner Familie, Ruth, Andreas und Angelika Page, für ihre stetige Unterstützung und Halt in allen Lebenslagen.

Vielen Dank an alle, die mir meinen Traum der Infektionsforschung ermöglicht haben.

7.6 Eigenständigkeitserklärung

Eidesstattliche Erklärung

Hiermit erkläre ich an Eides statt, dass ich die Doktorarbeit *„Entwicklung und präklinische Evaluation immunologischer und nuklearmedizinischer diagnostischer Tests für Schimmelpilz-assoziierte Hypersensitivität und invasive Mykosen“* eigenständig, d. h. insbesondere selbstständig und ohne Hilfe eines kommerziellen Promotionsberaters angefertigt und keine anderen als die von mir angegebenen Quellen und Hilfsmittel verwendet zu haben.

Ich erkläre außerdem, dass die Dissertation weder in gleicher noch in ähnlicher Form bereits in einem anderen Prüfungsverfahren vorgelegen hat.

Ort, Datum _____ Unterschrift

Affidavit

I hereby confirm that my thesis entitled *“Development and preclinical evaluation of immunological and nuclear medical diagnostic assays for mould-associated hypersensitivity and invasive mycoses”* is the result of my own work. I did not receive any help or support from commercial consultants. All sources and / or materials applied are listed and specified in the thesis.

Furthermore, I confirm that this thesis has not yet been submitted as part of another examination process neither in identical nor similar form.

Place, Date _____ Signature